Update Knowledge Base for Long-term Core Cooling Reliability

OECD
BETTER POLICIES FOR BETTER LIVES

NEA
NUCLEAR ENERGY AGENCY

Organisation de Coopération et de Développement Économiques
Organisation for Economic Co-operation and Development

20-Dec-2013

_____

English text only

NUCLEAR ENERGY AGENCY
COMMITTEE ON THE SAFETY OF NUCLEAR INSTALLATIONS

Updated Knowledge Base for Long Term Core Cooling Reliability

ORGANISATION FOR ECONOMIC CO-OPERATION AND DEVELOPMENT

The OECD is a unique forum where the governments of 34 democracies work together to address the economic, social and environmental challenges of globalisation. The OECD is also at the forefront of efforts to understand and to help governments respond to new developments and concerns, such as corporate governance, the information economy and the challenges of an ageing population. The Organisation provides a setting where governments can compare policy experiences, seek answers to common problems, identify good practice and work to co-ordinate domestic and international policies.

The OECD member countries are: Australia, Austria, Belgium, Canada, Chile, the Czech Republic, Denmark, Estonia, Finland, France, Germany, Greece, Hungary, Iceland, Ireland, Israel, Italy, Japan, Luxembourg, Mexico, the Netherlands, New Zealand, Norway, Poland, Portugal, the Republic of Korea, the Slovak Republic, Slovenia, Spain, Sweden, Switzerland, Turkey, the United Kingdom and the United States. The European Commission takes part in the work of the OECD.

OECD Publishing disseminates widely the results of the Organisation's statistics gathering and research on economic, social and environmental issues, as well as the conventions, guidelines and standards agreed by its members.

This work is published on the responsibility of the OECD Secretary-General.
The opinions expressed and arguments employed herein do not necessarily reflect the official
views of the Organisation or of the governments of its member countries.

NUCLEAR ENERGY AGENCY

The OECD Nuclear Energy Agency (NEA) was established on 1 February 1958. Current NEA membership consists of 31 countries: Australia, Austria, Belgium, Canada, the Czech Republic, Denmark, Finland, France, Germany, Greece, Hungary, Iceland, Ireland, Italy, Japan, Luxembourg, Mexico, the Netherlands, Norway, Poland, Portugal, the Republic of Korea, the Russian Federation, the Slovak Republic, Slovenia, Spain, Sweden, Switzerland, Turkey, the United Kingdom and the United States. The European Commission also takes part in the work of the Agency.

The mission of the NEA is:

– to assist its member countries in maintaining and further developing, through international co-operation, the scientific, technological and legal bases required for a safe, environmentally friendly and economical use of nuclear energy for peaceful purposes, as well as

– to provide authoritative assessments and to forge common understandings on key issues, as input to government decisions on nuclear energy policy and to broader OECD policy analyses in areas such as energy and sustainable development.

Specific areas of competence of the NEA include the safety and regulation of nuclear activities, radioactive waste management, radiological protection, nuclear science, economic and technical analyses of the nuclear fuel cycle, nuclear law and liability, and public information.

The NEA Data Bank provides nuclear data and computer program services for participating countries. In these and related tasks, the NEA works in close collaboration with the International Atomic Energy Agency in Vienna, with which it has a Co-operation Agreement, as well as with other international organisations in the nuclear field.

THE COMMITTEE ON THE SAFETY OF NUCLEAR INSTALLATIONS

"The Committee on the Safety of Nuclear Installations (CSNI) shall be responsible for the activities of the Agency that support maintaining and advancing the scientific and technical knowledge base of the safety of nuclear installations, with the aim of implementing the NEA Strategic Plan for 2011-2016 and the Joint CSNI/CNRA Strategic Plan and Mandates for 2011-2016 in its field of competence.

The Committee shall constitute a forum for the exchange of technical information and for collaboration between organisations, which can contribute, from their respective backgrounds in research, development and engineering, to its activities. It shall have regard to the exchange of information between member countries and safety R&D programmes of various sizes in order to keep all member countries involved in and abreast of developments in technical safety matters.

The Committee shall review the state of knowledge on important topics of nuclear safety science and techniques and of safety assessments, and ensure that operating experience is appropriately accounted for in its activities. It shall initiate and conduct programmes identified by these reviews and assessments in order to overcome discrepancies, develop improvements and reach consensus on technical issues of common interest. It shall promote the co-ordination of work in different member countries that serve to maintain and enhance competence in nuclear safety matters, including the establishment of joint undertakings, and shall assist in the feedback of the results to participating organisations. The Committee shall ensure that valuable end-products of the technical reviews and analyses are produced and available to members in a timely manner.

The Committee shall focus primarily on the safety aspects of existing power reactors, other nuclear installations and the construction of new power reactors; it shall also consider the safety implications of scientific and technical developments of future reactor designs.

The Committee shall organise its own activities. Furthermore, it shall examine any other matters referred to it by the Steering Committee. It may sponsor specialist meetings and technical working groups to further its objectives. In implementing its programme the Committee shall establish co-operative mechanisms with the Committee on Nuclear Regulatory Activities in order to work with that Committee on matters of common interest, avoiding unnecessary duplications.

The Committee shall also co-operate with the Committee on Radiation Protection and Public Health, the Radioactive Waste Management Committee, the Committee for Technical and Economic Studies on Nuclear Energy Development and the Fuel Cycle and the Nuclear Science Committee on matters of common interest."

EXECUTIVE SUMMARY

Background

Following the Barsebäck-2 incident in 1992, several OECD member countries initiated research and development programs to investigate the event. These studies confirmed the inadequacy of the existing guidance and resulted in substantial backfitting of plants in several OECD countries. The research also helped to identify essential parameters and physical phenomena important to the issue that had not been previously recognized. An international working group (IWG) was formed under the auspices of the CSNI and given the assignment to establish a knowledge base on the reliability of ECC systems during sump recirculation. The IWG was composed of members from Germany (GRS), Sweden (SKI), Finland (STUK), Japan (NUPEC), and the United States (US). The United States representation included the USNRC and the BWR Owners Group. In addition, there was participation by insulation vendors. This IWG produced a SOAR entitled "Knowledge Base for Emergency Core Cooling System Recirculation Reliability" documenting suction strainer and sump screen clogging research findings as of 1995.

A Workshop on "Debris Impact on Emergency Coolant Recirculation" was held on February 25-27, 2004 in Albuquerque, NM (USA) under the auspices of the CSNI, in collaboration with US NRC. This workshop was aimed at discussing the impact of new information made available since 1996, at promoting consensus among NEA member countries on the remaining technical issues important for safety, and possible paths for their resolution. The proceedings of this workshop were published in 2004 under the title "Debris Impact on Emergency Coolant Recirculation". The Plenary session of the Workshop recommended that special attention be paid to the debris generation assessment method, head loss assessment, chemical effects, development of emergency procedures to handle potential debris blockage events, downstream effects including clogging of fuel elements, and plant cleanliness, particularly the containment.

Following the International Workshop titled "Taking Account of Feedback on Sump Clogging" jointly organized on December 4-5, 2008 by the CNRA and the CSNI, the latter entrusted its Working Group on the Analysis and Management of Accidents (WGAMA) and its Working Group on Fuel Safety (WGFS) to prepare a concise document explaining how the issue of chemical effects and the issue of downstream effects and long term core cooling could be addressed in the CSNI working group or task group frame. Following a WGAMA and WGFS proposal, a CSNI Task Group on Sump Clogging was set-up in December 2009, and its mandate was approved by the CSNI in June 2010 with the following objectives:

- Review the SOAR on the "Knowledge Base for Emergency Core Cooling System Recirculation Reliability" and identify open issues that need to be answered.
- Review relevant findings from international meetings and national reports.
- Identify answers to the open issues of the 1995 SOAR and any further progress achieved or any new open issues raised, in particular regarding chemical effects and downstream effects.
- Update the 1995 SOAR to reflect additional knowledge gained and R&D results achieved since 1995.
- Review the advantages/possibilities to establish a web-based portal for information exchange in sump clogging.
- Report and document to CSNI.

The CSNI Task Group on Sump Clogging started to work in the fall of 2010, with the following participating countries:

- Canada, as lead country
- Finland
- France
- Germany
- Japan
- Korea
- Spain
- Sweden
- The United States.

The Slovak Republic joined the Group in January 2012.

2. Approach and implementation of the mandate

The principal mechanism for the implementation of the Task was through technical meetings and e-mail exchanges. Five technical meetings were held to implement the Task; the first meeting was organised at the OECD/NEA Headquarters on 23-24 November 2010 while the last was organised on 8-9 April 2013, also at the OECD/NEA Headquarters. Several members of the Group also had the opportunity to meet, to exchange information and to visit the IRSN/VUEZ integral test facility (VIKTORIA) in December 2011 at Vuez, Slovak Republic, and the AREVA integral test facility at Erlangen, Germany in May 2012. Besides exchanges by e-mails, the Sump Clogging web page, set up by the NEA Secretariat in November 2010, was used for information exchange between the Task Group members, who provided a lot of documents that were uploaded and shared within the Group.

It was recognized from the beginning (i.e., during the kick-off meeting) that differences in the issue status and the methods (regulatory aspects, resolution of issues and R&D actions) used to address the strainer clogging remained a challenge, and the Group decided to focus on generic issues, starting from the U.S.NRC list of issues. Three sub-groups were formed:

- Sub-group one to address chemical effects; coordinated by David Guzonas of AECL (Canada) and with the support of the other members;

- Sub-group two on downstream effects, coordinated by Ingo Ganzmann of AREVA with FORTUM support; and,

- Sub-group three to address the update of the original 1995 SOAR, originally coordinated by Gilbert Zigler of Science & Engineering Associates, Inc., and completed by John Burke (US NRC).

The report outline was discussed and a revised Table of Contents developed that covered the topics being reviewed by the three sub-groups and reflected the progress in R&D work as well as analytical methods (e.g., Computational Fluid Dynamics to address blow down transport and containment pool transport) and risk-informed approaches to address the whole issue of sump clogging. Therefore, the content of the present report goes beyond the 1995 SOAR and includes not only an update of the previous information, but also two new topics on:

- Chemical effects, about which a significant amount of non-proprietary information is available and discussed in the dedicated chapter and in the appendix on "Experimental Investigations and Test Facilities"; and

- Downstream effects, considering ex-vessel and in-vessel aspects, and where the limited amount of information available has been discussed in the dedicated chapter and in the appendix on "Experimental Investigations and Test Facilities".

It has also to be noted that while the previous SOAR focused on BWRs, the present update includes a significant amount of new information related to PWRs, leading in particular to a very much expanded Appendix on "Experimental Investigations and Test Facilities". The Appendices on "Terminology" and "Debris Characteristics" have also been updated and expanded.

In parallel, a group working web page was set-up by the NEA Secretariat not only to allow information exchange between the Group members but also to investigate the advantages/possibilities of a maintaining a public web-based portal for information exchange on the sump clogging issue.

3. Results and their significance

The significant amount of testing and strainer replacements carried out for PWRs since the original SOAR was published has led to a deeper understanding of many of the phenomena addressed in that document. For example, the US NRC no longer accepts the use of the US NRC/SEA Head Loss Correlation for new strainer design qualification as a result of conditions and limitations realized during resolution of GSI-191. Therefore, the lengthy discussion on this correlation was eliminated from this revision. The understanding of debris properties, especially non-fibrous debris, has improved significantly. There have been major test programs to address the two "new" phenomena of chemical effects and downstream effects (better characterized as previously poorly recognized than truly new). There has been a recognition that integrated effects tests may provide a better assessment of ECCS reliability issues than single effects testing. Many of the conclusions presented in NEA/CSNI/R(95)11 remain valid, and the discussion that follows highlights advances, gaps and new phenomena.

Any assessment of ECCS and core cooling reliability must start with quantification of the amounts of debris generated *for the postulated events* (these events can be dependent on plant-specific or country-specific design bases). Assessments must consider all materials known to be problematic. It is equally important that the key characteristics of the destroyed material be known, e.g., the size distribution of released fibers and particles.

The major mechanisms for dislodging material have been identified as the pressure wave associated with pipe rupture, jet impingement on insulated targets, and erosion due to interaction with the high-velocity fluid. While conceptual models have been established in order to quantify the amount of debris, in general, the assessment of the models is rather limited. In general, the conclusions regarding debris generation have not changed significantly since the original SOAR. While new information on paint chips, latent debris and chemical effects are available, little new information on size distributions of released material is available.

Most debris transport/strainer head loss correlations rely on a few types of debris and the formation of homogeneous filter bed on the strainer surface. Recent head loss testing experiments have concluded that the use of correlations is difficult to justify, and plant-specific head loss testing with representative quantities and combinations of debris of types is recommended. The scaling effects associated with debris transport add uncertainties.

A reference plant study developed a methodology that considers both transport phenomenology and plant features and divides the overall complex transport problem into many smaller problems amenable to solution by a combination of experiment and analysis or engineering judgment. The use of CFD for debris transport analyses is promising but complex, as analyses require a large number of nodes, the inclusion of turbulence in the model requires refined techniques, there is a lack of benchmarking of multi-phase flow models, and there is a need for more validation and verification. In general, conservatisms in debris transport evaluations are related to the unavailability of relevant

data; in the absence of such data, the analysis should conservatively hedge toward assuming transport to the strainers.

The phenomena referred to as chemical effects take place in a complex recirculating water system in contact with a large number of different materials. Most materials present within containment can undergo corrosion or dissolution under the right physical and chemical conditions, as determined by the sump water chemistry and temperature. A significant knowledge base now exists with respect to the behaviour of chemical effects source terms under post-LOCA sump conditions, and this knowledge base has been summarized in this update. While the fundamental principles underlying chemical effects are reasonably well understood, the post-LOCA sump is a non-equilibrium chemical system. Therefore, prediction of precipitate formation from first principles can be extremely difficult and testing based on results obtained in single-effects tests can be excessively conservative. The use of integrated test facilities can reduce this conservatism. Another, related effect (but different from chemical effects) is the impact of the corrosion undergone by metallic components inside containment (especially when coupled with other phenomena such as erosion) and its indirect effect (e.g., particle release) on the behavior of some debris, mainly the fibers, at the screens. Under some post-LOCA water chemistry conditions, erosion-corrosion can also be a concern.

The effect of debris by-pass on the potential for blockage of flow channels in fuel assemblies is an active area of research as relatively small amounts of debris captured by the fuel assemblies can have a drastic impact on thermal-hydraulics in the core under post-LOCA conditions. A significant knowledge base on downstream effects has also been developed, but unfortunately for the Task Group mandate, much of these data are proprietary. Downstream effects investigations are on-going and will continue to be performed in the upcoming years for both existing and new plant designs.

Much research and development work has been performed to understand and optimize the performance of sump strainers, focusing on both high debris retention capacity and a low pressure loss at the debris-covered strainer. As the debris layer itself is the effective filtering agent the performance of the strainer with respect to debris retention is better the faster a closed debris bed is built up. The Task Group highlights the seemingly conflicting requirements between a high degree of debris removal by the screens to minimize downstream effects and minimizing strainer head loss.

While differences in plant design and configuration (e.g., choice of insulation) make it impossible to specify a single solution to the problem of ensuring ECCS and containment spray reliability and long-term core cooling, the large knowledge base now available, supported by the extensive suite of test facilities described in the Appendix on "Experimental Investigations and Test Facilities", has made it possible for some member states to consider this issue closed.

It is clear that work will continue on the topic of the Task Group mandate for some time into the future, and the Task Group highlighted the need to ensure that this new information is shared when possible. Most of the Task Group effort focused on updating the SOAR; while much less time was spent investigating the feasibility of web-based information exchange, the Group was very positive concerning the usefulness and feasibility of such a tool. To minimize the burden on the NEA Secretariat to continuously update the NEA sump clogging web page, the Task Group members agreed to provide links to their national web pages on this issue to be included on the NEA sump clogging web page. In this way, updates to the various national web pages will be directly reflected in the latter, recognizing that issues such as language and availability of test data will be challenging. The NEA sump clogging web page will be cleaned up, restructured for easier use and made public as soon as the present report is published.

4. Recommendations

Given the differences in issue resolution status and approaches taken to achieve resolution, it is not possible to make specific recommendations that might become proscriptive. However, several

generic recommendations can be made:

- Careful consideration of the materials used inside containment (mainly thermal insulation materials, but also coatings and others) will decrease the risk of sump clogging by reducing the debris source term in case of a LOCA. Special care must be taken to try to avoid the presence of certain combination of materials which together could make the problem much severe.

- Good housekeeping to minimize latent debris is also important, especially when the interaction between LOCA-generated debris and latent debris (i.e. particulate vs. fibrous) is concern.

- The large number of test facilities that now exist should continue to be used, for example, in collaborative projects.

- There is a need to ensure that new information generated by on-going work is shared when possible. Maintaining and expanding the Task Group web page set-up by the NEA Secretariat could be an effective means of facilitating information exchange in the future. Availability (public vs. non-public) of some test reports and test data varies by individual member country practices. An investigator should contact the utility or safety authority in the country of interest to determine availability of existing information.

LIST OF ACRONYMS

ABB	Asea Brown Boveri
ABWR	Advanced Boiling Water Reactor
ACRS	Advisory Committee on Reactor Safeguards
AECL	Atomic Energy of Canada Limited
ANL	Argonne National Laboratory
ANSI	American National Standards Institute
ARL	Alden Research Lab
ASN	French Nuclear Safety Authority
ASTM	American Society for Testing and Materials (now ASTM International)
BMU	German Federal Ministry for the Environment, Nature Conservation and Nuclear Safety
BMW	German Federal Ministry of Economics and Technology
BWR	Boiling Water Reactors
BWROG	BWR Owners Group
CAD	Computer Aided Design
CANDU	CANada Deuterium Uranium
CCI	Control Components Inc.
CDF	Core Damage Frequency
CDI	Continuum Dynamics, Inc.
CESSI	Colorado Engineering Experiment Station Inc.
CFD	Computational Fluid Dynamics
CFR	Code Of Federal Regulations
CIIT	Chicago Illinois Institute of Technology
CNSC	Canadian Nuclear Safety Commission
CPVC	Chlorinated Polyvinylchloride
CSHL	Clean Strainer Head Loss
CSN	Consejo de Seguridad Nuclear (Spain)
CSNI	Committee on Safety of Nuclear Installations
CSS	Containment Spray System
CST	Condensate Storage Tank
CVSS	Containment Vessel Spraying System
DBA	Design Basis Accident
DDTS	Drywell Debris Transport Study
DEGB	Double-Ended Guillotine Break
DVI	Direct Vessel Injection
ECC	Emergency Core Coolant
ECCS	Emergency Core Cooling System
EDX	Energy Dispersive X-ray
EOP	Emergency Operating Procedure
EPR	European Pressurized Reactor
EPRI	Electric Power Research Institute
ESEM	Environmental Scanning Electron Microscope
FA	Fuel Assemblies
FME	Foreign Material Exclusion
F-HELO	FNC Head Loss Loop
F-WACH	FNC Water Chemistry Test Reactor
GE	General Electric
GENE	General Electric Nuclear Energy
GKSS	Gesellschaft fur Kernenergieverwertung in Schiffbau und Schiffahrt*
GL	Generic Letter

GSI	Generic Safety Issue
HDR	Heissdampfreaktor
HELB	High-Energy Line Break
HEW	Hamburg Electrizitatswerk
HPSI	High-Pressure Safety Injection
HSZG	University of Applied Sciences Zittau/Gorlitz
HZDR	Helmholtz-Zentrum Dresden-Rossendorf
HVT	Hold-up Volume Tank
IAEA	International Atomic Energy Agency
ICET	Integrated Chemical Effects Test
ICP-AES	Inductively Coupled Plasma - Atomic Emission Spectroscopy
IOZ	Inorganic Zinc
IRSN	L'Institut de Radioprotection et de Sûreté Nucléaire
IRWST	Inside-Containment Refueling Water Storage Tank
IT	Intermediate Temperature
IWG	International Working Group
JNES	Japan Nuclear Energy Safety
KINS	Korea Institute of Nuclear Safety
KWU	Kraftwerk Union (Siemens)
LANL	Los Alamos National Laboratory
LDFG	Low-Density Fiberglass
LBLOCA	Large Break Loss-Of-Coolant-Accident
LLOCA	Large Loss-Of-Coolant-Accident
LOCA	Loss-Of-Coolant-Accident
LPSI	Low Pressure Safety Injection
LWR	Light Water Reactor
MCL	Main Circulating Loop
MIJIT	Metallic Insulation Jet Impact Tests
MLOCA	Medium Loss-of-Coolant Accident
MSL	Main Steam Line
NEA	Nuclear Energy Agency
NEI	Nuclear Energy Institute (USA)
NISA	Nuclear and Industrial Safety Agency (Japan)
NPP	Nuclear Power Plant
NPSH	Net Positive Suction Head
NRC	Nuclear Regulatory Commission
NUCC	Nuclear Utilities Coating Council
OECD	Organization for Economic Co-operation and Development
OPG	Ontario Power Generation
OPR	Optimized Power Reactor
ORP	Oxidation-Reduction Potential
PE	Polyethylene
PCI	Performance Contracting Inc.
PCT	Peak Cladding Temperature
PHWR	Pressurized Heavy Water Reactor
PIRT	Phenomena Identification And Ranking Table
PNNL	Pacific Northwest National Laboratory
POP	Proof-of-Principle
PP&L	Pennsylvania Power and Light
PVC	Polyvinyl Chloride
PWR	Pressurized Water Reactor
PWROG	Pressurized Water Reactor Owners Group
RCS	Reactor Coolant System
RHR	Residual Heat Removal
RMI	Reflective Metallic Insulation

RPV	Reactor Pressure Vessel
RG	Regulatory Guide
RSK	Reactor Safety Commission (Germany)
RWST	Refueling Water Storage Tank
SAS	Sodium Aluminum Silicate
SBLOCA	Small Break Loss of Coolant Accident
SE	Safety Evaluation
SEA	Science and Engineering Associates, Inc.
SEM	Scanning Electron Microscope
SER	Safety Evaluation Report
SI	Safety Injection
SIS	Safety Injection System
SKI	Swedish Nuclear Power Inspectorate
SNI	Sandia National Laboratories
SOAR	State of the Art Report
STP	South Texas Project
SRTC	Savannah River Technical Center
SRV	Safety Relief Valve
SSM	Swedish Radiation Safety Authority
STUK	Säteilyturvakeskus (Finnish Centre for Radiation and Nuclear Safety)
TSP	Trisodium Phosphate
TVO	Teollisuuden Voima Oy
UCN	Ulchin Nuclear Power Plant
UFSAR	Updated Final Safety Analysis Report
URG	Utility Resolution Guidance
US	United States
USI	Unresolved Safety Issue
VGB	Verband der Großkessel Besitzer e.V.
VVER	Vodo-Vodyanoi Energetichesky Reactor (Water-Water Power Reactor)
WGAMA	Working Group on Accident Management and Analysis
WOG	Westinghouse Owners Group
XRD	X-ray Diffraction
ZOI	Zone of Influence

* Renamed "Helmholtz-Zentrum Geesthacht Centre for Materials and Coastal Research"

TABLE OF CONTENTS

TABLES

FIGURES

1.   INTRODUCTION

This revision of the Knowledge Base for Emergency Core Cooling System Recirculation Reliability (NEA/CSNI/R (95)11) [1-1] describes the current status (late 2012) of the knowledge base on emergency core cooling system (ECCS) and containment spray system (CSS) suction strainer performance and long-term cooling in operating power reactors. New reactors, such as the AP1000, EPR and APR1400 that are under construction in some Organization for Economic Co-operation and Development (OECD) member countries, are not addressed in detail in this revision.   The containment sump (also known as the emergency or recirculation sump in pressurized water reactors (PWRs) and pressurized heavy water reactors (PHWRs) or the suppression pools or wet wells in boiling water reactors (BWRs)) and associated ECCS strainers are parts of the ECCS in both reactor types. All nuclear power plants (NPPs) are required to have an ECCS that is capable of mitigating a design basis accident (DBA). The containment sump collects reactor coolant, ECCS injection water, and containment spray solutions, if applicable, after a loss-of-coolant accident (LOCA). The sump serves as the water source to support long-term recirculation for residual heat removal, emergency core cooling, and containment atmosphere clean-up. This water source, the related pump suction inlets, and the piping between the source and inlets are important safety-related components. In addition, if fibrous material is deposited at the fuel element spacers, core cooling can be endangered.

The performance of ECCS/CSS[1] strainers was recognized many years ago as an important regulatory and safety issue. One of the primary concerns is the potential for debris generated by a jet of high-pressure coolant during a LOCA to clog the strainer and obstruct core cooling. The issue was considered resolved for all reactor types in the mid-1990s and the OECD/NEA/CSNI published report NEA/CSNI/R(95)11 in 1996 to document the state of knowledge of ECCS performance at that time.

Subsequent to the publication of NEA/CSNI/R(95)11, a number of new issues (e.g., chemical effects, downstream effects and long-term effects) have been identified that have reopened the topic of strainer performance. This revised knowledge-base document has been developed to update the knowledge base by incorporating the considerable quantity of research completed, and the lessons learned, since 1996. It was recognized from the beginning that differences in the issue status and the methods (regulatory aspects, resolution of issues and research and development actions) used to address the strainer clogging remained a challenge, and the NEA Sump Clogging Task Team chose to focus on generic issues. The present report includes not only an update of the previous information, but also two new topics on chemical effects and downstream effects.   In addition, while NEA/CSNI/R(95)11 focused on BWRs, the present update includes a significant amount of new information related to PWRs, leading in particular to a very much expanded Appendix on "Experimental Investigations and Test Facilities".

This document was prepared by the NEA Sump Clogging Task Team which included in alphabetic order:

Maria Agrell	SSM, Sweden
Abdallah Amri	OECD/NEA
Young S. Bang	KINS, Korea

---

[1]   Wherever the term ECCS suction strainer is used, it is understood that it also applies to other similar suction strainers that may exist, such as for the containment spray system.

Philippe Blomart	EDF, France
Annette Bröcker	GRS, Germany
John Burke	NRC, USA
Ingo Ganzmann	AREVA NP
David Guzonas	AECL, Canada
Christophe Herer	IRSN, France
Bruno Lenogue	AREVA NP
Hideaki Masaoka	METI, Japan
Jean-Marie Mattéi	IRSN, France
Winfried Pointner	GRS, Germany
Oddbjörn Sandervag	SSM, Sweden
Vojtech Soltesz	VUEZ, Sloavak Republic
Seppo Tarkiainen	FORTUM, Finland
Matthieu Tricottet	IRSN, France
Atsushi Ui	JNES, Japan
Cristina Villalba	CSN, Spain
Gilbert Zigler	Science and Engineering Associates, Inc.

The lead authors of the specific chapters are as follows:

Executive Summary	Chair + Secretary
Chapter 1: Introduction	J. Burke
Chapter 2: Debris generation and sources	J. Burke
Chapter 3: Blow down transport (incl. CFD)	J. Burke
Chapter 4: Containment pool transport (incl. CFD)	J. Burke
Chapter 5: Chemical effects	D. Guzonas
Chapter 6: Strainer pressure drop	J. Burke
Chapter 7: Downstream effects	I. Ganzmann
Chapter 8: Risk assessment and Severe Accident-related issues	J.M. Mattéi
Chapter 9: Conclusions and recommendations	Chair
Appendix A: Terminology	Ph. Blomart
Appendix B: Historical background	J. Burke
Appendix C: Summary of debris characteristics	D. Guzonas
Appendix D: Experimental investigations and test facilities	All
Appendix E: Potential CFD support calculations	J. Bailey (AECL)

There are many acronyms and terms commonly used when discussing the issue of ECCS suction strainer clogging that are used throughout this report. The acronyms are defined at the start of the report; more details on the terminology can be found in Appendices A and C.

1.1   Description of the Safety Concern

In the event of a LOCA or a high-energy pipe break within the containment building, piping thermal insulation and other materials in the vicinity of the break can be dislodged because of the

ensuing steam/water-jet impingement. The area near the break where insulation debris is generated is called the zone of influence (ZOI). This debris would be driven away from the ZOI by the high-velocity fluid flow from the break. Some of this debris will eventually be transported to and accumulate on the recirculation pump suction strainers, which are typically located at lower levels in containment. Debris accumulation on the pump strainers could challenge the plant's capability to provide adequate long-term cooling water to the ECCS and to the CSS pumps. This accumulated debris on the sump strainer may increase the differential pressure across the sump strainer and thus decrease the net positive suction head (NPSH) margin (i.e., head loss) available to the ECCS pumps and challenge the structural stability of the strainer assembly. Another purpose of the suction strainer is to minimize the amount of debris entering the ECCS suction lines. Debris can block openings or damage components in the systems served by the ECCS pumps or impede the flow of cooling water into the reactor core.

To function properly, the ECCS pumps need an adequate margin between the available and required NPSH. An inadequate NPSH margin could result in cavitation and subsequent failure to deliver the amount of water needed for cooling during a DBA. The available NPSH is a function of the static head of water above the pump inlet, the pressure of the atmosphere above the sump water surface[2], and the temperature of the water at the pump inlet.

The United States (US) Nuclear Regulatory Commission (NRC) Regulatory Guide (RG) 1.82 [1-3] is a widely accepted guidance document for design considerations related to ECCS suction strainers. The US NRC first published this document in 1974, issuing Revision 0 "Water Sources for Long-Term Recirculation Cooling Following a Loss-of-Coolant Accident". This first revision of the RG recommended that the design coolant velocity at the strainers be approximately 6 cm/sec (0.2 ft/sec) and that the strainer surface area be determined by assuming one-half of the free surface area of the fine screen (strainer) area to account for debris blockage.

Because of questions raised in the late 1970s, research was sponsored to study the accumulation of debris on suction strainers. In January 1979 the NRC declared suction-strainer blockage to be Unresolved Safety Issue (USI) A-43, "Containment Emergency Sump Performance". Based on this additional research, the US NRC concluded that its regulatory guidance needed to be revised and issued Revision 1 of RG 1.82 in 1985 to require a more deterministic approach. The 6 cm/s approach velocity and the 50% blockage assumption in Revision 0 were replaced by a recommendation to conservatively determine the coolant velocity and debris blockage based on actual insulation destruction and transport properties.

USI A-43 was closed in 1985 based on the revision to the RG. The US NRC concluded that no additional regulatory action was warranted for operating NPPs at that time, but indicated that new NPPs would need to satisfy the guidance in RG 1.82 Revision 1, and that operating NPPs should consider the guidance in the revised RG 1.82 when making plant modifications, namely, to change thermal insulation.

A typical accident sequence, including the timing of debris generation for a US PWR, is shown in Table 1-1. In this table it is observed that the debris generating phase can be very short (40 seconds in this Large Break LOCA (LBLOCA) example). After the recirculation phase is initiated the different debris can be drawn to the pump suction strainers and start to accumulate at the screens. Minor breaks would have different evolution and time responses. A BWR would have a similar response, with some exceptions; for example, BWRs take suction from the suppression pool for the duration of the event and do not switch suction paths.

---

[2] Not all Regulatory Authorities permit the use of containment accident pressure to increase the calculated NPSH available.

Table 1-1: PWR LOCA Sequences (from NUREG/CR-6762, Vol. 1 Table 2-4)

Time after LOCA (s)	Accumulator (SI Tanks)	High Pressure Safety Injection (HPSI)	Low Pressure Safety Injection (LPSI)	Containment Spray (CS)	Comments
0-1	Reactor scram. Initially high containment pressure, followed by low pressure in pressurizer. Debris generation begins due to initial pressure wave, followed by jet impingement. Blowdown flow rate is large; flow at the break is mostly saturated water. Quality $\leq$0.05. Saturated jet-models are appropriate. Sandia National Laboratories (SNL)/American National Standards Institute (ANSI) models suggest wider jets, but static pressures decay rapidly with distance.				
2		Initiation signal	Initiation signal	Initiation signal	Initiation signal from low pressurizer pressure or high containment pressure/temperature
5	Accumulator injection begins	Pumps start to inject into vessel	Pumps start (pressure of reactor coolant system greater than pump dead head)	Pumps start and sprays on	In a cold-leg break, ECCS bypass is caused by counter-current injection in the downcomer. Hot-leg break does not have this problem.
10	Blowdown flow rate decreases steadily from $\approx$20,000 lb/s to 5000 lb/s. Cold-leg pressure falls considerably to about 1000 psia. At the same time, effluent quality increases from 0.1 to 0.5 (especially that from steam generator side of the break). Flow at the break is vapor continuum with water droplets suspended in it. Saturated water or steam jet models are appropriate. At these conditions, SNL/ANSI models show that jet expansion induces high pressures far from break location.				
25		End of bypass; high-pressure safety injection.			
25-30	Break velocity reaches a maximum > 1000 ft/s. Quality in excess of 0.6. Steam flow at less than 500 lb/s. Highly energetic blowdown is probably complete. However, blowdown continues as residual steam continues to be vented.				
35	Accumulators empty		LPSI ramps to design flow.		
40	Blowdown is terminated, and therefore debris generation is mostly complete. Blowdown pressure at nozzle <150 psi. Debris would be distributed throughout the containment. Pool is somewhat turbulent.				
55-200	Reflood and quenching of fuel rods (T_{max} about 1036 ^{o}F). In the cold-leg break, quenching occurs between 125 and 150 s. In hot-leg break, quenching occurs between 45 and 60 s (T_{max} about 950 ^{o}F).				

200-1200	Debris added to lower containment pool by spray washdown drainage and break washdown. Containment pool keeps filling. Heavy debris may settle down.				
1200	Low-level indication in RWST received by operator. Operator prepares to turn on ECCS in sump recirculation mode.				
1500		Switch suction to sump	Switch suction to sump	Terminate or to sump	Many plants have containment fan coolers for long-term cooling.
1500-18000	Debris may be brought to the sump strainer. Build-up of debris on sump strainer may cause excessive head loss. In general, containment sprays may be terminated in large dry containments at the 2-h mark.				
>36000		Switch to hot-leg recirculation.	Switch to hot-leg recirculation		

1.2   Sump Performance Issues

After closure of USI A-43, several BWR plant events in the 1990s affecting ECCS strainers prompted another review of strainer design requirements.

On July 28, 1992, a steam line LOCA occurred when a safety relief valve (SRV) inadvertently opened in the Barsebäck-2 NPP, a BWR in Sweden. The steam jet stripped fibrous insulation from adjacent pipework. Part of that insulation debris was transported to the wetwell pool and clogged the intake strainers for the drywell spray system after about one hour. Although the incident in itself was not very serious, it revealed a weakness in the defense-in-depth concept which under other circumstances could have led to the ECCS failing to provide water to the core.

The Barsebäck incident spurred immediate action on the part of regulators and utilities in several OECD countries (e.g., Sweden, Finland, Germany, Switzerland and France). Research and development efforts of varying intensity were launched in many countries and in several cases resulted in findings that earlier strainer clogging data were incorrect because essential parameters and physical phenomena (such as insulation aging) had not been recognized. Such efforts resulted in substantial backfitting being carried out for BWRs and some PWRs in several OECD countries.

To accelerate exchange of information and experience, and to provide feedback on actions taken to the international community, a workshop on the strainer clogging issue was hosted by the Swedish Nuclear Power Inspectorate (SKI) in Stockholm, Sweden on January 26-27, 1994, under the auspices of the CSNI/PWG-1 committee. The objectives of the workshop were to:

1. Give an overview of decisions and work performed recently on this issue;

2. Address the actual safety issues with regard to the reliability of ECC recirculation; and

3. Discuss further actions needed.

The workshop revealed a rather confusing picture of the available knowledge base, examples of conflicting information, and a wide range of interpretation of guidance provided in U.S. NRC Regulatory Guide 1.82, Rev. 1. Following this workshop, SKI requested the formation of an International Working Group (IWG) under the auspices of the CSNI/PWG-1 committee to establish an internationally agreed-upon knowledge base for assessing the reliability of ECC water recirculation systems. That led to the working group developing CSNI State-of-the-Art Report (SOAR) NEA/CSNI/R(95)11 "Knowledge Base for Emergency Core Cooling System Recirculation Reliability" in 1996.

1.2.1   Update of the Knowledge Base (1999 to 2009)

A number of corrective actions have been taken in NPPs around the world since the Barsebäck event in 1992. For a number of plants, actions were taken as direct responses to requirements issued by regulating authorities, while other plants introduced back-fitting measures voluntarily or because of anticipated requirements. The actions taken as response to the strainer issue, and the rationale behind these actions, had never been reported internationally in a systematic fashion. As a result, the CSNI decided to set up an international task force to revisit the strainer clogging issue. An OECD/NEA workshop was organized as a part of this effort on May 10-11, 1999 in Stockholm, Sweden, and its results are collected in the proceedings of the "Workshop on Update of the Knowledge Base for Sump Screen Clogging, Proceedings", dated May 1999, Stockholm, Sweden [1-11]. One recommendation from that workshop was to conduct a survey of actions taken in various countries.

Report NEA/CSNI/R(2002)6, dated July 2002, presents the findings of that survey of modifications performed primarily in the ECCS and CSS of NPPs in different countries following the Barsebäck event in July 1992. The information about these modifications was gathered through a

study of published reports, contacts with the regulatory bodies of the different countries, and in some cases, directly from utility specialists and plant representatives. The information reflected the plant and research status in 15 countries as of December 2001; nine with PWRs, seven with BWRs, five with Vodo-Vodyanoi Energetichesky Reactors (VVERs) and one with PHWR (CANDU[®3]) reactors.

The review indicated that:

1. Many countries had carried out very thorough and expeditious actions in response to the Barsebäck event, often within a noteworthy constructive and co-operative climate between the regulatory body and the plant owners;
2. All countries had performed extensive studies;
3. Many countries had performed extensive experiments;
4. Corrective actions had been taken in:
   a. most BWRs,
   b. a limited number of PWRs, and
   c. a significant number of VVERs and CANDU reactors (installation of new strainers /materials);
5. Experiments and theoretical studies were still ongoing in some countries, mostly for PWR designs.

Following that report, and as a result of further studies on the vulnerability of PWRs to strainer clogging documented in NUREG/CR-6771 that indicated that strainer clogging could increase the core damage frequency (CDF) by one to two orders of magnitude, it was decided to hold another workshop. The workshop on Debris Impact on Emergency Coolant Recirculation was held in February 2004 in Albuquerque, New Mexico, USA, organised under the auspices of the CSNI in collaboration with the US NRC. The purpose of this workshop was to discuss the impact of new information made available since 1996 and to promote consensus among member countries on identification of remaining technical issues important to safety, and on possible paths for their resolution.

The specific purposes of the workshop were to:

1. Review the knowledge base which had been developed since NEA/CSNI/R(95)11 was issued, and in particular, information developed after 1999, and to consider the validity of the conclusions drawn;

2. Exchange information on the current status of research related to debris generation, debris transport, and sump strainer clogging and penetration phenomena, in particular for PWRs, and to assess uncertainties. In particular, to critically review and then consolidate and expand the current, still incomplete and partially ambiguous, knowledge base;

3. Exchange and disseminate information on recent and current activities and practices in these areas;

4. Identify and discuss differences between approaches relevant to reactor safety; and

5. Identify technical issues and programs of interest for international collaborative research and develop an Action Plan outlining activities that CSNI should undertake in the area of strainer or sump screen clogging during the next few years.

The summary and conclusions of the Albuquerque workshop are documented in report NEA/CSNI/R(2004)2, "Debris Impact on Emergency Coolant Recirculation - Summary and Conclusions".

---

[3] CANDU, CANada Deuterium Uranium, is a registered trademark of Atomic Energy of Canada Limited (AECL).

Another workshop was held in December 2008 in Paris to discuss the lessons learned related to PWR strainer clogging since the Albuquerque meeting. The attendees felt that an update of NEA/CSNI/R(95)11 was warranted, in particular for the following topics:

- Review the State-of-the-Art report (SOAR) prepared in 1995 on the "Knowledge Base for Emergency Core Cooling System Recirculation Reliability" and identify any remaining open issues;

- Review relevant findings from international meetings and national reports;

- Identify answers to the open issues raised in the 1995 SOAR, any progress made, and any new open issues identified, in particular regarding chemical and downstream effects;

- Update the 1995 SOAR to reflect additional knowledge gained and research and development results achieved since 1995;

- Review the advantages/possibilities of establishing a web-based portal for information exchange on the subject of sump clogging;

- Report and document to CSNI.

Report NEA/CSNI/R(2009)14, "Proceedings of the CNRA/CSNI International Workshop on Taking Account of Feedback on Sump Clogging" documents that workshop.

At a CSNI meeting the following year on December 9-10, 2009, in Paris, its members agreed, based on the WGAMA and WGFS proposal, to set-up a CSNI Task Group on the sump clogging issue including the updating of the SOAR on the "Knowledge Base for Emergency Core Cooling System Recirculation Reliability" [1-1], issued in 1996. The mandate for the group was approved at that meeting, as recommended during the December 2008 workshop

1.2.2 *Assessment of Plant Vulnerability*

In 2001/2002, the US NRC commissioned several studies of the risk associated with suction strainer blockage to better understand the risk significance and change in CDF for ECCS strainer blockage in PWRs.

NUREG/CR-6762 "Assessment of Debris Accumulation on PWR Sump Performance," identified a range of conditions under which a PWR ECCS could fail in the recirculation mode of operation. These conditions stem from the destruction and suspension of piping insulation materials, coatings (paints), and particulate matter (e.g., dirt) by the steam/water jet emerging from a postulated break in reactor coolant piping. Under certain circumstances, this debris can be transported to the floor of the containment and accumulate on the recirculation suction strainer in sufficient quantity to severely impede recirculation flow. The likelihood that these conditions could occur during a postulated LOCA is plant-specific. However, a review of the design features for US PWRs conducted as part of research carried out to address Generic Safety Issue (GSI)-191 clearly indicated that adverse conditions existed in several plants. NUREG/CR-6771, "GSI-191: The Impact of Debris Induced Loss of ECCS Recirculation on PWR Core Damage Frequency", published in August 2002, examined the risk significance of those findings. Specifically, the goal was to estimate the amount by which the CDF would increase if failure of PWR ECCS recirculation cooling as a result of debris accumulation on the sump screen were accounted for in a manner that reflected the results of the recent experimental and analytical work. The results suggested that the conditional probability of recirculation sump failure (given a demand for recirculation cooling) was sufficiently high at many U.S. plants to cause an increase in the total CDF of an order of magnitude or more.

1.3 Operational Events Rendering the ECCS Inoperable

Operational events that occurred at both BWR and PWR plants pertaining to the issue of suction-strainer blockage further raised awareness of vulnerabilities of some ECCS strainer designs, and are

briefly reviewed below. These events are described in the general order of their relative severity, starting with operational events that have rendered systems inoperable with regard to their ability to complete their safety mission. Two of these events resulted in the generation of insulation debris by jet flow from a LOCA caused by the unintentional opening of SRVs. Other events have resulted in accumulation of sufficient operational debris to effectively block a strainer or to plug a valve. Some event reports simply noted debris found in containment, as well as inadequate maintenance that would likely cause potential sources of debris within containment. Related event reports identified inadequacies in a sump strainer whereby debris could potentially bypass the strainer and enter the respective system. Appendix B contains more details of the events discussed in this section.

1.3.1   *LOCA Debris Generation Events*

There were two LOCA events involving the unintentional opening of SRVs that generated insulation debris; these occurred at:

- German reactor Gundremmingen-1 (KRB-1) in 1977, where the 14 SRVs of the primary circuit opened during a transient; and

- Barsebäck-2 NPP on July 28, 1992, during a reactor restart procedure after the annual refueling outage.

Both of these reactors were BWRs with similarities to BWRs in the U.S. and other countries.

1.3.2   *Inadequate Maintenance Leading to Potential Sources of Debris*

In operating BWR and PWR plants, numerous events have occurred in which inadequate maintenance within containment could have potentially resulted in significant debris generation. In general, these events involved degraded or unqualified protective coatings, and degradation of piping insulation materials where these materials could be transported to the strainer and significantly affect head loss. Some of the more significant events are the subject of US NRC Information Notices, Generic Letters or Bulletins, and are discussed in Appendix B.

1.3.3   *Generic Safety Issue (GSI) 191*

As a result of the lessons learned from research conducted to address the events mentioned in Sections 1.3.1 and 1.3.2, the issue of sump clogging was revisited in the US for PWR reactors beginning in approximately 1997. This re-investigation of PWR suction strainer issues was labeled GSI-191, "Assessment of Debris Accumulation on PWR Sump Performance". The new and/or updated research investigated all aspects of PWR ECCS suction strainer performance following a LOCA; debris generation, debris fragmentation, protective coating performance, debris transport, chemical effects, suction strainer prototype testing, downstream effects, and risk assessment and CDF probabilities. NUREG/CR-6808 [1-10] summarizes the publically available research performed until 2002 on strainer blockage.

1.4   Regulatory Considerations

This section presents a general review of the different regulatory approaches followed by some of the member countries.

It is important to note that, because of the large uncertainties associated with the analytical methods used to evaluate some of the main phenomena affecting this issue, there is almost full agreement among regulators as well as industry on the need to use the results of appropriate and representative testing to evaluate the significant phenomena, including debris generation, debris transportation near the strainer, pressure drop at the filters and chemical effects. In all cases it is important to ensure that the test conditions reflect the actual conditions in the plant, and use representative quantities and combinations of debris types (including the way samples are mechanically prepared for the test and the degree of aging), timing of the testing, etc.

In the US, regulations were established to govern design and operational aspects of nuclear power reactors. These regulations are codified in Title 10 of the U.S. Code of Federal Regulations (CFR), Part 50 (10CFR Part50) [1-2] and are similar to regulations in other OECD countries. These regulations, promulgated by the NRC, provide for the licensing of nuclear facilities. The NRC also publishes regulatory guidance documents for the nuclear power industry to aid in compliance with the regulations. Regulatory guidance on ensuring adequate long-term recirculation cooling following a LOCA is contained in RG 1.82, "Water Sources for Long-Term Recirculation Cooling Following a Loss-of-Coolant Accident" [1-3]. This guide describes acceptable methods for implementing applicable general design criteria requirements with respect to the sumps and suppression pools functioning as water sources for emergency core cooling, containment heat removal, or containment atmosphere cleanup.

As mentioned briefly in Section 1.1, the US NRC first published regulatory guidance on the performance of ECCS suction strainers in 1974. Revision 0 of the RG recommended that the design coolant velocity at the strainers be approximately 6 cm/sec (0.2 ft/sec) and that the strainer surface area be determined by assuming one-half of the free surface area of the fine screen (strainer) is available to account for debris blockage.

Revisions of RG 1.82 were issued in November 1985 and May 1996, respectively. Revision 1 reflected the staff's technical findings related to USI A-43 reported in NUREG-0897. One key aspect of this revision was the staff's recognition that the 6 cm/s velocity and 50% strainer blockage criteria of Revision 0 did not adequately address the issue and was inconsistent with the technical findings developed for the resolution of USI A-43. The title of the RG was also changed to "Water Sources for Long-term Recirculation Cooling Following a Loss-Of-Coolant Accident" to better reflect its applications. US NRC Generic Letter-85-22 was issued recommending the use of Revision 1 of RG 1.82 for changeout and/or modification of thermal insulation installed on primary coolant system piping and components.

Revision 2 of RG 1.82 updated the strainer blockage guidance for BWRs because operational events, analyses, and research following the issuing of Revision 1 indicated that the previous guidance was not comprehensive enough to adequately evaluate a BWR plant's susceptibility to the detrimental effects caused by debris blockage of the suction strainers. Revision 2 of RG 1.82 addressed operational debris as well as debris generated by a postulated LOCA. Specifically, this revision stated that all potential debris sources should be evaluated, including, but not limited to, insulation materials (e.g. fibrous, ceramic, and metallic), filters, corrosion products, foreign materials, and paints and coatings. Operational debris includes corrosion products such as BWR suppression pool sludge and foreign materials. This revision also noted that debris could be generated and transported by the washdown process as well as by the blowdown process. Other important aspects of Revision 2 included: the use of debris interceptors (i.e., suction strainers) in BWR designs to protect pump inlets and NPSH margins; the design of passive and/or active strainers; instrumentation and in-service inspections; suppression pool cleanliness; evaluation of alternate water sources; analytical methods for debris generation, transport, and strainer blockage head loss; and the need for appropriate supporting test data.

Revision 3 of RG 1.82, issued in 2003, was the first time chemical effects were identified as a strainer clogging concern but did not provide details on acceptable methods for their evaluation.

Revision 4 of RG 1.82 was published in March 2012. This revision brings the regulatory guidance up to the current state-of-knowledge, addressing lessons learned from the on-going resolution of GSI-191 for PWRs. In particular, the guidance is greatly expanded in the areas of chemical effects, treatment of protective coatings, downstream ex-vessel effects and physical head loss testing performed to qualify suction strainers. Revision 4 does not address the acceptance criteria for downstream in-vessel debris blockage (i.e., debris that passes through the suction strainer and is entrained in the coolant water injected into the reactor core). It acknowledges that there is on-going research on this topic and that a future revision will be needed. Regulatory guidance for downstream

effects continues to evolve and remains under development.

Considering the lessons learned from the Barsebäck strainer clogging incident, the SKI decided to close the five oldest reactors which had strainers with relatively small surface area. Significant improvements were required before restart such as access to much larger sources of clean water for emergency core cooling, and installation of much larger strainers and backflush capabilities to prevent strainer clogging. Further discussion of the Swedish regulatory decisions after the incident is given in the Appendix, Chapter B.1.2.4.3.

In Germany, "The Federal Ministry for the Environment, Nature Conservation and Nuclear Safety (BMU), after consulting the Länder and, generally, with their consent, issues regulatory guidelines regarding technical and administrative questions arising from the licensing and supervisory procedure […]. These guidelines specify the administrative practice which, generally, is followed verbatim by the competent Länder authorities in the individual case." [1-4] "The RSK advises the Federal Ministry for the Environment, Nature Conservation and Nuclear Safety (BMU) on matters concerning the safety and security of nuclear facilities such as nuclear power plants or interim storage facilities for spent fuel elements. It also plays a major part in the ongoing development of safety standards for nuclear facilities." [1-5]

References [1-6], [1-7] and [1-8] provide guidance from the German regulatory authority on the issue of strainer clogging in PWRs. The RSK statements from 2004 and 2008 are basically for the verification of the proof of evidence.

Reference [1-7] gives the following assessment criteria:

"The general criterion for the safety-related assessment of the release of insulation material during a loss-of-coolant accident is the assurance of core cooling. For this purpose it has to be demonstrated for each plant that:

- The amount of the insulation material deposited inside the core remains below the amount at which core cooling is no longer guaranteed,
- Load transfer from the pressure differential due to insulation debris deposited on the suction strainers does not jeopardise structural integrity of the strainer,
- No cavitation takes place in the residual-heat removal pumps that will lead to an inadmissible reduction in flow rate. […]
- The procedure recommended here applies to PWRs. Individual aspects where plant configuration is comparable can also be applied to BWRs.
- The present findings mainly rest on experiments and do not allow a fully analytical treatment of the topic. They do show, however, that it is not possible to preclude without corresponding evidence that there may be an inadmissible pressure loss at the sump strainers or a pressure drop in the core, caused by insulation material released during a LOCA. The procedure described in the following represents the conditions to be fulfilled in future upon the provision of evidence.

The requirements listed below for the provision of evidence and the measures apply to all leak sizes requiring sump operation during the course of the accident."[1-7]

The 2008 RSK statement 1-8 deals with parameters that influence the build-up of head loss across the strainer and the requirements on measures for the removal of strainer deposits. All other aspects, in particular the requirements on coolability of the core, are not subject of this statement.

Principles

Core cooling as a protection goal (Translator's note: in the IAEA standards referred to as fundamental safety function) must be ensured at any time.

- It is to be ensured by the insulation concept, the cleanliness in the containment and the design of the sump strainers that in the first ten hours after occurrence of a loss of coolant the design limits of the sump strainers are not reached and the NPSH values required for cavitation-free operation of the emergency core cooling and residual-heat removal pumps do not fall below the specified values. The function of the components required for core cooling must not be impaired inadmissibly in the short and the long term.
- The pressure differential across the sump strainers must be monitored by means of correspondingly reliable measuring instruments.
- The limitation/reduction of high pressure differences has to be performed by measures that do not lead to an inadmissible impairment of core cooling.
- The limitation/reduction of high pressure differences by removal of deposits on the sump strainers should – under consideration of a safety margin to the design limits of the sump strainers and the required NPSH values – be performed as late as possible, i.e., at a pressure as high as possible and still admissible. This approach is aimed at the limitation of high pressure differences and, at the same time, minimisation of the transport of insulation material through the sump strainers and thus minimisation of depositions on the core.

The details of the RSK requirements can be found in Reference [1-8].

In Spain, plants from different technologies coexist and the guidelines on this topic from the countries in which the technology originated are generally accepted by the regulator (Consejo de Seguridad Nuclear, CSN). This means that the US and RSK guidelines mentioned above are both applicable to Spanish NPPs, depending on the plant type. To ensure consistency among plants and also to retain margins and conservatisms, the regulatory body can set up additional requirements to those set forth in the corresponding guidelines. The approaches and methodologies used by the utilities are evaluated by the regulator, along with implementation of plant-specific inspection programs. These tasks are publicly documented by issuing reports and other official documents.

In Japan, the Nuclear and Industrial Safety Agency (NISA) established a "NISA Guide" in 2005 which contains the evaluation criteria for BWR strainers. In February 2008, NISA revised the NISA Guide (NISA-324c-08-2) to include PWRs. NISA ordered PWR operators to submit their evaluation and countermeasures according to the NISA Guide. PWR operators designed new, larger sump screens based on tests, and NISA examined and approved the strainer design. The PWR operators were then required to install the new, larger sump strainers before the end of March 2011. The NISA Guide also provides some important points for operators on the methods of evaluation to use for chemical effects. The NISA Guide does not provide specific requirements for downstream effects; the Japan Nuclear Energy Safety (JNES) organization is conducting additional tests on downstream effects and will consider revising the NISA Guide as appropriate based on new knowledge and experience gained. More detailed information on the NISA Guide can be found on the Japanese regulator's web-site [1-9].

For the Canadian designed CANDU reactor, a LOCA involves the leakage of primary coolant (D_2O) from the main Heat Transport System. This immediately triggers a shut-down of the reactor, but coolant flow through the reactor must be maintained by the ECC for at least 90 days to remove decay heat. For CANDU 6 stations, the ECC system has three main stages. First, high pressure injection of water into the reactor building is triggered by the LOCA. This is followed by medium-pressure injection, from water in the dousing tank located at a high elevation in the reactor building. Finally, during the low-pressure stage, the water in the reactor building sump is pumped through the core to cool the reactor. The mission period for this stage is typically 90 days.

The Canadian nuclear industry has made significant advancements in its ECC strainer knowledge base over the past decade. All the licensees have implemented design changes in their ECC systems and in other relevant areas, such as impeding debris transportation by water flow. The regulator has accepted the solutions presented by the licensees on the basis of the low probability of the accident event, the constraints on the strainer area that could be installed as a back-fit, the risk reduction due to the timely implementation of the design change, the conservatism applied to the test results, the

defence-in-depth principle of CANDU stations, and the station-specific testing performed [1-10].

In Korea, KINS (Korea Institute of Nuclear Safety) issued the regulatory rule for the ECCS, contained in the "Regulation of Technical Standards of Siting and Equipment of Nuclear Power Plants", at the 10th Nuclear Safety Information Conference, Daejeon, Korea, April 2005. This rule requires the application of new technical standards to be used in the licensing review of new plants and in the periodic safety review of existing plants. The KINS position on the sump clogging issue is addressed in "Technical Guide on Water Sources for Long Term Recirculation following a Loss-of-Coolant-Accident" [1-11], issued in April, 2007 as document number KINS/GT-N016. The contents of the guide are similar to US NRC RG 1.82, Rev.3.

In Korea three types of PWR are operating and/or are under construction: (1) Westinghouse (WH) plants and Combustion Engineering (CE) plants, (2) CANDU plants, and (3) APR1400 plants.

(1) WH plants and CE plants: ECCS and CSS take suction from the containment sump during the recirculation phase. The pH of the collected water at the containment floor is initially low due to the boric acid in the Reactor Coolant System and the tanks for safety injection and then increases to a value greater than 7 due to spray additives such as NaOH or TSP as buffering agents.
(2) CANDU plants: Only ECCS takes suction from the containment sump during the low pressure injection stage. The pH of the water discharged from the break and collected at the containment floor is initially near 7.0 and then increases to 10 due to the presence of TSP canisters located at the containment floor.
(3) APR1400 plants: ECCS and CSS always take suction from the IRWST (In-containment Refueling Water Storage Tank) without recirculation. Initially the borated water is stored in the IRWST with a low value of pH. Since the IRWST is located at the lowest elevation and inside the containment, water from the break is collected in the IRWST through the Holdup Volume Tank having a TSP basket. Thus the pH of the IRWST water will eventually reach a value higher than 7.0

In France, leak before break or break preclusion are not applied to the design of Generation II reactors. The design of the sump filters is based on agreement with RG 1.82. The break preclusion concept is applied for Generation III reactors, in particular the EPR, in agreement with the Technical Guidelines recommended by the French Standing Group.

In 2003, using the results of a research program carried out by IRSN, the French Permanent Group recommended a global reassessment of the sump plugging issue. At the end of 2004, the French Permanent Group performed a review on the utility guidelines for reassessment of the sumps and requested investigations on the chemical effects in all the situations which require the recirculation mode. In April 2005, the French ASN (Nuclear Safety Authority) endorsed the advisory committee conclusions. The utility reply to the ASN request was mainly to increase filtering area and to carry out additional investigations on chemical effects. This topic is still under discussion.

As evident from the above discussion, regulations vary by country. An investigator should contact the utility or safety authority in the country of interest to determine availability of existing information.

The International Atomic Energy Agency (IAEA) Safety Guides [1-12] present international good practices and increasingly reflect best practices to help users striving to achieve high levels of safety. IAEA Safety Guide NS-G-1.9 "Design of the Reactor Coolant System and Associated Systems in Nuclear Power Plants" issued in 2004 addresses design considerations for the ECCS in sections 4.68 through 4.91. There are many similar elements between this IAEA safety guide and US NRC RG 1.82.

Some suction strainer designs provide for a backflush capability or have an active device for cleaning debris off of the strainer surface; a more detailed discussion can be found in Chapter 6.2.

Where this capability is provided, it should be able to prevent the accumulation and entry into the system of debris that may block restrictions found in the systems served by the ECCS pumps. The operation of the active component or backflush system should not adversely affect the operation of other ECCS components or systems. Under some operational modes, an active system may allow more debris to pass through the strainer. If this is the case, then the downstream effects analysis should be performed accordingly. Performance characteristics of an active system should be supported by appropriate test data that address head loss performance. Active systems should meet the requirements for redundancy for active components.

Figure 1-1 presents the overall elements that need to be considered in designing a suction strainer. These elements are discussed in more detail in the chapters that follow.
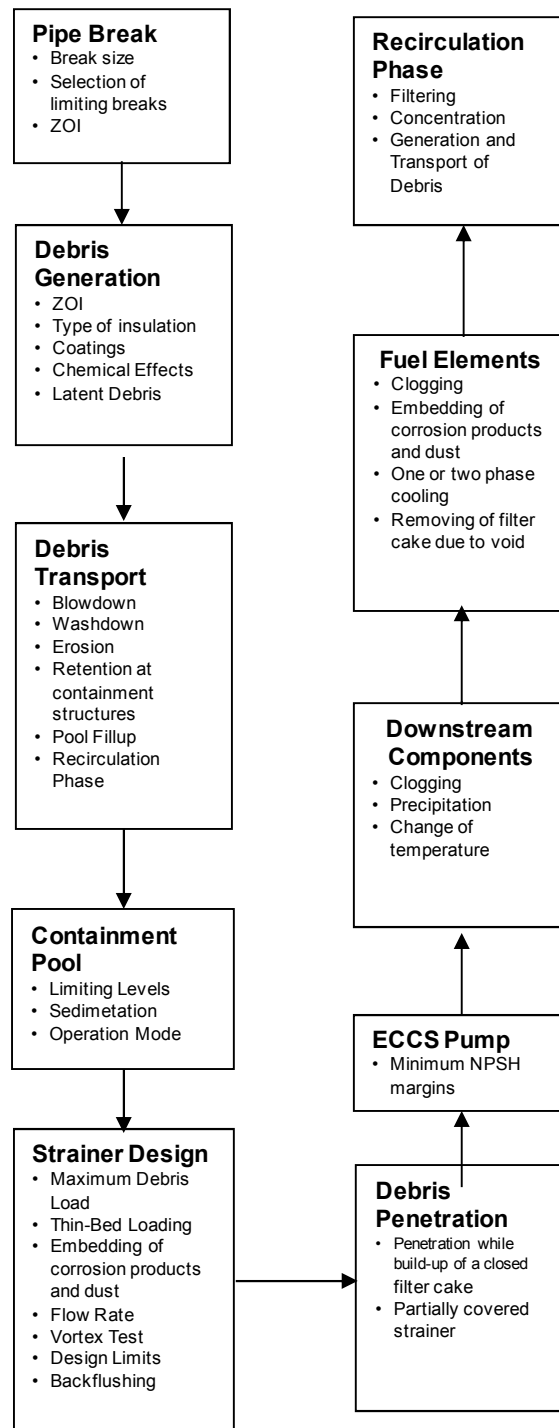
Figure 1-1: Elements of Suction Strainer Qualification

1.5   Report Structure

The report is structured as follows. Chapters 2-5 discuss debris generation and transport, including chemical effects. Chapter 6 covers strainer pressure drop, and Chapter 7 discusses downstream effects, i.e., the effect of debris flowing through or not captured by the strainers. Chapter 8 discusses risk assessment, and Chapter 9 presents conclusions and recommendations. The five appendices provide supplemental information on the terminology used in discussions of sump clogging, the historical background, relevant debris characteristics, the use of Computational Fluid Dynamics (CFD) codes for debris-related calculations, and an extensive summary of relevant

experiments and test facilities.

1.6   Advanced Light Water Reactors

The methodology used and regulatory expectations for advanced reactors (e.g., AP1000, APR1400, European Pressurized Reactor (EPR), Advanced Boiling Water Reactor (ABWR)) to evaluate ECCS suction strainer clogging are similar to what has been done for operating PWRs to address GSI-191. ECCS strainer head loss testing using plant-specific debris loads and flow rates is expected to be required by the regulatory authorities. The debris types to be evaluated include fibrous insulation, particulate, coatings, latent debris and chemical precipitates. No detailed discussion on advanced reactors is given in this report as work is on-going.

References

1-1   CSNI report NEA/CSNI/R(95)11 "Knowledge Base for Emergency Core Cooling System Recirculation Reliability".

1-2   Title 10 of the U.S. Code of Federal Regulations (CFR), Part 50 (10CFR Part50) 'Energy '.

1-3   US NRC Regulatory Guide 1.82 "Water Sources for Long-Term Recirculation Cooling Following a Loss-of-Coolant Accident".

1-4   BFS, Nuclear Safety in Germany, "Report under the Convention on Nuclear Safety by the Government of the Federal Republic of Germany for the First Review Meeting in April 1999", September 1998, http://www.bfs.de/www/kerntechnik/CNS_99_E.pdf.

1-5   BMU Homepage, March 26, 2012, http://www.bmu.de/english/the_ministry/tasks/independent_advisory_bodies/doc/3103.php.

1-6   RSK Statement, "Wirksamkeit der Notkühlsysteme bei Freisetzung von Isoliermaterial bei Kühlmittelverluststörfällen", RSK, 16.09.1998.

1-7   RSK 374, RSK Statement, "Requirements for the Demonstration of Effective Emergency Core Cooling during Loss-of-coolant Accidents involving the Release of Insulation Material and other Substances", RSK, 22. July 2004 (374th meeting), http://www.rskonline.de/English/downloads/stnsumpfengl.pdf.

1-8   RSK 406, "RSK Statement, Loss-of-coolant Accidents involving the Release of Insulation Material and other Substances in Pressurised Water Reactors - Removal of Deposits on Sump Strainers", RSK, 13.03.2008 (406th meeting), http://www.rskonline.de/English/downloads/sumpfsieberskstellungnahmee.pdf.

1-9   www.meti.go.jp/policy/tsutatsutou/tuuti1/aa508.pdf [in Japanese].

1-10   C. Harwood, Vinh Q. Tang , J. Khosla, D. Rhodes, A. Eyvindson, "Uncertainties in the ECC Strainer Knowledge Base – The Canadian Regulatory Perspective", NEA workshop proceedings, Debris Impact on Emergency Coolant Recirculation, p. 149, Albuquerque (NM),   2004 February 25-27.

1-11   Korea Institute of Nuclear Safety, "Technical Guide on Water Sources for Long Term Recirculation following a Loss-of-Coolant-Accident", KINS/GT-N016, KINS, April 2007.

1-12   IAEA Safety Guide NS-G-1.9 "Design of the Reactor Coolant System and Associated Systems in Nuclear Power Plants", September 2004.

1-13 NUREG/CR-6808 "Knowledge Base for the Effect of Debris on Pressurized Water Emergency Core Cooling Sump Performance", February 2003, US NRC.

1-14   Available at http://www.oecd-nea.org/download/sumpclog/info.html.

2. DEBRIS SOURCES AND GENERATION

In the event of a failure of the reactor pressure boundary inside the containment building of a NPP, insulation materials, coatings, and other materials present can suffer severe destruction, dislodgement and transport throughout containment. The initial blast waves exiting a break, followed by the ensuing break jet expansion, are the dominant contributors to debris generation in the event of a LOCA. Thus, both break jet forces and materials characteristics and location relative to the break location must be taken into account.

Estimating the quantity and type of debris, and identification of other debris sources which the LOCA can further destroy and transport to the ECCS, will affect the course of events that determine ECCS strainer reliability. A universal description of LOCA event progression and corresponding debris generation is not possible due to the variability of plant designs, potential break locations and the wide range of insulation materials and other materials present (see Table 1-1 for a typical PWR LOCA sequence). However, the existing information and understanding of break blast and jet phenomena can be combined with evidence of damage to targeted materials to estimate, perhaps with large uncertainties, the amount of debris generated.

This chapter is organized as follows:

Section 2.1: A brief description of break blast and jet phenomena and insights gained from large-scale experiments;

Section 2.2: A description of debris sources;

Section 2.3: A description of available small-scale experiments (key experiments are summarized in Appendix D);

Section 2.4: A discussion of models currently employed for estimating debris generation;

Section 2.5: A summary of the current knowledge base for estimating LOCA-generated debris.

2.1 Break Blast and Jet Phenomena

Debris generation first occurs due to the initial shock wave that emerges from the pipe rupture, and, after the onset of blowdown, due to erosion caused by jet impingement. Different insulation materials may display different degrees of sensitivity to each of these two phases of the accident. There are also important differences between steam and liquid break flows. The load from steam jets is, in general, larger than the load from flashing liquid for equal break areas. Steam jet loads are also more concentrated about the centreline than those of flashing jets. Break blast and jet phenomena can, therefore, not be treated in a generic way. The nature of a break depends on the system fluid conditions upstream of the break. The system pressure is also important in determining the amount of debris generated.

Jet impingement and break blast have been studied in large-scale experiments such as those performed at Marviken in Sweden, the Heissdampfreaktor (HDR) in Germany, the Siemens-KWU facility in Karlstein, Germany, Ontario Power Generation (OPG) in Canada, and the Colorado Engineering Experiment Station, Inc. (CESSI) facility in Colorado, USA. The Finnish PAROC tests are not included as the results are not publicly available. Although considerable information for

predicting discharging jets is available, the knowledge base for estimating quantities and debris characteristics of impacted targets is very limited. In addition, the ability to predict expanding jet characteristics derived from particular experiments should not be considered equivalent to being able to calculate the quantities and composition of the debris that would be generated by a break.

2.1.1 The HDR Experiments

The HDR reactor was used for safety experiments in the late 1970s and the 1980s [2-1], [2-2]. Typical initial conditions for blowdown were 11 MPa (110 bar) and 310 °C, and the break diameter was 0.45 m. Early blowdown tests conducted in the HDR ([2-2] Appendix C) showed that there were high dynamic loads in the immediate vicinity of the break. Inspections following those blowdown tests revealed spalled concrete (attributed to thermal shock), blown-open and damaged hatchways (in some compartments, doors were torn from their frames), bent metal railings, damaged protective (or painted) coatings, peeled and heavily damaged thermal insulation on piping, and insulation debris scattered throughout the containment building. The damage to, and the scattering of, glass wool insulation was particularly severe. The original insulation was badly damaged in the first experiments and other insulation types were applied to limit the damage. Conventional fibrous insulation (mineral wool reinforced with wire mesh and jacketed with galvanized carbon steel sheet) was blown away as soon as the cover was damaged. Material located within a radius of 3 to 5 m from the break nozzle was dislodged. Foam glass insulation was resistant against pressure from the outside, but was destroyed when the pressure wave loading penetrated beneath the surface and lifted off the protective sheaths.

Later HDR experiments included installed NUKON™ insulation assemblies ([2-1] Appendix F) and reflective metallic insulation (RMI) assemblies ([2-1] Appendix E). Derivation of debris generation models from these experiments was complicated by the fact that the break jet first hit a force plate and then expanded to the installed insulation specimens. Thus break-to-target separation insights (L/D comparisons) were difficult to model.

The tests ([2-2] and [2-1] Appendix F) demonstrated that unjacketed NUKON blankets, or NUKON blankets covered with metal mesh located within nine pipe diameters of the simulated pipe break, could be totally destroyed, although the extent of damage depended on the orientation (i.e., over 90 % of the wool insulation was reduced to fine fibers). However, NUKON blankets enclosed in the standard NUKON 22-gauge stainless steel jackets withstood the blast to such an extent that less than 50 % of the metal-jacketed wool insulation was reduced to fine fibers (for pipe insulation within seven pipe diameters from the simulated pipe break).

RMI panels were also tested (Appendix E in [2-1]); one of the two panels located at about 2.2 L/D from the break broke apart completely and the other was badly deformed. The next nearest panels were located at about 7 L/D; none of these suffered significant damage. No large, flat pieces of foil were released in these tests. Photographs taken after the experiments show a few crumpled but not very balled-up pieces of various sizes. Neither the size distribution nor mass balance of the destroyed panel could be established, which hints at the possibility of generating some non-negligible quantity of fairly small inner foil pieces.

Damage to insulation generally occurred up to distances of about 2 m (L/D=4), with the exception of conventional insulation, which was destroyed at greater distances. Moreover, the degree of damage depended on geometry, e.g., due to shielding effects. According to the investigators, the damage seemed to be caused mainly by the dynamic pressure wave which occurs at rupture and the forces exerted by the outflowing jet.

2.1.2 The Marviken Experiments

The reactor vessel was about 24 m high and about 420 m³ in volume. Typical initial conditions were 5 MPa, subcooled or at saturation. Both steam and water blowdowns were performed. The containment was essentially a pressure suppression system of Mark II design. The containment had a

relatively complex compartment structure.

Two series of experiments were of relevance for debris generation. The first series of containment response tests in Marviken [2-3] was performed to study containment response to a break in the feedwater line or in the steam line. In a later experiment series [2-4], load distributions from jets were investigated.

2.1.2.1 Containment Response Tests [2-3]

These were the first blowdown tests, and the original vessel and piping insulation, rockwool and calcium silicate, had been retained. The insulation was supported by a sheath of steel or aluminum. The qualitative judgment after the second test, which was a simulated steamline break with an initial flow rate of about 170 kg/s, was that the damage in the upper part of containment was large. Although not directly hit by the jet, the insulation of the vessel cupola, which initially was covered by a steel sheet, was blown away. Heavy equipment (cable terminal cabinet) was moved and destroyed, and five containment spray pipes were torn off. Sheets of aluminum, which initially covered the pipe insulation, were found a long distance from the break locations. Large amounts of insulation debris were found in the wetwell pool, on the floor of the lower containment where it was caught by the strainer over the drain pipe, and stuck to the walls and floors. No clogging of the strainer for the recirculation line was reported.

As a result of this experience, a total of 16 test pieces of heat insulation, prepared in accordance with 8 different specifications, were installed along the wall and near the exit of the compartment in which the feedwater breaks were performed. All were located significantly more than 7 diameters from the break. The test pieces were exposed during blowdown runs Nos. 4 through 16.

The overall impression was that the jet impingement force from the rupture was the major destructive factor for the types of heat insulation tested. The test pieces were all exposed to forces representative of deflected jets. Test pieces shielded from the break location by concrete structures were not destroyed. The surrounding metallic supports of some of the test pieces were blown away or otherwise destroyed. Examples were found of insulation melting, compaction, and dislodging.

2.1.2.2 Marviken Jet Impingement Testing [2-4]

A vertical discharge pipe had been installed in the vessel. Nozzles with diameters ranging from 300 mm to 500 mm were attached to the discharge pipe. Loads were measured in a free expanding jet and also at a flat circular plate with a diameter of 3 m. The evaluated thrust coefficients showed values that were close to the theoretical ones. For non-flashing water, the measured thrust coefficient was close to 2. Steam experiments showed values close to 1.3. Stable flashing jets showed values less than 1.3. One important conclusion was that flashing jets had a much larger cross-sectional area than steam jets. An example of this is shown in Figure 2-1. The thrust coefficient was about 2.0 during the initial impact of cold water, decreased to 0.5 during subcooled flashing flow, was about 0.7 for upstream saturated conditions, and increased to about 1.3 during steam flow. This occurred because only a portion of the flashing jet was intercepted by the 3-m-diameter impingement plate.

In pressurized systems discharging saturated or subcooled water, the blowdown will be terminated by a steam blow, when the break location is uncovered. Depending on the system pressure, the steam jet near the end of a blowdown could give rise to significant impingement forces and additional debris generation.

Another important result is that a flashing jet significantly overexpands and causes pressures lower than ambient near the center. This caused the target to lift a few pipe diameters away from the break location.

The free jet data from Marviken were used to develop and assess calculation tools for estimating two-phase jet loads [2-5].

Thrust Coefficient, defined as

$$\frac{\left(\dfrac{F^{total}}{A^{nozzle}}\right)}{\left(pstag - pcontain\right)}$$
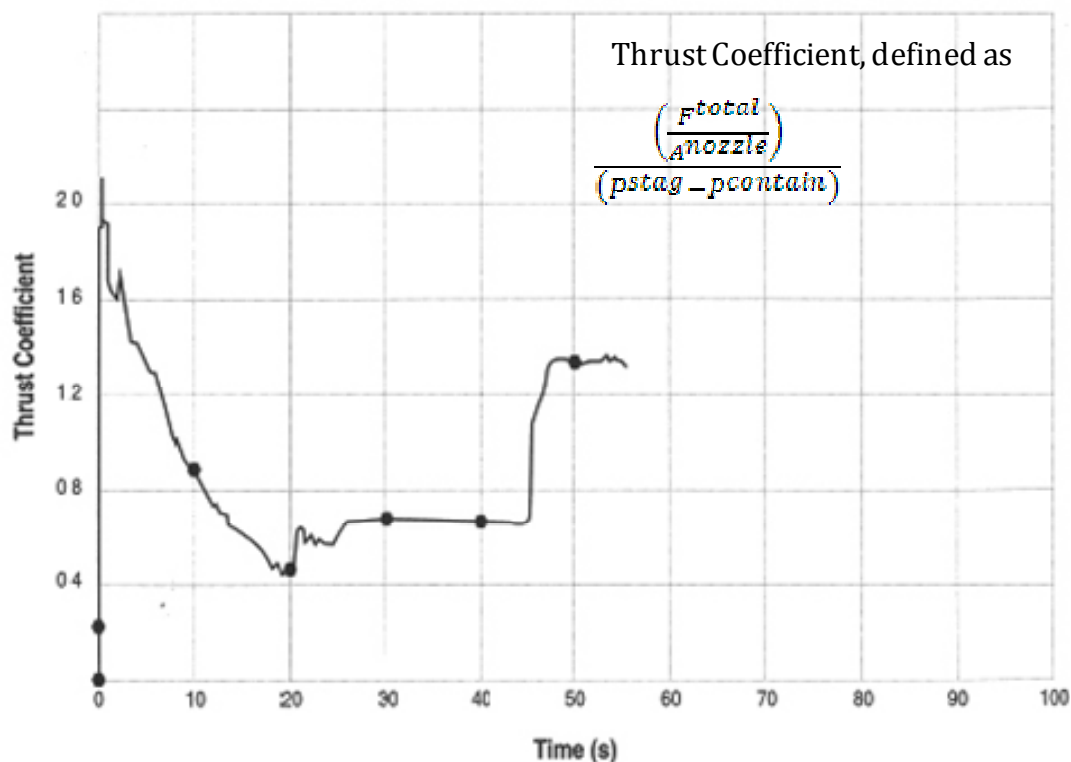
Figure 2-1: Thrust Coefficient Plot from [2-4], Test 8.

2.1.3 The Swedish Metallic Insulation Jet Impact Test (MIJIT) [2-6]

2.1.3.1 Reflective Metallic Insulation Testing

In late 1994 and in 1995, a group of Swedish utilities contracted for large-scale jet impingement tests at the Siemens-KWU facility in Karlstein, Germany. The objective of these tests was to investigate the behavior of metallic insulation under realistic conditions.

The tests were performed with both water and saturated steam. The facility consisted of a tall vessel and a blowdown line. The break was simulated by double rupture disc. The tests were typically performed from 80-bar pressure with nozzle diameters of 200 mm. One of the conclusions in the report is that saturated water jets are much less destructive than steam jets. Target materials hit by the steam jet core could be destroyed within a range up to 25 L/D.

Most of the tests were performed so that the discharging jet hit the target from the side. There were also a limited number of tests performed with saturated water which simulated a double-ended guillotine break (DEGB) so that the insulation was broken up from the inside.

The following conclusions were made:

- All insulation directly hit by a steam jet will be more or less fragmented. The tested distances (up to 25 L/D) envelope typical dimensions of reactor containments;

- Insulation outside the core of a steam jet will not be fragmented;

- Saturated water jets are much less destructive than steam jets;

- Steam breaks should also be taken into account for PWR systems since a blowdown will always be terminated by a steam jet when the break location is uncovered.

Typical debris from the testing by Vattenfall [2-6] is shown in Figures 2-2 and 2-3. A calculation methodology that can predict the type of damage observed is not available.

2.1.3.2   Fibrous Insulation Testing

Full scale hydraulic testing of debris disintegration, settlement and build-up on strainers during post-LOCA water flow under PWR conditions was performed as well as measurements on pressure drop from recirculating flow having fibers and fines in the water. The debris bed build-up on a small scale one-dimensional filter plate and on a vertical cylindrical half-scale strainer of Ringhals 1 type showed that the head loss was as high as in earlier tests for Ringhals 1 with steam-fragmented fiberglass insulation. This test was performed by Vattenfall Utveckling AB at Alvkarleby Laboratory as part of the qualification program for the new strainers at Ringhals 2 [2-37].

Possible combination effects of oil and fiber in the water and effects of fiber and carbon powder in the recirculation water were studied in the small one-dimensional test rig. No extra pressure drop was found for the small but typical concentrations tested.

CFD calculations of the flow pattern in the bottom region of containment were performed and revealed that quite high velocities could be present in areas close to the existing strainers.

2.1.4   NRC-Funded Test at the Siemens Facility at Karlstein [2-7]

The same facility as described above was used to simulate a DEGB of a steam line [2-7]. A typical RMI cassette of American design was placed around the break location. The initial pressure was 80 bar and the blowdown lasted for about 11 seconds. This test was designed to investigate the destructive nature of a circumferential weld break in a steam line located beneath an RMI assembly. Severe damage and fragmentation of the RMI inner foils were also observed in this test. Figures 2-4 and 2-5 illustrate the damage to the inner and outer skin and the shrapnel-type debris generated. Models do not exist that can predict destruction characteristics or estimate quantities of this type of debris. RMI debris fragments from this blast test were used to investigate suspension characteristics of such materials and the findings are discussed in Section 2.3. In addition, this debris was used for further investigations of strainer clogging at Alden Research Laboratory (ARL) [2-36] and by the U.S. BWR Owners Group (BWROG) in the mid-1990s.
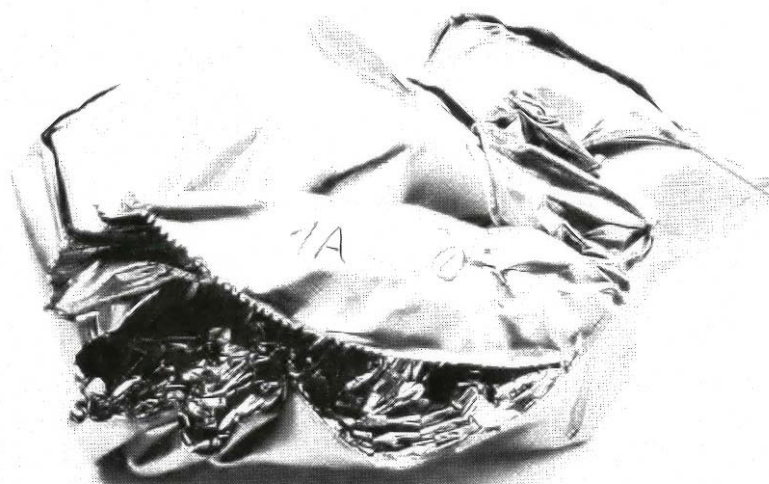
GRÜNZWEIG + HARTMANN - TARGET NO. 1

PANEL NO. 1A

AFTER THE TEST
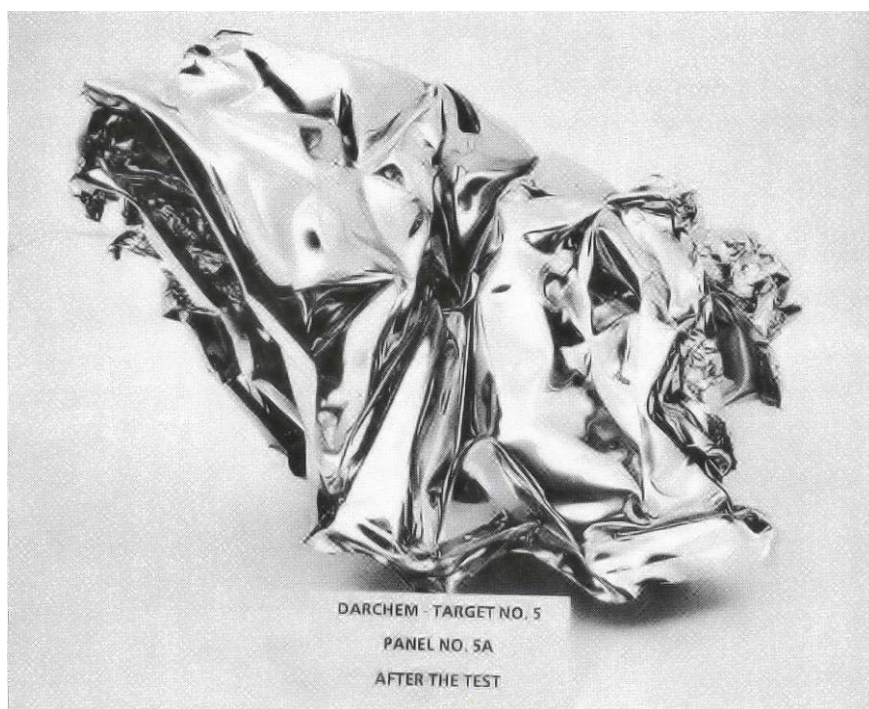
DARCHEM - TARGET NO. 5

PANEL NO. 5A

AFTER THE TEST

Figure 2-2: Saturated Water Jet Debris
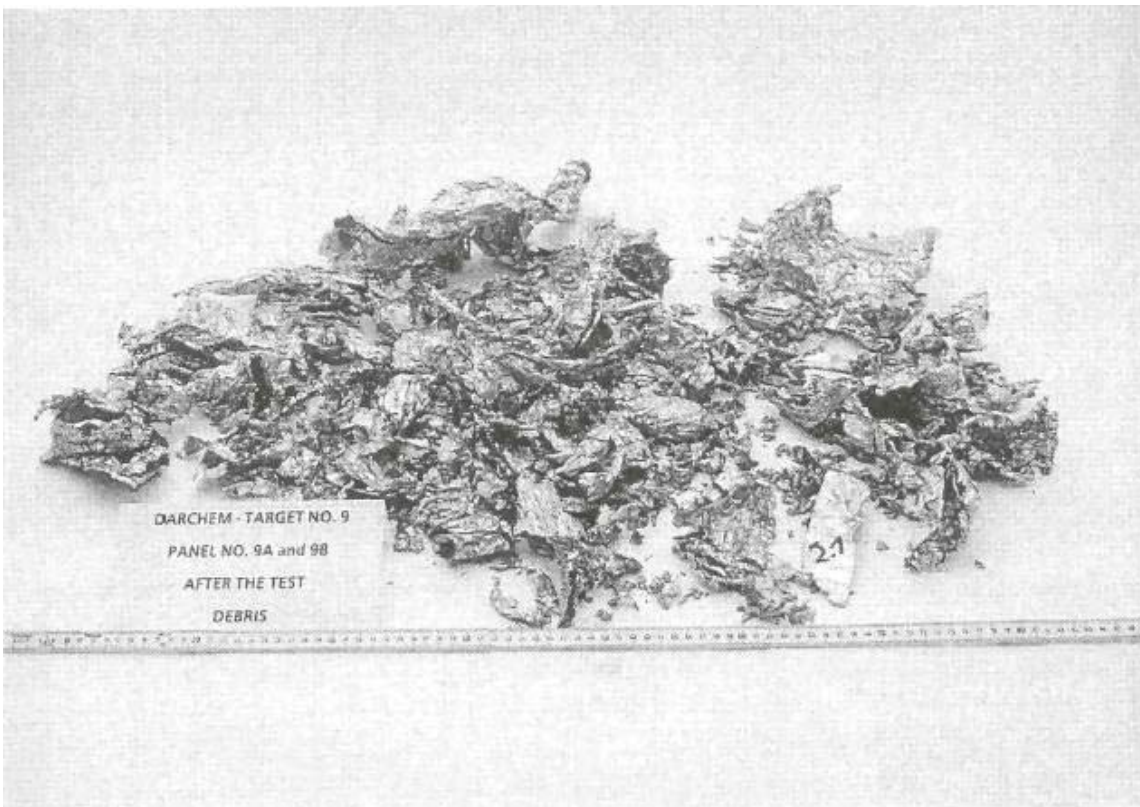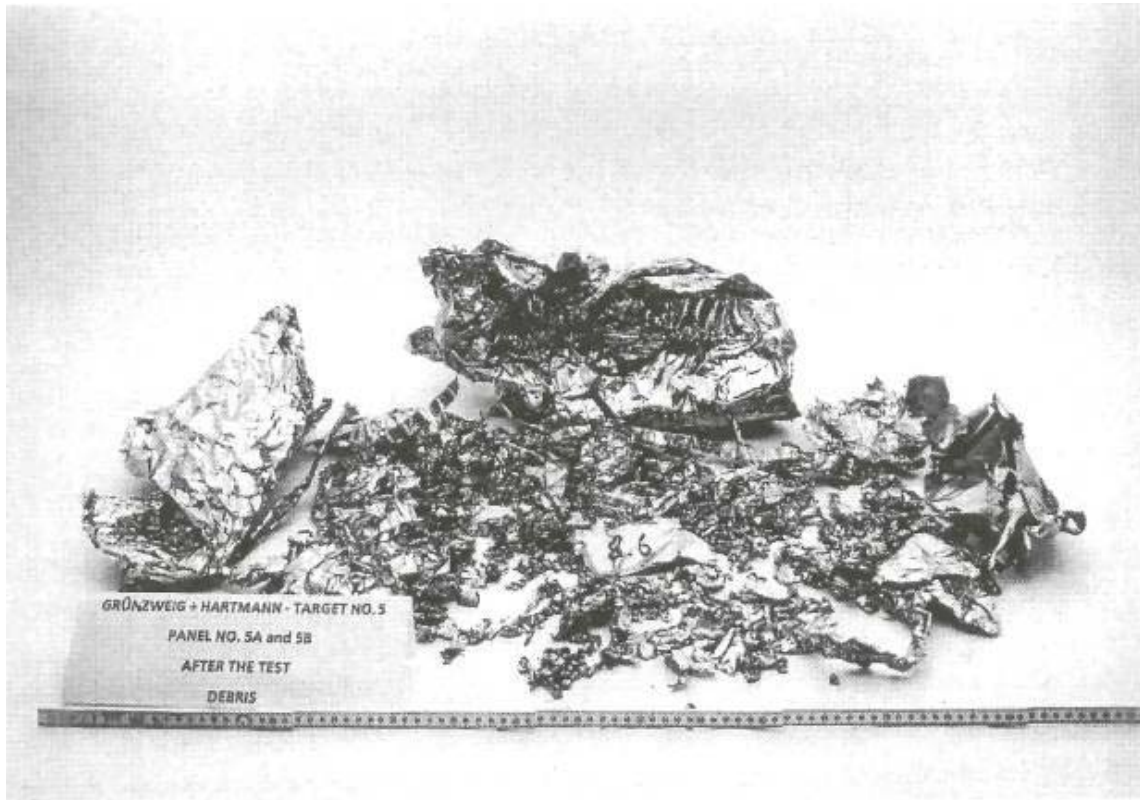
Figure 2-3: Saturated Steam Jet Debris
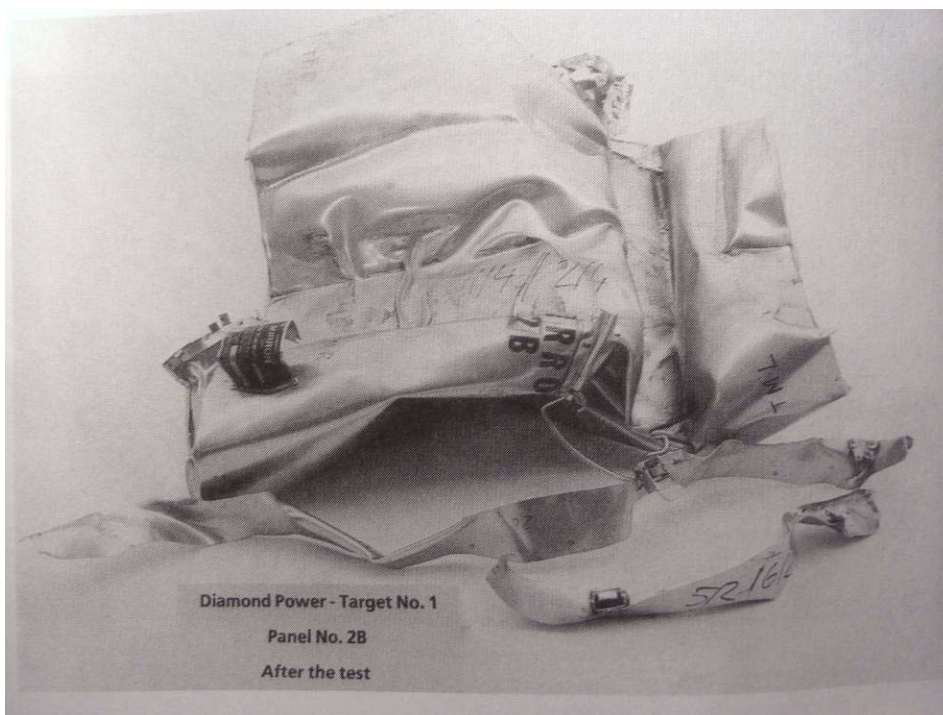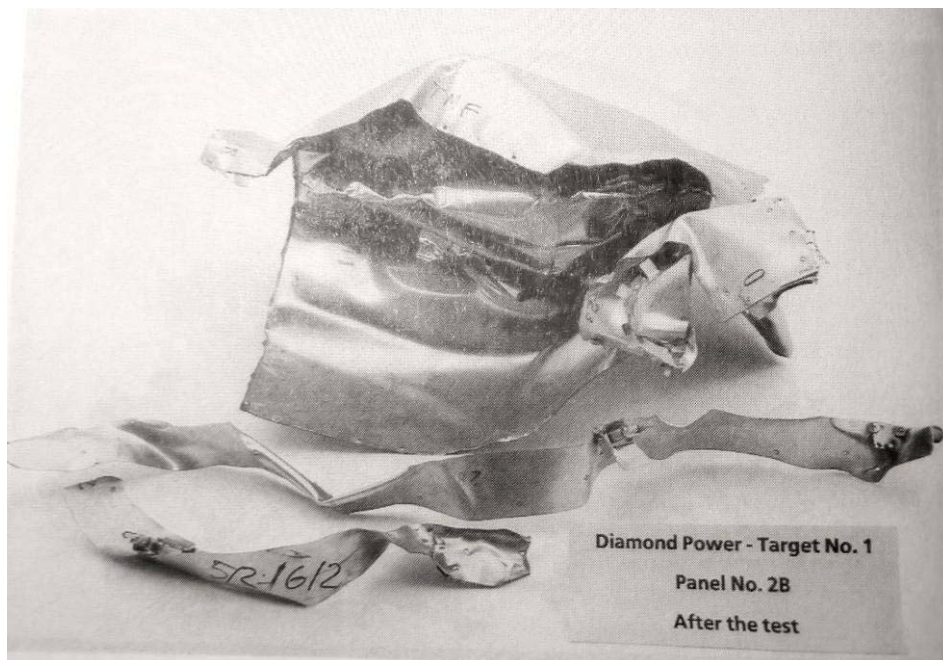
Figure 2-4: RMI Outer Panels after Steam Blast Test
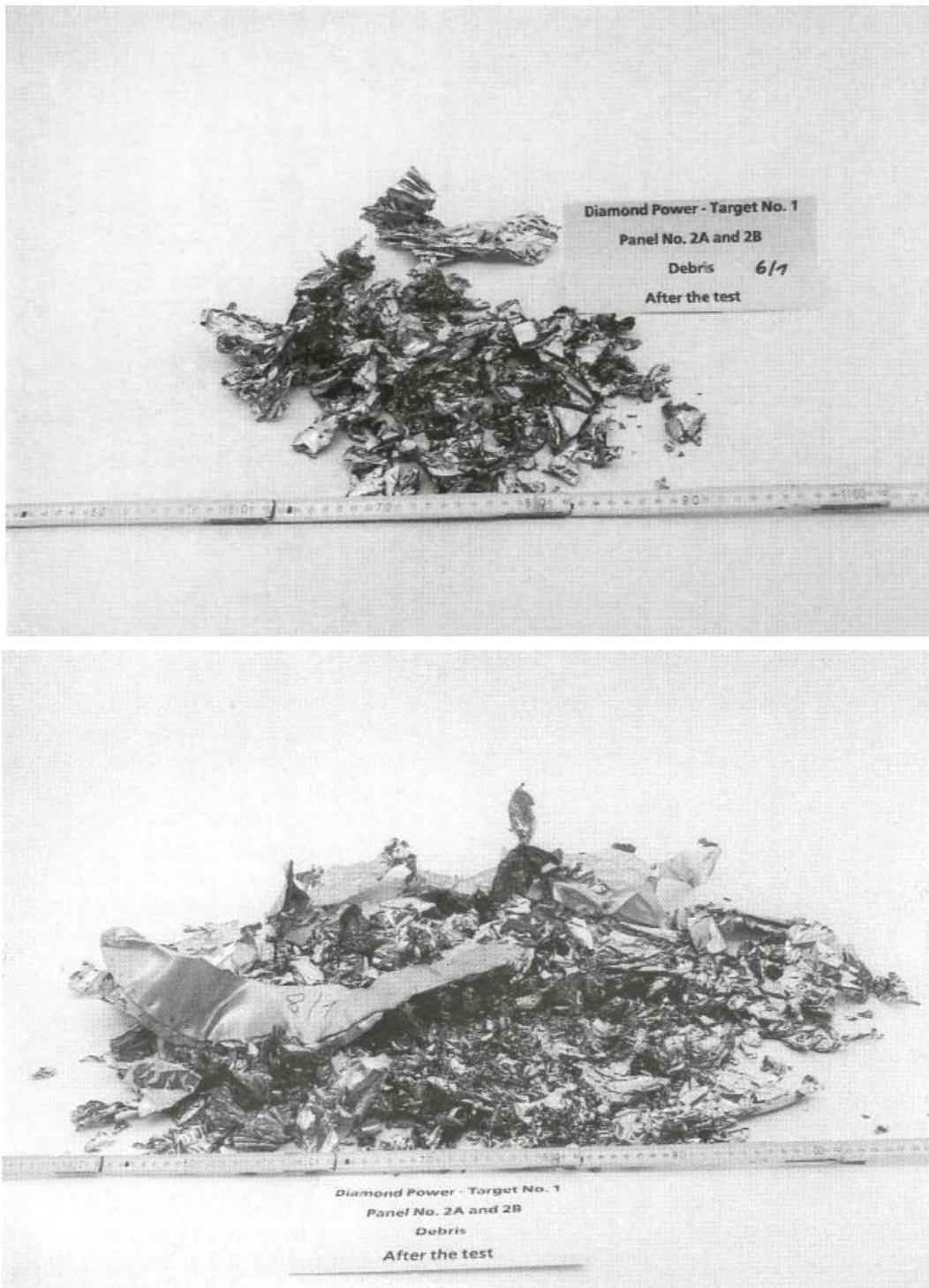
Figure 2-5: RMI Foil Debris after Steam Blast Test

2.1.5 *Fragmentation Experiments at Karlstein*

Fragmentation experiments were performed by Framatome-ANP at the large scale test facility in

Karlstein (Figure 2-7). It was the goal to fragment encapsulated insulation material as realistically as possible and to generate fragmented material for strainer testing. Determination of the fiber spectrum was not a focus of the experiment. Therefore the cassettes were hit by a hot water jet under simulated PWR conditions. The blow-out of fine fibers was accepted as a behavior similar to the transport by steam within the containment to more distant parts and therefore no transport to the sump.

The test facility consisted of a pressure tank of volume 125 m³. The operational pressure was 110 bar and the temperature was 310 °C. Between the pressure tank and the blow-out tank a DN 250 pipe was installed. The opening of the pipe was directly in front of the cassettes with insulation material. The blow-out time was between 4.6 and 8.7 s. Due to the evaporation of about 40 % of the water it was not possible to observe the destruction of the cassettes themselves. After cooling down, the water was drained and the fibrous material collected by means of a hole plate. The collected insulation material was dried afterwards.

Experiments were performed for used mineral wool of type Isover MD2 produced between 1980 - 1982 from NPP Krümmel, and mineral wool of type Rockwool RTD2 produced in 1983 from NPP Gundremmingen. Due to its use in plants the insulation material was no longer hydrophobic.

Figure 2-6: Photograph of the Large Scale Test Facility in Karlstein used for the Fragmentation Experiments performed by Framatome-ANP.

Figure 2-7 shows the collection chamber from outside. 7 out of 8 vertical wall segments are made of wire mesh of 2 by 2 mm mesh width. One vertical segment and the cover on top of the collection chamber are made of perforated plates with a hole diameter of 2 mm and a 3.5 mm pitch.

Figure 2-7: Outside View of the Collection Chamber.

The mineral wool was encapsulated by half-shell cassettes produced by G+H Montage and by Kaefer. The photo shows two cassettes positioned edge to edge in front of the blow-out line. Tests were performed with cassettes positioned that way or with one cassette face-to–face to the blow-out opening.

2.1.5.1   Results

Table 2-1 gives a short overview of the experimental results. More detailed information is given in report [2-43].

The fragmented material was evenly distributed in terms of fiber length. No significant differences were found for different places of deposition of the fragmented material. Rockwool RTD2 was more finely fragmented compared to Isover MD2.

Cassettes within zone 1 according to the NUREG cone model were not destroyed by the jet hitting from outside. Only in the case where the face-to-face edge of the cassettes was in front of the jet were the cassettes partially destroyed.

In case of tearing off cassettes from the pipe a remarkable amount of insulation material remained within the cassettes due to the retention at the inner wire mesh.

It is supposed, that especially finer fibers were taken out from the collection chamber together with the steam. Within the containment of a NPP more fine fibers ought to be transported by steam far away from the leak position due to the missing retention like at the collection chamber. These fine fibers don't reach the sump area and the material at the strainers will be a mixture of longer and less fine fibers in a real sump.

Table 2-1: Summary of the Results of the Fragmentation Experiments at Karlstein

Test	Cassette Type	Position	Mineral Wool	Mass within the Cassette		Collected Amount of Released Material [%]
				Before test [kg]	After release [kg]	
1	G+H	Vertical centered Gap-to-Jet	MD2	23.5	0.0	45
	G+H	Vertical centered Gap-to-Jet		23.5	0.0	
2	G+H	Upper Gap-to-Jet	MD2	24.1	0.0	39
	G+H	Upper Gap-to-Jet		23.1	0.0	
	G+H	Lower backside		22.6	22.6	
	G+H	Lower Face-to-Jet		23.2	23.2	
3	Kaefer	Upper Gap-to-Jet	MD2	23.5	16.7	67
	Kaefer	Upper Gap-to-Jet		21.0	0.0	
	Kaefer	Lower Gap-to-Jet		20.5	0.0	
	Kaefer	Lower Gap-to-Jet		19.0	8.2	
4	Kaefer	Upper Gap-to-Jet	MD2	22.5	0.0	82
	Kaefer	Upper Gap-to-Jet		22.5	0.0	
	G+H	Lower Gap-to-Jet		23.5	13.6	
	G+H	Lower Gap-to-Jet		23.4	0.0	
	Kaefer	At the floor, not fixed and with the inner side to the jet		21.0	21.0	
	G+H	At the floor, not fixed and with the inner side to the jet		22.6	0.0	
5	Kaefer	Vertical centered Gap-to-Jet	RTD2	21.0	0.0	25
	Kaefer	Vertical centered Gap-to-Jet		16.0	16.0	

2.1.6 Colorado Engineering Experiment Station Inc. (CEESI) Air Jet Testing

BWROG Air-Jet Testing

The BWROG debris generation testing was conducted at CEESI, where a high-pressure jet of air was focused on an insulation target [2-8]. Air pressurized to 1110 psig in a large tank was piped to a nominal 76 mm- (3-inch) diameter test nozzle through a control valve assembly. When the control valves were opened, air pressure built up behind a single rupture disk designed to burst at a pressure of 1000 psig. Targets of various insulation types and jacketing were placed at various distances from the jet with the objective of determining the minimum threshold pressures for generating insulation debris. The BWROG placed a differential pressure transducer in a target-mounting pipe to measure the actual jet pressure at specific distances from the jet nozzle to benchmark a CFD model used to define jet stagnation pressures at any targeted distance so that target damage could be correlated with the jet stagnation pressure. A 20 L/D pressure measurement confirmed the results of the CFD predictions inside 20 L/D and other, more distant measurements were used to interpolate pressures between 20 and 117 L/D.

NRC-Sponsored Air Jet Testing

The NRC-sponsored air jet testing for the Drywell Debris Transport Study (DDTS) [2-9] was conducted at CEESI using the same basic equipment as in the BWROG testing. Initial testing used a nominal 76 mm (3-in.) jet nozzle, but after an initial exploratory testing phase, the 76 mm nozzle was replaced with a 102 mm (4-in.) nozzle to enhance the destruction of the insulation blankets. The objective of these tests was to study the transport behavior of Low Density Fiberglass (LDFG) debris as the debris passed through or impacted a prototypical representation of BWR drywell congestion of structural obstacles such as gratings. An array of pitot tubes was used to measure the downstream flow velocities in an axial and radial configuration for comparison with a CFD flow simulation used to estimate stagnation pressures. The targets were LDFG blankets mounted on a test pipe and generally placed to maximize blanket destruction, thereby generating the greatest potential density of debris transiting the chamber test obstructions. At 30 L/D the fraction of debris small enough to pass through the test gratings was typically greater than 90% of the original insulation material. At 10 L/D and 20 L/D, the target was too close to the jet to be completely engulfed by it so that substantial insulation at the target ends became debris too large to pass through the first grating. A video camera focused directly on the test target showed that destruction was essentially instantaneous. The destruction appeared to be immediate in nature rather than due to erosion processes.

2.1.7 OPG Debris Generation Testing

Ontario Power Generation conducted debris generation testing in 2001 to support its programs. A test report for aluminum-clad calcium silicate insulation [2-10] was made available for review. A dual rupture disk assembly attached to a 73 mm- (2.87-in.) diameter test nozzle was used to release water pressurized to 10 MPa (1450 psia) and heated to saturation. Piping heaters were installed to maintain the initial test conditions within the piping before initiating the test. Because OPG did not measure test pressures downstream of the jet nozzle, NRC staff calculated the pressures associated with insulation destruction by using the jet model in the ANSI/ANS-58.2-1988 standard. Target placement at the greatest test distance from the nozzle (20 L/D) was used to estimate the threshold damage pressure for calcium silicate insulation; however, the target at this position still sustained substantial damage. In addition, the target may have been too close to the jet for prototypicality considerations.

2.2 Debris Sources

All materials that could be entrained and reach the strainers when the pumps in the ECCS or the containment vessel spray system (CVSS) are activated are defined as strainer debris. This means in practice that all kinds of loose materials that are present in containment prior to a LOCA could be possible sources of strainer debris.

The LOCA event progression shown in Figure 2-8 will proceed to generate debris. The first debris source is at and near the break location where different types of materials such as thermal insulation, protective coatings, and concrete would disintegrate. Latent debris such as dirt and dust on horizontal surfaces could be washed down by the break stream flow or containment spray flow to the suction strainers. There are also other types of material such as rust particles (sludge) in a BWR suppression pool that must be included as possible debris material.

TIME > LOCA (seconds)	LOCA EVENT PROGRESSION	DEBRIS GENERATION	DRYWELL TRANSPORT	SUPPRESSION POOL PHENOMENA	SUPPRESSION POOL TRANSPORT	ECCS RESPONSE
0	• Pressure wave • Dynamic piping response	• Impulse load on insulation • Peeled covers • Insulation destroyed	• Drywell pressurization • Recirculating vapor flows • Entrainment and transport of debris	• Water jet impingement • Vent clearing • Pool swell	• Resuspension of suppression pool sludge	• Initiation on drywell high pressure
1 10	• Reactor pressure vessel blowdown • Choked flow and quasi-steady jet expanding into drywell	• Destruction under steady loads • Dislodgement • Erosion of solid insulation • Concrete spallation • Paint chips	• Transport by vapor flow • Deposition on structures	• High energy phase • Chugging, condensation oscillations • High intensity turbulence	• Addition of drywell debris • Continued resuspension • Fully mixed conditions • Debris break up	• RPV pressure > shut-off head • Minimum flow through bypass (10% of rated flow)
50 100	• End of blowdown • ECCS injection commences	• Termination of debris generation	• Rapid depressurization	• Rapid decrease in pool dynamics	• Washdown of insulation • Start of sedimentation	• Ramps to design flow
	• Flooded reactor core • Design flow from break		• Pressure equalization • Transport by breakflow • Formation of water pool on drywell floor	• Low energy phase • Recirculation flow patterns	• Transport to strainers	
1000				• Low intensity turbulence		• May operate in suppression pool cooling mode

Figure 2-8: LOCA Event Progression and its Effects on Debris Generation and Transport

The following sub-sections briefly review materials identified in experiments and incidents as possible problematic debris sources based not only on primary effects such as release and transport, but also secondary effects such as chemical reaction and long term effects. The properties of different insulation materials are described in more detail in Appendix C.

It should be highlighted that the determination of the realistic properties of materials in case of a LOCA is very difficult, e.g.:

• Size of fragmented materials;

• Aging effects due to high temperature and radiation;

• Interaction of different materials;

• Transport of materials;

• Influence of pH, temperature, etc. and their post-LOCA evolution.

Therefore experimental results must be checked very carefully with respect to their conservatism and realism. Many experiments in this field have yielded results that were unexpected and difficult to explain.

2.2.1 Insulation Materials

The most significant effects on head loss across strainers and fuel elements are caused by released insulation materials. Many different insulation materials are used in containment. It has been shown in experiments that different materials behave differently. Only a few materials have been systematically assessed. Insulation materials can be divided into two major classes: (1) reflective metallic and (2) conventional or mass-type insulation, such as calcium-silicate or low

density fiberglass.

2.2.1.1   Reflective Metallic Insulation

These materials consist of several layers of thin metallic sheets, typically 0.05- to 0.07-mm thick, which usually are encapsulated in a shell of a thicker metal sheet. The insulation is normally welded together in panels which are fitted to the component (pipe or vessel). The dimensions, thickness of the sheets and number of layers differ among manufacturers. The sheet metal used for RMI in the US is often half the thickness of the sheet metal used in some European-designed RMI. The material of construction is typically either stainless steel or aluminum. Steam blast tests have revealed high levels of destruction of the panels.

RMI is used in newer NPPs as well as in design modifications to replace problematic insulation as a corrective action. For example, Spanish plants undertook a major campaign to replace fibrous insulation by RMI.

This insulation material has several characteristics that make it suitable to deal with the strainer clogging issue:

- Most of the debris generated by the LOCA jet is large enough to remain near the break location;

- The transported RMI fragments typically sink to the bottom of the containment pool and do not arrive at the strainers, especially when the sump strainers have large surface area (as now used in many plants), which implies very low flow velocities;

- RMI is very stable under different humidity, temperature and radiation conditions and does not contribute to chemical effects; and

- Its relevance when analyzing downstream effects in system piping and in the reactor core is negligible.

The drawback of RMI is its weight. It weighs considerably more than fibrous insulation and handling of RMI cassettes for maintenance work is more cumbersome.   There are also reports that the thermal efficiency is less in some applications.

2.2.1.2   Conventional or Mass-Type Insulation

This class of insulation includes low-density fiberglass (38.45 kg/m^3 (2.4 lbm/ft^3)), medium-density fiberglass, and pre-formed fiberglass, as well as fiber felt materials. It also includes microporous insulation such as MinK and Microtherm, as well as calcium silicate insulation.

There are three principal types of mass insulation:

1. Fibrous insulation (including asbestos);

2. Granular insulation (calcium silicate and microporous);

3. Cellular insulation

In mass-type insulation, the materials used as the insulation filler come from one or two broad categories, fibrous and other. Fibrous insulation includes mineral wool and fiberglass. Other materials include foam glass and various silicates which may or may not be reinforced by fibers. The density of mineral wool is higher than that of glass wool.

Mineral wool and glass wool are commonly used as high-pressure spun or woven material in the form of mattresses, reinforced with wire mesh, jacketed, encapsulated or totally encapsulated. Mass-type insulation may be enclosed in a shell or jacket or cloth covers, and may be totally encapsulated or

semi-encapsulated in order to hold the insulation together. The encapsulated material has an outer shell, generally made of a sheet of metal which is joined by welding. Semi-encapsulated insulation resembles encapsulated material but is clamped together. Cloth covers forming various types of pillows are used to preserve the integrity of the insulation. Jacketed insulation contains mass-type insulation as the principal heat barrier. The jacket, which is usually a separate metal cover, is basically for protection. The jackets are only provided at the outside. Thus, a jacket does not protect the insulation on the pipe that breaks.

For US plants, the metal jacket encapsulation can be stainless steel or aluminum. The thickness is typically 0.41 mm (0.016 inch). When used on vessels such as steam generators, the encapsulation jacket thickness could be as high as 0.79 mm. Total encapsulation in French plants uses stainless steel of 1 mm thickness on the inner and outer sides of the jacket. Encapsulation in German plants consists of stainless steel metal outside (0.8 mm thickness) and metal foil on the inner side. The cassettes are fixed by snap fits.

The fiber length produced by destruction by a high pressure jet ranges from micrometers to millimeters. The fiber length is important for assessing the penetration through retention devices. It has to be emphasized that for mesh widths smaller than the fiber length, fibers can penetrate through a strainer due to the small fiber diameter and orientation in the flow direction. Short fibers can accumulate, especially in case of a low flow velocity, and the agglomerates can clog strainers and spacers of fuel elements.

Experiments have shown that metal covers can provide some protection against LOCA loads. The insulation in the vicinity of the break will normally be destroyed. Different types of insulation materials are affected differently during a LOCA. Mineral wool is affected by the initial blast and could be further converted to small particles by erosion. Fiberglass is more affected by jet impingement forces. Metal insulation covers may also be deformed or removed by the dynamic pressure wave from the initial blast. Materials like calcium or aluminum silicate offer special problems. These types of insulation materials disintegrate mostly because of erosion by the jet. The resistance to elevated stagnation pressure is limited and it must be assumed that debris may be generated in narrow sections where the flow velocity is high. This process results in disintegration into very small particles, as has been shown in tests [2-11], [2-12], [2-13]; the size distributions observed in these tests are shown in Table 2-2 for illustration. If new experiments are conducted the length distribution for fibrous debris should also be determined in sufficient detail to better characterize its behavior.

The hot environment to which the insulation is normally exposed will change the structure of the material. Mass-type insulation materials contain different organic binders which hold the fibers together. These binders are affected at high temperatures and may eventually dissipate. This process can make the insulation more brittle [2-14], causing more "fines" to be generated which later can be entrained in the debris bed on the strainer. These effects have not been quantified and differences between various fibrous insulation materials have not been fully investigated.

When the binders dissipate, the insulation fragments will settle more readily and may reduce the quantity of material transported to the strainer. Where this type of settlement is credited in the analyses it must be justified by representative experiments.

Table 2-2: Measured Particle Size Distribution (as Mass of Material (g)) of Steam-Jet Dislodged Newtherm 1000

Test Number	Particle Size Range (µm)			Total	Amount Before Test	% Material Missing After Test
	>0.85	850-20	<20			
1	1135.3	43.8	71.1	1550.2	1475.4	15.5
2	1002.4	77.6	73.6	1153.6	1404.5	17.9
Average 1 and 2	1068.6	60.7	72.4	1209.9	1439.95	16.6

2.2.1.2.1   Granular insulation (calcium silicate and microporous)

Granular insulation (e.g., calcium silicate, Min-K, and Microtherm) subject to post-LOCA environmental conditions can erode and release fine particulates that could contribute to strainer head losses, especially in the event of release of mixed fibrous and granular materials. In general, for granular insulation the released particles should be small enough not to plug strainers or fuel elements. Larger pieces may settle depending on factors such as the flow velocity.

A wide variety of calcium silicate-based insulation is installed in NPPs. Some include fiberglass fibers as reinforcement, others use organic fibers, and some of the calcium silicate used up to the late 1950s used asbestos fibers. Calcium silicate dissolution varies by manufacturer, with some types of calcium silicate dissolving rapidly in hot water while others dissolve at a significantly lower rate. This variability is due in part to the method of manufacturing, either a press-shaping process or a molding-shaping process. Some calcium silicate insulation with asbestos fibers was manufactured by a press-shaping process, and this material seems to be more resistant to water erosion than calcium silicate manufactured by a molding-shaping process. It is apparent that at least some erosion would occur for any calcium silicate insulation. The same conclusion should be assumed to hold for Min-K and Microtherm unless adequate research is conducted to support a different conclusion.

During one NRC-sponsored separate-effects testing program, one type of calcium silicate was tested for its dissolution behavior in water [2-15]. In these tests, pieces of debris that had been created by shattering the calcium silicate insulation were dropped into water at both ambient temperature and at 80°C. The water was quiescent or was stirred to induce turbulence. Within 20 minutes in the stirred 80 °C water, about 75% of the material became suspendable fines due to the disintegration process. This process was found to increase with temperature and to increase with turbulence.

When erosion tests are conducted, the tests should last for a sufficient length of time to adequately determine the rate of erosion. The lower the rate of erosion, the longer the test duration needed to accurately determine the erosion rate. Even a low rate could be important over the long-term post-LOCA mission time of the containment sump. The hydraulic conditions that the test debris are subjected to should be prototypical (or conservative) with respect to the plant sump pool. In addition, steps should be taken to ensure that the samples are properly dried before weighing to ensure accuracy. Because the measured mass differences during the testing can range from hundredths to tenths of a gram, small variations in the quantity of water adhering to the samples at the time of weighing could easily influence differential mass measurements.

Publicly available size distribution data on the reaction of an unspecified calcium silicate to a two-phase jet can be found in Table 3-6 of NUREG/CR-6808. The results of Test 5 indicated that the size categories adopted by this guideline would be 50 percent for small fines and 50 percent for large calcium silicate pieces. Given the uncertainties in the subsequent erosion by the post-DBA water, the recommended assumption is that 100 percent of calcium silicate in a ZOI is destroyed as small fines.

2.2.2 Other Potential Strainer Debris Sources

Materials other than insulation could also be transported to the strainers under LOCA conditions. Of special importance is particulate material. Examples of materials which could disintegrate into small particles are:

Concrete

Concrete may be eroded by the jet flow and disintegrate into small chips and particles. Examples of this are shown in [2-1]. Concrete particles can also be released from concrete walls and transported to the sump area in the case of unpainted walls or the use of unqualified coatings. There are no publicly available experimental reports where the objective was to investigate concrete disintegration and, therefore, no data are available on the amount of debris or size distribution.

Protective Coatings

Industrial protective coatings are applied to a large number of systems, structures, and components housed in the containment of both PWRs and BWRs to protect the surfaces from corrosion, to facilitate decontamination, and to provide for wear protection during plant operation and maintenance activities. These coatings are of several types (primer, sealer, topcoat, surfacer, etc.) and encompass a wide variety of chemical formulations, including alkyd, vinyl toluene modified alkyd, epoxy, urethane, acrylic, styrenated acrylic, basic zinc carbonate, and inorganic zinc-rich materials. It has been estimated that a medium-sized US PWR containment has approximately 60,385 m^2 (650,000 ft^2) of coated surfaces (NUREG/CR-6808) [2-17]. The amount of coating debris generated in a LOCA event depends upon the failure characteristics of the coating as well as the size of the region (i.e., ZOI) over which coating failure is expected for a given accident scenario. The amount of this debris that actually reaches the ECCS strainer further depends upon the transport characteristics of that debris under the accident conditions in question.

Both qualified and unqualified coatings have been extensively tested in the US under simulated DBA conditions, and the debris characteristics and transport behavior have also been studied. The regulatory/safety authority position is that all coatings within the ZOI fail as small particulate material, approximately 10 μm in diameter. Coatings qualified by tests to withstand LOCA temperature, pressure and radiation effects outside the ZOI are assumed not to fail. Coatings not qualified by testing are assumed to fail in a LOCA environment.

According to the US NRC Safety Evaluation Report on NEI-04-07, "Pressurized Water Reactor Sump Performance Evaluation Methodology" [2-16], the following has to be assumed for testing of paint chips: "However, for those plants that can substantiate no formation of a thin bed at the sump, this assumption would be nonconservative with regard to sump blockage because fine particulates would pass through the sump screen and generate no blockage concerns. Therefore, for those plants that can substantiate no formation of a thin bed at the sump at which particulate debris can collect, the staff finds that debris generated should be assumed to be sized with realistic conservatism based on the plant-specific environment and susceptibilities identified for that facility, with appropriate justification for the sizing used."

Latent Debris

Dirt, fiber, and other foreign materials that are generally found in NPP containment buildings are referred to as "latent debris." The most important latent debris sources are dust, rust and sludge. Consideration should be given to the potential for latent debris to gather in containment during plant operation. This debris may transport to, and affect the head loss across, the ECCS strainers. Therefore, it is necessary to determine the types, quantities, and locations of latent debris sources. Due to variations in containment design and size from unit to unit, miscellaneous sources should be evaluated on a plant-specific basis.

Dust can be mobilized from walls, step gratings and other building structures (e.g. cable trays) by water flowing down to the sump. The amount of dust transported to the sump strongly depends on the coatings on the walls, the use of the containment spray system, and general plant cleanliness.

It is unlikely that foreign materials exclusion (FME) programs can entirely eliminate sources of miscellaneous debris within containment.

Reasonably conservative estimates for latent debris need to be included in the overall debris source term unless plant-specific walkdowns verify lower values. Plant-specific walkdown results can be used to determine a conservative amount of dust and dirt to be included in the debris source term. Section 3.5 of Reference [2-35] is one source for further guidance on determining quantities of latent debris.

For German NPPs transport of less than 10 kg of dust to the sump area was shown by sampling and extrapolation. The method for estimation of dust within the containment for German NPPs is described in [2-18].

France provided a set of walkdown results performed in some plants at the end of their outage; the provisions taken for the dust is specified at 200 kg (conservative value with large margins).

For Canadian CANDU plants, the following method was used to determine latent debris. The quantity of floor debris to be used for the strainer performance evaluation was estimated based on plant walk-downs and a review of FME programs. Floor swipes were used to estimate the quantity of rust, dust or dirt particulate per unit area; this was then multiplied over the entire area of interest to give an overall estimate. Larger debris such as plastic gloves, rubber boots, garbage cans and their contents were assumed to be removed as part of plant FME programs. Despite the walkdowns and floor swipes, it was determined that it would not be possible to obtain a precise measurement of the amount of floor debris that could exist at the time of an accident, and some conservatism was applied to account for these uncertainties. First, the amount of rust, dust and dirt in the entire area of interest was calculated based on the upper range of measured debris per unit area (as determined by the floor swipes), rather than on the mean value. Second, all this debris was assumed to be transported to the strainer; no credit was allowed for any debris that might fall out of suspension along the way or get caught in stagnant areas. Third, although FME programs were assumed to prevent large debris such as rubber boots or gloves from reaching the strainer, some testing was performed to confirm the ability of the strainer to withstand limited quantities of this type of debris.

Spanish plants have undertaken plant-specific quantification activities to estimate the amount of latent debris in containment expected to be transported toward the sumps. The estimates range from on the order of 20 to 100 kg, depending on whether the adopted value is generically accepted or experimentally obtained. In the particular case of KWU Spanish plants an extra contribution to the latent debris equal to 2 % of the total debris inventory (on the order of 5 kg) was assumed.

Eight kg of dust was estimated for the Wolsong Unit 1 in Korea from a plant walkdown. For the newly constructed Korean plants, latent debris in the amount of 91 kg was conservatively assumed.

For US plants the amount of fibrous and particulate debris ranges from 30 kg to 265 kg with a typical split of 85 % particulate and 15 % fibers. Most plants used the NEI 04-07 methodology to

determine that values.

In the case of uncoated concrete walls the amount of dust generated is expected to be higher than the amount from painted walls.

Chemical Precipitates

The water chemistry has a strong influence on the head loss across debris beds. The following effects must be considered:

- Chemical reactions within the cooling water and formation of precipitates;
- Chemical reactions of the water and building structures;
- Physical-chemical reactions such as erosion-corrosion;
- Chemical degradation of released insulation material.

Some specific observations include:

- While under conditions relevant for French NPPs, degradation of glass fibers was observed for high pH values, rock wool was found to be chemically stable under German post-LOCA chemical conditions;
- Unbuffered boric acid within the cooling water strongly increases erosion and corrosion of zinc-coated ferritic materials. German experiments showed embedding of corrosion products in the debris bed can increase head loss after 10 hours. In the longer term, experiments show that destruction of zinc-coated ferritic materials occurs when covered by borated water;
- Japanese experiments showed that corrosion of carbon steel can increase the head loss significantly.

Chemical reactions strongly depend on temperature, pH, concentration and mixing ratios. It is also noted that these conditions can change relatively quickly when a pH buffer is used in the pool and/or the containment spray systems are in use. As a result, experimental verification by head loss testing can be difficult. A detailed discussion of chemical effects testing can be found in Chapter 5.

Aluminum

Chemical precipitates formed from aluminum released by corrosion of aluminum-based materials can greatly increase the head loss across a fibrous debris bed (see Chapter 5). Additionally, any coating on aluminum surfaces must be considered as an unqualified coating, therefore becoming an additional coating debris contribution. Another downside of having aluminum components in containment is the potential for hydrogen gas generation in the post-LOCA environment; the corrosion of aluminum produces hydrogen and the inventory is administratively controlled in many plants.

No aluminum is utilized in the containment of German and French NPPs. In Spanish PWRs of Westinghouse standard design, aluminum in containment is found in some NSSS parts, e.g., nuclear instrumentation system detectors, Control Rod Drive Mechanism (CRDM) connectors, radiation monitors, in-core and ex-core instrumentation, some parts of RCP, rod control indicators, etc. In US plants the quantity of aluminum varies greatly (150 kg to 3000 kg) depending on the type of insulation encapsulation used and the materials of construction used for ventilation systems. Plant-specific walkdowns and review of documentation for all Korean plants showed that plants generally have aluminum in containment in metallic form in detectors, miscellaneous valves, refueling machine, etc. The amounts range from a few to a few hundred kilograms. For evaluation of chemical effects, the major portions of aluminum including the submerged portion of the total amount were considered.

Zinc

In Spanish NPPs zinc (Zn) is another metallic material that can be problematic in a DBA containment environment. Zinc is used in containment in HVAC elements, liner containment coatings, illumination parts, cable trays, conduits, connecting boxes, etc. The corrosion of Zn produces hydrogen and its inventory is administratively controlled in the plants. Zn from galvanized steel and IOZ coatings was included in the chemical effects testing program in the form of coupons. No chemical precipitate from the Zn was observed.

Experimental investigations were performed for German NPPs to study the erosion and corrosion of zinc-coated step gratings within a waterfall or submerged by water. An increasing head-loss was observed in the case of a waterfall of borated water after 10 hours. The head loss increase was not due to the Zn particles, but rather was attributed to iron oxide particles generated by erosion corrosion when the protective Zn layer had been dissolved or eroded away by the break flow hitting the ferritic grating. When demineralized water was used the corrosion rate was much slower (Chapter 5).

Zinc is present in Korean plants in the form of paint, galvanized steel, etc.

Carbonation

Carbonation can increase the head loss across a debris bed due to complex chemical interactions. One source of carbonation is calcium release in the water from concrete walls without coating or with a damaged coating.

Corrosion Products [2-19]

Sludge consists of corrosion products often found in BWR pressure suppression pools. The formation of particles of corrosion products is mostly associated with carbon steel piping. Corrosion products could be released as a result of a LOCA, and also may exist, for instance, in the wetwell pool, as "sludge." Significant amounts of sludge have been reported. Such material could easily be stirred up and generate strainer debris during a LOCA. In an incident at Limerick Unit 1 in 1995, a mixture of sludge and fibrous material built up a "mat" at the strainers resulting in pump cavitation. It was noted that "The licensees removed about 635 kg of debris from the pool" [2-38]. Section 4.13 further discusses this and has data on accepted size distributions of the sludge particles.

Microorganisms

According to Swedish experience from experiments on chemical effects for assessment of the Ringhals strainers, microorganisms can grow under these conditions. The high initial temperature in containment and the weakly acidic boric acid in the spray are likely to disinfect any surfaces at high temperatures that are hit by the solution. However, it cannot be excluded that resistant spores may survive or that organisms protected from the high temperatures in cracks and crevices may also survive.

When recirculation of the water in containment begins, the pH is relatively favorable for growth of organisms that can withstand the water temperature and circulating radioactivity. Leaching of organic substances from painted surfaces, the availability of phosphate and a nearly neutral pH provide an environment that may promote microbial growth, despite the relatively high boron content.

Unfortunately, it is almost impossible to predict to what extent this will happen. Experience shows, however, that microorganisms have a surprisingly large capacity to live even in very extreme environments, such as in hot springs and black smokers on ocean bottoms. It can be expected that the formation of large amounts of biological material would require a relatively long time. The occurrence of large amounts of such material might be expected weeks after an accident and could continue for months. The US position is that there will be insufficient formation of microorganisms

during the design basis event duration (30 days) to significantly affect head loss.

2.2.3 Other Materials Present in Containment

Other materials have been reported in containment [2-19], [2-20]. Foreign materials that have inadvertently been left in containment include marking tapes, plastic bags and filter material; an air filter which had been dropped in the wetwell pool was identified as the cause of the strainer troubles at the Perry plant in the US. Cleaning of the wetwell pools, which now is recommended, has revealed many foreign objects. However, most of these would not form strainer debris due to their size. Appendix B contains a listing of plant events in which debris has been identified.

Other materials with unknown effects on strainer behavior, such as, lubricating oil, are present in containment. A reactor circulation pump has approximately 1 m^3 of oil. Head loss tests of strainers have shown little impact from oil.

2.3 Small-Scale Experimental Work Available

Miscellaneous sources of small-scale test data are reviewed in this section. Details of the experiments are given in Appendix D.

2.3.1 Studsvik Materials Experiment (Sweden)

The main objective of the test was to produce representative steam blown fibrous insulation material to be used for experiments on strainer head loss. Experiments were conducted using various types of fiber insulation and also using Caposil and Newtherm, which contain larger fractions of particles. The insulation was aged through exposure to elevated temperatures. The tests were conducted using steam in a small vessel at an initial pressure of 30 bar. The inner diameter of the steam pipe was 16 mm and the distance between the nozzle and the pillow was varied from 2 to 40 L/D.

Three series of experiments were performed [2-11], [2-12], [2-21]. The observations were correlated with current conceptual models used for estimating insulation debris in power plants. Destruction was observed at larger distances. The disintegration was severe for L/Ds up to 15. The subsequent head loss tests which were performed with the insulation material after the tests gave high pressure drops. Some of the insulation was disintegrated up to 35 L/D. In these tests, erosion was found to be a dominant debris generator. The longer time the material was located in the jet, the greater the debris.

2.3.2 Karlshamn Experiments in Sweden ([2-22], [2-23])

Steam from the Karlshamn power plant was led into a scaled-down model of a containment that was built using containers. Although the objective of the experiments was to study insulation transport in a BWR containment under LOCA conditions (see Chapter 3), some observations were made on dislodgement.

The distance between the nozzle and the thermal insulation was 250 mm (approximately 8 L/D). The fibrous insulation was destroyed and dislodged in all the tests. The debris was not characterized. Insulation installed in metallic cassettes showed less destruction for a distance of 5 L/D.

Tests on Newtherm 1000 insulation, which basically is a particulate material, showed that erosion is the main contributor to the disintegration of this kind of material. The resistance of the insulation to stagnation pressures was determined in the experiments.

2.3.3 NUKON™ Experiments in Colorado [2-24]

The purpose of these tests was to characterize the extent of NUKON insulation destruction and the nature of the debris that would result from a sudden pipe break. The LOCA was simulated by an

air blast using rupture discs.

The tests showed that metal jacketing can provide significant protection. The protection may be somewhat dependent on how it is installed relative to the blast. Less than 30% of the material located within the zone of destruction was fragmented to small pieces. Subsequent testing sponsored by the BWROG (documented in Ref. 2-8) of jacketed and unjacketed NUKON™ insulation produced different conclusions. Those test results indicated similar behavior for both jacketed and unjacketed material unless the jacket seam was oriented such that it was not impacted by the jet. As a result the US NRC recommends the same destruction pressure be used for both types of installations unless stronger banding straps are used.

Since the tests were performed with compressed air and there is no systematic basis for comparison with other fluids, caution is needed when extending use of the test results for LOCA conditions. However, it is noted that the US NRC accepted the use of air jet tests to determine the destruction pressure for materials. The air jet tests compare relatively well with saturated water tests.

2.3.4   The Transco Tests [2-25]

The objective of this study was to investigate the effects of a jet-like blast of air on RMI, fibrous insulation with various types of coverings, and electric cables. The experiments were conducted using a shock tube with a rupture disc, and the insulation was placed at various distances from the exit of the tube. The strength of the shock wave could be studied by varying the initial pressure in the tube.

For the RMI, the damage was not very great and depended on the longitudinal seam in the cassette. The distortion volume increased with pressure. Increased damage was observed when exposing the debris to repeated shock waves. Tests with metal-jacketed fibrous insulation showed less damage. It was speculated that the fibrous insulation was able to take up more of the energy in the blast. Tests with unjacketed blankets showed that only a small amount of material was dislodged. Tests with electrical cables showed that they remained essentially intact.

The same caution regarding test medium noted in Section 2.3.3 should be exercised for these experiments.

2.3.5   NUKON Experiments by the PWROG and Westinghouse

Numerous jet impingement tests were conducted on NUKON insulation and other systems at Wyle Laboratories by the PWROG and Westinghouse in the 2005-2007 time frame. However, the data are all non-public information.

2.4   Break Jet Modeling

A jet model is dependent on an in-depth understanding of the physical phenomena occurring and the capability to translate such phenomena into a calculation algorithm. As noted in Section 2.1, modeling of the initial blast wave is not easy, jet expansion modeling is feasible, and estimating debris generation (quantities and types) from limited experiments is complex with a high degree of uncertainty, and therefore conservative methods should be used. Since it has not been possible to develop a singular generic LOCA debris generation model, a number of approaches have evolved, largely based on engineering judgment, to apply to this situation.

2.4.1   The Cone Model or Multiple Region Conceptual Model

Historically the cone model or multiple region model has played an important role since it has been used in many countries for the design basis for strainer capacity. It must be borne in mind that this is a conceptual model and it was not intended to be a predictive tool. The model has been widely

used in PWRs and BWRs to obtain order-of-magnitude estimates for the amount of debris generated by a postulated LOCA. The uncertainties are deemed to be substantial under certain circumstances, and a few comparisons are discussed below. The model does not pretend to give information about the characteristics of the debris. It is recommended that the cone model be used with caution, taking into account known limitations, engineering judgment, and allowing for a reasonable margin for uncertainty.

The development of the model is the result of analyses of two-phase jet behavior [2-26], two-phase jet calculations [2-5] and the degree of insulation damage found in the HDR experiments [2-1]. It is noted that the early developmental work was focused on two-phase jets. Little public information is available on single-phase discharge with steam. The model is actually based on conversion of a specific stagnation pressure (P_{stag}) to insulation damage [2-26].

The debris generation model adopted by the U.S. NRC in Regulatory Guide 1.82 [2-27] prior to GSI-191 is based on the distance from the break, measured in break diameters (L/Ds). There are different suggestions of the top angle of the cone. A 90-degree angle was assumed to be a conservative estimate. The following regions are considered:

Region 1. L/D < 3. Complete destruction to fine fibers;

Region 2. 3< L/D <7. A high level of destruction or damage is possible. Different materials give different amounts of debris in this zone;

Region 3. L/D > 7 to P_{stag} = 0.5 psi, or major wall boundary from the break. Destruction is likely to be in the as-fabricated mode, or as modules.

Figure 2-9 illustrates the model.
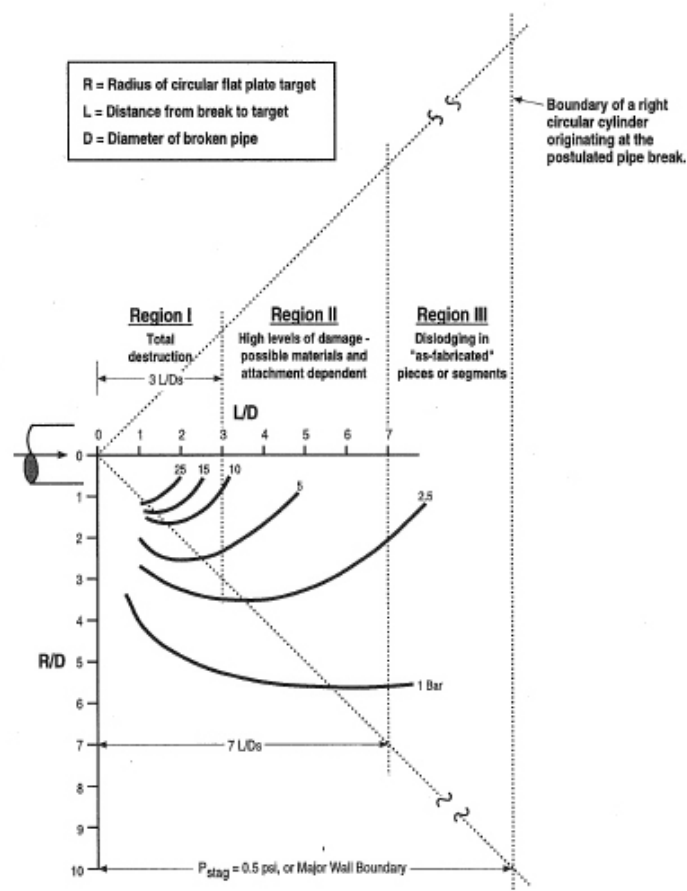
Figure 2-9: NRC Cone Model or Multiple Region Insulation Debris Generation Model

The model has been compared qualitatively with experimental data and operational incidents:

- NUKON experiments in HDR demonstrated that jacketed and unjacketed NUKON insulation blankets within 7 L/D will be almost totally destroyed. NUKON blankets enclosed in standard stainless steel showed greater resistance to the blast. Note that the jet first hit a deflection plate;

- NUKON experiments in Colorado indicated that the destruction zone is narrower than the cone model. Compressed air was used as a debris generation medium and there is no straightforward comparison between air and two-phase flow;

- The Barsebäck incident indicated that the destruction went further than 7 L/D. The model has been extrapolated down to 30 bar;

- MIJITs in Karlstein were performed in order to study metallic insulation debris generation in a large-scale environment. Tests with flashing water gave results that were in accordance with the model. Tests with steam indicated a zone of destruction which was longer and narrower than that predicted by the model;

- Studsvik material steam jet destruction of thermal insulation material showed that insulation material in the form of pillows was damaged up to 35 L/D;

- Karlshamn steam jet experiments used mineral wool packed into silicon-coated fiberglass fabric. The insulation was wrapped around a pipe with a distance of 8 L/D between the nozzle and the thermal insulation. The insulation was damaged in all the tests and blown away, which indicates that unprotected thermal insulation could be damaged beyond 7 L/D;

- A double-ended guillotine steam break test performed in Karlstein for the U.S. NRC on an RMI assembly indicated that the destruction factors were more severe than those obtained from tests with air.

The uncertainties with this model that should be taken into account are related to the protection of insulation material and the jet characteristics. Unprotected insulation normally experiences higher destruction than the model would suggest. Insulation protected with, for example, metal jacketing will often experience less destruction. Steam jets are capable of destroying insulation at a large distance. The cross-sectional area of a steam jet is much smaller than that of jets of flashing water. These examples are provided to remind users that jet modeling does not constitute debris generation estimation. The user should also be aware that the orientation of seams in metal jacketing can also affect the results.

2.4.2 Sphere Model

A sphere model [2-33], [2-34], [2-35] has been derived from the cone model and has been used for analyzing U.S. BWRs and PWRs since the mid-1990s. The use of a spherical ZOI is intended to encompass the effects of jet expansion resulting from impingement and reflection on structures and components.

BWRs and PWRs used different analytical approaches to determine the radius of the spherical ZOI. BWRs used a NPARC CFD model, the details of which can be found in NEDO-32686 [2-34]. For PWRs, the ANSI/ANS 58.2-1988 standard [2-31] provides the guidance necessary to determine the geometry of a freely expanding jet from a variety of reservoir conditions, including subcooled conditions.

1. The mass flux from the postulated break was determined using the Henry-Fauske model for subcooled water blowdown through nozzles, based on a homogeneous non-equilibrium flow process. No irreversible losses were considered;

2. The initial and steady-state thrust forces were calculated based on the postulated reservoir conditions;

3. The jet outer boundary and regions were mapped for a circumferential break with full separation. The input to the equations for the thermodynamic conditions at the asymptotic

plane was calculated using principles of thermodynamics and the postulated conditions in the reservoir;

4. A spectrum of isobars was mapped. Several isobars were considered of interest, including the 10 psi isobar. The 10 psi isobar was of interest for BWRs as NEDO-32686 [2-34] identifies 10 psi as the destruction pressure of jacketed NUKON insulation with standard bands or unjacketed NUKON. For PWRs, the NRC reduced this value to 6 psi because of the uncertainties associated with saturated water jets from a PWR RCS break vs. air jets used in the testing.

5. The volume encompassed by the various isobars was calculated using a trapezoidal approximation to the integral. Since the volume result only represents the volume encompassed by the isobars in a free jet, the volume encompassed by results was doubled to represent a DEGB;

6. The radius of an equivalent sphere was calculated to encompass the same volume as twice the volume of a freely expanding jet calculated from step 5, above. The radius calculated was taken to be the radius of the ZOI to be used to calculate the volume of debris generated from a postulated break;

7. A circular break geometry was used for the calculations. This break geometry is representative of both a postulated DEGB of primary piping as well as the DEGB of piping attached to the RCS. The complete breaking of a pipe, either primary piping or piping attached to the RCS, provides for a maximum debris generation volume as there are two ends of the break to release fluid;

8. Ambient pressure of 14.7 psia was used. This is conservative since no credit is taken for containment backpressure (the increase in containment pressure that would result from the release of mass and energy into the containment as a result of the postulated break).

The resulting ZOI is expressed as the ratio of the radius of the equivalent ZOI sphere to break size diameter. This allows the ZOI to be expressed independently of the break size.

The results of the DEGB steam blast test [2-7] support adoption of a destruction factor of 1.0 for $L/D \leq 3$ for steam line-type breaks. The sphere model is illustrated in Figure 2-10.
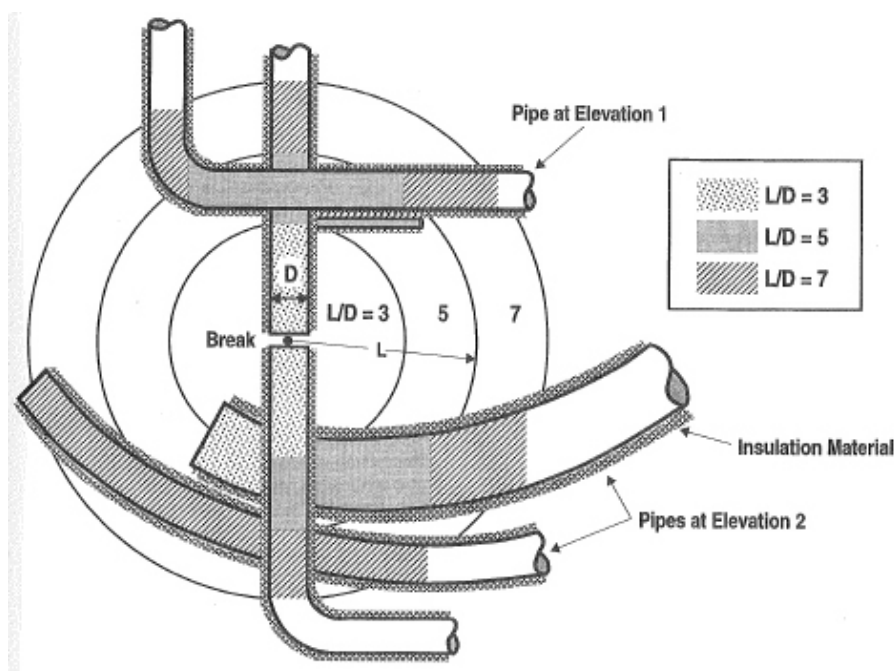
Figure 2-10: Sphere Model from NUREG/CR-6224

2.4.3   Stagnation Pressure Models

Before the cone model was developed, a stagnation pressure model was employed. This model assumes that all insulation inside a zone, the boundary of which is 0.5 psig (0.1035 MPa), is completely destroyed. The stagnation pressure model was far more conservative than the cone model and is not used today [2-26].

Asea Brown Boveri (ABB) Atom found that the cone model was not applicable to breaks in narrow parts of containment and developed a new model. This model [2-29] is specifically used for calculating debris between the reactor vessel and the biological shield, is only valid for calcium silicate insulation and assumes that erosion is the dominant debris generator. This model is purely empirical and is based on small-scale experiments that were performed at Karlshamn. It was found that the material was eroded for stagnation pressures exceeding 1.6 bar. All insulation which experiences higher pressures is assumed to be destroyed. This is an example of a purely empirical approach to the debris generation problem.

2.4.4   CIIT Eddy Model (Chicago Illinois Institute of Technology)

The CIIT eddy model [2-25] assumes that the local shear stresses created by the turbulence in the jet will break up the fibers of the insulation. The model addresses the sizes of the generated particles which are assumed to be related to the sizes of local turbulent eddies. Effects of binders in the insulation are ignored. The model has not been validated.

2.4.5   Jet Impingement Models

Models for evaluation of protection against the effects of postulated pipe ruptures (ANSI/ANS-58.2-1988) are presented in [2-31]. Methodology is provided to evaluate hydraulic forces like impingement loads, pipe whip, and internal loads. This report does not address debris generation and a model for converting forces into destruction of material is needed to use such results. Jet impingement models have traditionally been used to define the region surrounding a break where the impingement pressures would be larger than the ambient pressure.

The model divides the distance from the break into three regions. In the region closest to the break the full stagnation pressure is recovered on a target. This region extends to about half a break diameter and increases with upstream subcooling. The jet expands to its asymptotic area in the next region. The model proposed by Moody [2-33] is used to calculate the asymptotic area and a method is provided for calculating the asymptotic pressure. Downstream of this region the jet is assumed to expand with a half angle of 10 degrees.

The predictions of the jet impingement loads provided by the ANSI models have been thoroughly validated for the blowdown phase [2-31], [2-33]. The major drawbacks associated with the jet impingement models are as follows:

1. The Moody two-phase model does not address the issue of pressure loadings on the structures surrounding the break due to the initial blast phase. As noted in the HDR and Siemens-Karlstein tests, considerable potential exists for debris generation during this phase of a LOCA;

2. Usage of the jet impingement model ultimately requires an analytical model or experimental data relating potential for debris generation to the local jet impingement loads.

In this context, it should be noted that usage of jet impingement models for defining the ZOI over which debris may be generated has not been validated. As a result, they should be used with caution, after accounting for the fact they do not model the blast phase.

JNES performed two-phase jet analysis with a two-fluid model considering fluid compressibility [2-39], [2-40]. The results showed that the initial blast wave was not generated in the analyses. Regarding estimation of ZOI, the two-fluid model and the ANSI/ANS model are comparable in a high jet pressure region, while the latter is conservative in a low jet pressure region approaching

atmospheric pressure.

2.4.6 *RSK/NRC cone model*

In Germany the assumptions for the release of insulation material are based on experimental results. For German NPPs the ZOI model was modified. The release of encapsulated fibrous material (cassette-type insulation) was significantly increased compared to the NRC cone model. The model is described in RSK statement 374 from 2004 [2-41], which states that the calculation of the amount of insulation material released shall be done according to the "so-called NRC Cone Model" [2-1]. The amount released is calculated as shown in Table 2-3 as a function of leak size, distance from leak location, and the type of insulation material, with a 90° opening angle of the cone.

Table 2-3: Dependence of Amount of Debris Released on Leak Size (Equivalent Diameter D), Distance from Leak Location (L), and Type of Insulation Material.

Region	Distance	Release		
		Cassette-type insulation	Mat insulation	Conventional insulation
1	L ≤ 3D	100 %	100 %	100 %
2	3D < L ≤ 7D	50 %	100 %	100 %
3	7D < L ≤ 30D	0 %	0 %	100 %

Experiments were performed to demonstrate the validity of these assumptions (Figure 2-11) [2-42]. In the calculation of the amount of insulation material released from cassette-type insulation, those half cassettes that surround the assumed circular leak location on the pipe affected have to be fully considered. For cassettes which are partly hit by the jet cone in regions 1 and 2 and which mostly lie outside the jet cone, the cassette region lying outside the jet cone has to be attributed to region 2. Regarding insulation material protected within the cassettes, e.g. by canvas jackets, these must be assessed case-by-case as to whether additional assumptions have to be made for areas lying outside the jet cone.

The effect of a shift of the jet direction upon the rupture of pipes (pipe whipping), which may lead to a widening of the area of insulation material that will be hit, has to be considered on a case-by-case basis for each plant in the determination of the release.

Modification of the NRC Cone Model was necessary due to experimental results from Battelle-Kaefer in 1995 [2-42] and AREVA/FRAMATOME in 2003 [2-43]. For the Battelle-KAEFER tests the pressure within the break pipe was 95 bar and the temperature ~300 °C. The pressure at the break location was around 54 bar. Release of insulation material occurred in zones 2 and 3 as well as in zone 1.
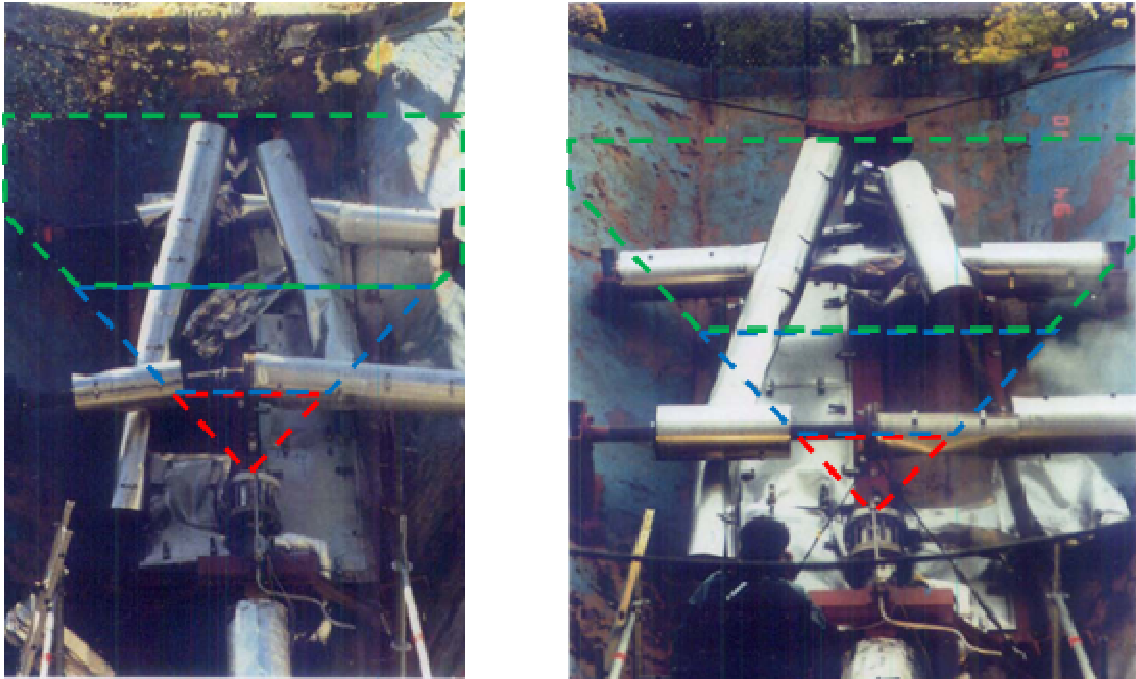
Figure 2-11: Release of insulation material in zone 1 (red1), 2 (blue) and 3 (green) [2-42].

There were two important mechanisms for higher release than predicted by the NRC cone model: peeling and secondary destruction of cassettes. Peeling means that cassettes were hit in the direction of the jet and were destroyed after destruction of a cassette closer to the break location. Secondary destruction happened due to cassettes outside the jet being struck by other destroyed cassettes. Release of insulation material from cassettes could happen for distances L/D > 7. It has to be mentioned that Battelle-KAEFER tests were also performed for RMI and glass wool.

The FRAMATOME tests at Karlstein were performed with a distance between the jet outlet and cassettes of 40 cm (according to zone 1), a pressure of 100 bar at the burst disk and a temperature of 285 °C. The blowout-time ranged from 4.6 to 8.7 s.

The AREVA/FRAMATOME tests (Figure 2-12) showed that:

- Cassettes with their outer surface in front of the jet in zone 1 (facing the jet) were usually only deformed and not destroyed;
- 2 cassettes with a position of the interface in front of the jet and in zone 1 were partially destroyed and almost totally washed out; for 8 out of 10 cassettes the insulation material was totally washed out, from 1 cassette 30 % was washed out, and from 1 cassette there was no release

Figure 2-12: Left: Position of lower cassettes with one in front of the jet and one away from the jet and upper cassettes with the interface in front of the gap, jet outlet at the right side Right: Removed and destroyed upper cassettes at the floor and deformed lower cassette faced to the jet, jet outlet out of the picture bottom right [2-43].

2.5 Summary of the Knowledge Base for Debris Generation

The uncertainties and future research needs in the topic of debris generation are discussed in this section. Adequate evaluation of LOCA-generated debris is needed to assess the design specifications of the intake strainers to the recirculation system. Several features of dislodged material have to be addressed in plant-specific examinations.

Most of the experimental studies have focused on the destruction pressure and the amount of debris generated. This is an important factor since it represents the source term for transport through the containment to the strainers. It has been shown that the concentration of very fine material (particles or fibers) could have a large effect on the head loss of the strainers. Since the significant safety concern is strainer clogging, it has become equally important to characterize the destroyed material, such as the measuring the fraction of released fine particles, in plant-specific safety assessments. The database for the assessment of such issues is limited. In estimating the amount of strainer debris, it is also necessary to consider other materials, such as concrete, paint chips, latent debris and corrosion products which may come loose under a LOCA, as well as chemical effects. Good housekeeping to minimize the latent debris source term will help in preventing strainer clogging. Understanding of the various debris sources has increased significantly since the first revision of this document was issued.

The major mechanisms for dislodging material are the pressure wave associated with pipe rupture, jet impingement on insulated targets, and erosion due to interaction with the high-velocity fluid. Conceptual models have been established in order to quantify the amount of debris. Two of the conceptual models for debris generation, the cone model and the sphere model, address the interaction between the fluid jet and the insulation and define affected zones in terms of the number of break diameters from the break location. Results from some experiments indicate that zones with dislodging of insulation may be larger than these models predict for unprotected insulation. Jacketed insulation could give smaller amounts of debris than indicated by the model. Water jets can dislodge insulation material when reflected from nearby structural features or other hard surfaces. Pipes with large diameters or steam generator (SG)-vessel outer surfaces offer an arching surface for the jet to reflect from and expand the area of influence. The spherical model accepted by the NRC is intended to account for this. However, it is based on judgment, not on experiments.

The models are considered to be adequate for debris generated by flashing jets when used with due consideration of uncertainties and engineering judgment. Experience from experiments, and also

from the incident at Barsebäck, indicate that the destruction zone is different for water or steam/air jets than from that of flashing water jets, being narrower and more extended for steam jets than for flashing water jets. Since most LOCAs will turn into steam blowdown when the break location is uncovered, consideration of the topology of the destruction zone may be warranted in the evaluation of amount of generated debris. The effect of fluid type may also have an effect on the characteristics of the debris. It has, for instance, been shown that material fragmented by steam produces higher strainer head losses than material which is mechanically fragmented. This may be caused by differences in the distribution of particle sizes. In general, the assessment of the models is rather limited.

Experiments performed for the BWRs in the 1990s often used air jets while many of the experiments performed for GSI-191 resolution for PWRs have used 2-phase water jets. Much of the debris generation testing for fibrous insulation and protective coatings is not public information. An interested party could contact the safety authority or NPP licensee in the country of interest to ascertain what non-public information might be available.

No model specifically addresses the effects of possible pressure waves within containment to separate the effect of the pressure wave from the effects of impingement and erosion. This was considered to be a significant contributor to debris generation in the HDR experiments. The main effect seems to be the potential for deformation or removal of metallic insulation coverings, which may later cause increased interaction with the fluid jet. One of the models [2-29] addresses dislodging in narrow gaps. The main parameter is the stagnation pressure. The model rests mainly on empirical evidence relating stagnation pressure and mechanical destruction of material. Another model [2-30] also addresses particle sizes generated in a turbulent jet. No assessment case is available for this model. Experiments at CEESI [2-24] demonstrate that a shock wave contributes significantly to debris generation.

The various insulation materials used in NPPs show different destruction behaviors. Materials like mineral wool seem to disintegrate more quickly than fiberglass under impact from a jet. Insulation material that has been subjected to realistic ambient temperatures prior to testing behaves differently than new material. RMI material has been used in many applications to replace fibrous insulation. Experiments indicate that such RMI material will be fragmented and form loose debris beds that induce relative low head loss ([2-16], Chapter 6). However, it is important to note that even though there have been many experiments on destruction pressures of various materials, there has not been a concerted effort to consistently capture the destroyed material to determine the size distribution.

References

2-1   U.S. Nuclear Regulatory Commission, "Containment Emergency Sump Performance", NUREG-0897, Rev.1, October 1985.

2-2   Owens/Corning Fiberglass Corporation, "HDR Blowdown Tests, With NUKON™ Insulation Blankets", March 1985.

2-3   Studsvik Energiteknik, "The Marviken Full Scale Containment Experiment Component Tests. Paint and Heat Insulation", MXA-4-206, September 1973.

2-4   Studsvik Energiteknik, "The Marviken Full Scale Jet Impingement Tests, Summary Report", MXD-301, September 1982.

2-5   U.S. Nuclear Regulatory Commission, "Two Phase Jet Loads", NUREG/CR-2913, January 1983.

2-6   Vattenfall Energisystem, "Metallic Insulation Jet Impact Tests (MIJIT)", Report GEK 77/95, June 6, 1995.

2-7   Siemens, "RMI Debris Generation Testing. Pilot Steam Test with a Target Bobbin of Diamond Power Panels", Technical Report NT34/95/e32, July 3, 1995.

2-8   Continuum Dynamics Inc. "Air Jet Impact Testing of Fibrous and Reflective Metallic Insulation", CDI Report 96-06 September 1996.

2-9   NUREG/CR-6369, Vol. 1 & 2, "Drywell Debris Transport Study", SEA97-3501-A:14 and -A15, September 30, 1999.

2-10   Ontario Power Generation "Jet Impact Tests-Preliminary Results and their Applications", N-REP-34320-10000-R00, April 2001.

2-11   Studsvik Energiteknik, "Steam Jet Dislodgement Tests of Thermal Insulating Material of Type Newtherm 1000 and Caposil HT1", Material Report M-93/41, April 7, 1993.

2-12   Studsvik Energiteknik, "Steam Jet Dislodgement Tests of Two Thermal Insulating Materials", Material Report M-93/60, May 1993.

2-13   ABB-Atom, "Barseback 1 & 2, Oskarshamn 1 & 2, Ringhals 1. Report from Tests Concerning the Effect of a Steam Jet on Caposil Insulation at Karlshamn, Carried Out Between April 22-23, 1993, and May 6, 1993", SDC 93-1174, June 1993.

2-14   ABB-Atom, "Barseback 1 and 2, Oskarshamn 1 and 2 - Strainers in Systems 322 and 323. Results from Blowdown Experiments in a Test Rig", RVA 92-340, November 27, 1992.

2-15   NUREG/CR-6772 "Separate-Effects Characterization of Debris Transport in Water", US NRC August, 2002.

2-16   US NRC Safety Evaluation Report on "Pressurized Water Reactor Sump Performance Evaluation Methodology" (ADAMS Accession Number ML043280007).

2-17   NUREG/CR-6808 "Knowledge Base for the Effect of Debris on Pressurized Water Reactor Emergency Core Cooling Sump Performance", USNRC, February 2003.

2-18   AREVA Work-report NGPS4/2005/de/0055, "Estimation of Dust Relevant Surfaces within the Containment", AREVA, 09 September 2006.

2-19   U.S. Nuclear Regulatory Commission, "Debris in Containment and the Residual Heat Removal System", Information Notice 94-57.

2-20   U.S. Nuclear Regulatory Commission, "Potential for Loss of Emergency Core Cooling Function Due to a Combination of Operational and Post-LOCA Debris in Containment", Information Notice 93-34.

2-21   Studsvik Energiteknik, "Steam Jet Dislodging of Thermal Insulating Material", Material Report M-93/24, March 1, 1993.

2-22   ABB-Atom, "Karlshamn Tests 1992, Test Report. Steam Blast on Insulated Objects", RVE 92-205, November 30, 1992.

2-23   ABB-Atom, "Karlshamn Tests 1992, "Steam Blast on Insulated Objects, Logbook", RVE 92-202, November 1992.

2-24   Colorado Engineering Experiment Station, Inc., "Air Blast Destructive Testing of NUKON™ Insulation -Simulation of a Pipe Break LOCA", October 1993.

2-25   Transco Products, Inc., "Experiments to Assess Jet and Debris Damage to Metal Reflective and Fibrous Insulation", June 1995.

2-26   U.S. Nuclear Regulatory Commission, "Methodology for Evaluation of Insulation Debris Effects", NUREG/CR-2791, September 1982.

2-27   U.S. Nuclear Regulatory Commission, "Sumps for Emergency Core Cooling and Containment Systems", Regulatory Guide 1.82, Revision 1, 1985.

2-28   U.S. Nuclear Regulatory Commission, "Parametric Study of the Potential for BWR

ECCS Strainer Blockage Due to LOCA Generated Debris", NUREG/CR-6224, October 1995.

2-29   ABB-Atom, "A Calculation Model for Reactor Tank Insulation in Case of a Pipe Break", NT 93-034, May 1993 (in Swedish).

2-30   Transco Products, Inc., "Postulation of the Range of Fibrous Insulation Debris Size Generated by High Energy Jet Impact", ITR-93-01N, August 1993.

2-31   American Nuclear Society, "Design Basis for Protection of Light Water Nuclear Power Plants Against the Effects of Postulated Pipe Rupture", ANSI/ANS-58.2-1988, October 1988.

2-32   Organization for Economic Cooperation and Development/Nuclear Energy Agency, *Proceedings of the OECD/NEA, Workshop on the Barseback Strainer Incident, Stockholm, January 26-27, 1994,*1994.

2-33   F. J. Moody, "Prediction of Blowdown Thrust and Jet Forces", Paper 69-HT-31, American Society of Mechanical Engineers, 1969.

2-34   NEDO-32682-A "Utility Resolution Guide for ECCS Suction Strainer Blockage", Vol 1 to 4, October 1998 by BWR Owners' Group.

2-35   NEI 04-07 "Pressurized Water Reactor Sump Performance Evaluation Methodology Revision 0", December 2004 by Nuclear Energy Institute.

2-36   SEA No. 95-970-01-A:2 "Experimental Investigation of Head Loss and Sedimentation Characteristics of Reflective Metallic Insulation Debris", May 1996 by Science and Engineering Associates, Inc. for US NRC.

2-37   PWR Sump Performance Workshop July 30-31, 2002 in Baltimore, Maryland "The Ringhals 2 Experience - The Discovery of a Strong Debris Disintegration Mechanism", Mats Henriksson, Vattenfall Utveckling AB.

2-38   G. H. Hart, "A Short History of the Sump Clogging Issue and Analysis of the Problem", Nuclear News, March 2004.

2-39   H. Utsuno et al., "Application of Compressible Two-Fluid Model Code to Supersonic Two-Phase Jet Flow Analysis", NURETH-13, N13P1368, September 2009.

2-40   JNES/NTCG09-017, "Flow Analysis Concerning to PWR Sump Screen Clogging Issue", February 2010 [in Japanese].

2-41   RSK-Statement, "Requirements for the Demonstration of Effective Emergency Core Cooling during Loss-of-Coolant Accidents Involving the Release of Insulation Material and other Substances", 374th RSK meeting, July 22, 2004.

2-42   Final Report, "Blow-down Investigations on the Performance of Insulating Systems", Battelle Ingenieurtechnik GmbH, August 1995.

2-43   Technischer Bericht NGES1/2002/de/0210, "Experimenteller Nachweis der Gesicherten Sumpfansaugung nach einem Kühlmittelverluststörfall bei KWU-Druckwasserreaktoren", FRAMATOM ANP, 06.11. 2003 (Report in German, details available from I. Ganzmann, ingo.ganzmann@areva.com)

3.   BLOWDOWN / WASHDOWN DEBRIS TRANSPORT

This chapter deals with the transport of insulation debris generated by a LOCA and the transport of other debris from the drywell/upper containment regions into the wetwell, suppression pool, or containment ECCS sump. Three phases of transport can be distinguished: initially, the debris is distributed by blast forces within the containment; during blowdown, the debris is transported by steam and air flow; and finally "washdown" occurs, that is, transport by water. During this phase, transport depends on whether the containment spray system is activated in the plant. If not, washdown is only driven by water streaming out of the leak and condensate accumulating on cold surfaces.

Debris transport depends on various parameters, for example, the insulation type, the layout of the containment compartments, and the location of the break. The following aspects of the problem are addressed in this chapter:

• Transport of debris by blast forces, blowdown (by steam and air), and washdown (by water);

• Influence of insulation type;

• Deposition;

• Effect of floor and stair gratings;

• Effect of vent pipes; and

• Influence of containment layout.

Experiments dealing with transport over weirs are also discussed in this chapter. These tests are important for reactors having structures that would act similarly to weirs as obstacles in the flow path. The transport and settling behavior of insulation debris in water pools in general is discussed in Chapter 4, 'Transport of Containment Pool Debris."

3.1   Debris Transport Evaluation

The debris generation methodology from Chapter 2 is used for estimating bounding quantities of debris that could potentially be generated from dislodged piping thermal insulation, fire barrier materials, coatings, and other materials in the vicinity of the break due to the impingement of the LOCA break jet. Subsequently, the debris would be chaotically propelled by these same jet effluences as the primary system depressurization pressurizes the containment. RCS depressurization flows would dynamically propel debris, which could, due to inertial forces, subsequently impact structures causing the debris to stick to those structures. Larger debris could be captured by structures such as gratings, and whenever and wherever depressurization flows slowed, debris would settle due to gravity. Because containment pressurization results in air and vapor flow into all containment free space, fine debris would also enter all free space. At the end of the primary system depressurization, debris would be dispersed into both the upper and lower containment, where debris would be both inertially captured onto surfaces of all orientations and gravitationally settled onto compartment floors and equipment. These transport processes are referred to as "blowdown transport." For PWRs, some debris would reside on the sump pool floor before the sump pool is established. For BWRs, some

debris would reside on the drywell floor and within the suppression pool.

This LOCA-generated debris, along with the pre-existing containment latent debris, would then be subject to subsequent transport by the drainage of the break overflow, the containment sprays, and the accumulated condensate flow. These transport processes are referred to as "washdown transport." For PWRs, debris that is either initially deposited onto the sump pool floor or washed down from the upper containment to the sump pool would subsequently undergo transport within the sump pool, first as the sump pool fills before the recirculation pumps start, and then within the established sump pool. Debris transport in the containment pool, driven by pump flow is sometimes referred to as recirculation transport. It is discussed further in Section 4. For BWRs, the debris is either deposited within the suppression pool by the depressurization flows through vent downcomers or subsequently by the break, spray, and condensate drainage flows. For BWRs, the blowdown and chugging associated with RCS depressurization have a large influence on transport (and erosion) within the suppression pool, as well as the fact that the ECCS recirculation starts immediately, while for PWRs there is some significant delay. Within this pool of water, debris transport would be governed by various physical processes including the settling of debris in agitated pools, tumbling/sliding of settled debris along the pool floor, re-entrainment of settled debris, lifting of debris over structural impediments, retention of debris on strainers of various orientations, and further destruction of debris as a result of pool flow dynamics, thermal effects, and chemical effects. Some types of debris residing within a pool can be further degraded by pool flow dynamics (e.g., individual fibers can detach from fibrous shreds). Some portion of the debris within the pool would subsequently be transported to, and accumulated on, the recirculation suction strainers.

Blowdown/washdown processes also have the potential to generate additional debris due to the interactions of flows, elevated temperatures, and moisture with various otherwise undamaged materials within containment. These materials include, but are not limited to, unjacketed insulation, unqualified coatings, and equipment labels. For example, a deluge of spray drainage over unjacketed/uncovered fibrous insulation could erode transportable fibers from that insulation. The primary concern has been the generation of coating debris from unqualified coatings, but all potential sources should be considered. Of more recent concern is the potential for corrosion or dissolution of materials in containment and the subsequent formation of precipitates that can deposit on a strainer debris bed, so-called 'chemical effects' (Chapter 5).

Long-term recirculation cooling must operate according to the range of possible accident scenarios. A comprehensive debris transport study should consider an appropriate selection of these scenarios, as well as all engineered safety features and plant operating procedures. The maximum debris transport to the strainer will likely be determined by a small subset of accident scenarios, but this scenario subset should be determined systematically. Many important debris transport parameters will be dependent on the accident scenario. These parameters include the timing of specific phases of the accident (i.e., blowdown, injection, and recirculation phases) and pumping flow rates. The blowdown phase refers to primary-system depressurization. The injection phase corresponds to ECCS injection into the primary system, a process that subsequently establishes the PWR sump pool. The recirculation phase refers to long-term ECCS recirculation.

The physical processes of all these transport phases are so varied and complex that detailed analysis is difficult at best and is typically considered to be too complex to pursue, except in specific areas. Because the primary analytical objective is the conservative bounding of the maximum quantity of debris by type and size category, the more difficult-to-analyze processes can be conservatively bounded, while processes more amenable to analysis can be more realistically yet conservatively estimated. An analytical approach referred to as the "logic chart" approach was developed during the BWR DDTS [3-1]. It uses event-tree models to decompose the complex overall process into many smaller steps, some of which may be solved analytically or estimated based on data obtained from small-scale experiments. In quantifying such a chart, conservatively estimated fractions are used for steps where data or analyses are not available to resolve that step, and more realistic fractions are used for steps where data or applicable analyses are available. The

multiplication of step fractions throughout the logic chart results in a distribution of debris following complete transport that is conservative with respect to debris accumulation on the strainer. An example logic chart is shown in Figure 3-1.

The transport of each debris type and size category should be considered separately because each has unique transport characteristics. The important transport characteristics are whether the debris is buoyant, prone to settling, or likely to be transported as relatively uniformly dispersed suspended debris. The size categories are (1) fines that remain suspended, (2) small-piece debris that is transported along the pool floor, (3) large-piece debris with the insulation exposed to potential erosion, and (4) large debris with the insulation still protected by a covering, thereby preventing further erosion.

The level of detail employed by the analyst depends on resources and resolution tolerance to conservatism. The easiest analysis uses the conservative assumption of complete transport and accumulation onto the strainer, but this oversimplification typically produces unacceptable head loss at the strainer. When complete transport of debris is assumed, and the resulting strainer design is verified by testing, then the debris should be added to the test flume in smaller batches. This method of adding debris will envelope the thin bed effect. A more detailed evaluation could use CFD simulations to predict flow metrics of a PWR sump pool in combination with experimental data to determine whether a given size and type of debris would transport and/or conducting small-scale plant-specific experiments. It can be difficult to benchmark CFD analyses with physical effects due to scale effects. Appendix E provides more information on CFD analyses. The remaining subsections discuss (1) blowdown/washdown debris transport, (2) sump or suppression pool transport, and (3) erosion of containment materials and further degradation of debris. The final subsection discusses the importance of identifying the size characteristics of the debris estimated to arrive at the recirculation strainers (i.e., characteristics that affect debris accumulation).

Debris Size	Blowdown Transport	Washdown Transport	Washdown Entry Location	Pool Fill Up Transport	Pool Recirculation Transport	Debris Erosion in Pool	Path	Fraction	Deposition Location
		Trapped Above					1		Not Transported
						Erosion Products	2		Sump Screen
					Stalled in Pool	Remainder	3		Not Transported
			Sump Area		Transport				Sump Screen
						Erosion Products	4		Sump Screen
					Stalled in Pool	Remainder	5		Not Transported
	Deposited Above		SG #4		Transport		6		Sump Screen
							7		Sump Screen
					Stalled in Pool	Remainder	8		Not Transported
			Eq. Room		Transport		9		Sump Screen
						Erosion Products	10		Sump Screen
					Stalled in Pool	Remainder	11		Not Transported
		Transports to Pool	SG #3 (Stairs)		Transport		12		Sump Screen
						Erosion Products	13		Sump Screen
					Stalled in Pool	Remainder	14		Not Transported
			Opposite Side		Transport		15		Sump Screen
						Erosion Products	16		Sump Screen
					Stalled in Pool	Remainder	17		Not Transported
			SG #2 (Elevator)		Transport		18		Sump Screen
						Erosion Products	19		Sump Screen
					Stalled in Pool	Remainder	20		Not Transported
			SG #1 (RV Cavity)		Transport		21		Sump Screen
			To Near Screen				22		Sump Screen
						Erosion Products	23		Sump Screen
					Stalled in Pool	Remainder	24		Not Transported
	Break Room Floor		Away From Screen		Transports		25		Sump Screen
			Inactive				26		*Inactive Pools*
Small Pieces			To Near Screen				27		Sump Screen
						Erosion Products	28		Sump Screen
					Stalled in Pool	Remainder	29		Not Transported
	Sump Floor		Away From Screen		Transports		30		Sump Screen
			Inactive				31		*Inactive Pools*

POOL TRANSPORT LOGIC CHART

FIBROUS DEBRIS

Figure 3-1. Logic Chart for Sump Pool Debris Transport

3.2   Blowdown/Washdown Debris Transport

This section discusses the blowdown and washdown transport methodology that provides an estimate for the transport of debris from its points of origin to the containment pool. The transport analysis consists of two components: blowdown debris transport, where the effluent from a high-energy pipe break destroys insulation near the break and then transports that debris throughout containment; and washdown debris transport due primarily to operation of the containment sprays. Along the debris-transport pathways, substantial quantities of debris would come into contact with containment structures and equipment on which the debris can be retained, thereby preventing or delaying further transport. The blowdown/washdown debris-transport analysis provides the source term for the subsequent recirculation transport (i.e., within a PWR pool or a BWR suppression pool), such as RMI debris where the primary difference would be the mechanisms of debris capture. The methodology would also be similar for particulate insulation (e.g. calcium silicate) where the primary difference might be in the erosion process. Further detailed guidance includes (1) a detailed blowdown/washdown transport analysis performed for a PWR reference plant that had a Westinghouse reactor and large-dry containment, Appendix VI of NRC-SER for NEI 04-07[3-2] and (2) the DDTS [3-1].

3.2.1   Blowdown/Washdown Debris-Transport Phenomenology

A spectrum of physical processes and thermal-hydraulic phenomena govern the transport of debris within containment. The physical processes involved range from the transport/deposition physics of aerosols to the dynamic impaction of larger pieces of debris onto containment surfaces. The design of a particular containment will influence the flow dispersion, thereby affecting debris transport and deposition. Because of the energetic blowdown flows following a LOCA, insulation destruction and subsequent debris transport are rather chaotic. For example, on the one hand, a piece of debris could be deposited directly near the sump strainer or take a much more tortuous path, first going to the dome and then being washed back down to the sump by the sprays. On the other hand, a piece of debris could be trapped in any number of locations. Aspects of debris transport analysis include characterization of the accident, design and configuration of the plant, generation of debris by the break flows, and both air- and water-borne debris dynamics.

Many features in NPP containments significantly affect the transport of insulation debris. As the RCS depressurizes, the break effluents will flow towards the pressure suppression pool in BWRs and towards the large containment dome in PWRs. Structures such as gratings located in the paths of the dominant flows likely would capture substantial quantities of debris. For PWRs, the lower compartment geometry, such as open floor areas, ledges, structures, and obstacles, defines the shape and depth of the sump pool area and is important in determining the potential for airborne debris to deposit directly onto the sump floor. Furthermore, the relative locations of the sump, LOCA break, and drainage paths from the upper regions to the sump pool are important in determining the distribution of debris deposition onto the sump floor. For BWRs, the geometry of the drywell floor and entrances into the vent downcomers influence the transport of debris into the suppression pool.

Transport of debris is strongly dependent on the characteristics of that debris, including the type (insulation, coating, dust, etc.), size distribution, and form of the debris. Each type of debris has its own set of physical properties, such as density, specific surface area, buoyancy (including dry, wet, or partially wet), and settling velocity in water. Pooled water can form within upper containment regions, e.g., the drywell floor in a BWR or a refueling pool in a PWR. The size and form of the debris, in turn, depends on the method of debris formation (e.g., jet impingement, erosion, aging, and latent). The size and form of the debris affect transport of the debris to the sump or suppression pool. For example, fibrous debris may consist of individual fibers or large sections of an insulation blanket, and all sizes between these two extremes.

The complete range of thermal-hydraulic processes affects the transport of insulation debris, and the containment thermal-hydraulic response to a LOCA includes most forms of thermal-hydraulic process. Debris transport is affected by a full spectrum of physical processes, including particle deposition and re-suspension for airborne transport and both settling and re-suspension within calm and turbulent water pools for both buoyant and non-buoyant debris. The dominant debris-capture mechanism in a rapidly moving flow likely would be inertial capture; however, in slower flows, the dominant process likely would be gravitational settling. Much of the debris deposited onto structures would likely be washed off by the containment sprays or possibly even by condensate drainage. Other debris on structures could be subject to erosion. Relatively complete discussions of the range of transport phenomena are found in the BWR and PWR Phenomena Identification and Ranking Table (PIRT) panel reports [3-3], [3-4]. The BWR DDTS and the PWR SE Appendix VI provide analysis processes that focus on the phenomena determined to most govern the transport processes.

3.2.2 *PWR Blowdown/Washdown Transport*

PWR Blowdown Containment Dispersion

Following a break, primary system depressurization effluents flow toward the upper containment dome in a PWR. For large dry and sub-atmospheric containments, the SG compartments are designed to direct the flows directly into the upper containment. For ice condenser containments, the flows are directed into the ice condenser banks, which exit into the upper containment. Debris generated by a LOCA would be carried by these flows until the debris was either captured by or deposited onto a structure, or the debris gravitationally settled onto equipment and floors. The dominant deposition mechanism for larger airborne debris ejected from a SG compartment into the upper containment dome would be gravitational settling. For very fine particulate, the containment spray fallout may become the dominant mechanism. The reference plant blowdown transport analysis presented in Appendix VI of the US NRC SE of NEI 04-07 [3-2] provides further guidance for conducting a detailed debris dispersion analysis.

The source of all insulation debris is the region immediately surrounding the LOCA break, which is typically a SG compartment. This region would be subject to the most violent containment flows where the primary debris capture mechanism would be inertial capture. For these reasons, the transport of debris within the region of the pipe break should be solved separately from that of the rest of the containment.

The first step in determining the dispersal of debris near the break is to determine the distribution of the break flow from the region, specifically, the fractions of the flow directed to the dome vs. other locations. In the Appendix VI analysis of [3-2], the containment thermal-hydraulics code MELCOR was used to determine the flow distribution within and out of the break SG compartment for a large dry PWR containment.

The LOCA-generated debris not captured within the region of the break would be carried away from the break region by the break flows. The primary capture mechanism near the break would be inertial capture or entrapment by a structure such as a grating. The break-region flow that occurred immediately after the initiation of the break would be much too energetic to allow debris simply to settle to the floor in that region.

The inertial capture of fine and small debris occurs when a flowpath changes directions, such as flowpaths through doorways from a SG compartment into the sump-level annular space. These flowpaths often have at least one 90° bend, and because the structural surfaces are wetted by steam condensation and the liquid blowdown from the break, a portion of this debris could stick to the impacted surfaces. Debris-transport experiments conducted at CEESI [3-1] demonstrated an average capture fraction of 17% for fine and small debris that make a 90° bend at a wetted surface. The flow in any of the flowpaths could encounter bends as the break effluents interact with various equipment and walls.

Platform gratings within the break region SG compartment will capture substantial amounts of debris, even if the gratings do not extend across the entire compartment. The CEESI debris-transport tests demonstrated that an average of 28% of the fine and small debris was captured when the airflow passed through the first wetted grating that it encountered, and that an average of 24% was captured by the second grating. The large and intact debris would, by definition, be trapped completely by a grating. In addition, equipment such as beams and pipes were shown to capture fine and small debris. In the CEESI tests, the structural congestion of a typical BWR drywell was simulated using gratings, beams, and piping. Air-jet generated fibrous debris was driven through this structural simulation to determine realistic capture fractions that could be applied to containment analysis. An average of 9% of the debris passing through the entire test section was captured.

To evaluate transport and capture within the break region, the evaluation is best separated into many smaller problems that are amenable to resolution. Appendix VI of [3-2] analysis accomplished this separation using a logic-chart approach similar to that in Figure 3-1, but based on the structural details of the break region compartment. The headers across the top of the chart alternated among volume capture, flow split, and junction capture as the debris transport process progressed through the nodalization scheme. The nodalization scheme was constructed to place the gratings at junction boundaries. Chart header questions asked (1) how much debris would be captured in a specific volume, (2) what is the debris transport distribution at a flow split, and (3) how much debris would be captured at a flow junction between two volumes? This analytical approach is rather detailed; therefore, the interested reader is directed to the detailed example presented in Appendix VI of [3-2] for a more detailed discussion. The answers were based on estimates of inertial capture on structures within a sub-volume region and at gratings at specific junctions, and the airflow distributions at junction flow splits. For fine and small-piece debris, it is reasonable to assume that the debris split is approximated by the flow split. For large and intact-piece debris, the debris split may differ substantially from the flow split, depending on the geometry. The break region chart is used to track the progress of small debris from the pipe break until the debris is captured or is transported beyond the compartment. Each application of this methodology should develop a plant-specific chart.

Outside the break region compartment, debris dispersion and capture throughout containment could also be handled by such detailed modeling, but the effort would be highly resource-intensive. Figure 3-2 shows an example of a small section of a potentially very large logic chart to further illustrate the number of decisions possible in a detailed transport analysis. In this chart, the regions are designated as Region j and Region j+1, indicating that the total number of regions into which containment was subdivided is determined by the depth of the analysis and could be substantial. A simpler method, used in the reference plant study, is based on dispersion of the debris by free volume followed by surface orientation within specific free-volume regions. First the free volume of each specific volume region is divided by the total containment free volume and then these fractions are multiplied by the quantity of each debris type and size category to arrive at distributions for dispersing the debris among the volume regions. Then, in a similar manner, area fractions are used to distribute the debris among the surface areas within each volume region. Dispersion distributions should be based on actual volumes and areas and adjusted with weighting factors based on engineering judgment. Obviously, debris will preferentially settle to the floor, hence the weighting factors should be adjusted to make most of the debris deposit onto the floors; however, some of the fines will stick to vertical surfaces. Wetted versus relatively dry areas are used to distribute debris within areas impacted by containment sprays and areas not impacted by the containment sprays.
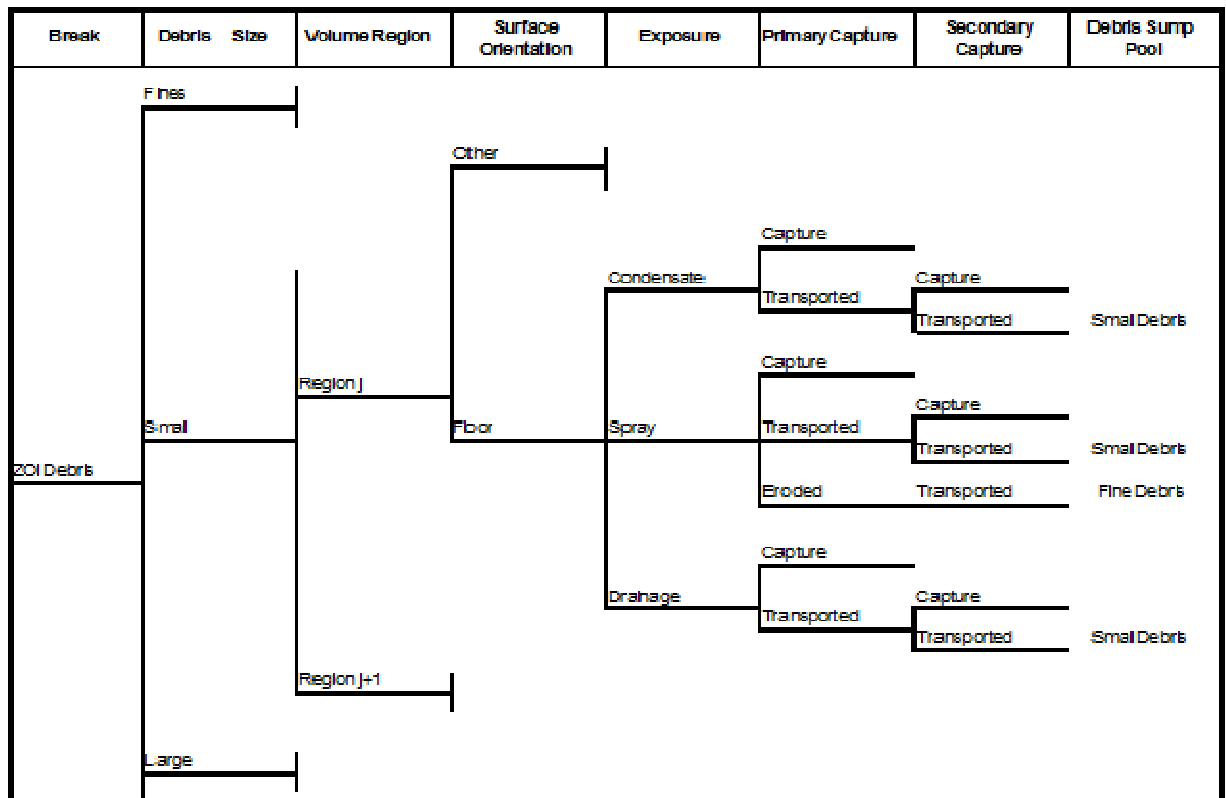
Figure 3-2: Example of a Section of a Debris Transport Chart

Once debris is dispersed to a specific volume region, it is assumed to have deposited within that region. Some residual fine debris could remain airborne in regions not affected by the sprays; however, the total quantity of this residual airborne debris is not expected to be significant. The surface area within each volume region is subdivided into subsections reflecting both the differing surface orientations and the extent of their exposure to moisture. The floors are separated from all of the other surfaces because they would receive gravitationally-settled debris. The spray water would not accumulate on the walls, ceilings, and equipment. The surface moisture conditions are considered in the analysis: surfaces wetted directly by the containment sprays, surfaces not directly sprayed but washed by spray drainage (most likely floor surfaces), and surfaces wetted only by steam condensation. All surfaces are likely to be wetted by condensation. The surface exposure determines the likelihood that debris deposited onto that particular surface would subsequently be transported by the flow of water. This process also uses a system of weighting factors to implement engineering judgment.

PWR Containment Spray and Condensate Drainage Washdown

Debris deposited throughout containment would subsequently be subjected to potential washdown by the containment sprays, by drainage of the spray water to the sump pool, and (to a lesser extent) by drainage of condensate. Debris on surfaces hit directly by the sprays would be much more likely to be transported with the flow of water than would debris on a surface that is merely wetted by condensation. The transport of debris entrained in spray water drainage is not as easy to characterize. If the drainage flows were substantial and rapidly flowing, the debris likely would be transported with the water. However, at some locations, the drainage flow could slow and be shallow enough for the debris to remain in place. That is, the force that the water exerts on a piece of debris depends on both the localized velocity of the water flow and on the projected contact surface area. When the water depth is shallow, then only a portion of the piece of debris (depending on its size) may be in contact with the water and the water would simply flow around the piece. With deeper water, a sheeting effect can be effective at moving the debris, and when the debris is completely submerged, the water velocity may slow accordingly. Flows will speed up nearer the drains. As drainage water drops from the pipe flow, containment spray or condensation from one level to another, as it would through floor drains, stairwells, or by falling over floor edges, the impact of the water on the next lower level could cause sufficient splashing to transport debris beyond the main flow of the drainage, thereby essentially capturing the debris a second time. In addition, the flow of water could further erode the debris, generating more fine debris. These considerations should be factored into the analysis.

The drainage of spray water from the location of the spray nozzles down to the sump pool and condensation flow should be included in the transport analysis, such as identifying areas that would not be affected by the sprays, the water drainage pathways, likely flowpaths for drainage water to the sump pool, and locations where drainage water would plummet from one level to the next. A key result of the washdown analysis is an estimation of how much debris is washed to the sump pool via each of the main drainage pathways, based on the assumption that the debris is uniformly mixed with the flows entering the pool. This information is typically needed for the evaluation of sump pool debris transport.

The spray and condensate drainage analysis can contribute to the upstream effects analysis, which addresses the potential holdup of drainage water in the upper containment to the extent that the holdup can adversely affect the sump pool water level, which can, in turn, affect strainer submergence, vortexing, and recirculation pump NPSH. The blockage of any water drainage could result in water holdup, but the primary locations of concern are the refueling pool drains because the refueling pool represents a substantial potential volume of water. An adequate understanding of water drainage from the upper containment to the sump pool is needed to ascertain potential locations for water holdup, as well as debris washdown transport.

Certain types of insulation debris could potentially continue to erode to form smaller debris during containment washdown. Experiments conducted in support of the DDTS analysis [3-1] demonstrated that fibrous insulation debris could be eroded further by the flow of water. The primary concern of the DDTS analysis was LDFG debris deposited directly below the pipe break and, therefore, inundated by the break overflow. Debris erosion in that case was substantial (i.e., ~9 %/h at full flow). Debris erosion due to the impact of the sprays and spray drainage flows was certainly possible but was found to be much less significant. The DDTS concluded that <1% of the LDFG was eroded due to direct impact of the containment sprays. Debris caught within cascading flows of accumulated spray drainage could be subjected to more forceful erosion than that caused by direct spray droplets, although in many situations falling water flows could simply push the debris aside. Debris erosion due to condensation and condensate flow was neglected. Debris with its insulation still in the cover was not expected to erode further. For RMI debris, erosion was not a consideration. However, for microporous insulation such as calcium silicate or Min-K, the washdown erosion has not been determined, and the outcome could vary substantially with the type of insulation and even by the insulation's manufacture process (e.g., one vendor's calcium silicate readily dissolves while

another's does not). The key PWR debris erosion process for evaluation would be erosion of debris that was impacted directly by the sprays and possibly debris layered on any gratings located below the break overflow. The erosion of debris on the sump pool floor would typically be evaluated under the sump pool transport processes, and most of the debris located directly below the break likely would be pushed away from the break area and become part of the sump pool.

Because the byproduct of the erosion process is very fine and easily transportable debris, the process should be evaluated. All erosion products should be assumed to transport to the sump pool. Furthermore, this debris would also likely remain suspended in the sump pool until filtered from the flow at the sump strainers. Therefore, even a small amount of erosion could contribute significantly to the likelihood of strainer blockage.

To estimate the volume of debris eroded, the volume of small and large debris impacted by the sprays should be estimated first. In the reference plant study, 1% of the small- and large-piece debris directly impacted by the sprays was considered to have eroded on the basis of the DDTS conclusion that erosion by sprays was <1%. Note that the 1% value was based on small-scale tests in which the spray flow rates were scaled to the volunteer BWR plant. If the spray flow rate were increased, the erosion rate could possibly increase; however, the 1% erosion value represented a conservative conclusion for a minor rate of erosion. Even if the spray-driven rate of erosion was increased, its contribution to the overall erosion within containment would likely remain relatively minor compared to the recirculation pool erosion. Note that erosion does not apply to fine debris because that debris is already fine, and it does not apply to intact debris because the cover would likely protect the enclosed insulation.

Retention of debris on surfaces during washdown needs to be estimated for the debris postulated to be deposited on each surface (i.e., the fraction of debris that remains on each surface). The estimates should be based on a combination of experimental data and engineering judgment. Generic assumptions used in the reference plant study included:

- For surfaces that would be washed only by condensate drainage, nearly all deposited fine and small debris would likely remain. The study assumed 1% of the fibrous debris would be washed away (99% retention on the surface) in a realistic central estimate and 10% for an upper-bound estimate.

- For surfaces hit directly by sprays, the DDTS assumed 50% and 100% were washed away for the central- and upper-bound estimates for small fibrous debris, respectively, but that large and intact debris likely would not be washed down to the sump pool (complete retention).

- For surfaces not sprayed directly but that subsequently drain accumulated spray water, such as floors close to spray areas, the retention fractions are much less clear. These fractions likely would vary with location and drainage flow rates and, therefore, should be area-location specific, with more retention for small pieces than for fine debris.

- All erosion products are completely washed to the sump pool.

The overall blowdown/washdown transport fraction is the total quantity of debris entering the sump pool divided by the total volume of insulation generated within the ZOI.

In conclusion, the reference plant study in Appendix VI of NRC-SER-2004 [3-2] developed a methodology that considered both transport phenomenology and plant features, and that divided the overall complex transport problem into many smaller problems that are either amenable to solution by combining experimental data with analysis or able to be judged conservatively based on the foundation of debris-transport knowledge. The reference plant methodology resulted in predicted transport fractions that were conservative. The conservatism in the transport decisions is related to the availability of applicable data; without data, the results should be conservatively hedged toward transporting the debris to the sump pool. The results also depended upon the analytical objective (i.e., bounding versus realistic results). Plant-specific analyses must consider a range of break locations.

In performing blowdown/washdown analyses, it is important that (1) the debris-size categories match the characteristics of the debris-transport behavior, (2) the break region and the break region exits are analyzed in substantial detail because a significant portion of the debris capture may occur there, (3) the containment spray drainage patterns should be determined to support the washdown analysis and to determine where the debris would enter the sump pool and how the spray drainage would affect sump pool turbulence, and (4) the spray-drainage pathways where potential debris blockage might occur should be identified. The complexity of a plant-specific methodology could vary significantly from one plant to the next.

In general, for fine LOCA-generated debris, it is likely that realistic analysis will show that a high percentage of the fines would be transported to the sump pool via the spray drainage flows. The fines retained in the upper containment would be the fines blown into areas not impacted by the containment sprays or spray drainage. Transport fractions tend to decrease as the debris size increases. Realistically speaking, RMI might be expected to transport less readily than would fibrous debris because it is heavier. During the resolution of GSI-191, the licensees typically chose to make highly conservative blowdown/washdown assumptions rather than perform the detailed analyses outlined herein. This conservative approach was not unreasonable, considering that the majority of the fines blown into the upper containment would be predicted to wash down to the sump pool, and that the majority of the larger debris residing or entering the sump pool would typically settle in the sump pool rather than accumulate on the strainer.

3.2.3   BWR Blowdown/Washdown Transport

BWR Blowdown Containment Dispersion

The physical processes governing BWR blowdown dispersion are basically the same as those described in Section 3.2.2 for PWRs. Pressure relief in BWR containment results in primary system depressurization with flows through the downcomer vents to the suppression pool. Debris generated by a LOCA would be carried by these flows, with portions of the debris being captured along the way by deposition onto structures or by gravitationally settling onto equipment and floors. The blowdown dispersion within a BWR drywell was studied in the DDTS.

BWR containments differ from PWR containments in both size and design. The BWR suppression pool allows BWR containment volumes to be significantly smaller than PWR containments. The break discharge from a BWR primary system, Main Steam Line (MSL), or feedwater line break would flow directly toward the vent downcomers leading to the suppression pool. Gratings rather than solid floors typically separate the elevation levels in BWR drywells. A break above a continuous grating would trap the larger debris. Debris trapped on a grating directly below the break overflow would be subjected to substantial erosion. In addition to the break flows, the containment sprays would transport debris. Depressurization flows entering a vent downcomer may undergo turns, resulting in inertial debris capture at the vent entrances or debris fallout onto the drywell floor. A pool of water would form on the drywell floor, with its depth governed by the elevation of the entrances into the vent downcomers. The transport of debris in the drywell floor pool could be evaluated similarly to PWR sump pool transport. A CFD code was used in the DDTS to simulate the drywell floor pool for each of the BWR Mark I, II, and III designs. Debris transport within a BWR suppression pool is unique to BWRs and is discussed in Chapter 4.

The DDTS employed the logic-chart approach to decompose the overall transport process into individual steps, similar to the evaluation process described in the preceding section for PWRs. Typically, these charts treat each debris type and size category and each break scenario separately. The analyst can choose the level of detail based on the application requirements and the information available.

A system level code, e.g., MELCOR, can be used to estimate containment conditions, flow dispersions, rates of flow, flow composition, condensation rates, etc. This information is useful when applying engineering judgment to transport models. The dominant debris capture mechanisms considered were inertial capture from fast moving flows and gravitational settling once flows slowed down.

Inertial capture of flow-driven fibrous debris was studied in the DDTS [3-1]. The CEESI facility air jets were used to destroy fibrous insulation blankets and then to carry the debris downstream through a series of structural obstacles based on prototypical BWR containment congestion. The tests demonstrated the ability of structural components to capture debris. The average overall transport fraction for small debris in the CEESI tests was 33% of the total debris generated (i.e. ~2/3 of the generated debris was captured, primarily by inertial impaction) within the test facility. Gratings were found to be the most effective debris catchers. Figure 3-3 shows a plot of the available debris capture data on a specific test grating, where the capture efficiency is plotted versus the debris loading approaching the grating. The capture efficiency did not seem to depend significantly upon the debris loading but did depend upon surface wetness. MELCOR analyses showed that steam condensation onto containment surfaces would happen relatively rapidly. The average fractions of small debris captured by each test structure component are shown in Table 3-1. The first continuous test grating stopped almost all of the larger debris but the capture fraction for that grating was not obtained due to the failure of the test mister system to adequately wet the continuous grating (i.e., this grating illustrated dry behavior). The subsequent two gratings in the test were successfully wetted and it was found that second of these two wetted gratings captured less efficiently than the first wetted grating (downstream of the first grating that failed to become wetted), as might be expected as the second wetted was loaded with finer debris that had passed through the first wetted grating. The 90-degree bend between two test chambers captured debris. The bend was maintained wet by a mister in the auxiliary chamber. About 17% of the debris entering the second auxiliary chamber was trapped on the chamber wall as a direct result of the bend. The pipes and I-beams captured a smaller, but still substantial, amount of debris.
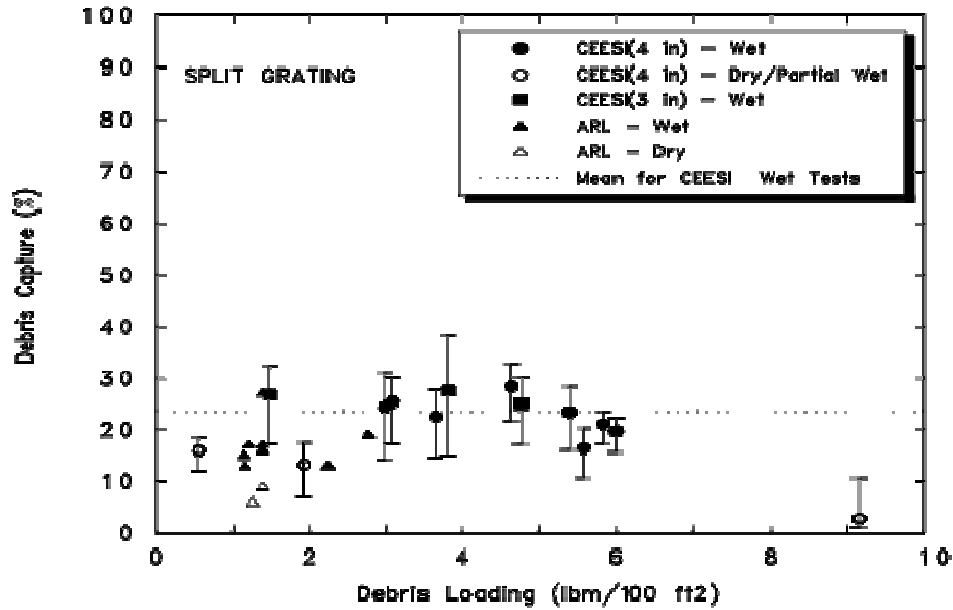
Figure 3-3. Capture of Small Debris by a Grating

Table 3-1: Small Debris Capture Fractions

Structure Type	Debris Capture
I-Beams and Pipes (Prototypical Assembly)	9%
Gratings	
V-Shaped Grating	28%
Split Grating	24%
90° Bend in Flow	17%

Following the blowdown process, the containment sprays and/or condensate drainage would wash debris from surfaces and down into the drywell pool with overflow into the vent downcomers. Debris on surfaces hit directly by the sprays would be much more likely to transport with the flow of water than would debris on a surface that is merely wetted by condensation.

In PWRs, water would often flow across a floor to a floor drain but in BWRs the sprays pass through a grating from one level down to the next level. The DDTS included a small-scale experiment in which debris was placed on top of a prototypical section of grating and then exposed to water spray to study the erosion of the fibrous debris at various flow rates and to determine the ability of debris to remain on the grating. These tests, described in Volume 2 of [3-1], demonstrated that nearly all captured fibrous debris (generally) smaller than the grating openings would be washed through the grating, and that larger debris remaining trapped on top of the gratings would erode into finer debris, with the erosion fraction dependent upon flow rate. For a full characteristic break overflow rate, the debris directly under that flow eroded at approximately 9%/hr. Debris erosion due to the impact of the sprays and spray drainage flows was certainly possible but was found to be much less significant. The DDTS concluded that <1% of the LDFG was eroded due to the containment sprays. The spray experiments were carried out for 30 min., which was estimated to be the maximum credible time spray would be operated following a LOCA in a BWR. Furthermore, the <1% result was based on tests with debris large enough to not be washed down through the support grating, thereby distinguishing erosion from the washdown transport fraction typically associated with fines and small piece debris. Debris erosion occurring because of condensation and condensate flow was neglected. Debris with its insulation still in the cover was not expected to erode further. These tests did not test the erosion of microporous insulation debris.

The DDTS studied the turbulence levels within a drywell pool for each of the BWR Mark I, II, and III containment designs using a CFD code (Volume 3 of [3-1]). The turbulence levels were correlated with debris settling by using the same CFD code to simulate flume tests that studied debris settling within a pool. That is, if the turbulence levels as modeled with this code were sufficiently high to keep debris from settling within the test flume, then the debris would not likely settle within the drywell pool. The turbulence levels were studied for scenario conditions where the drywell pool received full break-water overflow and for conditions where the break steamed so that the pool was driven by condensate and/or spray drainage. Under full flow the debris would most likely tend to transport into vent downcomers, but under more quiescent conditions, the debris could remain in the drywell pool.

3.3 Review of Operational Events and Debris Transport Experiments

The following incidents and experiments were analyzed with regard to the transport of insulation debris:

- The incident at Barsebeck-2 in July 1992;

- Blowdown experiments carried out in the HDR Kahl (Germany) during the seventies and eighties;

- Experiments at the fossil-fueled power plant Karlshamn (Sweden) that were performed after the incident at Barsebäck by ABB-Atom utilizing scaled containment structure models to investigate the release and transport of insulation debris;

- Experiments performed for the German utility HEW (Hamburg Electrizitatswerk) at GKSS (Gesellschaft fur Kernenergieverwertung in Schiffbau und Schiffahrt) to study the transport behavior of fibrous insulation debris in water;

- Tests performed by ABB-Atom at NPP Oskarshamn to investigate the transport by the containment spray system;

- Experiments at the Alden Research Laboratory (ARL) to determine the transport and entrainment characteristics of various types of insulation material and other debris;

- Experiments described in NUREG/CR-2982, "Buoyancy, Transport, and Head Loss of Fibrous Reactor Insulation" [3-15]; and,

- Experiments described in NUREG/CR-6773, Integrated Debris Transport Tests [3-19].

Some of the experiments are applicable to blowdown debris transport and some are applicable to debris transport in recirculation flow in the containment pool. It was decided to discuss both types of experiment here.

3.3.1 *Incident at Barsebäck-2 in July 1992*

Description. A more detailed description of this incident is given in Appendix B to this report. Of special significance with respect to this chapter and debris transport is the containment layout. In Barsebäck-2, the containment is basically an upright cylinder with the drywell in the upper part and the wetwell directly beneath. The reactor pressure vessel is located at the top of the drywell. The drywell and the wetwell are connected by vertical pressure relief pipes, the openings of which are flush with the drywell floor, where they are covered with gratings. No other obstacles are installed at the openings of the pressure relief pipes.

The incident started with the spurious opening of a SRV in the lower part of the drywell, whose discharge was directly to the drywell atmosphere at a pressure of 3.0 MPa (440 psi). Only steam was ejected by the valve. The containment spray system was started automatically shortly afterwards.

About 200 kg (440 lb) of fibrous insulation debris was generated [3-5], [3-6]. Approximately

50% of it reached the wetwell, resulting in a large pressure loss at the strainers about 70 minutes after the beginning of the event. Gratings in the drywell did not effectively hold back the insulation material.

The distribution of the insulation debris found in the drywell was approximately as follows:

• 50% on the structural steel, mainly concentrated within three areas: inside the drywell "gutter"; near the outer containment wall; and on and near the grid plates over the blowdown pipes;

• 20% on the wall next to the affected pipe, from which most of the insulation originated, and on components around the safety valve;

• 10% on the wall opposite the affected pipe;

• 12% on the walls above the grating lying above the safety valve;

• 8% on the grating above the safety valve.

The insulation material was transported by steam and air flow generated by the blowdown, and by water from the containment spray system. It cannot be determined how the transport developed with respect to time and whether the major part of the debris found in the wetwell was transported there by blowdown or washdown.

The following phenomena were observed:

• Generation and transport of large amounts of fibrous insulation debris;

• Short-term transport of this debris by steam and air blast; and

• Long-term transport of this debris by water delivered by the CSS. The debris was transported from the break location in the lower part of the drywell through pressure relief pipes into the wetwell (sump).

The extent of damage and the extent of transport from the drywell to the wetwell appear remarkably large given the small leak size (one failed valve) and the low reactor pressure.

Applicability and appropriate use of data. These phenomena can be expected at all NPPs with a similar containment layout and similar insulation material. Knowledge about the general behavior of fibrous insulation debris is gained for all NPPs of this type from this incident.

Major uncertainties. The development of the transport with respect to time and the fraction of the insulation debris transported into the wetwell within a short time by blowdown effects are not known.

3.3.2   *Blowdown Experiments at the HDR Facility in Germany*

Description. A detailed description of the test facility and experiments is found in Appendix D to this report and in NUREG-897 [3-7].

The objective of these tests was to determine the capability of NUKON insulation to withstand a high pressure steam-water blast and to determine the size distribution of the debris. Since the original insulation was badly damaged in the first experiments, four other insulation types were tested in search of a robust solution:

• Conventional insulation (mineral wool reinforced with wire mesh and jacketed with galvanized carbon steel sheet);

• Foam glass insulation;

• Fiberglass encapsulated in steel cases; and

• Insulation mats with glass wool inserts and pure textile or wire-weave strengthened covers.

For two tests, the behavior of NUKON insulation blankets was investigated by attaching them to

a strut and the ceiling in the vicinity of the nozzle [3-8]. MIRROR RMI was also tested in one HDR test [3-7].

The break compartment was situated about 25 m (82 ft) above the sump inside the tall and slim containment of the HDR, which measures about 20 m (66 ft) in diameter and 60 m (200 ft) in height. It is subdivided into a larger number of compartments than are modern NPPs. Therefore, the water had to pass four floors on the way from the break nozzle to the sump.

The following observations were made regarding transport of insulation material and other debris:

- Debris of every type was found in the break compartment as well as in adjacent rooms.

- Pieces of RMI were only found in the break compartment. However, only one test specimen was installed and destroyed during the MIRROR insulation test. Therefore, the results are not really representative of the behavior of large amounts of RMI debris.

- After the first blowdown experiment, conventional mineral wool insulation was torn off the pipes. The debris was caught in large flocks at railings and at other obstacles, as well as in stagnation areas.

- Almost no insulation material or other debris was found in the sump four floors beneath the break compartment. However, the distribution of individual fibers was not determined; therefore, individual fibers, which are almost invisible, could have reached the sump.

In evaluating these results, recognize that containment was subdivided into many compartments and that the containment spray system was not activated. Released insulation material was, therefore, transported merely by steam and water flowing from the break nozzle and by displaced air.

The following phenomena were observed:

- Generation of various types of insulation debris, and
- Blowdown transport inside a real containment.

Applicability and appropriate use of data. The results can be used to gain insights into the transport behavior of various types of insulation debris by steam and air blast. They can be applied to containments that are subdivided into a large number of compartments.

Major uncertainties. Apart from the tests with NUKON and MIRROR RMI, no detailed information about the insulation materials used in the HDR is available.

- In none of the experiments could the total amount of insulation material previously installed be found in the containment afterwards. Therefore, it cannot be concluded that no fibers were transported into the sump. However, no visible parts of the debris were found there.

- The distribution of insulation debris within compartments adjacent to the break nozzle was not quantified.

3.3.3   Experiments Performed by ABB-Atom at Karlshamn

Description. Tests were performed by ABB-Atom to determine the relative distribution of insulation debris in containment. The experiments took place at the Karlshamn fossil-fueled power plant utilizing scaled and vertically connected test volumes which had plates and gratings to simulate compartment connections representative of Swedish BWRs with external recirculation pumps and Series 69 German BWRs ([3-9] to [3-13]). Figure 3-4 illustrates the experimental layout.

Fibrous insulation material was attached to a pipe in the upper section of the containment simulation model. It was exposed to a steam jet, the pressure of which is not exactly known. The steam was produced in a vessel in the power plant at a pressure of about 8.0 MPa (1160 psi) and transferred to the nozzle from the steam source via a pipeline 75 m (250 ft) long. The insulation debris generated was distributed by the steam flow and displaced air. Fig. 3-4 illustrates the test setup for Swedish BWRs, and the distribution of insulation debris at the blowdown experiments is listed in Table 3-2.

The main results were as follows:

- Most of the fibrous insulation debris was distributed in the upper parts of the containment. It was held back by gratings and adhered to walls at which steam condensed, or accumulated in areas of low-flow velocity.

- Shreds of insulation material adhered to the inner side of the blowdown pipes.

- Only minor quantities of the debris reached the wetwell. For both containment types investigated, the amount was less than or equal to approximately 3 percent of the total quantity of dislodged insulation. The share of debris transported into the wetwell depended on the steam flow rate: at higher velocities, more debris was transported.

Note that in these experiments, the insulation material was transported by steam and air, not by water.
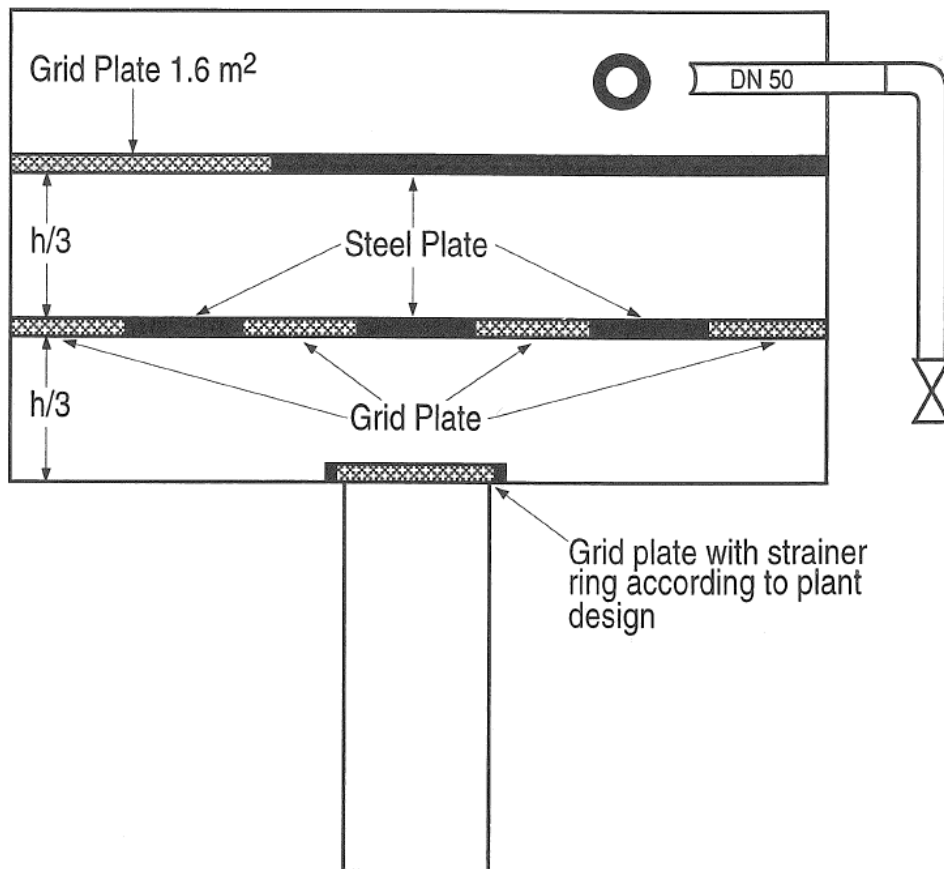
Figure 3-4: ABB-Atom Containment Experimental Arrangement

From the test results at Karlshamn [3-13], the authors concluded that in a plant of the Barsebäck

type at a maximum steamline break, about 10% of the dislodged insulation material would be transported into the wetwell by blowdown. For German BWRs, it was conservatively assumed that 20% of the displaced debris would reach the suppression pool. It has to be noted that this number applies to transport by blowdown only, because the sump and the suppression pool are separated in German BWR designs. Therefore, insulation debris can be transported into the suppression pool by blowdown only, whereas washdown results in transport into the sump.

Debris Type: Aged mineral wool (Rockwool, 100 mm thick, 600 mm wide, used for 60,000 hours at 250 °C) was used in Test 1. In the other tests, insulation from a sugar refinery subjected to a temperature of 250 °C was used.

Mode of Debris Generation: Steam blast.

Generation Fraction and Transport Data: A summary of the debris generation fractions and data corresponding to the transport in rooms simulating the drywell and wetwell is provided in Table 3-2.

Table 3-2: Summary of Debris Generation Fractions and Data Corresponding to the Transport in Rooms Simulating the Drywell and Wetwell.

	Test 1	Test 2	Test 3	Test 4	Test 5	Test 6
Initial Weight	8.0 kg	6.2 kg	5.6 kg	5.2 kg	6.0 kg	6.0 kg
Pipe DN 200	3.2 kg	2.2 kg	1.5 kg	1.0 kg	1.8 kg	1.2 kg
Room 1 Upper	3.3 kg	2.8 kg	2.8 kg	1.2 kg	1.8 kg	2.9 kg
Room 1 Interim	0.4 kg	0.5 kg	0.5 kg	0.5 kg	0.6 kg	0.8 kg
Room 1 Lower	0.4 kg	0.6 kg	0.5 kg	1.2 kg	1.0 kg	1.2 kg
Room 2	37.5 g	13.8 g	51.2 g	134 g	69.2 g	30.5 g
Pipe DN 600	3.1 g	0.3 g	1.1 g	6.1 g	7.1 9 g	2.3 g

The following phenomena were addressed:

• Transport of fibrous insulation debris by steam and air flow, and

• Effect of gratings and other obstacles inside containment.

Applicability and appropriate use of data: The test results can be used to estimate the fraction of fibrous insulation debris transported by steam and air flow into the suppression pool, considering the uncertainties. Because the experiments dealt with various containment layouts, they give general insights into the transport behavior of fibrous insulation debris, but only for the materials tested.

An appropriate safety margin should be added when referring to these test results, rather than using the results for a design basis because of atypicalities introduced by the experimental arrangement. Even the utilities performing these tests used care and conservative assumptions to derive the quantities transported by blowdown as an input for strainer design.

When comparing the results with the experience from the incident in Barsebäck-2, take into account that at the experiments in Karlshamn only blowdown was investigated, whereas the observations in Barsebäck were made after blowdown and washdown.

Major uncertainties: The experiments were carried out in relatively small-scale models. The scale and the geometry gave them dimensions in which the ratio of available wall surface to free volume was too large, which led to an overestimation of the amount of insulation that adhered to the walls in an NPP. No systematic scaling analysis was performed on which the size of the break (i.e., the steam jet) would be based, and the orientation and number of samples of insulation installed in the models did not represent the prototype plant in any way. Furthermore, the experiments were performed with an almost steady steam flow. From these experiments, the experimenters were not certain whether other results may occur at blowdown conditions with high-energy blast effects. The pressure at the nozzle of the pipe cannot be determined exactly from the reports.

3.3.4   Experiments Performed at GKSS Geesthacht for HEW

Extent of Experimental Effort: The transport behavior of fibrous insulation debris in water and the pressure drop at strainers were investigated at the research institute GKSS Geesthacht for the German utility HEW [3-9]. One test setup was significant in determining the transport behavior in the containment of German BWRs. In this setup, the effect of a sill located in the containment above the sump was investigated, for which a wall was installed in the test basin. Insulation debris was put into the water at one side of the wall, and water was pumped from the other side so that the water had to flow over the wall. The amount of insulation debris transported over the wall was determined. The flow velocities were about 0.06 m/s (0.2 ft/s) in the basin and 0.83 m/s (2.7 ft/s) above the wall.

ISOVER mineral wool of various ages was inserted into the water on the surface or on the bottom. In all cases, only negligible amounts of insulation debris (less than 1 % of the inserted mass) were transported over the wall.

The following phenomena were addressed:

- Long-term transport of mineral wool insulation of various ages in water; and,
- Effect of a sill in containment.

Applicability and appropriate use of data: These results can be used to assess the effects of sills and sedimentation pools in containment. The results are valid for ISOVER mineral wool of various ages. As the transport behavior of fibrous insulation debris depends on material characteristics, the results can only be transferred to fibrous insulation that has the same sinking behavior as ISOVER mineral wool.

Major uncertainties:

- The insulation debris was generated by mechanical shredding and its size distribution may have been different than if it had been destroyed by blast forces.
- After a LOCA, water streaming out of the leak flows down inside containment into the sedimentation pool above the sump. Therefore, the water in this area is disturbed and does not stay calm as in the experiments. The influence of this deviation of the test conditions from those expected in a plant raises uncertainties in applying these findings.

3.3.5   Experiments Performed at Oskarshamn NPP

Extent of Experimental Effort: At the Oskarshamn plant, which is the same type as that at Barsebäck-2, ABB-Atom investigated the transport of insulation material by the CSS [3-12]. After old and new insulation material was spread out on the diaphragm floor between the drywell and

wetwell, the CSS was started. After the experiments, the distribution of the insulation material was determined.

In these experiments, a maximum of 5 % of the insulation material was transported into the wetwell.

The following phenomena were addressed:

•   Long-term transport of old and new insulation material by water from the CSS; and,

•   Effect of shielding frames at the blowdown pipes of Swedish BWRs of older design.

Applicability: These data can be used to estimate the fraction of insulation material transported by the CSS into the wetwell of older Swedish BWRs. However, the major uncertainties listed below have to be considered.

The results of these experiments are inconsistent with the Barsebäck experience, where roughly 50% of the dislodged material ended up in the wetwell after blowdown and washdown. However, in the tests in Oskarshamn only washdown was investigated.

Major uncertainties:

•   The type of insulation material investigated is not mentioned in [3-12]. Therefore, more data would have to be obtained before applying the results from this report.

•   The material was spread out on the diaphragm floor before starting the CSS. This situation may not be comparable to the situation after a LOCA, when the insulation debris is distributed all over containment, and water and steam ejected out of the leak swirl around the insulation debris.

3.3.6   *Experiments Performed at Alden Research Laboratory*

Description: Debris transport experiments were performed in a laboratory flume at the ARL in Holden, Massachusetts [3-14]. The study was conducted to determine the transport and entrainment characteristics of different kinds of insulation material and other debris found in the Susquehanna NPP.

The test flume had a rectangular cross-section with a width of 56 cm (22 in.), a depth of 41 cm (16 in.) and a length of about 5.5 m (18 ft). A collection screen was installed at the end of the flume. Three types of tests were performed:

1. Transport in steady, horizontal flow with flow velocities ranging from 6 cm/s (0.2 ft/s) to 30 cm/s (0.98 ft/s).

2. Horizontal transport flow with simulated vertical downcomer jets. In these tests, water was injected into the flume through three vertical model downcomers. The horizontal flow velocities in the flume varied between 6 cm/s (0.2 ft/s) and 18 cm/s (0.6 ft/s). The vertical downcomer flow was increased until the debris within the water was observed to be completely mixed.

3. Weir tests with a 30-cm (12-in.) high weir at the end of the flume. The velocities in the flume ranged from 4 cm/s (0.12 ft/s) to 10 cm/s (0.34 ft/s) corresponding to water heads above the weir of between 3 cm (0.11 ft) and 8 cm (0.25 ft).

The following phenomena were addressed.

Various types of debris were investigated:

•   Individual fibers of NUKON fiberglass insulation (grade A);

•   NUKON shreds of varying shapes and sizes (grade B);

- Sludge, corrosion products, paint particulates and flakes (grade C); and
- "Koolphen K paper" (polyethylene (PE) foam insulation with a paper cover for low-temperature application) fibers and shreds, reflective metal pieces of varying sizes (grade D).

The debris tested is described qualitatively. The report gives detailed information only on the pieces of metallic insulation.

The test results were mainly obtained by visual observation of the degree of vertical mixing of the debris in the water flow and of the amount of debris being transported. The main results with regard to horizontal transport in steady flow are as follows:

- Individual fibers of NUKON fiberglass insulation were transported to the collection screen at the end of the flume at all velocities tested (minimum 6 cm/s or 0.2 ft/s);
- Clumps of fibrous insulation had a tendency to be swept along the floor. At 6 cm/s (0.2 ft/s), none of the material was transported to the collection screen. At higher water velocities, the shreds were moved to the collection screen along the bottom of the flume;
- The behavior of sludge, corrosion products, and paint chips depended on particle size and density. Generally, large and heavy particles sank to the floor, whereas lighter dust was mixed in the water and moved to the collection screen. Some paint chips stayed afloat on the surface and were transported downstream. Of course, the portion of particles transported to the screen grew with rising water velocity;
- Finer particles of "Koolphen K paper" were easily moved to the screen. Larger strips were only transported at velocities greater than 12 cm/s (0.4 ft/s);
- At velocities equal to or higher than 24 cm/s (0.8 ft/s), all metal strips were moved to the screen along the bottom of the floor. At lower flow velocities, only smaller, crumpled pieces were transported.

Some major results of the downcomer tests were:

- Rust and metal strips were not entrained within the flow, even at the highest downcomer flow rates tested;
- Higher downcomer flow rates are needed to entrain shreds of fibrous insulation than to entrain individual fibers.

Applicability and appropriate use of data: The tests give a qualitative and quantitative impression of the transport behavior of various debris types. These results can be used for assessing the assumptions made for debris transport and for comparison with other test results. In addition, the results can be useful for developing transport models to determine the influence of vertical jets streaming into a steady, horizontal flow.

The main results of the weir tests were as follows:

- Most of the fibrous debris and the "Koolphen K paper" shreds were drawn over the weir when the debris was introduced into the water in the vicinity of the weir. Results are given for the critical distance at which transport over the weir occurred. The fraction transported increased as the velocity increased, corresponding to increasing water head above the weir;
- Only small paint flakes were drawn over the weir. Rust particulates, larger paint flakes, and pieces of metallic insulation were not transported over the weir;
- When all pieces of "Koolphen K paper" and metal were placed on the flume bottom in still water and the flow was initiated afterwards, none of the debris was transported over the weir.

The following phenomena were addressed:

- Transport of various debris types - fibrous and metallic insulation, sludge, paint chips, PE foam with paper cover ("Koolphen K paper") in steady flow;

- Influence of vertical jets streaming into a steady, horizontal flow on the transport behavior of debris; and,

- Transport of various debris types over a weir.

Applicability and appropriate use of data: The tests give a qualitative and quantitative impression of the transport behavior of various debris types. These results can be used for assessing the assumptions made for debris transport and for comparison with other test results. In addition, the results can be useful for developing transport models to determine the influence of vertical jets streaming into a steady, horizontal flow.

The weir test results indicate that the effectiveness of a weir as an obstacle for debris transport depends on the type of debris, the flow conditions, and the geometrical properties of the weir. Therefore, without investigation of the actual situation in a plant, a weir should not be considered to be an effective obstacle in the flow path. Furthermore, the test method limits the usefulness of the results of these experiments because the transport behavior of debris depends on whether it is introduced into the established flow or put on the flume bottom in still water and the flow initiated afterwards.

Major uncertainties:

- The debris tested is mainly described qualitatively. The size distribution of the fibrous debris is not known. Test results provided detailed information only for RMI;

- The test results were mainly obtained by observation. With the exception of one test series, no quantitative data on the transport behavior are given in the report;

- The influence of the weir shape is not known. The tests were performed with a straight weir at the end of a laboratory flume. How the results can be transferred to circular weirs corresponding to the openings of downcomer pipes protruding above the floor of the drywell was not investigated.

3.3.7 Experiments Described in NUREG/CR-2982, "Buoyancy, Transport, and Head Loss of Fibrous Reactor Insulation"

Extent of Experimental Effort: Investigations of buoyancy, transport, and head loss characteristics of fibrous insulation are presented in [3-15]. Three types of insulation pillows were tested:

1. Mineral wool insulation with a cover of asbestos cloth, coated with a 13-μm (0.5-mil) Mylar film;

2. Oil-resistant insulation pillows with a core insulation material of fiberglass Filomat (high-density, short-fiber E-glass in needled pack) and a cover consisting of an inner stainless steel knitted mesh and an outer silicone glass cloth; and

3. Insulation pillows with a core insulation material of fiberglass Filomat and a cover of 18-ounce fiberglass cloth.

The following phenomenon was addressed: Transport behavior of various insulation types in a water flume. All pillows had an area of 0.6 m by 0.6 m and a thickness of 0.1 m (2 ft by 2 ft by 4 in). The tests were carried out with insulation pillows in three states: undamaged whole pillows, pillows with covers opened on one side or cut in half, pillows with covers ripped off and inside insulation material in pieces of various sizes (from unbroken insulation layers to shreds). Additionally, small samples of RMI and of foam glass insulation were investigated. The RMI measured 20 cm by 20 cm by 8 cm (8 in. by 8 in. by 3 in.) with 6 sheets of reflective metal and a fastening clasp. The foam glass insulation sample measured 15 cm by 10 cm by 5 cm (6 in. by 4 in. by 2 in.).

Applicability and appropriate use of data: The test results can be used to estimate the water velocity needed to initiate motion of sunken insulation debris. The influence of the size distribution of the debris on the transport behavior during the various phases is not known yet and cannot be modeled at this time. Owing to the properties of the test specimen, the results for RMI are not representative of the behavior of individual pieces of sheet metal.

The transportation tests were performed in a 1.8 m (6 ft) wide flume with a water depth of 0.8 m (32 in.). In some tests, vertical piles were installed in the flume as turbulence generators, similar to the obstructions that can be present in NPPs near the sump screens. The main parameters measured were the velocities needed to initiate the transport of sunken insulation and to bring all the insulation pieces against the screen. The following are the main results:

- Water velocities needed to initiate the motion of sunken insulation are on the order of 6 cm/s (0.2 ft/s) for individual shreds, around 18 cm/s (0.6 ft/s) for individual pieces with a size of up to 10 cm (4 in.) on the side, and between 27 cm/s and 46 cm/s (0.9 ft/s to 1.5 ft/s) for individual large pieces with a size of up to 60 cm (2 ft) on the side;

- Insulation shreds, once in motion, tend to become suspended in the water column and collect over the entire screen area;

- Insulation pillows broken up into finite size fragments tend to congregate near the bottom of the screen;

- The RMI sample tested needed a velocity of 80 cm/s (2.6 ft/s) to start moving. Note that this sample was not representative of individual pieces of reflective sheet metal;

- The tests were conducted in water heated to a temperature as high as 60 °C (140 °F);

- The sample of foam glass insulation did not sink, but remained afloat at the water surface.

Major uncertainties: In the description in [3-15] there is no mention as to whether the tested samples were treated thermally before the experiments. Therefore, the test results might not be representative of aged insulation material present in NPPs.

The size distribution of the fibrous insulation material tested is not given.

3.3.8 Experiments Described in NUREG/CR-6772, "Separate-Effects Characterization of Debris Transport in Water" [3-18]

Description: The purpose of this research program was to experimentally determine the transport characteristics of various types of LOCA-generated debris within a PWR containment, focusing exclusively on debris transport on the containment floor.

The experiments measured the following properties for several types of debris:

- Terminal settling velocity in quiescent pools and in water pools in planar (lateral) motion;

- Incipient tumbling velocity (i.e., the minimum fluid velocity at which an individual stationary fragment resting on the containment floor would begin to move);

- Bulk tumbling velocity (i.e., the minimum fluid velocity required to induce "bulk-scale" movement of a population of debris fragments);

- Lift-at-the-curb velocity (i.e., the minimum fluid velocity required to lift a fragment of debris over a vertical curb (typically 4 or 6 in. in height) that impeded forward motion along the floor).

In all cases, the velocities were measured in terms of the pool average flow velocity.

Applicability: The data presented focus exclusively on debris transport in the water pool present on the containment floor following a LOCA. Experiments were performed under planar and turbulent flow conditions (and repeated several times) to evaluate and quantify the degree of data variability in

such circumstances. In addition to the transport properties, experiments were performed to measure other important characteristics of post-LOCA debris behavior, such as:

- The buoyancy characteristics of fibrous debris fragments, i.e., the rate at which low density fiberglass insulation fragments become sufficiently saturated with water to sink into the pool as a function of temperature;

- The disintegration rate of calcium silicate insulation when submerged in hot water; and

- The extent to which the threshold velocities listed above are affected by the simultaneous presence of other types of debris (i.e., mixtures of fiber fragments and calcium silicate).

Major Uncertainties

- Variations in pool velocity as a result of (for example) large-scale turbulence may cause significant variability in measured values for these threshold velocities;

- The emphasis of this test program was to measure transport properties of LOCA-generated debris fragments, not to perform scaled tests that would determine the quantity of debris that might transport to a screen in a particular plant.

3.3.9 *Experiments Described in NUREG/CR-6773 "GSI-191: Integrated Debris Transport Tests in Water Using Simulated Containment Floor Geometries" [3-19]*

Description: Experiments were conducted to examine insulation debris transport under flow conditions and geometric configurations typical of those found in PWRs.

The following phenomenon was addressed: Small-scale three-dimensional (3-D) tank tests were conducted at the University of New Mexico Open-Channel Hydrology Laboratory.

The tests were conducted in a large tank with provisions to simulate a variety of PWR containment and sump features. Debris transport was studied in such a way that all the separate effects studied in the separate-effects testing (See Section 3.3.8) could be integrated into tests that were more typical of PWR geometries. The important physical processes that took place in the 3-D tank tests included settling of debris in turbulent pools, tumbling/sliding of settled debris along the floor, re-entrainment of debris from the containment floor, lifting of debris over structural impediments, retention of debris on vertical screens, and the further disintegration of debris as a result of sump-pool dynamics. The integrated phenomena included early debris transport as the sump filled and later debris transport after a steady-state flooded condition was achieved. The flow regimes established during the tests included quiescent, turbulent, and rotational flow in geometries comparable to the complexity of PWR containment floors.

Applicability: The tests provided insights into the relative importance of the various debris-transport mechanisms and are directly applicable to creating or validating models capable of estimating debris transport within a PWR plant containment sump. Furthermore, these tests provided debris particle tracks and bulk debris transport data needed to validate CFD code applications to estimate debris transport within a PWR plant containment sump.

Major Uncertainties:

- The measured transport fractions of the integrated tests should not be applied directly to plant-specific analyses because there is no apparent means of scaling those transport fractions from the test geometry to an actual plant. Rather, the CFD simulation models must apply the debris-transport phenomenology to all of the individual plant features for each specific plant;

- The potential for pool turbulence to generate additional fine debris that would remain suspended in the pool was demonstrated; however, the tests did not provide a means of quantifying that disintegration as a function of turbulence levels.

3.4   Knowledge Base for Blowdown- Washdown Transport

The amount of insulation debris transported into the containment pool depends, among other parameters, on the layout of containment, the break location, and the insulation type. Tests have been performed, or experience from incidents is available, for only a few containment designs, break locations, and insulation types. A conservative approach for strainer qualification, taken by some licensees, is to assume all debris that is generated will be transported to the containment pool.

For experiments dealing with special aspects of transport, the influence of initial conditions is not known. Whether these experiments reflect the situation after a LOCA with sufficient accuracy is not clear. This becomes obvious when comparing the results of the tests in Karlshamn and Oskarshamn with the experience from Barsebäck. The viscosity of the water varies with temperature; the impact of this viscosity change on debris transport has not been extensively studied.

A commonly accepted assumption is that RMI debris does not transport to the strainer surface with the low velocities typical of most plants. The available information concentrates on transport in water (see Chapter 4).

To supplement the missing information, research in the following area is desirable:

•   The use of CFD simulations to predict debris transport is not universally accepted. It can be difficult to benchmark CFD analyses with physical tests due to scale effects. Topical report NEI-04-07 and the NRC staff safety evaluation [3-2, 3-17] provide more information on the use of CFD simulations; also see Appendix E for a summary of relevant CFD studies.

3.5   References

3-1   NUREG/CR-6369 Vol 1 – Vol 3, Drywell Debris Transport Study, US NRC September 1999

3-2   Safety Evaluation by the NRC for Nuclear Energy Institute Guidance Report (NEI 04-07) "Pressurized Water Reactor Sump Performance Evaluation Methodology", ML043280007, December 2004.

3-3   BWR-PIRT, G.E. Wilson et al., "BWR Drywell Debris Transport Phenomena Identification and Ranking Tables (PIRTs)", INEEL/EXT-97-00894, September 1997.

3-4   PWR-PIRT, B.E. Boyack, et al., "PWR Debris Transport in Dry Ambient Containments – Phenomena Identification and Ranking Tables (PIRTs)", LA-UR-99-3371, Rev. 2, December 14, 1999 (ADAMS ML003698506).

3-5   Incident Reporting System (OECD/NEA), "Clogged Pump Suction Strainers in the Wetwell Pool", Report No. 1294, received on July 8, 1992.

3-6   Sydkraft, Barseback Nuclear Power Plant, "Report Concerning the Quantity of Insulation Which was not Washed Down in Connection with the 314 Event", Reference No.: PBM-9211-23, November 26, 1992.

3-7   NUREG-0897, Rev. 1 "Containment Emergency Sump Performance", October 1985. U.S. Nuclear Regulatory Commission.

3-8   Owens/Corning Fiberglass Corporation, Internal Report, Granville, Ohio, March 1985.

3-9   H. Ohlmeyer, "Investigations and Modifications in the German BWR Plants"

3-10   "KKB and KKK after the Barseback Incident" *Proceedings of the OECD/NEA Workshop on the Barseback Strainer Incident,* Vol. 1; Stockholm, January 1994, https://www.oecd-nea.org/nsd/docs/1994/csni-r1994-14.pdf.

3-11   T. Riekert, "Survey of the Investigations and Actions Taken at German NPPs", *Proceedings of the OECD/NEA Workshop on the Barseback Strainer Incident,* Vol. 1; Stockholm, January 1994, https://www.oecd-nea.org/nsd/docs/1994/csni-r1994-14.pdf.

3-12   L. Ohlin, "Upgrade of Emergency Core Cooling Systems in Swedish BWRs - Research and Experiments", *Proceedings of the OECD/NEA Workshop on the Barseback Strainer Incident,* Vol. 2; Stockholm, January 1994.

3-13   ABB-Atom, "Karlshamn Tests 1992. Test Report. Steam Blast on Insulated Objects", RVE 92-205, November 30, 1992.

3-14   Alden Research Laboratory, Inc., "ECCS Strainer Model Study - Transport and Entrainment Studies in a Laboratory Flume", Holden, MA; May 1994.

3-15   NUREG/CR-2982, Rev.1 "Buoyancy, Transport, and Head Loss of Fibrous Reactor Insulation", July 1983. U.S. Nuclear Regulatory Commission.

3-16   T. Kanzleiter, K.O. Fischer, H.J. Allelein, S. Schwarz, and G. Weber, "The VANAM Experiments Ml and M2 — Test Results and Multi-compartmental Analysis", *Journal of Aerosol Science,* Vol. 22, Suppl. 1, pp. S697-S700, 1991.

3-17   NEI, 2004, "Pressurized Water Reactor Sump Performance Evaluation Methodology", Nuclear Energy Institute PWR Sump Performance Task Force, Rev. 0, NEI 04-07.

3-18   NUREG/CR-6772, "Separate-Effects Characterization of Debris Transport in Water", August 2002, U.S. Nuclear Regulatory Commission.

3-19   NUREG/CR-6773,"GSI-191: Integrated Debris Transport Tests in Water Using Simulated Containment Floor Geometries", December 2002, U.S. Nuclear Regulatory Commission.

4. TRANSPORT OF DEBRIS IN CONTAINMENT POOLS

This chapter summarizes pertinent information and presents understanding related to debris transport within the containment pool following a LOCA. The LOCA and post-LOCA transient will control debris generation and transport. Although the types and quantities of debris generated plus transport effects must be evaluated, the physical phenomena occurring in the containment pool and plant ECCS flow requirements will ultimately control the transport of debris materials to the ECCS suction strainers. Exact modeling of such a transient is difficult because of the complexity of physical phenomena occurring and the variabilities introduced by plant-specific containment and suction strainer designs.

Debris transport factors for BWRs will be discussed first, followed by those factors unique to PWRs

4.1   Factors Affecting BWR Debris Transport

Debris transport within a BWR suppression pool will be dependent on the following four factors:

1. Containment and suction strainer design features;

2. Levels of LOCA-induced turbulence and rate of decay following cessation of "chugging";

3. Types, quantities, and physical characteristics of the debris present;

4. Debris bed build-up and composition on the strainer as a function of time, which is influenced by strainer approach velocity;

Although this analysis concentrates on U.S. BWR suppression pool designs, the results can also be applied to other BWR designs.

4.1.1   Effect of the Containment Type on Debris Transport

Drywell and wetwell designs vary widely among the U.S. BWR Mark I, II, and III containment designs as well as between European BWR plants (i.e., Swedish versus German designs). Such variations will substantially affect suppression pool hydrodynamics which, in turn, will control debris transport within the suppression pool. Experimental studies carried out by the General Electric Company for each containment type in support of the resolution of suppression pool loads program [4-1] have clearly shown that LOCA hydrodynamic phenomena are strongly dependent on containment type. For example, the Mark III drywell blowdown into the suppression pool is through horizontal pipes, while the blowdown used in the Mark I and II designs is through vertical downcomers; therefore, condensation oscillations in a Mark III are somewhat different in nature from those in the Mark I and II.

Similar differences will exist in the long-term ECCS recirculation phase. U.S. Mark III recirculation-mode velocities are much larger than corresponding velocities in Mark I and II designs, thereby increasing the possibility that debris materials that may have settled out will resuspend.

Equally important is the containment design because drywell and wetwell transport pathways and downcomers and other design features (i.e., curbing) can control the amounts and types of

LOCA-generated debris introduced into the suppression pool. Containment drywell design features should not be ignored before embarking on an analysis of the transport of suppression pool debris.

4.1.2   LOCA-Related Suppression Pool Hydrodynamic Phenomena

Immediately following a postulated LOCA, the pressure and temperature of the drywell atmosphere increase rapidly. With the increase in drywell pressure, water initially standing in the downcomers accelerates into the pool, clearing the downcomers of water. This vent-clearing process generates a water jet capable of causing turbulent mixing of the suppression pool water. Immediately following vent-clearing, noncondensable gases from the inert drywell atmosphere are discharged at the exit of the downcomers for about 10 to 15 seconds for a large LOCA, swelling the suppression pool. During this initial stage of accident progression, the suppression pool flow fields are dominated by large-scale turbulence, leading to resuspension of a large fraction of the suppression pool sludge and other materials that may have been present.

With time, the flow in the vent pipe will consist increasingly of steam. As the flow of steam through the downcomers continues, pressure oscillations occur in the suppression pool. Experimental data show that these oscillations can be divided into two categories: (1) "condensation oscillations," which occur at relatively high vent-flow rates and are characterized by continuous periodic oscillations, with the neighboring downcomers oscillating in phase, and (2) "chugging," which occurs at lower steam-flow rates and is characterized by a series of pulses typically a second or more apart. Experimental data suggest that the amplitude, frequency, and duration of the condensation oscillations are primarily functions of the mass flow rate, concentration of the noncondensables in the mass flow, downcomer submergence, suppression pool temperature, and break size.

Chugging phenomena seem to occur over a short period toward the end of the drywell blowdown when the drywell pressure is not sufficient to keep the downcomer throat completely cleared of water. Experimental data suggest that condensation oscillations and chugging phases are both associated with turbulent flow fields. However, turbulence, in the case of condensation oscillations, appears to be nonisotropic when integrated over the entire height of the pool, as demonstrated by thermal stratification observed in some extreme cases. The chugging phase, on the other hand, appears to generate large-scale eddies that can propagate to the bottom of the pool. Turbulence generated by both of these phases is probably nonisotropic and exists at high levels at the exit of the downcomers where the debris is introduced into the pool. Sedimentation of debris introduced during the blowdown phase would be strongly influenced by suppression pool turbulence introduced by condensation oscillations and chugging. Another probable effect of condensation oscillations and chugging is resuspension of suppression pool sludge.

BWR safety systems are designed so that shortly after a LOCA, the ECCS will automatically start to pump water into the reactor vessel from either the condensate storage tank (CST) or the suppression pool. This water floods the reactor core and ultimately cascades into the drywell through the postulated break. The time at which this occurs will depend on the size and location of the break. Because the drywell will be full of steam at the time of vessel flooding, introduction of water into the drywell causes large-scale condensation and a rapid decrease in drywell pressure. At this stage, the vacuum relief valves open to enable noncondensable gases in the suppression pool to flow back into the drywell, leading to equalization of drywell and wetwell pressures. Thereafter, vapor flow to the suppression pool would be reduced to very low levels. Suppression pool turbulence levels start to decay because energy cannot be introduced into the bulk of the pool to maintain high levels of turbulence. This phase of the accident will have two significant effects on debris transport: (1) water cascading from the break will result in continued washdown of debris contained in the drywell, especially near the region of the break, and (2) decaying turbulence levels will no longer impede debris from settling in the suppression pool.

Since vent pipes and downcomers are generally uniformly spaced, it is reasonable to assume that the initial introduction of debris into the suppression pool will be uniform during the blowdown

phase. In contrast, debris transported into the suppression pool during the washdown phase may not be uniformly introduced, depending upon the location of the break, the volume and type of debris that still remain within the drywell, and intervening structures (e.g., gratings, curbs) that could impede debris transport to the suppression pool. The analyst should review the location of individual strainers relative to downcomer exits to determine if "pool averaged" conditions and assumptions are adequate to estimate debris transport, or if a multidimensional model is needed.
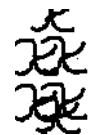
In the final stage of an accident, BWRs rely on long-term ECCS flow to the vessel for heat removal, containment sprays to control drywell pressure and temperature, and suppression pool cooling for ultimate heat removal from the containment. Break flow, aided by the containment sprays, will continue to wash down remaining insulation originally damaged by the LOCA to the suppression pool. This debris will enter the wetwell through the vent paths and the downcomers. The majority of the debris introduced into the pool during this stage is likely to be composed of large or partially damaged insulation pieces and drywell particulates.

At a later time, actuating the suppression pool cooling systems will result in establishment of large-scale recirculation flow patterns within the suppression pool. During this stage, the residual turbulence is due to (1) the horizontal momentum component introduced by the recirculation flow, and (2) the vertical momentum component introduced by the jets of water exiting the downcomers. Although the resulting turbulence may not be sufficient to completely prevent sedimentation, if pool recirculation velocities are sufficiently large, the drag in the boundary layer may reach the critical value required to cause resuspension of a small portion of the sediment at the bottom of the suppression pool. This resuspension may lead to the formation of a more uniform sediment layer and may result in transport of a small fraction of the resuspended debris to the strainer. In general, this phase will be characterized by continued washdown of debris from the drywell and sedimentation of the debris present in the suppression pool.

4.1.3   Debris Types, Quantities, and Characteristics

Insulation debris in the form of fines and shredded pieces (ranging from singular or multiple fibers to clumps of fibers) can be introduced into the suppression pool through a network of vent pipes and downcomers connecting the drywell to the suppression pool. Table 4-1 illustrates potential fibrous debris characteristics and identifies the current understanding associated with settling and filtration characteristics of such materials. Pictures of NUKON insulation fragments Classes 3, 4, 5 and 6 are shown in Figure 4-1. These classes of fibrous debris were selected for testing because they represent the type of debris that can remain in suspension for a long time and be transported to strainers.

Table 4-1: Fibrous Debris Classification

Class		Description	Settling Characteristics	Settling Velocity in Calm Pools	Strainer Filtration Efficiency
1		Very small pieces of fiberglass material, "microscopic' fines which appear to be cylinders of varying LTD.	Drag equations for cylinders are well known, should be able to calculate fall velocity of a tumbling cylinder in still water.	1-3.5 mm/s Based on Cal. for 0.5 - 2.54 cm long fibers	Unknown
2		Single flexible strand of fiberglass, essentially acts as a suspended strand.	Difficult to calculate drag forces due to changing orientation of flexible strand.	Same as above	Nearly 1.0
3		Multiple attached or interwoven strands that exhibit considerable flexibility and which due to random orientations induced by turbulence drag could result in low fall velocities.	This category is suggested since this class of fibrous debris would likely be most susceptible to re-entrainment in the recirculation phase if turbulence and/or wave velocity interaction becomes significant.	0.04 ft/s - 0.06 ft/s (measured)	1.0 (measured)
4		Formation of fibers into clusters which have more rigidity and which react to drag forces more as a semi-rigid body-	This category might be represented by the smallest debris size characterized by PCIs air blast experiments.	0.08-0.13 ft/s (measured)	1.0 (measured)
5		Clumps of fibrous debris which have been noted to sink. Generated by different methods by various experimenters but easily created by manual shredding of fiber matting.	This category was characterized by the PCI air test experiments as comprising the largest two sizes in a three size distribution.	0.13-0.18 ft/s (measured)	1.0 (measured)
6		Larger clumps of fibers. Forms an intermediate between Classes 5 and 7.	Few of the pieces generated in PCI air blast tests consisted of these debris types.	0.16-0.19 ft/s (measured)	1.0 (measured)
7		Fragments of fibers that retain some aspects of the original rectangular construction of the fiber matting. Precut pieces (i.e. .25" by .25") to simulate small debris. Other manual/mechanical methods to produce test debris.	Dry form geometry known, will ingest water, should be able to scope fall velocities in still water assuming various geometries.	0.25 t/s (calculated)	1.0 (estimated)

CLASS 3 AND 4 INSULATION FRAGMENTS

CLASS 5 AND 6 INSULATION FRAGMENTS

Figure 4-1: Examples of Fibrous Debris Fragments Tested

Other materials, sometimes referred to as "sludge," are known to be present in U.S. BWR suppression pools. Sludge has been identified by the U.S. BWROG [4-2] as being principally composed of iron oxides having the particle size distribution given in Table 4-2.

Table 4-2: Particle Size Distribution of Iron Oxides in US BWR Suppression Pool Sludge

Particle Size Range (μm)	Average Size (μm)	% Present in Suppression Pool Sludge
0 - 5	2.5	81
5 - 10	7.5	14
10 - 75	42.5	5

Estimates of the amount of sludge present in U.S. BWRs vary widely, depending on whether the suppression pool has been regularly cleaned during refueling outages. The severity of head loss associated with filtration of such materials by fibrous debris transported to the suction strainer supports cleaning of suppression pools when the plant is in a refueling outage.

Mineral wool (extensively used in European reactors) has also shown evidence of "fines" that are apparently the result of deterioration of this material with time at operating temperatures. Previous experiments have demonstrated that mineral wool "fines" will be entrapped and result in high head losses. Some analysts have noted the severity and rapidity of blockage experienced in the Barsebäck-2 event as possibly related to the effect of "old" mineral wool debris with "fines." Aged, or old, mineral wool should always be used in head loss testing to accurately reflect the material behavior after the organic binders have dissipated.

In addition, other debris materials, such as paint chips, concrete particles, chemical precipitates, dust, and so forth, which may be present or which might be generated by a LOCA, should not be overlooked because these materials will also be filtered by fibrous bed buildup on suction strainers.

RMI debris is also a concern since such insulation is used in various NPPs, and LOCA destruction of such insulation is possible as discussed in Section 2.1. Breaks in steam lines will generate highly fragmented RMI debris, crumpled larger foil pieces and make missiles of outer casings [4-3]. Findings related to settling rates for such materials are provided in Section 4.2.

4.1.4 Debris Bed Buildup and Composition

Debris transport within the suppression pool will be inherently influenced by the types of debris being transported and the composition of the debris bed forming on the suction strainer over time. Historically, analyses have assumed homogeneous mixing of debris and uniform deposition on strainers. Numerous head-loss correlations have been developed on the basis of this assumption. However, recent separate-effects experiments indicate that while this assumption may be true for only fibrous debris shreds, it is not true when sludge particles of 1 to 10 μm are present.

Debris bed formation with sludge present is somewhat different. Initially a thin layer of fibers is formed on the strainer, but sludge particles can easily penetrate this layer, apparently because the fibrous layer does not have the required structure or strength to filter very small sludge particles. During these initial stages of bed buildup, visual observations as well as concentration measurements suggest that the majority of particles penetrate the bed. However, with time, continuous transport of fibrous debris will result in a more rigid structure and the bed will start to filter out sludge particles. Concentration measurements have shown that filtration efficiency initially is very small, but increases to approximately 50% efficiency as the bed builds up (but see Section 6.1 for additional discussion of filtration efficiency).

Although small particulates can pass through the initial formation of fibrous debris beds, as

larger particles are entrained, a fibrous "cake" starts to form. As material that initially passed through the strainer returns to it, the "cake" characteristics begin to change and pool "turnover" time becomes important because of the transient nature of debris transport and changing head-loss characteristics of the debris bed being formed. Experiments performed in the United States by industry groups in the 1990s suggested that formation of thin layers of fibrous debris plus some sludge can quickly lead to high head losses. Thus coupling of material transport (fibers and particulates) within the suppression pool and debris bed formation (which is material- and time-dependent) on suction strainers is necessary to arrive at reliable plant predictions.

Figures 4-2 and 4-3, extracted from [4-4], illustrate the need for a transient analysis model that couples these effects. These fiber and particulate transport calculations show that the majority of debris transport to the strainers occurs in less than two pool flushing times for the reference plant analyzed and also show significant differences in transport characteristics of fibers and particulates. Therefore, plant calculations addressing when loss of NPSH margin would occur should employ a model coupling debris transport with debris filtration effects.

4.2   Debris Transport and Settling in Turbulent Pools

Sedimentation, also referred to as gravitational settling, is a primary mechanism for removal of debris suspended in the suppression pool. The rate at which the debris settles is a complex function of debris characteristics (e.g., density, shape, and size) and pool dynamics (e.g., turbulence levels and the flow velocity profiles). The sedimentation rates, also referred to as the settling velocities, can be calculated for debris with well-defined shapes under still-pool conditions using existing analytical models ([4-5] to [4-8]). For undefined shapes under turbulent pool conditions, a few approximate models can be used to estimate the settling rates [4-9]. However, such models are usually based on assumptions regarding debris shape and turbulence conditions that may be present. More recent information about sedimentation of insulation materials used in NPPs under still-pool conditions can be found in References [4-10] to [4-15], and this information has been used to develop models.

Given the importance of settling rates for fibers, sludge, and other particulate materials, the prediction of transport in the suppression pool, the NRC-sponsored experiments at the ARL in 1994 to gain insights into debris behavior during and after the high-energy phase of a LOCA. These approximately 1/2-scale experiments focused on studying the debris behavior during in-phase chugging, which is typical of a medium loss-of-coolant accident (MLOCA) and also allowed for visual observation of the debris behavior (Fig. 4-4) as well as for measuring debris concentrations.

4.2.1   Settling Rates for the High-Energy Phase

The ARL experiments provided the following insights about fibrous debris behavior during the high-energy phase:

• The turbulence created during the high-energy phase will resuspend all of the sludge initially contained at the bottom of the suppression pool;
• The turbulence is sufficiently strong to keep the sludge as well as the fibrous debris in suspension throughout the high-energy phase;
• The turbulence also results in further disintegration of fibrous debris.

Although these insights were gained from experiments simulating moderate-energy chugs typical of an MLOCA, they are judged to be valid for condensation oscillations that characterize a large loss-of-coolant accident (LLOCA) since measurements confirmed that total suspension of debris components occurred. The results are applicable to both Mark I and II containments because of the downcomer geometry. However, unconditional applicability of these results to Mark III containments (where the vent pipes are arranged in the horizontal direction) should be carefully assessed before using the results in a Mark III study.
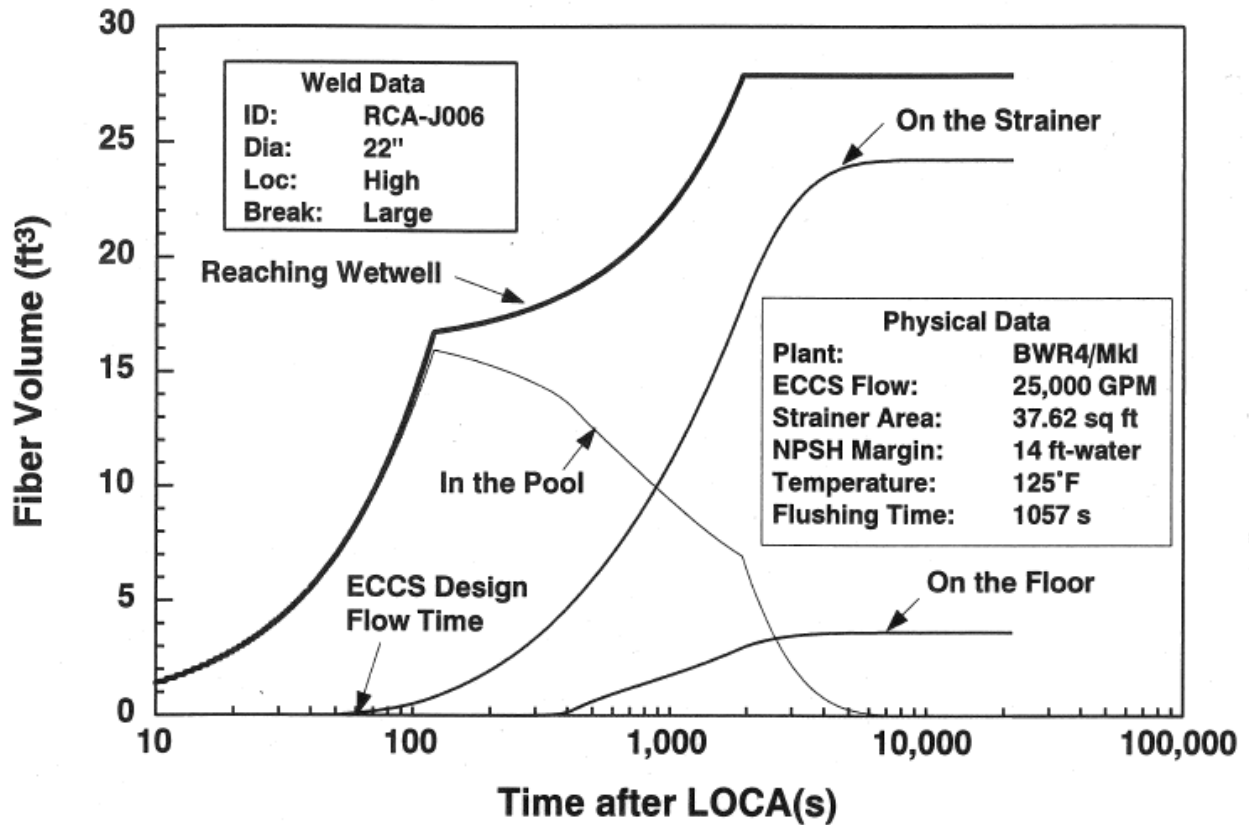
Figure 4-2: Calculated Transient Fibrous Debris Transport in a BWR Suppression Pool. Note that that the trapping efficiency for fibers is 1.0. No fiber penetrates the strainer.

Figure 4-3: Calculated Transient Particulate Debris Transport in a BWR Suppression Pool
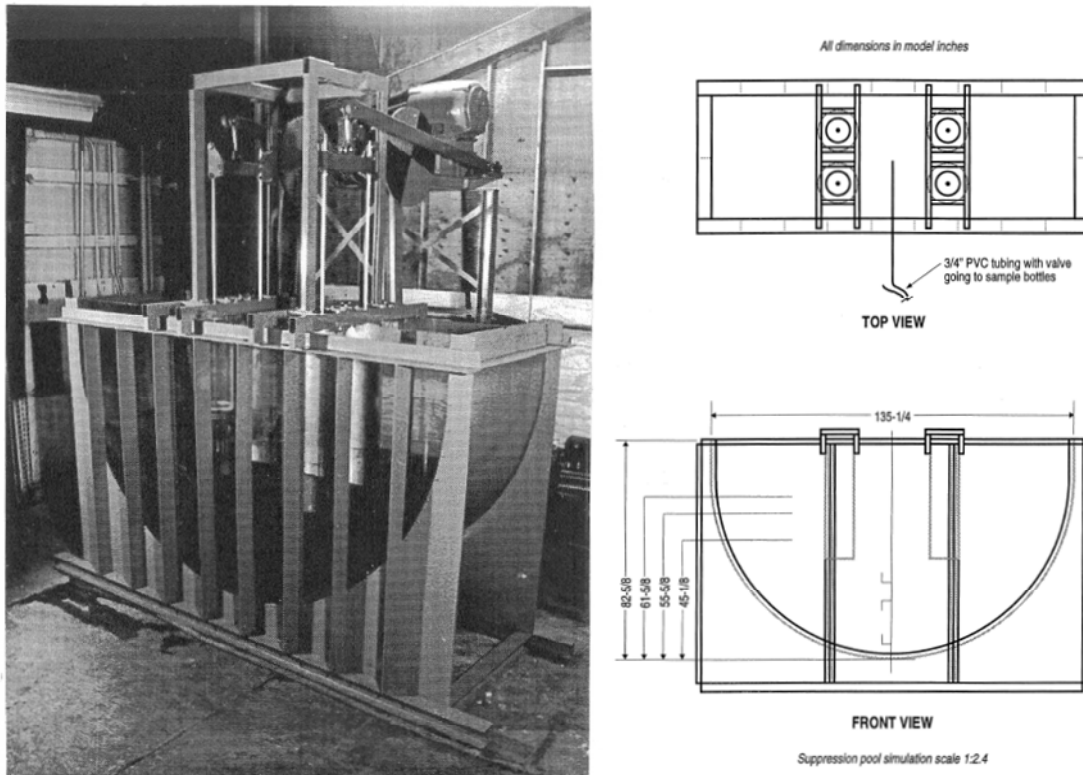
Figure 4-4: Suppression Pool Scaled Facility at ARL to Investigate Debris Settling and Concentrations

4.2.2 Settling Rates for Post-High-Energy Phase

After cessation of the high-energy phase, the suppression pool returns to quiescent pool conditions.[4] During the post-high-energy phase, the residual turbulence in the pool is expected to decay rapidly, allowing for sedimentation of the suspended debris. As a result, researchers have postulated that sedimentation would play an important role in debris removal from the pool during this stage of accident progression. In the ARL experiments, the suppression pool was initially brought to a fully mixed condition by simulated chugging. After 9 to 10 minutes, the chugging was terminated and the turbulence in the suppression pool was allowed to decay naturally. Visual observations revealed that soon after termination of chugging, the debris began to settle to the pool floor. Water samples were drawn from five locations in the suppression pool at predetermined intervals to measure debris concentrations. The debris concentrations were then used to estimate settling rates for each species, that is, fibrous debris and particulate sludge. Figure 4-5 presents settling velocities measured from tests A-l, A-1R, A-2, and A-2R for fibrous debris of shape Classes 3 and 4, and shape Classes 5 and 6. Figure 4-6 presents settling velocities for sludge and fiber mixtures of different mass ratios measured from the remaining tests. The following conclusions were based on these measurements:

1. The fibrous debris underwent large-scale destruction under the influence of shear forces induced by eddies created by the chugging. The fibrous debris usually resembled shape Classes 1, 2, and 3 at the end of the chugging tests. This visual observation was further confirmed by settling velocity measurements; the measured settling velocities of 0.1-10 mm/s fall in the range of previously

---

4   This assumption may not be accurate for BWRs that are equipped with pool mixers or other systems that are intended to mix the pool water by turbulent means to prevent thermal stratification. Such pool mixers can be found in some European BWRs and some of the Mark III U.S. BWRs.

established settling velocities for shape Classes 1, 2, and 3. Figure 4.7 also shows that the settling velocities are weakly dependent on the shape class of the debris initially added to the pool.

2.   Two different equations were developed for each of Classes 3 and 4 and Classes 5 and 6:

$$\frac{C}{C_0}(\%) = \frac{31}{\left(V_{s-test}^{3\&4}\right)^{\frac{2}{3}}}$$

Equation 4-1

$$\frac{C}{C_0}(\%) = \frac{40}{\left(V_{s-test}^{5\&6}\right)^{\frac{1}{2}}}$$

Equation 4-2

where,

V_{s-test} is the settling velocity measured in the tests in mm/s

$\frac{C}{C_0}(\%)$ is the mass percentage of debris with settling velocity greater than V_{s-test}.

In both cases more than 60% of the total debris, by mass, exhibit settling velocities less than 1 mm/s. Such low settling velocities suggest that the potential for fibrous debris settling in the suppression pool is small.

The ARL experiments demonstrated that on average, the sludge particles settle faster than the fibrous shreds. About 30 percent of the sludge particles, by mass, exhibit settling velocities exceeding 10 mm/s, and about 60 percent of sludge particles, also by mass, exhibit settling velocities exceeding 2 mm/s. However, about 10 percent of the sludge particles exhibit settling velocities less than 0.1 mm/s. The median particle settling velocity is about 3 mm/s.
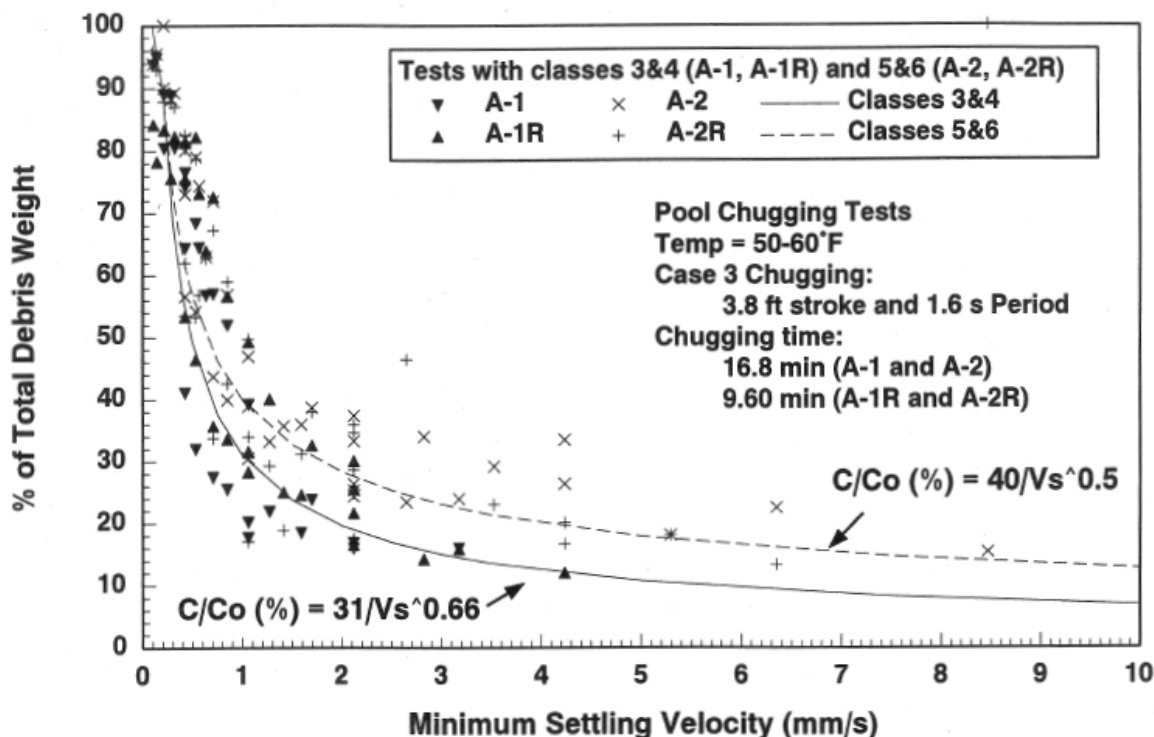
Figure 4-5: Settling Velocities for Shreds of Fiber Following Suppression Pool Turbulence Simulation
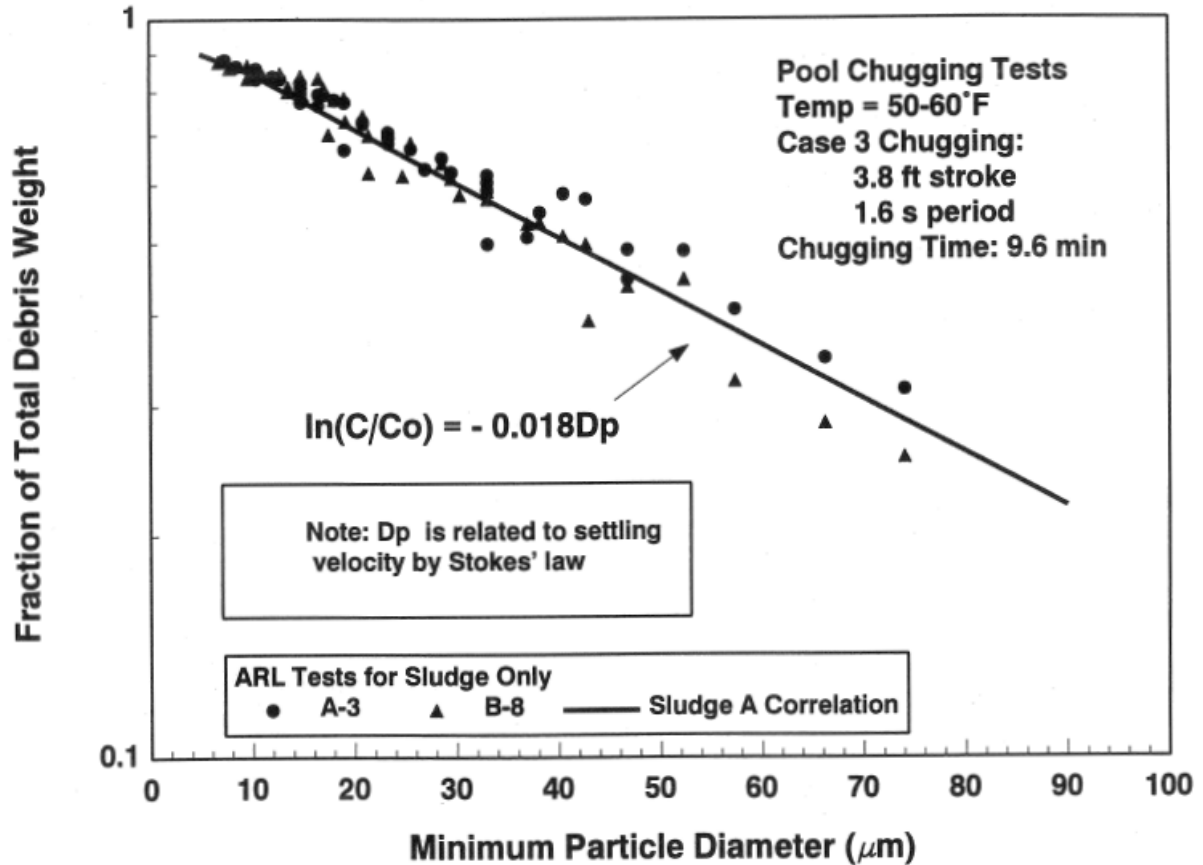
Figure 4-6: Settling Velocity Data for Sludge A Particulates and Fiber

The relationship between sludge concentration and particle diameter derived from the ARL experiments is given by:

$$ ln\left(\frac{C}{C_0}\right) = -0.018 D_p $$

where D_p is the minimum particle diameter related to the settling velocity via Stokes' law as:

$$ V_{s-test}^{sludge} = g D_p^2 \frac{(\rho_p - \rho_w)}{18\mu} $$

Equation 4-4

where:

V_{s-test}^{sludge} is the terminal velocity for sludge particles measured in the experiments;
g is the acceleration due to gravity (m/s^2);
ρ_p is the sludge particle density (kg/m^3)
ρ_w is the water density (kg/m^3);
μ is the water viscosity (Pa·s)

The settling velocities of sludge and fiber mixtures increase as the sludge-to-fiber mass ratio increases (see Figure 4-7). The settling velocities for these mixtures can be estimated via superposition by assuming that fibers and sludge settle independently of each other.

The ARL experiments also showed that reintroduction of small levels of turbulence reinitiated suspension of fibrous shreds.

In 1992, ABB Atom in Vasteras [4-15] conducted experiments to investigate the behavior of mineral wool insulation debris when it enters the wetwell. The objective was to gain insights into the behavior of old and new mineral wool debris following blowdown. These experiments showed that (a) old mineral wool was pulverized into small fractions ("fines") and did not float to the surface following blowdown, (b) sedimentation of larger particles occurs directly after blowdown but that small particles settle slowly, and (c) the behavior of new insulation was completely different.

ABB Atom's Experiment A2 was directed at investigating sedimentation following blowdown, and ABB Atom reported the following observations:

1. Sedimentation of small particles occurs slowly; the concentration dropped from 13 mg/L to 8 mg/L within an hour;

2. Scanning electron microscope studies showed that the fibers were stick shaped with an estimated diameter of 3 to 10 μm and that the fibers were completely unstructured and interwoven;

3. Cakes (about 80 mm by 80 mm) of large fiber deposits were coherent and could be lifted off at the corner without breaking.

These experiments demonstrated that "old" mineral wool with "fines" is a two-component system that exhibits settling characteristics similar to fiberglass and "sludge." Careful study of the limited settling data presented in this report can be used to derive settling velocities greater than 5 mm/s for 70 percent of the debris, 1 to 5 mm/s for 10 to 15 percent of the debris, and less that 1 mm/s for the remainder of the debris.

4.2.3   Debris Resuspension

Resuspension is the phenomenon by which sediment located at the bottom of the suppression pool is swirled upwards. The purpose of the resuspension model is to simulate resuspension of suppression pool sludge during the high-energy phase of the blowdown and possible resuspension of sludge and debris sediment during the long-term recirculation phase, if sufficient pool velocities occur.
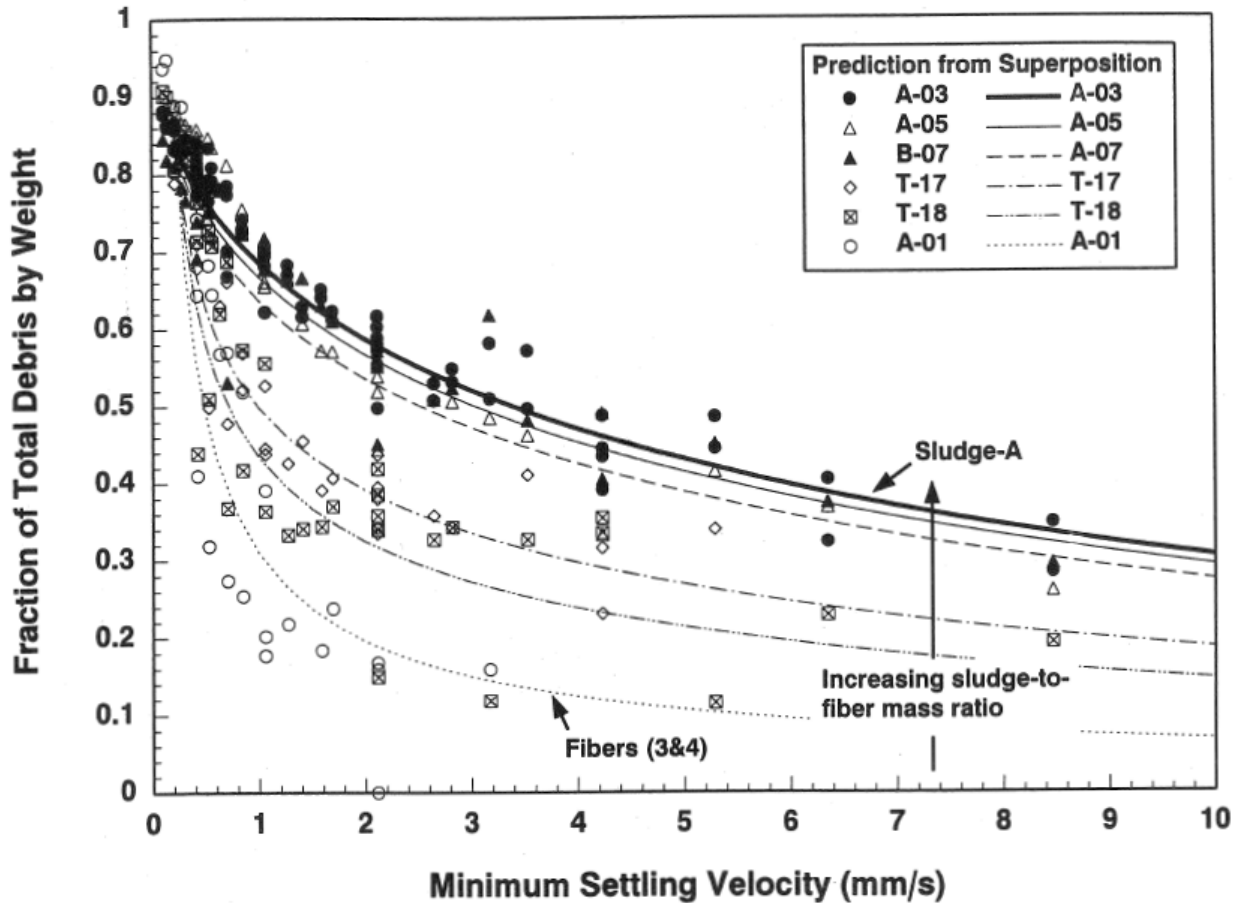
Figure 4-7: Settling Velocities for Various Sludge and Fiber Mixtures Predicted using the Principle of Superpositioning

Resuspension is possible when turbulence levels or recirculation velocities in the boundary layer are capable of providing net upward drag on the debris to overcome gravitational forces. This phenomenon can be seen as the opposite of sedimentation and has been widely studied for settling tanks. The resuspension mass-flux of debris class "I" is usually expressed as a product of the sediment mass and a coefficient, $K_R^I(t)$, referred to as the resuspension coefficient:

$$M_{Resuspension}^I = K_R^I(t) \cdot M_{Pool}^I$$

Equation 4-5

where:

$M_{Resuspension}^I$ = resuspension mass flux (lbm/s);

$K_R^I(t)$ = resuspension coefficient (1/s);

M_{Pool}^I = total mass of Ith debris species contained in the suppression pool floor (lbm)

This parametric resuspension model described in NUREG/CR-6224 [4-4] allows for a variety of scenarios to be simulated through the usage of resuspension coefficients. For example, one scenario of interest is instantaneous resuspension of all suppression pool sludge at the start of the blowdown and no resuspension thereafter. This situation can be modeled by assigning the following time-dependent function for the resuspension coefficient:

$$K_R^I(t) = 1.0 \; for \; 0 < t < 1s$$

Equation 4-6

$$K_R^I(t) = 0.0 \; for \; t > 1 \, s$$

In general, $K_R^I(t)$ is a complex function of sediment particle size and shape, pool velocity profiles, and pool turbulence levels. The model developed does not attempt to model resuspension mechanistically, that is, it does not attempt to relate the resuspension coefficient to the suppression pool turbulence levels or recirculation velocities. Instead, it assumes that the resuspension coefficient is directly proportional to turbulence intensity.

Accordingly, $K_R^I(t)$ can be visualized as having the temporal dependence shown in Figure 4-8. The resuspension coefficient is close to 1.0 during the high-energy phase as demonstrated by the ARL experiments; this conclusion is judged equally valid for both LLOCA and MLOCA. The coefficient falls to essentially zero once the turbulence associated with the high-energy phase decays. It may possess a non-zero value in the recirculation phase, depending on recirculation flow velocity profiles and containment design.
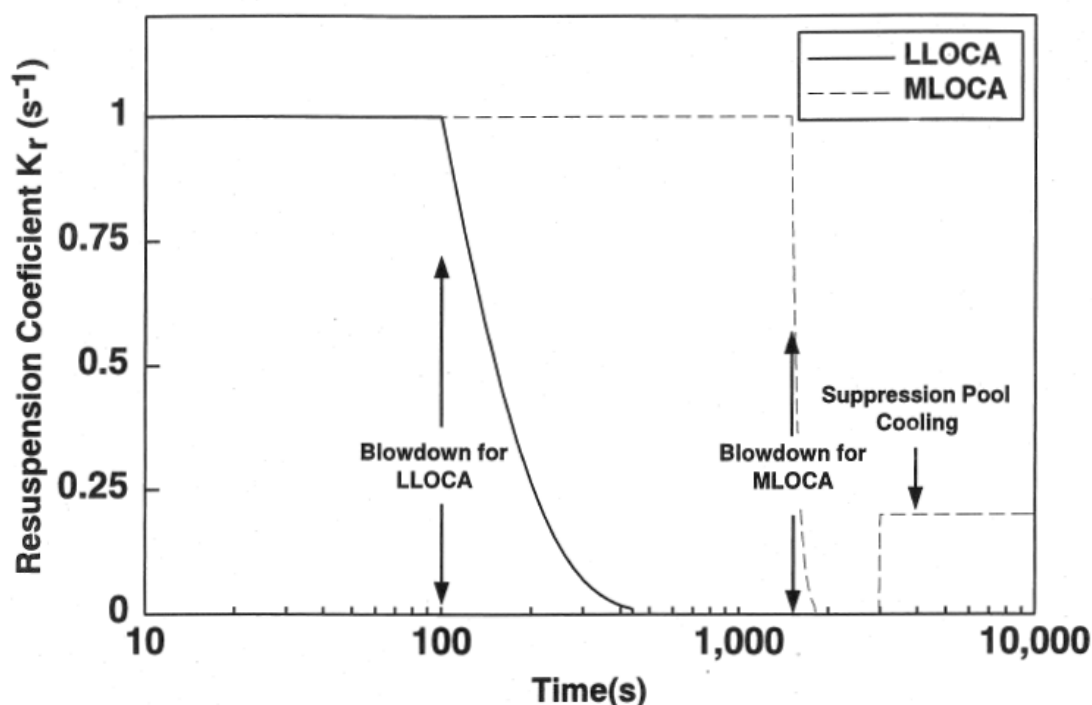
Figure 4-8: Resuspension Constant as a Function of Time

Appropriate values for $K_R^I(t)$ should be obtained from experimental studies, either full-scale experiments or experiments that are appropriately scaled. At present, appropriate data are lacking for the post-high-energy phase of an accident. Engineering judgment formed the basis of the values used in NUREG/CR-6224 [4-4].

Additional insights can be derived from [4-10] and [4-11]. Although these experiments were designed to study fibrous debris transport within the suppression pool during the blowdown phase of a LOCA, these investigators concluded that the sunken debris can be easily resuspended by relatively small turbulence levels. The resuspension studies were done using a submersible mixing fan that introduces turbulence mechanically. The resuspension of the debris studied, when under the influence of the mixing fan, was described by the investigators as resembling a rising cloud. The investigators also noted complete resuspension of the debris when the fan was on, and quick settling when the fan was off. The shreds used to conduct these experiments were 30 mm by 30 mm by 20 mm mineral

wool pieces, which had been disintegrated during blowdown experiments.

4.2.4   *RMI Debris Settling Characteristics*

Tests were conducted at ARL [4-16] to investigate still pool settling characteristics of RMI debris generated by the steam blast test of May 31, 1995 [4-3] conducted by Siemens-KWU. These tests suggest that all such RMI debris will settle with a typical velocity of 120 mm/s, indicating a high probability of RMI debris settling in a relatively short period of time (e.g., less than five minutes) in suppression pools with little or no turbulence. This is an important difference when compared to the much lower settling velocities associated with fibrous insulation debris.

In addition, tests were conducted to examine the impact of chugging on settling. The qualitative results, which should not be used for unconditional extrapolation, can be described as follows:

1.   A fairly high fraction of the RMI debris (between 1/3 and 2/3) appears to settle in the pool region for the lowest energy chugging tested. A lower fraction of the debris, estimated to be 1/4 to 1/2 based on visual observations, settles at a higher chugging energy level considered more typical of the entire chugging event;

2.   The larger debris is kept in suspension more readily than the smaller debris. It appears that larger pieces of RMI debris coupled with higher turbulence levels present a worst-case scenario, but unconditional conclusions are not possible due to the visualization limits;

3.   Settling was observed to take place at regions of the curved torus wall that are not directly below the downcomers where local velocities are higher;

4.   From visual observations it can be speculated that debris size, shape, and concentration can play a role. In some cases it appeared that RMI debris was lodged on the floor because one piece would become entangled with another, forming a heavier cluster more difficult to entrain.

Figure 4-9 shows the experimental facility and suspension characteristics exhibited by the RMI debris tested.

4.3   Transport of Reflective Metallic Insulation

Experiments were conducted at the Finnish Centre for Radiation and Nuclear Safety (STUK) to test the transport and clogging properties of RMI [4-17]. The basic test facility consisted of a 25 m^3 water tank, a water recirculation water system, and a pressure vessel for the air supply. The first three experimental sets investigated the transport properties of insulation foil pieces, starting with sedimentation in a stagnant water pool and proceeding to transport in horizontal and vertical flows. The clogging experiments addressed the differential pressures resulting from accumulation of both pure metallic and a mixture of metallic and fibrous (mineral wool) debris. The results showed that transport of RMI would occur and that the shape, velocity, and circulatory patterns were controlling factors. These tests also illustrated that under certain circulation conditions, larger pieces could remain suspended. Mixtures of fibrous and RMI pieces resulted in larger pressure differentials than would be caused by either of the constituents alone. This is an important finding because the significance of fibers and other debris bridging flow gaps is now becoming more evident from head-loss experiments directed at obtaining data for modeling thin layers of fibrous debris and attendant particulate (i.e., "sludge") filtering effects.

Transport characteristics of RMI debris are also reported in NUREG/CR-3616, "Transport and Screen Blockage Characteristics of Reflective Metallic Insulation" [4-18], based on experiments conducted at the ARL. Although those transport experiments were conducted in a flume versus a large pool [4-14], the observed motions of foils and pieces of foils reported are similar.
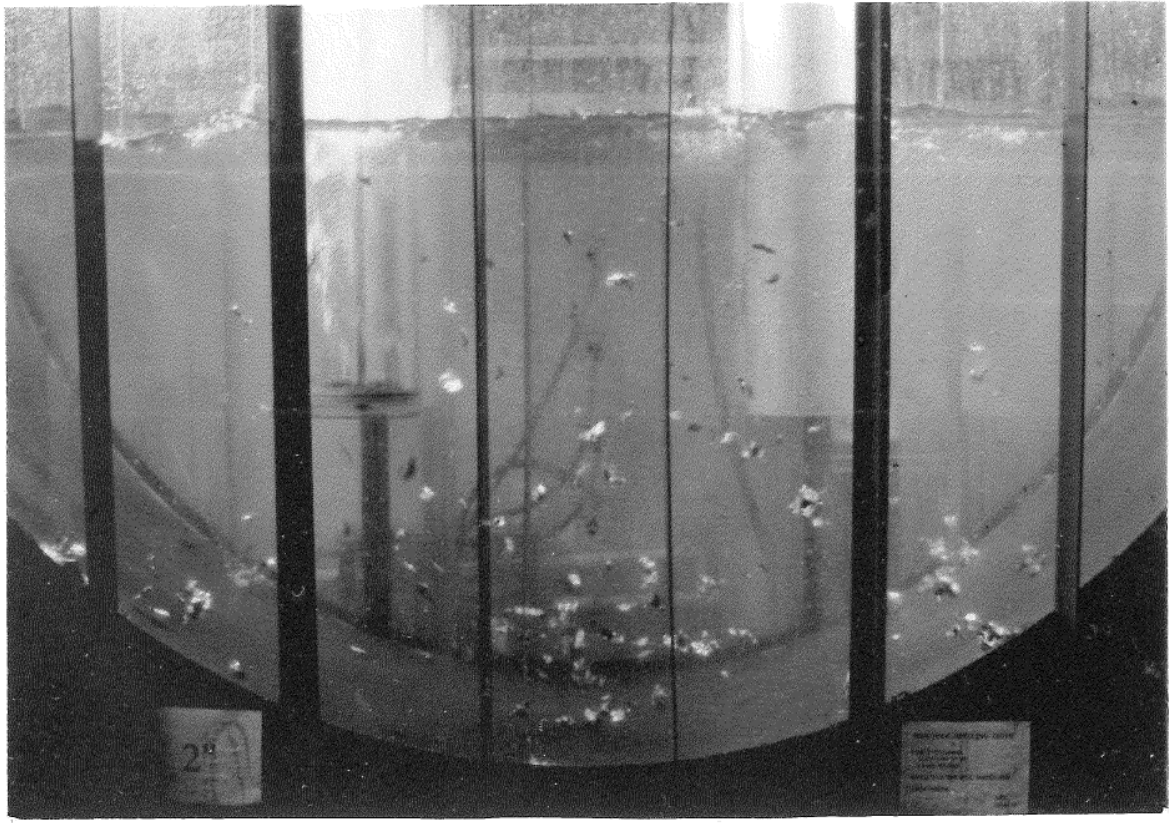
Figure 4-9: RMI Debris Suspension Characteristics

4.4   PWR Containment Pool (Sump) Debris Transport

The PWR containment pool debris transport evaluation considers two relatively distinct phases. The first phase involves the transport of debris as the pool fills, before activation of the recirculation mode. The second phase examines the transport of debris within the established pool with the recirculation pumps operating. The further erosion of debris within the pool is considered to be a relatively long-term process and is, therefore, evaluated in the second phase rather than the first.

The information requirements for the containment pool transport analyses include the structural geometry that shapes the pool, the locations and rates of flows entering the pool, the location and flow through the recirculation strainer, and the debris source terms from the blowdown/washdown analyses (Chapter 3). The geometry description includes any debris interceptors designed to preclude or reduce debris transport. A common debris interceptor is a curb-like device designed to inhibit debris from moving across the sump pool floor, at least until sufficient debris piles up behind the interceptor to form a ramp that allows additional debris to slide over the top. Another type of interceptor is a grating or perforated plate across a flow pathway that traps debris at that pathway; once blocked by debris, the interceptor effectively reroutes that flow over the interceptor or through a more torturous pathway to the recirculation strainer.

4.4.1   Containment Pool Formation Debris Transport

The PWR containment pool would begin to fill with water immediately after the LOCA break due to both RCS blowdown effluents and the drainage of the containment sprays and continues to fill until a relatively steady-state water level is achieved. Analytically, the pool formation period is generally assumed to range from break initiation to ECCS switchover to the recirculation mode. After

switchover, the analysis is described in the pool recirculation debris transport section. The primary driving force for moving debris during pool formation, especially for the large debris, is sheeting flow as the initial water from the break spreads across the sump floor. This behavior was observed during the integrated debris transport tests [4-19] in which debris, initially deposited on the floor, was observed to be pushed along with the wave front. These observations demonstrated that sheet-flow driven debris can be transported a considerable distance, even to the other side of the sump pool, and that once in motion, a piece of debris can readily gain enough momentum to carry it past openings where water would otherwise flow, such as a doorway from the primary sump area into an interior space such as the reactor cavity. Once the water depth becomes significant, further transport that occurs due to the drag forces of the water flow past the debris becomes substantially less dynamic than the original sheeting flow transport, especially for the larger debris, so that further debris movement can effectively cease. Individual fibers will move as suspended debris in the water flow.

Substantial quantities of debris may be initially deposited on the floor of the compartment where the LOCA break occurred (e.g. a SG compartment), and the subsequent break compartment sheeting flow could likely transport substantial portions of that debris from the break compartment and into other sump locations (e.g., the annular sump pool area via personnel access doorways). As the pool fills, water will flow into spaces located below the pool floor, such as a reactor cavity, and that flow will carry debris into such spaces. However, in some situations, the pathway is sufficiently tortuous that larger debris would not follow that flow into such a space. When the water filling one of these spaces becomes completely filled and relatively quiescent, that space is referred to as an inactive pool or inactive volume. Once debris enters an inactive pool, that debris may be considered as permanently trapped there unless there is subsequent sufficient flow through that pool to once again entrain the debris. Once large-piece debris enters an inactive pool region, it is likely to remain there, but the situation is less clear with respect to fine suspended matter because even natural circulation could allow the suspended matter to escape.

The debris entering the pool during the pool fill transport period would include debris initially deposited in the pool during blowdown and then any debris washed back down into the containment pool by the containment sprays during this period. The sump formation period would likely be relatively short compared to the time it would take for the containment washdown to complete; therefore most of the washdown debris would typically be expected to transport into the pool during the recirculation transport phase. While the larger debris may be moved around during pool fill, such debris would likely remain on the pool floor unless buoyant. Such debris would not accumulate on the strainer prior to switchover to recirculation and after switchover the large replacement strainer perimeter approach velocities would typically be too slow to lift the large debris from the floor and onto the strainer. Fine suspended matter would likely become relatively uniformly mixed within the pool, with the possible exception of the inactive pool regions.

The quantity of fine debris trapped within inactive pools has been estimated by multiplying the total quantity of fine debris estimated to be in the sump pool as a result of blowdown transport[5] by the ratio of the inactive pool volume to the total sump pool volume. Regarding the distribution of the larger debris on the sump pool floor following pool fill, it is not conservative to assume that all such sump pool debris is uniformly distributed across the containment floor as settled debris. If it can be shown that debris of a specific size category would be settled debris, and that the subsequent established sump pool flow velocities and flow turbulence were insufficient to cause such debris to accumulate on the strainers (i.e., entrainment), then the issue of debris distribution is of no consequence. Otherwise, an analysis with conservative assumptions will be required to initially

---

[5] Because transport of debris by washdown processes is time-dependent, washdown debris will enter the sump pool both before and after the pool has filled and the recirculation pumps have started. Analytical capabilities have not been sufficiently developed to determine how much washdown debris enters before and how much enters after the pool has filled. Therefore, the only reasonable conservative assumption is that only debris deposited in the sump pool area by blowdown processes can be transported into inactive pool volumes.

distribute the debris before operating the recirculation pumps. For example, it could be conservatively assumed that the pool fill relocated all such debris near the recirculation strainers. A more detailed analysis could be used to relax the conservatism.

4.4.2   *Containment Pool Recirculation Debris Transport*

This phase in the debris transport evaluation estimates the quantities of debris, by type and size classification, that would arrive at the recirculation strainer for potential accumulation. The source debris includes the debris already in the sump pool when the recirculation pumps start and the subsequent debris entering the pool due to washdown processes. The typical recirculation transport analysis deals with the overall potential quantities of debris transported, i.e., the transport processes are sufficiently complex that time-dependent analyses are not practical. However, if the only debris with the potential for accumulation on the strainers consisted of suspended matter such that settling and other forms of deposition could be neglected, and the time frame for the washdown processes was reasonably short compared to that for the recirculation processes, a first-order estimate could be made of time dependency based on a uniform concentration within the pool.

The three main types of debris resulting from prototypical behavior for recirculation sump pool transport are: (1) suspended debris, (2) buoyant debris, and (3) settled debris. Suspended debris matter typically consists of fine debris (i.e., basically individual fibers and fine particulates). Although these fine debris types will settle in still or relatively calm water, the settling process can take substantially more time than the typical sump pool turnover times. An actual plant containment pool is not necessarily calm water due to the continuous entrance of break overflow and containment spray drainage into the sump pool. This drainage added to the recirculation flow, especially at channels through passageways induces turbulence. It is conservative and reasonable to assume complete transport of the suspended fines to the strainer.

Debris that remains buoyant will float on the surface of the pool and, therefore, may tend to drift toward the strainer. Examples of buoyant debris are types of closed cell foam insulations where water penetration is unlikely. Typically, such debris would not be a strainer blockage problem because the typical strainer would be submerged. Hence, the buoyant debris is typically dismissed from further consideration. The exception, of course, would be the partially submerged strainer where the accumulation of the buoyant debris against the strainer could contribute to the potential blockage problem.

Settled debris may or may not transport to the strainer. The settled debris of greatest concern is typically shreds of fibrous debris. Dry fibrous debris will initially float because most of its volume is free space filled with air. But over time, water will infiltrate the fibers, and eventually the debris will sink to the pool floor, whether it is a small shred or a complete intact pillow [4-20]. The rate of water infiltration is highly dependent on the temperature of the water (surface tension effect). Whereas cold water can take hours to days to infiltrate fibrous insulation, hot water can saturate shreds of fibrous debris rather rapidly. Aged fibrous insulation, where the binder has dissipated, will also absorb water quickly and settle. If large-piece fibrous debris (or an intact pillow) remains buoyant for a sufficient time, it could float over the top of the recirculation strainer and then sink onto the strainer. However, the probability of this behavior is relatively small so that it is unlikely that it would contribute significantly to the blockage of a large strainer, i.e., the large piece would either simply lie across the top of the strainer or fall to the floor beside the strainer.

Once fibrous debris has settled to the sump pool floor, its mode of transport would be to either slide or roll along the floor toward the strainer. Floor-transported debris would be subject to entrapment by obstacles such as curbs and debris interceptors. Small-scale testing has been conducted to measure the necessary velocities to cause the movement of various kinds of settled debris [4-21].

For a given type and size of debris, a certain flow velocity is needed to move the piece of debris along the floor. A greater velocity would be needed to cause the debris to become sufficiently

entrained to lift over an obstacle. If a piece of debris were to arrive at a strainer located above the sump floor, it may take a greater velocity to lift the piece onto the strainer resulting in accumulation. Further, for debris on a vertical strainer surface, a minimum velocity may be required to keep the debris attached to the strainer. Turbulence affects minimum transport velocities. Most separate-effects testing was conducted with uniform low-turbulent flows, and some testing has been conducted with turbulence induced. A flow assessment can estimate whether or not the flows approaching a strainer are sufficiently fast or turbulent to transport floor debris from the floor onto the strainer. A notable alternate strainer configuration would be a strainer recessed into a pit below the sump pool floor where the floor transported debris could simply fall into the pit and onto the strainer. Vendor head loss testing performed in conjunction with debris transport to the strainer via a flume designed to replicate licensee prototypical strainer approach velocities has shown a tendency for the heavier RMI debris and typical paint chips to settle within the flume rather than accumulate on the test strainer, i.e., the flume test velocities were less than the debris transport velocities for debris that has settled to the flume floor (note that a typical shred of LDFG insulation requires a velocity of approximately 0.12 ft/s to move along a floor). This vendor testing was plant-specific and therefore not generally applicable to all plants; however the trend noted would apply to a significant number of plants. There are, of course, exceptions such as a piece of RMI debris with an entrapped air bubble or a paint chip that floats. In addition, in vendor head loss testing, some fibrous insulation shreds may remain buoyant and float over top of the test strainer most likely due to air entrapment.[6]

Another concern is transport of failed coatings. The transport testing of coating debris is documented in NUREG/CR-6916 [2-25]. Five coating systems, typical of coatings applied to equipment and structures located in the containment buildings of PWR plants, were tested. The effects of chip size, shape, density, thickness, stream velocity, water saturation, and thermal curing on transportability were examined through two types of tests: quiescent settling and transport within uniform flow. The water in the test flume was unborated tap water at ambient temperature. The quiescent settling tests were conducted in a 0.3 m wide by 0.3 m long by 1.2 m deep (one ft wide by one ft long by four ft deep) acrylic tank. The goals of the quiescent water tests were to determine: (1) the time necessary for coating chips dropped onto the water surface to break the surface and begin to sink (time-to-sink tests), and (2) to determine the terminal settling velocity of submerged coating chips (terminal velocity tests). The transport tests were conducted in a 0.91 m wide by 0.91 m deep by 9.1 m long (three ft wide by three ft deep by thirty ft long) acrylic flume suspended in a large circulating water channel. The goal of the transport tests was to characterize the behavior of coating chips in moving water. The tests consisted of a tumbling-velocity test to study the behavior of coating chips placed on the flume floor and a steady-state velocity test to study the behavior of coatings debris released into the moving stream below the water surface. A statistically meaningful number of data tests were conducted for each coating type, chip size and chip shape in each test category in order to more accurately quantify observations.

The quiescent tests demonstrated that, when dropped onto the water surface, coating chips with a density close to that of water tended to remain on the surface indefinitely and heavier chips tended to sink almost immediately. The tumbling velocity tests demonstrated that all but the lightest chips and curled chips remained in their initial position at stream velocities in excess of 0.09 m/s (0.3 ft/s). The steady-state velocity test demonstrated that, at a uniform water velocity of 0.06 m/s (0.2 ft/s), all but the lightest chips settled to the bottom before reaching the end of the flume.

The final important aspect of floor debris transport is that some types of debris (e.g., fibrous and particulate insulation debris) are subject to erosion, resulting in additional suspendable fines that would likely be completely transported to the strainer. The erosion process is discussed in Section 4.5.

---

[6] In the US, vendor head loss testing was typically conducted with colder water that may not easily saturate fibrous debris. The usual test procedure would include a step in which the fibrous debris was pre-saturated before introduction into the test tank typically using heated water. The floating fibrous debris noted during vendor testing was likely due to improper and incomplete saturation.

Determination of the transport fractions for floor-transportable debris requires an assessment of sump pool flow velocities and patterns, together with flow turbulence. The best method for this hydraulic assessment is the application of a CFD code to the plant-specific sump pool. An example CFD application is the CFD study performed for a reference plant, found in the NRC SE for NEI-04-07 [4-22]. However, it is noted that horizontal swirls (eddy currents) can be difficult to accurately predict with a CFD code. CFD applications are discussed in more detail in Appendix E.

After a suitable CFD code is selected, a three-dimensional geometric model of the sump pool is typically developed. Models should include an appropriately detailed calculational mesh. The geometric model should be sufficiently detailed to include significant structures located within the sump pool and such details as stairwells and flow passageways. The height of the model should extend from the bottom of the pool to the maximum anticipated depth of water. Note that some CFD codes support the importation of Computer-Aided Design (CAD) models. The locations and flow rates of water sources to the sump pool, including effluents from the LOCA break and containment spray drainage, are simulated. There should be sufficient detail to reasonably capture the splash locations of the incoming water. The water drawn from the pool via the recirculation pump is simulated.

Analysts have typically focused on simulating the steady-state flows of a fully established pool but some have simulated the pool fill-up transient. A simulation typically requires appropriate boundary condition assumptions for surfaces, and inlet and outlet flows. Steady-state conditions must satisfy conservation of water mass within the pool; for example, the simulation might use a specified flow rate for mass inflow but then use a pressure boundary condition that allows the code to adjust the pressure at the bottom of the sump to balance the mass flow entering and exiting the pool without introducing numerical instabilities. Many CFD codes have user options for selecting numerical models for solving incompressible flow (Navier-Stokes equations), as well as for simulating turbulent kinetic energy and the dissipation of the turbulence. CFD codes that include features that model phenomena in sump pools should be selected. For example, codes should model specific sump pool flow behavior like turbulence dissipation of swirling flows. CFD codes require the analyst to specify appropriate initial conditions to initiate a simulation and to specify the numerical convergence criteria for the acceptance of a solution where the options available to the analyst vary the code.

The CFD results are typically two-dimensional figures showing either the velocity flow patterns or the patterns of flow turbulence at particular levels within the pool. An example of a flow velocity pattern is shown in Figure 4-10 (Figure III-36 in [4-22]). The scale on the right side of the figure shows the color codes used for the pool velocities. Referring to Figure 4-10, shreds of LDFG debris physically located in the yellow or red zones (i.e., velocities greater than about 0.06 m/s (0.2 ft/s)) would most likely move with the flows, and the shreds located in the blue zones (i.e., velocities less than about 0.03 m/s (0.1 ft/s)) would likely remain at those locations, but the movement of the shreds located with the green zones is less certain. In addition, CFD results can include streamline plots that would indicate how fine suspended debris moves within the pool.

The scenarios that need to be simulated likely include both Small Break Loss-of-Coolant Accidents (SBLOCAs) and LBLOCAs and the various break locations, e.g., alternate steam generator compartments. Activation of the containment sprays is dependent on containment pressurization, which in turn, depends upon the size of break. Both the pumping flow rate and the pool depth can vary with the size of the break. In addition, the debris source term under evaluation may depend upon the size of the break, as well as break location.
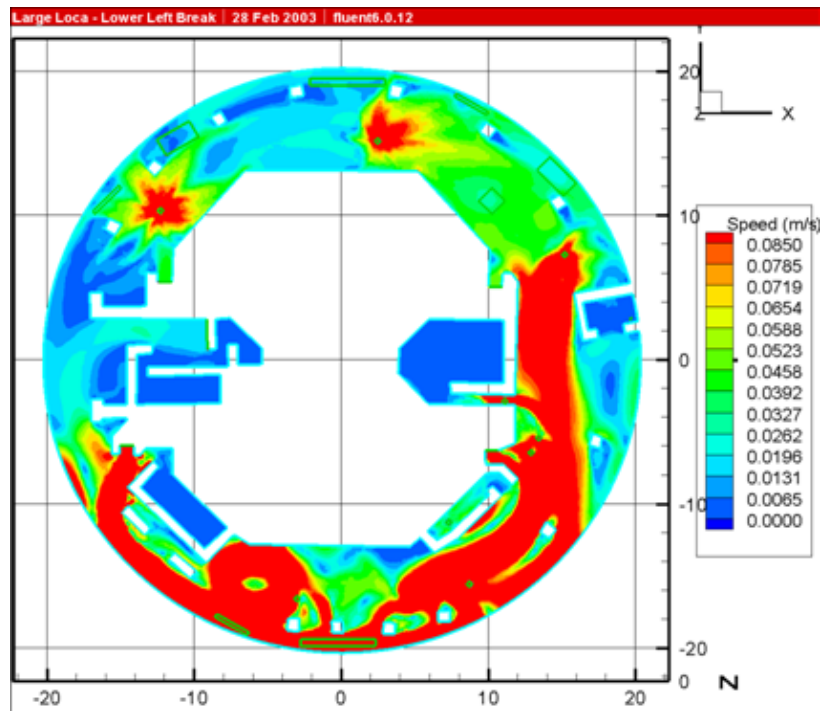
Figure 4-10: Example of CFD Sump Pool Flow Velocity Pattern

With the pool hydraulics simulated, debris transport should be estimated by using the velocity and turbulence patterns and an assessment of the initial debris location in the sump pool. Unfortunately, no debris transport model has been developed in which a straightforward application of a computer code could be used to calculate the transport. The primary method in use involves the application of engineering judgment of the CFD results to estimate transport fractions. As such, it can be useful to establish CFD plot contours corresponding to threshold transport velocities that determine whether specific floor-settled debris would likely be transported.

Refer to the logic chart for the debris-transport model shown in Figure 3-1, as an example of transport assessment. This figure included steps for debris transport during pool fill-up and during the recirculation phase for which the analyst could implement transport fractions based on analysis, or experimental data, or even conservative engineering judgment. During the chart's evaluation of the fill-up phase, the debris was either transported to the sump strainer or away from the sump strainer, or into an inactive pool. The debris transported to the strainer was added to the debris that was determined to be deposited at the strainer by the blowdown/washdown processes and the debris in the inactive pool was assumed to remain in the inactive pool. The fraction of debris predicted to be transported away from the strainer by the pool fill processes and that did not enter an inactive pool region would then be subjected to the recirculation transport processes. For this debris component, the debris is either transported to the strainer or is predicted to stall in the pool, where it may then be subject to further erosion.

Pool velocity and turbulence characteristics determine the areas of the pool where debris may be entrapped. Flow streamlines can be used to determine whether debris entering the pool at a discrete location would likely pass through a potential entrapment location. During the integrated debris transport tests [4-19], shreds of water-saturated fibrous debris were observed to accumulate in relatively quiescent locations within the simulated sump pool. Figure 4-11 is a test photo showing debris stalled within a slow-flowing region from a one-tenth scale simulation of a reference plant sump annulus. Most of these shreds tended to remain in these locations for the relatively short duration of these tests. However, during close observation, an occasional shred exited the low-flow area and was re-entrained in the surrounding flows. If such a shred subsequently encountered another quiescent location, it was likely to become stalled again. For a shred to be transported all the way to

the strainer, a continuous transport pathway was needed where the flow velocities along this pathway generally exceeded the minimum velocity required to keep the piece moving. This behavior suggests a method of estimating the fraction of debris transported along the floor within the sump pool.

Figure 4-11: Debris Stalled in a Slow-Flowing Region of the Simulated Annulus

CFD analyses can provide realistic descriptions of the flow conditions at floor level. By designating velocity contours based on experimentally measured thresholds for movement of the settled debris, the locations for debris entrapment become clearly indicated. By overlaying the CFD plots with estimates for conservative debris placement at the start of pump recirculation and also the introduction of washdown debris from above, a graphical integration can be performed to arrive at transport fraction estimates. Debris predicted to coincide with a region of flow moving slower than the threshold for debris movement would be considered as not being transported. The transport fraction is obtained by summing these quantities and subtracting the sum from the totals to calculate the quantities transported, then dividing the result by the original source terms. The actual calculation method could, for example, subdivide the pool floor into a fine mesh grid with each grid space independently assessed, the results of which are then quantified.

In addition to velocity contours, the streamline plots provide reasonable connecting pathways whereby a piece of debris would likely travel from its original location in the pool to the recirculation sumps. If a transport pathway passes through a slower portion of the pool, then debris moving along that pathway could stall and not be transported to the recirculation sump. Otherwise, transport to the strainer is more likely.

Effects of pool turbulence are more difficult to quantify. The transport results based on flow velocities may need to be adjusted by also overlaying the CFD-calculated turbulence level plots with the velocity plots. For example, turbulence levels may be relatively high near a location with a source of water plummeting into the pool. If high turbulence coincides with a flow velocity slower than the threshold transport velocity, it is prudent and conservative to assume that debris would be transported from that location. As noted above, stalled debris has been observed to resume movement, a behavior attributed to localized pulsations of turbulence that suddenly peaked at the position of that piece of debris. Although this behavior cannot be reasonably quantified, transport estimates should be

modified to consider these effects because turbulence is capable of moving debris where and when bulk flow will not or keeping debris suspended to move with the flow at any velocity. One method of accounting for turbulence effects might be to decrease the threshold velocities for transport. In addition, a certain amount of engineering judgment may be required to arrive at a reasonable solution. For more information on the use of CFD for debris transport analyses see Appendix E.

4.5 Erosion of Containment Materials and Debris

This section applies to both BWRs and PWRs. The post-LOCA containment environment can potentially damage containment materials or further degrade LOCA-generated debris. The damage to containment materials could generate additional debris, and the degradation of existing debris could generate transportable fines from relatively non-transportable larger debris. Although erosion could be considered a debris-generation issue, it is addressed in the transport section because the assessment of such damage requires knowledge of the containment environment, such as locations of pooled water, water flows, and the rates of flow.

4.5.1 Post-LOCA Damage to Containment Materials

The possibility of containment materials that were previously damaged by the LOCA being damaged by the post-LOCA environment of containment sprays and flowing water should be considered. One concern would be water flowing over materials such as insulation and fire barriers that were not protected by a cover or jacketing, such that the water could erode a surface resulting in production of fine fibers or fine particles. The water can also corrode or dissolve the materials, leading to chemical effects (Chapter 5). Evaluation of erosion has typically not resulted in the generation of significant additional insulation or fire barrier debris.

4.5.2 Erosion of LOCA-Generated Debris

The subject of further erosion of LOCA-generated debris with respect to washdown debris transport was discussed in Section 3.2. There, the postulated drivers for the erosion were the break overflow, the containment sprays, and/or spray and condensate drainage. The issue for discussion in this chapter is erosion due to immersion in a pool of water, with water flowing over and around the debris and perhaps being enhanced by turbulence. The types of debris of primary concern are fibrous debris and microporous particulate insulation debris.

4.5.2.1 Erosion of Fibrous Debris

Individual fibers will erode from fibrous debris residing within a pool then become readily transportable whereas the larger debris was not transportable. This behavior was observed in the NRC-sponsored integrated debris transport tests [4-19], which were designed to simulate the sump pool of a typical PWR plant. During four longer-term tests (3 to 5 h duration), debris accumulation on the simulated sump screen was collected every 30 min. Fine fibrous debris continued to accumulate on the test screen throughout these tests; the fineness of the eroded fiber is evidenced by the uniformity of the accumulation, which is illustrated in the photograph shown in Figure 4-12. The shreds (small clumps of fiber) typically accumulated in a heap at the bottom of the test screen. Sources of this fine fibrous debris included the initial fine fiber in the debris batches introduced into the test, as well as the eroded fibers. However, the initially suspended fibers would have been removed relatively early in the test, after a few turnovers of the tank volume. Therefore, the continued accumulation at a somewhat sustainable rate was concluded to have been primarily that of eroded fibers.

It was also apparent that the level of pool turbulence affected the rate of erosion, i.e., an increase in turbulence increased the rate of erosion. One test was conducted with a pool depth of 9 in. rather than the usual 16 in. but at the same volumetric rate of flow and the erosion rate was greater in the shallower pool. The water in the shallower pool flowed significantly faster with a corresponding

greater turbulence than the deeper pool. In fact, the accumulation was about eight times more rapid for the shallow pool test.

Figure 4-12: Typical Accumulation of Fine Fibrous Debris

These test data for debris erosion in a sump pool strongly indicate a sustainable rate of erosion that is affected by the relative turbulence in the pool. Although these longer-term tests ran for several hours, they were of shorter duration than those of the LOCA long-term recirculation tests, which ran for up to 30 days. If it is assumed that the erosion rate remains constant beyond the measured erosion rate until the end of the mission time, a conservative fraction for the quantity of debris eroded can be calculated. The following extrapolation equation takes into account the steadily decreasing mass of debris in the pool:

$$F_{eroded} = 1 - (1 - Rate)^{Hours}$$

Based on the erosion rate of 0.3% of the current tank debris per hour associated with the 16-in. pool tests, and extrapolating to 30 days (720 h), the analysis indicates that nearly 90% of the initial debris mass would become eroded. Again, this assumes a constant erosion rate, which is not likely to be true in practice.

While the application of this 90% value to the overall transport results would seem to be conservative, it may be overly conservative, and not realistic. The calculation had substantial sources of uncertainty, including (1) the integrated debris transport tests lasted only 3 to 5 h, (2) flow turbulence would in actuality depend on plant-specific geometry and flow rates, and (3) the tests did not study large-piece debris (note that fibrous debris still enclosed within a protective cover is not likely to erode). But the greatest uncertainties are whether the erosion rate declines with time and whether the erosion rate measured for small shreds applies to large pieces of relatively intact insulation. It was expected that this 90% value could be reduced with better or more extensive erosion rate data.

Several PWR vendors in the US have conducted independent testing to justify reducing the initial erosion rate after a period of time. In one test, samples of insulation of various sizes were placed within wire mesh baskets that were, in turn, placed within a linear flume. A turbulence suppressor and a flow straightener were used to condition the flow upstream of the sample baskets. Flume velocity was specified to approximately match a CFD-predicted maximum recirculation velocity for the post-LOCA sump pool. A nominal (average) flume velocity of 0.72 ft/s was used for the testing (greater than the velocities found in 98% of the containment pool). Note that this test velocity is much higher than the typical tumbling velocity for small pieces making the results conservative for debris lying on the floor and not retained by some object, such as a debris interceptor.

Debris samples were placed in the flume for a specific time period; removed, dried, and weighed, and then generally placed in the flume again later for one or more additional erosion test intervals (the intervals provided time-dependent information). The differences between the initial masses and the post-test masses were attributed to erosion. The measured erosion percentages for small and large pieces of NUKON and Kaowool®[7] debris from the test durations were extrapolated out to the 30-day test period, which resulted in a 30-day erosion estimate of 30% for NUKON and 10% for Kaowool; these numbers were then conservatively increased to 40% for NUKON and 15% for Kaowool in the debris transport calculation.

Alion Science and Technology also conducted erosion testing on fibrous debris using submerged small pieces of NUKON low-density fiberglass insulation exposed to water flows representative of a PWR containment sump pool following a LOCA. The proprietary test report concluded that a cumulative erosion percentage of 10% over a 30-day period following a LOCA is justified. Prior to plant-specific application of these erosion test results, licensees should verify that the test conditions (e.g., velocity and turbulence levels, debris material properties) are applicable to their plant-specific conditions. The Alion testing demonstrated that the previous NRC assessment of 90% based on extrapolating a few hours of test data out to 30-days was overly conservative and that more realistic values have been developed for PWRs (similar data have not yet been developed for BWRs).

Regarding BWRs, the turbulence that would occur in the suppression pool during the high-energy depressurization phase would further disintegrate fibrous debris including the generation of individual fibers [4-4]. Such fragmentation behavior was observed in scaled suppression pool tests investigating debris sedimentation of LOCA-generated debris and sludge, but a method was not developed for quantifying the fragmentation [4-23].

In the erosion of LOCA-generated debris, it is likely that destruction of the insulation leaves fibers rather loosely attached, so that moderate turbulence working these fibers back and forth will cause the fibers to detach. Testing during the DDTS [4-24] showed that fibers will also erode from undamaged insulation, but that typically requires more turbulent force to sustain an effective erosion rate. Therefore, it is reasonable to expect that the rate of erosion for LOCA-generated debris would taper off with exposure time, as the more loosely attached fibers have been detached so that the increasing total eroded mass is expected to approach an asymptotic limit. As such, it may be possible and reasonable to extrapolate test results that demonstrate a tapering-off effect from shorter test durations out to a 30-day test period.

The guidance that should be observed whenever such erosion testing is conducted includes:

- The conduct of such erosion testing should ensure that the velocity and turbulence test conditions are prototypical or conservative of the plant pool. Due to the turbulence associated with the often chaotic and multidirectional variations in prototypical flow conditions, a bounding flow velocity may not by itself guarantee the prototypicality of the turbulence;
- Preparation of debris samples should render debris prototypically representative of LOCA-generated insulation debris. For example, destroying insulation with a shredder would produce debris more prototypical of a LOCA than simply cutting insulation into pieces;
- The size distribution of the debris samples should be representative of and even conservative with respect to predicted debris size distributions. It is conservative to hedge test samples to the smaller size because smaller pieces have a higher surface-to-volume ratio than larger pieces, which tends to increase the erosion rate;
- Placement and grouping density within the test basket should be prototypical of the plant sump pool, in that the grouping should not shield individual debris pieces from turbulence in a non-prototypical manner;

---

[7] Kaowool® is a registered trademark of Thermal Ceramics Inc.

- If the measured erosion rates depend upon the size of the debris, then the overall erosion of the LOCA-generated debris necessarily would involve an integration of the rates with the predicted debris size distribution;
- Erosion test data are specific to the type of fibrous debris tested. There is no guidance regarding the adaption of erosion data for one type of fibrous insulation to another type of insulation. Erosion rate tests must be conducted in water representative of plant conditions, i.e., temperature, pH, chemical additives, etc.

4.5.2.2   *Erosion of Microporous Insulation Debris*

Microporous insulation debris subject to post-LOCA environmental conditions can erode and give off fine particulates that could contribute to strainer head losses. During NRC-sponsored separate-effects testing, one type of calcium silicate (obtained from Performance Contracting, Inc.) was tested for its dissolution behavior in water [4-21]. In these tests, pieces of debris that had been created by shattering this calcium silicate insulation were dropped into water at both ambient and 80 °C. The water was quiescent or was stirred to induce turbulence. Within 20 minutes in the stirred 80 °C water, about 75% of the material became suspendable fines due to the disintegration process. This process was found to increase with temperature and to increase with turbulence.

Similar vendor conducted tests were conducted by a licensee in the US. In this test the dissolution of two pieces of calcium silicate (identified as having asbestos-bearing fibres) were tested in 93.3 °C (200 °F) water for 2 h with stirring added for 30 min. This vendor testing had substantially different results from the NRC-sponsored tests. A calcium silicate insulation expert was consulted to help discern why the two sets of test results were so different. The primary reason for the behavior difference was attributed to the manufacturing process of the calcium silicate insulation i.e., either a press-shaping process or a molding-shaping process. The licensee's insulation contained asbestos fibers and it was manufactured by the press-shaping process, which results in a material that is resistant to water erosion, whereas the calcium silicate used in the NRC-sponsored testing was manufactured by the molding-shaping process, which results in a material that is apparently highly susceptible to water erosion.

The erosion rate depends on the type and manufacture of the calcium silicate, and it is apparent that at least some erosion would occur for any calcium silicate insulation. The same conclusion should be assumed for Min-K and Microtherm unless adequate research is conducted to support a different conclusion. When erosion tests are conducted, no matter what the debris type is that is being tested, the tests should last for a sufficient length of time to adequately determine the rate of erosion. The lower the rate of erosion, the longer the test duration needed to accurately determine the erosion rate. Even a low rate could be important over the long-term post-LOCA mission time of the containment sump. The hydraulic conditions being subjected to the test debris should be prototypical (or conservative) with respect to the plant sump pool. In addition, steps should be taken to ensure that the samples are properly dried before weighing to ensure accuracy. Because the measured mass differences during the testing can range from hundredths to tenths of a gram, small variations in the quantity of water adhering to the samples at the time of weighing could easily influence differential mass measurements.

There have been erosion experiments conducted in other countries (Germany and France), but they are not discussed here because the test results were not available.

4.6   **Knowledge Base for Containment Pool Debris Transport**

There have been a number of studies of pool debris transport since NEA/CSNI/R(95)11 was issued, most significantly related to PWR containment debris transport. The transport of failed coatings has also been studied. Most debris transport/strainer head loss correlations rely on a few types of debris and the formation of homogeneous filter bed on the strainer surface. More recent head loss testing experiments have concluded that the use of correlations is difficult to justify. The debris

beds rarely form homogeneously and the correlations used in the past did not include the contribution from chemical effects (Chapter 5).

Plant specific head loss testing with representative quantities and combinations of debris of types is now recommended in most member countries. However, the scaling effects associated with debris transport add uncertainties. Debris preparation methods and debris introduction into the test flume can have a great effect on test results. The test should be performed in a manner that resembles plant conditions as closely as practical.

CFD has been extensively used to assess debris transport by predicting sump pool floor velocity patterns and turbulence. The use of CFD analyses is complex; difficulties include:

- Analyses require a large number of nodes;

- Including turbulence in the model requires refined techniques;

- Multi-phase flow models need more benchmarking; and,

- Limited validation and verification data for the models exist.

References

4-1   General Electric Company, "The General Electric Pressure Suppression Containment Analytical Model", Topical Report NEDO-10320, April 1971; Supplement 1, May 1971; Supplement 2, January 1973.

4-2   BWR Owners' Group ECCS Suction Strainer Committee, Letter from T. Green to A. Serkiz (NRC), "Suppression Pool Sludge Particle Size Distribution", OG94-661-161, September 13, 1994.

4-3   Siemens-KWU, "RMI Debris Generation Testing - Pilot Steam Test with a Target Bobbin of Diamond Power Panels", Technical Report NT34/95/e32, Karlstein, July 3, 1995.

4-4   U.S. Nuclear Regulatory Commission, "Parametric Study of the Potential for BWR ECCS Strainer Blockage due to LOCA-Generated Debris", NUREG/CR-6224, October 1995.

4-5   E.S. Pettyjohn and E.G. Christiansen, "Effects of Particle Shape on Free Settling Rates of Isometric Particles", *Chemical Engineering Progress,* Vol. 44, No. 2, p. 157, 1948.

4-6   "Particle Dynamics," *Perry's Chemical Engineering Handbook,* McGraw-Hill Book Co., 1977, pp. 5-61.

4-7   H.A. Becker, "The Effects of Shape and Reynolds Number on Drag in the Motion of a Freely Oriented Body in an Infinite Fluid", *Canadian Journal of Chemical Engineering,* Vol. 37, Issue 2, pages 85–91, 1959.

4-8   J.W. Daily and D. Harleman, *Fluid Dynamics,* Addison-Wesley Publishing Company, Inc., 1966.

4-9   G.T. Orlob, "Eddy Diffusion in Homogeneous Turbulence", *Transactions of American Society of Civil Engineers,* Vol. 126, Part 1, 1961.

4-10   Oskarshamn Kraftgrupp, "Downward Transport and Sedimentation of Insulation Material and the Build-up of Pressure Loss in the Suction Filters", 92-07779, Stockholm, Sweden, March 1992.

4-11   Illinois Institute of Technology, "Measurements on the Sink Rate and Submersion Time for Fibrous Insulation", Test Report No. ITR-93-02N, May 22, 1993.

4-12   Performance Contracting, Inc., "NUKON Debris Sink Rate Test on Unexposed Base Wool in Room Temperature Neutral Water", ESD-TR-10B, December 11, 1984.

4-13   Alden Research Laboratory, Inc., "Tests of Particle Settling Velocity in Still Water", Report No. ARL/SEA/787/94/1, Alden Research Laboratory, Inc., June 1994.

4-14   ABB-Atom, "Guaranteed Emergency Core and Containment Cooling. Laboratory Experiments Concerning Insulation", Report No. RVD 92-192, November 1992.

4-15   ABB-Atom, "Barseback 1 and 2, Oskarshamn 1 and 2 - Strainers in Systems 322 and 323. Results from Blowdown Experiments in a Test Rig", Report No. RVA 92-340, November 27, 1992.

4-16   Alden Research Laboratory, Inc., "Reflective Metallic Insulation Settling Following a LOCA in BWR Suppression Pools", Report No. 1/4-95/M787F, August 1995.

4-17   Finnish Centre for Radiation and Nuclear. Safety, and Imatran Voima Oy "Metallic Insulation Transport and Strainer Clogging Tests", STUK-YTO-TR 73, DLV1-G380-383, June 1994.

4-18   U.S. Nuclear Regulatory Commission, "Transport and Screen Blockage of Reflective Metallic Insulation Materials", NUREG/CR-3616, December 1983.

4-19   U.S. Nuclear Regulatory Commission, "GSI-191: Integrated Debris Transport Tests in Water Using Simulated Containment Floor Geometries", NUREG/CR-6773, December 2002.

4-20   U.S. Nuclear Regulatory Commission, "Buoyancy, Transport and Head Loss of Fibrous Reactor Insulation", NUREG/CR-2982 Revision 1, July 1983.

4-21   U.S. Nuclear Regulatory Commission "Separate-Effects Characterization of Debris Transport in Water", NUREG/CR-6772, August 2002.

4-22   U.S. Nuclear Regulatory Commission Safety Evaluation (SE), Revision 0, December 6, 2004, "Pressurized Water Reactor Containment Sump Evaluation Methodology for NEI document number NEI 04-07".

4-23   U.S. Nuclear Regulatory Commission "Experimental Investigation of Sedimentation of LOCA-Generated Fibrous Debris and Sludge in BWR Suppression Pools", NUREG/CR-6368, December, 1995.

4-24   U.S. Nuclear Regulatory Commission "Drywell Debris Transport Study", Vol. 1 to 3 NUREG/CR-6369, September, 1999.

4-25   U.S. Nuclear Regulatory Commission "Hydraulic Transport of Coating Debris", NUREG/CR-6916, December 2006.

4-26   Letter from US NRC to Mr. Robert Choromokos, Manager, Energy Services Division Alion Science and Technology, dated June 30, 2010 "Proprietary Erosion Testing of Submerged NUKON Low Density Fibreglass Insulation in Support of Generic Safety Issue 191 Strainer Performance Analyses", ADAMS No. ML101540221.

5.   CHEMICAL EFFECTS

5.1   Introduction

In the 1990s, three nuclear plants experienced minor incidents that resulted in their ECCS becoming engaged but operation of the strainers was significantly hindered by debris [5-1]. Many countries began programs to address deficiencies in the ECCS strainer knowledge base [5-2], and many utilities replaced their existing strainers with larger units.

Around the time that new installations were nearing completion, chemical precipitates were identified as a form of debris not yet considered. In an assessment performed by Los Alamos National Laboratory (LANL) [5-3], it was noted that evaluations of hydrogen generation for DBAs include contributions from zinc and aluminum corrosion, although the effects of corrosion by-products were not yet considered for strainer performance. In 2003, the US Advisory Committee on Reactor Safeguards (ACRS) noted [5-4] that the recirculation water following a LOCA could facilitate chemical reactions because of the presence of:

1. RCS additives such as boric acid or lithium hydroxide;

2. Additives such as sodium hydroxide in sprays or trisodium phosphate (TSP) in the sump.

They suggested that the amount of additional debris generated by chemical reactions could be significant, and could interact differently with an existing debris bed than the materials from which the chemical reactants originated. The ACRS noted that the gelatinous debris found in the sump of Three Mile Island Unit 2 following the accident in 1979 was an example of the type of precipitate possible [5-5].

In a broad-scoped letter issued by the US NRC [5-1] regarding ECCS performance, the regulator identified that chemical effects may have an effect on head loss and that addressees should consider these effects in their responses. Small-scale [5-6] and medium-scale tests [5-7] were conducted at LANL to investigate the issue. The authors of that study concluded that:

1. Temperature-dependent corrosion of relevant metals (aluminum, zinc) occurs at temperatures and pH values typical of post-LOCA conditions;

2. Precipitation of dissolved metals present in the sump water at concentrations in excess of their solubility limits (which are relatively low) can produce transportable gelatinous material.

This combination of phenomena became known as 'chemical effects'.

Various industry groups and regulatory bodies subsequently developed comprehensive research programs to address the potential for debris accumulation on PWR sump screens, including the assessment of various simulated pool conditions on the formation of the possible chemical products, and measurements of the head loss associated with the formation of chemical products.

This chapter summarizes the available knowledge base on chemical effects, starting with an overview of the general concepts underlying the phenomenon. This is followed by detailed discussions of the key processes of chemical release and precipitation that govern the evolution of

chemical effects, and a summary of chemical effects testing. While not strictly a chemical effect as defined above, the long-term corrosion of materials will also be briefly discussed.

5.2   General Concepts

Although the collection of phenomena referred to as chemical effects take place in a complex recirculating water system in contact with a large number of different materials, it is helpful to consider the phenomenon of chemical effects as consisting of two key processes:

Process 1:   Release of various chemical species into the sump water by corrosion or dissolution; and

Process 2:   Chemical reactions between the various dissolved species leading to the formation of a precipitate.

A wide range of materials are present within containment, all of which can undergo corrosion or dissolution under the right physical (e.g., temperature) and chemical (e.g., pH) conditions; a partial list of materials is given in Table 5-1. The chemical reactions that occur in the post-LOCA sump are determined by the sump water chemistry, in particular the pH and concentrations of chemistry control reagents. The post-LOCA pH evolution is complex and depends in part on whether chemical buffers are added to minimize iodine release [5-8]. Table 5-2 summarizes the sump water buffering practices of a number of countries.

The expected behavior for most materials in Process 1 is shown in Figure 5-1; a plateau is reached either because of surface passivation or because the concentration of the dissolved species reaches a solubility limit. The time dependence of these release curves can often be modelled by equations of the form:

$$\text{Release} = (1\text{-exp}^{-kt})$$

<div align="right">Equation 5-1a</div>

or

$$\text{Release} = kt^{-1/2}$$

<div align="right">Equation 5-1b</div>

where k is a rate constant and t is the time. The former is a typical first order kinetic equation, and the latter is a parabolic rate law commonly found for corrosion processes where the rate is limited by diffusion of species through a corrosion film. By differentiating either equation with respect to time an instantaneous release rate can be obtained. Using a single value for the release rate obtained from short duration corrosion testing can be excessively conservative (by one or two orders of magnitude) when used to calculate release over long periods.

Table 5-1: Partial List of Materials Found in PWR Containments (adapted from Reference 5-9). Additional information on the various types of insulation materials can be found in Appendix C.

Class	Sub-class	Material	Composition
Metals		Aluminum	Al plus various alloying elements
		Carbon Steel	Fe plus various alloying elements
		Copper	Copper
		Galvanized Steel	Zinc-coated steel
		Zinc Coating (no top-coated)	
Concrete		Concrete	Calcium silicates and calcium aluminate
Insulation	Glass Fibre	Fiberglass	95% E-glass + < 5% fibers
		Tempmat	100% E-glass fibers
		Foamglas	100% E-glass
		Thermal Wrap	>95% E-glass and <5% binders
	Mineral-based	Asbestos	Fibrous minerals belonging to serpentine or amphibole

		groups. The most common are chrysotile $(Mg_3(Si_2O_5)(OH)_4)$, amosite, $(Fe_7Si_8O_{22}(OH)_2)$, and crocidolite $(Na_2Fe^{2+}_3Fe^{3+}_2Si_8O_{22}(OH)_2)$
	3M M20C	50% vermiculite $((Mg,Fe,Al)_3(Al,Si)_4O_{10}(OH)_2 \cdot 4H_2O)$, 13% Al silicate, foil, binders
	3M Interam	70% hydrated alumina, 25% aluminum silicate, 3% metal foil, organic binders
Calcium silicate	Unibestos	Calcium silicate and asbestos
	Calcium Silicate	Calcium silicate
	Kaylo	90% calcium silicate and 10% asbestos
	Mudd	>50% calcium silicate, >10% cement, 10% (SiO_2 and Al oxide), other metal oxides/silicates
	Transite	70% calcium silicate, 22% calcium metasilicate, organic fiber, fiberglass
	Marinite	70% calcium silicate, 22% calcium metasilicate, organic fiber, fiberglass
Mineral Wool	Cerablanket	100% aluminosilicate
	Kaowool	80% aluminum silicate and 20% kaolin clay (hydrated aluminum silicate)
	MinWool	Synthetic fiber derived from basalt (a mixture of various minerals rich in Mg and Ca, and low in Si content)
	PAROC Mineral Wool	95-99% mineral wool, 1-5% phenolic binder, 0.2-0.5% mineral oil
Microporous	Microtherm	90% (amorphous silica, silicon carbide), 10% E-glass
	Min-K	Amorphous silica, E-glass
Miscellaneous	Thermolag	6% SiO_2, 3% E-glass, epoxies
	CP-10	20% quartz, 12% hydrated alumina, 5% TiO_2, vinyl acetate
	Armaflex/Anti-sweat rubber/ Foam Rubber	Nitrile rubber, polyvinylchloride
	Benelex 401	Lignocellulose hardboard (pressed wood)

Table 5-2a: Summary of Post-LOCA Sump Water Chemistry Control Strategies used in PWRs by Various Countries. Numbers refer to the predicted pH. Adapted from Reference 5-8].

Additives	Korea	Finland	Spain	Belgium	Sweden	Czech Republic	France	Canada	The Netherlands	USA	Japan	Switzerland	Germany
No pH Control	X		X	X	X			X	X			X	X
NaOH	X		X	7-10 (Recirc phase)						>7	7[1]		
N_2H_4	X	X				X						X	
$Na_3(PO_4)_3$	7-10		7.2							> 7			
KOH		X				X							
$Na_2O[B_2O_3]_5$		8-9											

Na$_2$[B$_4$O$_5$(OH)$_4$]									>7			
B(OH)$_3$ + Soda		X				X	High					

Notes: (1) Added through containment spray line.

Table 5-2b: Summary of Post-LOCA Sump Water Chemistry Control Strategies used in BWRs by Various Countries.

Additives	Spain	Sweden	The Netherlands	USA	Japan	Switzerland	Germany
No pH Control	x		x	x	x	x	x
NaOH		8-8.5		>7			
Na$_3$(PO$_4$)$_3$				>7			
KOH							
Na$_2$O[B$_2$O$_3$]$_5$				>7			

Notes: (1) Added through containment spray line.

Some surface reactions can lead to inhibition or acceleration of release; for example, the inhibition of aluminum corrosion and release by silicates. Under extremely aggressive conditions, no passivation of the dissolving or corroding surfaces is possible and the release can be linear with time. This can lead to the complete destruction of gratings, ladders, etc., forming a mixture of dissolved metals and particulates.

After an initial delay time during which the chemical precipitants reach a solution concentration greater than the solubility limit of a precipitating phase, precipitates will be continuously formed in the solution and on all wetted surfaces until the source term is depleted. Both homogeneous (reaction between molecules in solution to form a precipitate in the solution) and heterogeneous (reaction between molecules and a suitable surface to form a precipitate on the surface) nucleation can occur; heterogeneous nucleation is more likely at lower degrees of supersaturation, while homogeneous nucleation will occur when the degree of supersaturation is very high. In the post-LOCA sump, the large surface areas in containment, including debris, will provide numerous sites for heterogeneous nucleation of precipitates.
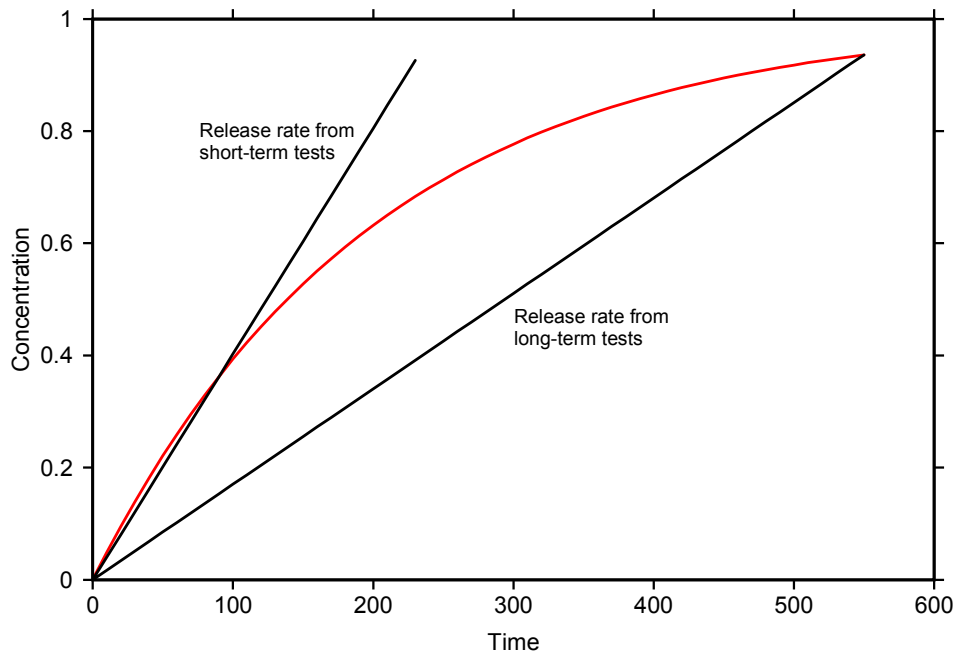
Figure 5-1: Hypothetical Release Curve for a Species into the Post-LOCA Sump Water as a Function of Time at Constant Temperature and pH. The two slopes (straight lines) give the integrated release rates that would be obtained from short duration tests and longer duration tests.

Process 2, precipitate formation, is more complex. Precipitation requires that the concentrations of species in solution or at a surface exceed the solubility limits with respect to a solid phase. This will not occur for some period after the start of the accident because it takes time for the various corrosion or dissolution reactions (Figure 5-1) to produce sufficient concentrations of dissolved species in solution. Two scenarios are possible:

1. At constant temperature and pH, the concentrations of the relevant species increase in solution due to their release, until the solubility limit for the precipitating phase is exceeded (e.g., condition A in Figure 5-2); or

2. A change in temperature and/or concentration results in a decrease in the solubility of the precipitating phase such that it is now lower than the solution concentration (e.g., condition B in Figure 5-2).

Typically, some amount of supersaturation (degree of supersaturation) is required before precipitation occurs (Figure 5-2). Clearly, in Scenario 2 a much higher degree of supersaturation can occur, increasing the likelihood of precipitation.
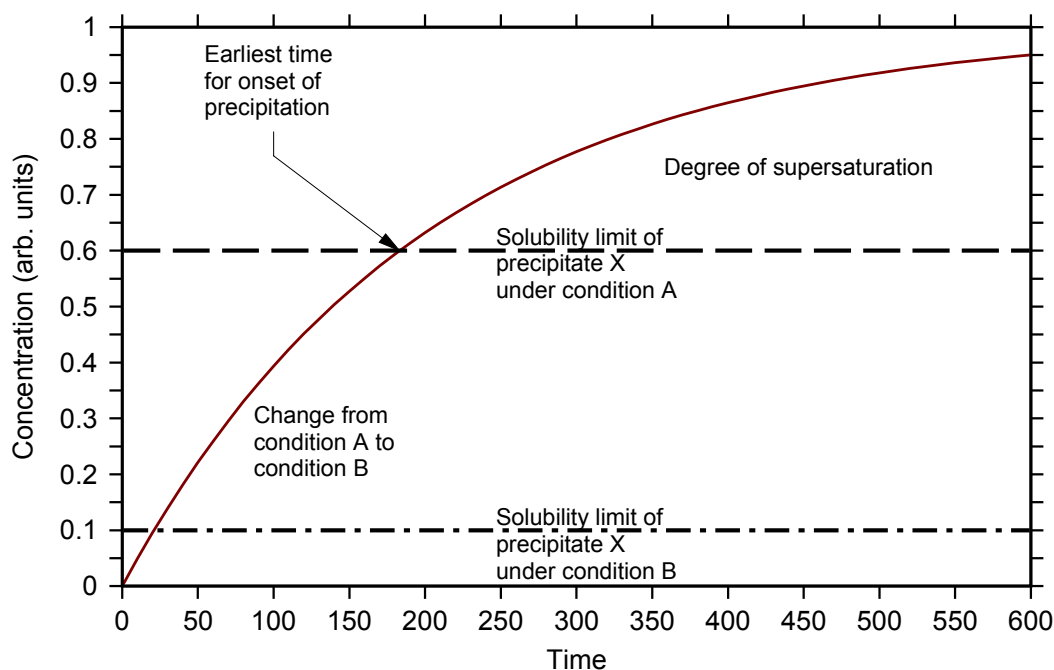
Figure 5-2: Release Curve from Figure 5-1 and Hypothetical Solubility Limits under Two Conditions (A and B) with Different Sump pHs and/or Temperatures. The assumed solubility limit for the precipitating phase (precipitate X) is assumed to be 0.4 concentration units under condition A and 0.1 concentration units under condition B.

Predicting the solubility of relevant precipitates is challenging, and a simple assumption is that 100% of the species of interest precipitates. This can be a very conservative assumption depending on the conditions. Recent measurements [5-10] of the solubility limits of aluminum in PWR sump water show that at pH 9 and 40 °C the assumption of complete precipitation overpredicts the amount of precipitate formed by 1-2 orders of magnitude. However, at pH values near 7 (e.g., if TSP or NaTB are used as pH buffers), the solubility of aluminum is very low and the assumption of 100% precipitation can give a more realistic answer. If the amounts of chemical precipitants expected in solution are low, this can simplify chemical effects testing.

The next level of sophistication is to use thermodynamic data to predict the type and quantity of precipitates formed. However, the post-LOCA sump is not an equilibrium system as the physical and chemical conditions change over the mission time. Therefore, equilibrium thermodynamics is unlikely to give accurate predictions concerning the formation of precipitates due to chemical effects. Instead, precipitate formation will be dominated by processes such as supersaturation, heterogeneous nucleation, colloid stabilization, and gel formation, leading to the formation of amorphous or poorly crystalline phases [5-11]. These latter phases are far more soluble than the thermodynamically most stable phases for the specified conditions. Typically, the nucleating phase possesses the lowest interfacial free energy of all candidate phases, with recrystallization to form more stable phases taking place over timescales that can be longer than the period of coolant recirculation. These mechanisms must be taken into account when attempting to predict the behavior of precipitates in the post-LOCA sump.

Kinetic factors can slow precipitation even when the solubility limit is reached, and typically some degree of supersaturation with respect to the solubility of the precipitating phase is required to initiate precipitation. The approach to equilibrium from supersaturated solutions can be very slow, involving the formation of one or more thermodynamically metastable phases with a higher solubility than the thermodynamically stable phase under the test conditions. Many studies of aluminum hydroxide precipitation carried out under PWR post-LOCA sump water conditions have found that the measured concentration of aluminum in these solutions is higher (by as much as 3 orders of

magnitude) than the reported solubilities of aluminum hydroxide or oxyhydroxide crystalline phases, as a result of the interactions of boric acid with aluminum and because of the formation of higher solubility, metastable phases. Kinetic factors also determine which precipitates will form, and their properties. Thermodynamic calculations predict precipitation of a number of silicate species not observed to form in the Integrated Chemical Effects Tests (ICET), as discussed in Section 5.1.1. While these silicates are the thermodynamically stable phases, their formation is kinetically slow. Testing with sodium aluminum silicate can therefore be excessively conservative; due to the much higher molecular weight of aluminosilicate species, adding Al as a silicate results requires addition of about three times more precipitate to the test rig than if Al is added as aluminum hydroxide.

5.2.1 *Experimental Findings for PWRs*

A key early test program was the ICET program, jointly sponsored by the US NRC and the US nuclear industry, and conducted by LANL at the University of New Mexico. The five ICET tests simulated postulated chemical environments in the containment water sump after a LOCA to quantify the formation of chemical precipitates and determine their characteristics [5-12]. The results are detailed in a series of reports ([5-13] to [5-17]), summarized in [5-7] and also reported in [5-18] and [5-19]. Each test represented a unique containment pool environment (Table 5-3) intended to represent conditions applicable to a portion of the commercial US PWR fleet. The environment in the ICET program was **not** intended to represent individual PWR plant conditions and further experiments were recommended to determine the formation of chemical products under plant specific conditions.

Table 5-3. pH Target and Control Agent, and Type of Insulation used in the ICET tests.

Test no.	Buffer	pH target	Insulation
1	NaOH	10	100% fibreglass
2	TSP	7	100% fibreglass
3	TSP	7	80% calcium silicate and 20% fibreglass
4	NaOH	10	80% calcium silicate and 20% fibreglass
5	no	pH allowed to drift to value determined by added borax	100% fibreglass

Figure 5-3 compares the concentrations of the major species measured in solution in ICET Tests 1-5. Sodium was the dominant element present because either NaOH or TSP was used to control the pH. The measured sodium concentration was roughly equal to that expected from the mass of NaOH added in Tests 1, 2 and 5, but increased to higher values in Tests 3 and 4, suggesting an additional sodium source. Argonne National Laboratory [5-20] noted that calcium silicate can contain sodium silicate as an impurity; sodium silicate is very soluble.
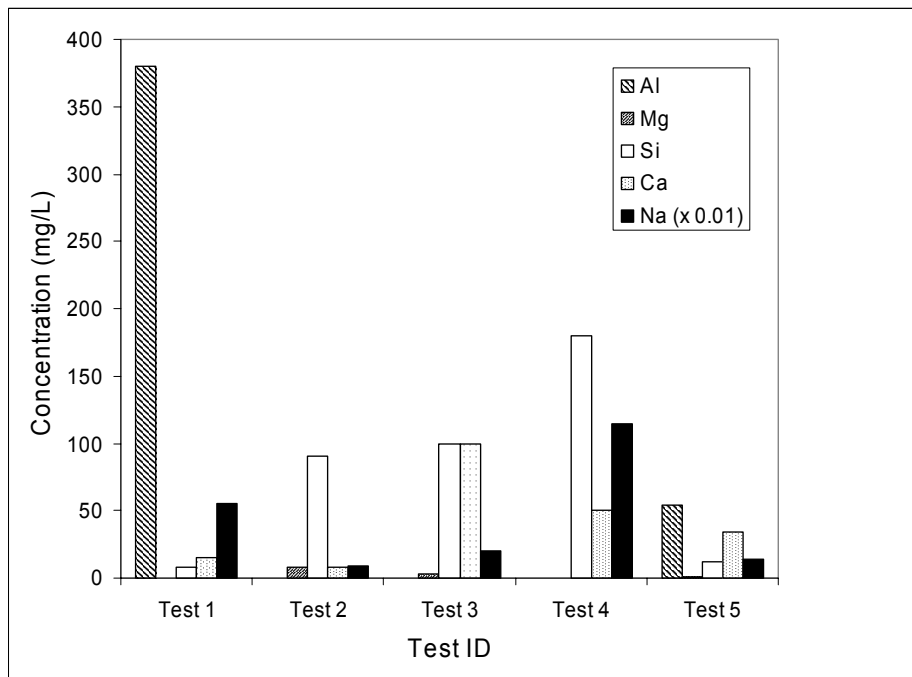
Figure 5-3: Comparison of the Concentrations of the Major Species Measured in Solution in ICET Tests 1-5. The sodium concentration data have been divided by 100 to facilitate comparison.

Table 5-4 summarizes the major precipitates identified in the ICET tests, and Table 5-5 lists the precipitates formed by the cooling of various simulated sump water solutions in the Westinghouse Owners Group (WOG) single tests [5-9]. Note that the chemical phases present were inferred from Scanning Electron Microscopy (SEM)/Electron Dispersive X-ray (EDX) data, and not directly determined by XRD or other phase-sensitive method and therefore the assignments are not unambiguous. Figure 5-4 shows the total mass release from the materials tested in WCAP-16530-NP. As noted in the original reference, the concrete mass used in the tests was not scaled properly to the amount of concrete present in PWR containment, so that the release from concrete is exaggerated in the graph.   Therefore the use of these data to calculate calcium release can be excessively conservative, and plant-specific tests are recommended.

Table 5-4: Summary of Chemical Phases Identified during ICET Tests

Test ID	Deposit	Formula	Comments
1	Tincalonite	$Na_2B_4O_7 \cdot 5H_2O$	
	Borax	$Na_2B_4O_5(OH)_4 \cdot 8H_2O$	
	Unknown	Compound containing Al, B, Na, CO_3^{2-}	
	Unknown	Compound containing Na, B, Al	
2	Calcium phosphate (hydroxyapatite?)	$Ca_5(PO_4)_3OH$?	
3	Tobermorite	$Ca_{2.25}(Si_3O_{7.5}(OH)_{1.5})(H_2O)$	Not a chemical reaction product - components of cal-sil
	Calcite	$CaCO_3$	
	Sodium calcium hydrogen carbonate phosphate hydrate	$(Ca_8H_2(PO_4)_6 \cdot H_2O \cdot NaHCO_3 \cdot H_2O)$	
	Lithium calcium hydrogen carbonate phosphate hydrate	$(Ca_8H_2(PO_4)_6 \cdot H_2O \cdot Li_2CO_3 \cdot H_2O)$	
	Calcium phosphate (hydroxyapatite?)	$Ca_5(PO_4)_3OH$?	
4	Tobermorite	$Ca_{2.25}(Si_3O_{7.5}(OH)_{1.5})(H_2O)$	Not a chemical reaction product - components of cal-sil
	Calcite	$CaCO_3$	
5	Unknown	Compounds containing O, Na, Al, C, Ca Mg and Si	Deposits a mixture of fibreglass and unidentified compounds

Table 5-5: Precipitates Formed by the Cooling of Various Simulated Sump Water Solutions in the PWOG Single Effects Tests [5-9]

Type of Test and Conditions	Precipitate (as identified by SEM)
Precipitation from cooling, Al at pH 4	Hydrated AlOOH
Precipitation from cooling, Al at pH 8	Hydrated AlOOH
Precipitation from cooling, Al at pH 12	Hydrated AlOOH
Precipitation from cooling, other fibreglass, pH 12	$NaAlSi_3O_8$ with minor calcium aluminum silicate
Precipitation from cooling, concrete, pH 4	Calcium aluminum silicate – Al rich
Precipitation from cooling, mineral wool, pH 4	Hydrated AlOOH
Precipitation from cooling, FiberFrax at pH 4	Hydrated AlOOH
Precipitation from cooling, FiberFrax at pH 12	$NaAlSi_3O_8$
Precipitation from cooling, galvanized steel, pH 12	$ZnSiO_4$ with Ca and Al impurities
Mixture of TSP and cal-sil	Calcium phosphate and a silicate
Mixture of TSP and powdered concrete	Calcium phosphate with AlOOH
pH 12, 265 fibreglass with high calcium from pH 4 cal-sil	Sodium calcium aluminum silicate
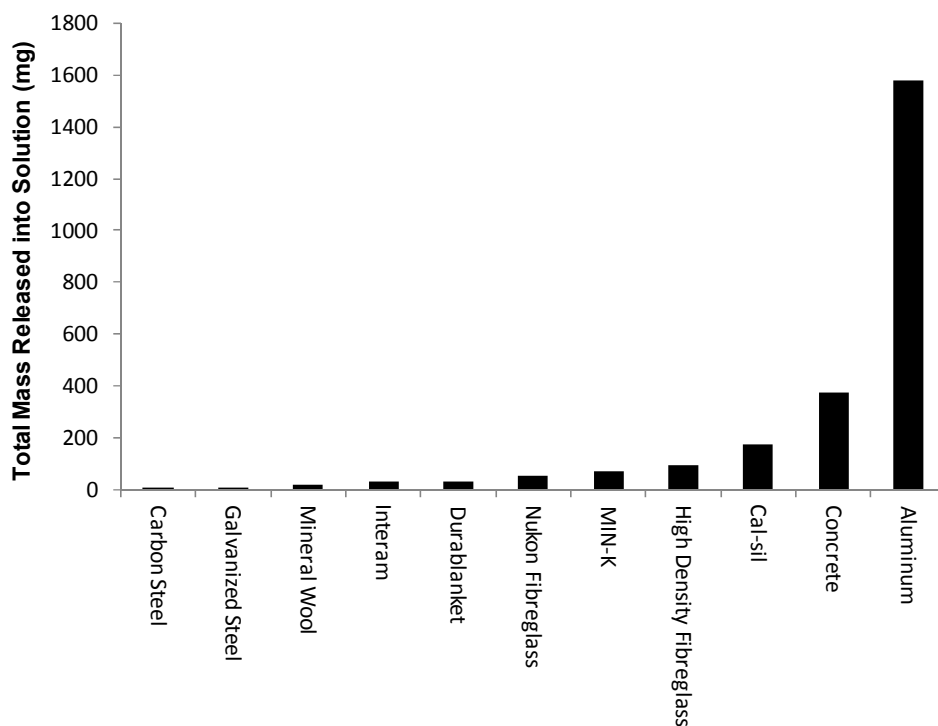
Figure 5-4: Comparison of the Total Mass Release from the Materials Tested in WCAP-16530-NP. Adapted from [5-9]. As noted in the original reference, the concrete mass used was not properly scaled to the amount of concrete present in a PWR containment, and release from concrete is exaggerated in this graph.

5.3   Release of Chemical Precipitants

As noted above, a wide range of materials are found in reactor containment, and many of these are susceptible to dissolution (corrosion) when contacted by the post-LOCA sump water, especially at

high temperature when the rates of chemical reactions are high. In various test programs worldwide, it has been established that aluminum, silicon, zinc, calcium and iron are the most problematic elements with respect to chemical effects, and this section reviews and summarizes the available data on their release from containment materials. These data can be used to calculate the expected concentrations of precipitants expected to be formed under a specific set of post-LOCA physical and chemistry conditions (i.e., a specific evolution of temperature, pH, etc.).

Many chemical effects tests have highlighted the important role of synergistic effects in the formation of precipitates in simulated post-LOCA sump water. Most of these effects involve inhibition of corrosion or dissolution reactions by other species present in the water. As an example, the weight changes of aluminum coupons in ICET Tests 1 and 4 were significantly different although both tests used NaOH to adjust the pH to the same target value (pH = 10). A high Al concentration, which increased with experimental time, was measured in solution in Test 1, while only trace concentrations of aluminum were present in ICET Test 4 solutions. While no explanation for this difference was given in the original ICET reports, it became clear that silicate species released by dissolution of calcium silicate present in ICET Test 4 but not in Test 1 inhibited aluminum corrosion in Test 4. It was also suggested [5-21] that surface passivation by calcium may have lowered the aluminum corrosion rate.

Additional experiments by the PWR Owners Group (PWROG) confirmed the inhibitory effects of silicates and phosphates on aluminum corrosion [5-22]. The inhibition by silicates was as high as a factor of 11. A comparison of the aluminum (Alloy 1100) release rate (mg/m^2 min) in the presence and absence of phosphate indicates a decrease in the aluminum corrosion rate by a factor of between 2 and 3 at pH 8- 9. The use of phosphates as a corrosion inhibitor is well known; TSP has been shown to reduce the corrosion of steel bars in alkaline solutions [5-23].

McMurry et al. [5-24] reported that in corrosion/leaching tests using aluminum and Nukon insulation, dissolved aluminum inhibited the leaching of silicon from the fibreglass under certain conditions. At pH 7, the presence of aluminum had no effect on release of various elements from Nukon, while at pH 10, the presence of aluminum in the test solution had significant inhibitory effects on Nukon dissolution. Dissolution tests with Nukon and aluminum in pH 10 containment water at 60 ºC gave concentrations of silicon and aluminum in the solution similar to those found in ICET Test 1.

These data show that synergistic effects must be considered when predicting what chemical reactions might be occurring in post-LOCA sump water. Therefore, care must be taken when using the results from single-effects tests.

5.3.1   *Aluminum Release*

Aluminum is present in nuclear containments in the form of fan blades, scaffolds, feeder pipe cabinets in CANDU plants, and parts of valves and other components. It is also a component of many types of fiberglass and other insulation.

The corrosion rate of aluminum is a function of pH, temperature, and exposure time. Thermodynamic calculations indicate that in the weakly acidic-weakly alkaline pH range (4 < pH <9), aluminum is in a passive region in the Pourbaix[8] diagram (Figure 5-5) [5-25]. Experimental data on aluminum corrosion rates show that aluminum alloys have a low corrosion rate in the pH range 4-7; at pH values less than 4 or greater than 7, the corrosion rate increases significantly (Figure 5-6) due to the increasing solubility of the passivating aluminum surface oxides [5-26].

---

[8]   Pourbaix diagrams are plots of electrochemical potential vs solution pH, and are often used in corrosion science to define regions of thermodynamic stability for metals and their corrosion products.
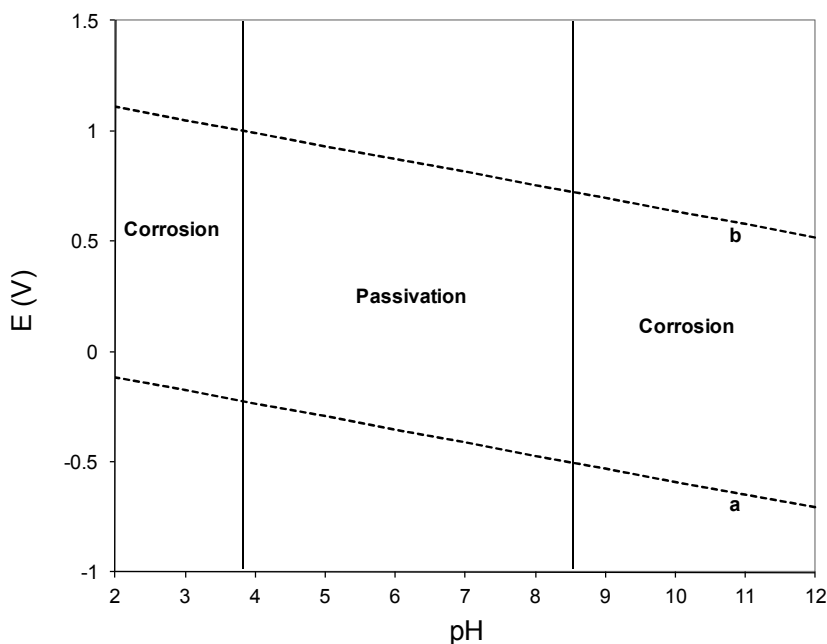
Figure 5-5. Pourbaix Diagram for Aluminum at 25 °C. All dissolved species are at activities of 10^{-6} g-equivalent/L. The dotted line labelled "a" represents the reaction $2H^+ + 2e^- \rightarrow H_2$, and the line labelled "b" represents the reaction $O_2 + 2H_2O + 4e^- \rightarrow 4OH^-$.
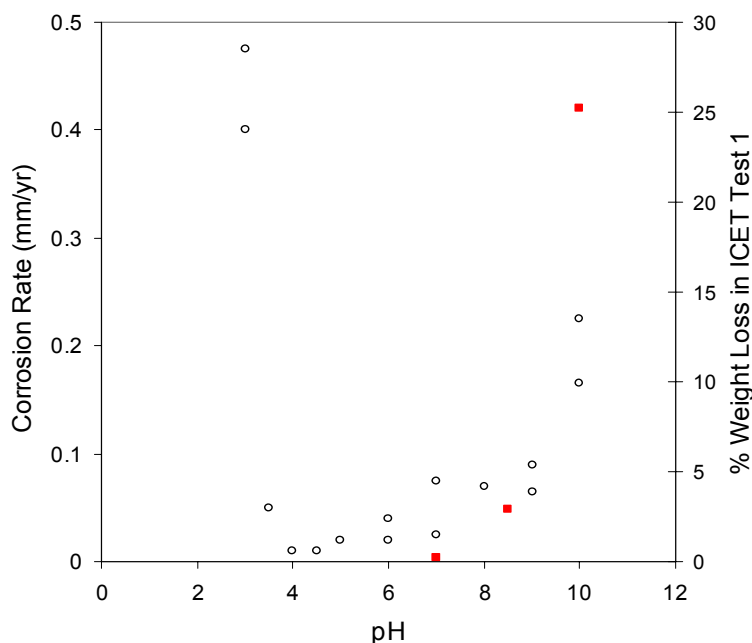
Figure 5-6. Corrosion Rate of Aluminum as a Function of pH [5-26] (Open Circles) and the Total Corrosion (as a Fractional Weight Loss, Solid Squares) from the ICET.

Table 5-6 lists the weight changes of the submerged and unsubmerged aluminum corrosion coupons in the ICET [5-9] tests. The weight loss data for the submerged coupons in ICET Tests 1, 2, and 5 are consistent with the existing literature observations. The unsubmerged coupons, subjected to the spray, all showed a weight gain, and while the coupons exposed to pH 10 water showed the highest weight gain, the change was less than 0.5% of the total coupon mass. In ICET Test 3, in which TSP was used as a buffer, the total dissolved aluminum concentration in the sump water,

expected to be the total release from both the submerged (0.15% weight gain) and unsubmerged (0.1% weight gain) aluminum coupons, was about 0.1 mg/L. In ICET Test 4, the submerged Al coupons showed no measurable weight change, while the unsubmerged Al coupons showed a 0.15% weight gain. The aluminum concentration in the solution was below the detection limit of ICP-AES (<1 mg/L).

Table 5-6: Percentage of Weight Loss (-) or Gain of Submerged Aluminum Coupons after 30 Days

Coupon Location	Test Number				
	Fibreglass			CalSil/Fiberglass	
	1	2	5	3	4
	(pH 10, no TSP)	(pH 7, TSP)	(pH 8.5, borax)	(pH 7, TSP)	(pH 10, no TSP)
submerged	-25.2%	-0.2%	-2.9%	0.15%	0%
unsubmerged	0.48%	0.1%	0.1%	0.1%	0.15%

Data on the corrosion rates of aluminum in water at various pH values and temperatures are available in the literature, and relevant data are summarized in Table 5-7. The corrosion rates of aluminum in the presence of boric acid are significantly higher than those reported in the absence of boric acid. The reported corrosion rates under what are nominally the same conditions can vary by at least one order of magnitude.

Table 5-7: Selected Corrosion Rate Data for Aluminum

Solution Composition	Temperature (ºC)	Corrosion rate (g/m^{2}h)	Reference
0.28 M (3000 ppm) B + 0.15 M NaOH (3450 ppm Na)	55	0.35-0.61	[5-27]
	100	14.0-18.0	
Not described	90	23.9	[5-28]
pH = 9.2 with NaOH, borated	90	1.45	[5-29]
pH = 10 with NaOH, aerated		0.012	
Borated Alkaline Containment Water at pH 10	60	0.986	[5-30]
	90	1.89	
	110	2.21	
pH 10 with NaOH	60	0.060	[5-26]
ICET Test 1 Data [a]	60	0.73	[5-7]
pH 4	88	0.56	[5-9]
pH 8		2.68	
pH 12		60.1	
pH 4	130	5.4	
pH 8		23.7	
pH 12		200	
pH 7	99	0.078	[5-31]
pH 8		2.2	
pH 9		12.96	

Solution Composition	Temperature (°C)	Corrosion rate (g/m²h)	Reference
pH 10		365	

Note: [a] Average corrosion rate based on coupon weight loss. Release rate data show that the corrosion rate is a function of time.

Aluminum release models were developed by Lane et al. [5-9]. Limited short-term (90-minute) corrosion tests were conducted on aluminum sheet in borated solutions at pH 4, 8 and 12, and data from other longer-term aluminum corrosion tests were compiled to create a data set that covered most pH and temperature regions of interest. Despite significant scatter in the data, an empirical model for aluminum release was produced that became the US industry standard:

$$RR_{Al} = 10^{A - B/T + C \cdot pH^2 - D \cdot pH \cdot T}$$

Equation 5-3

Using a very similar data set, AECL [5-36] produced a semi-empirical equation based on a first principles understanding of corrosion processes:

$$RR_{Al} = A \times \exp(B \cdot pH) \times \exp(-C/T)$$

Equation 5-4

Both models predict the aluminum concentration data for ICET tests 1 and 5 reasonably well (Figure 5-7). It can be shown by consideration of coupon weight change, mass balances and short spray duration that very little dissolved aluminum came from the sprayed coupons in these tests, making the "Submerged Al Only" curves in Figure 5-7 pertinent to the present discussion. It can be seen that the predicted 30-day release is in general agreement with the observed concentrations. The incongruity of the models is mainly a result of the inhomogeneity of the available data set because of the disparate methods used in testing by the separate groups, especially the test duration.

Aluminum release models such as Equations 5-3 or 5-4 can be used to predict the aluminum release as a function of ECCS mission time, in order to calculate the mass of precipitants or surrogate precipitates to be added to strainer head loss tests.
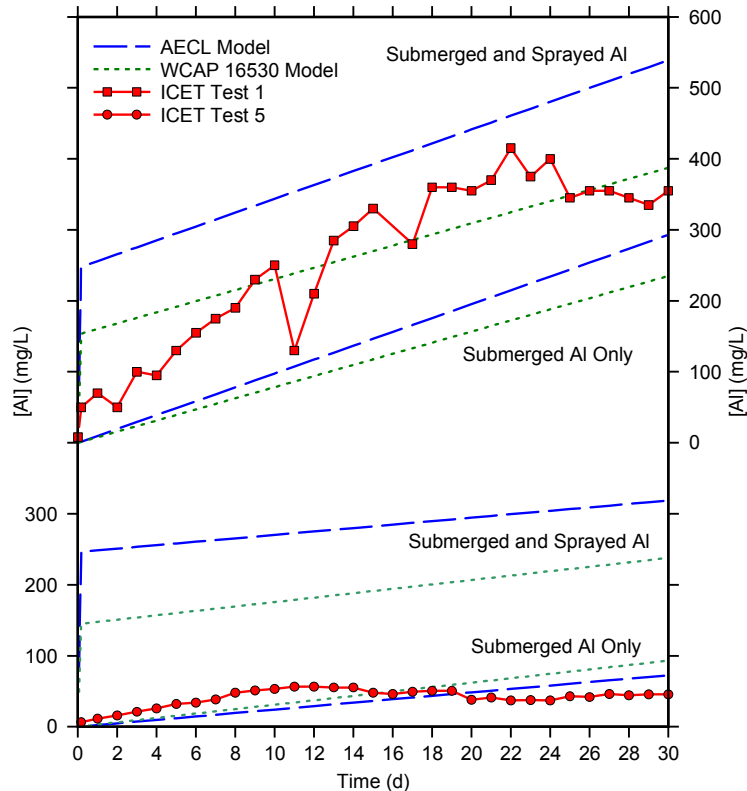
Figure 5-7: WCAP and AECL Aluminum Release Models Predictions of ICET Test 1 and Test 5 Aluminum Concentration [5-36]. ICET concentration data adapted from Dallman et al. [5-7]. Spray pH, reported as < 12, was taken to be 11 for calculations.

5.3.2   *Silicon Release*

There are two potentially significant sources of silicon in containment; fibrous insulation and calcium silicate. Fibrous insulation is used as a thermal insulation in many locations in containment, and can be damaged by the jet impact during a LOCA. The resulting debris can become immersed in the sump water, leading to dissolution of the fibers. Fibrous insulation is primarily made of glass fiber wool, with binders added to hold the glass fibers together. The binders can account for as much as 25 percent of the weight, and are typically phenol-formaldehyde resin-based. The compositions of different fibrous insulations do not differ significantly; the chemical composition of Nukon fiber insulation is given in Table 5-8 as an example.

Figure 5-8 shows the data for silicon release in the ICET tests. ICET tests 1, 2, and 5 contained concrete and fiber, while in test 4, calcium silicate was included in the debris mixture. When calcium silicate is present the concentration of Si in solution is significantly higher than it is without calcium silicate, showing that calcium silicate is the dominant Si source when present. The dissolution of calcium silicate will be discussed in further detail in Section 5.2.3.
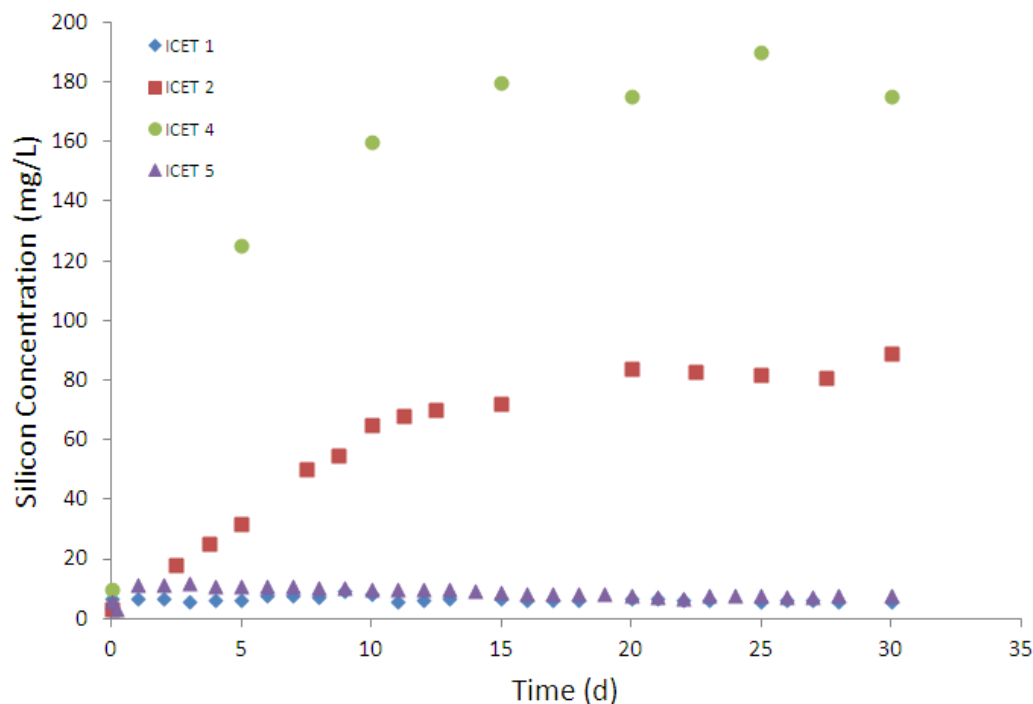
Figure 5-8: Release of Silicon from Containment Materials in ICET Tests 1, 2, 4 and 5 [5-7].

Although the dissolution of glasses has been well studied, these studies tend not to focus on dissolution in solutions containing a high concentration of boron. In general, the dissolution of glass involves the inward diffusion of hydronium ions into the glass and the outward diffusion of alkali ions. At the same time, the covalent silica network is hydrolyzed and dissolves; these hydrolysis reactions are known to be slow at pH values in the range 6-9. Silicon release rates from Nukon glass in typical PWR post-LOCA sump water were reported by Jain et al. [5-30], who carried out static leaching tests in polytetrafluoroethylene vessels for 14 days. The results (Figure 5-9) showed a non-linear dependence of release on time, with the concentration of silicon in solution tending toward a plateau at longer exposure times. Silicon release increased with increasing temperature and with increasing pH; the pH effect was obscured, however, by the choice of pH control agents. The pH 10 solution was prepared using NaOH, while the pH 7 solution used TSP. The possible formation of insoluble phosphate compounds (e.g., calcium or aluminum phosphates) on the fiber surfaces could inhibit dissolution. The results are, however, consistent with the known dissolution behaviour of glasses. Similar behaviour was found in the very short term testing reported in WCAP-16530-NP [5-9].

Soltesz et al. [5-32] performed experiments to measure the release of Ca, Si and Al from glass fibers. Figure 5-10 shows the results of a test carried out at pH 8.1 (adjusted using TSP) at 85 °C. The silicon release data obtained by Soltesz et al. at 85 °C are in reasonable agreement with the data of Jain et al. obtained at 90 °C. The work of Soltesz et al. [5-32] also showed that the choice of buffer affects the release and final solution concentration, due to the formation of soluble complexes that can enhance release, or by the formation of insoluble compounds that lead to precipitation or inhibition.

Table 5-8: Composition of Nukon (adapted from Reference 5-30).

Component	Composition	
	Weight Percent	**Mole Fraction**
SiO_2	62.5	0.64
Al_2O_3	3.6	0.02
CaO	8.2	0.09
MgO	3.5	0.05
Na_2O	15.8	0.16
B_2O_3	5	0.04
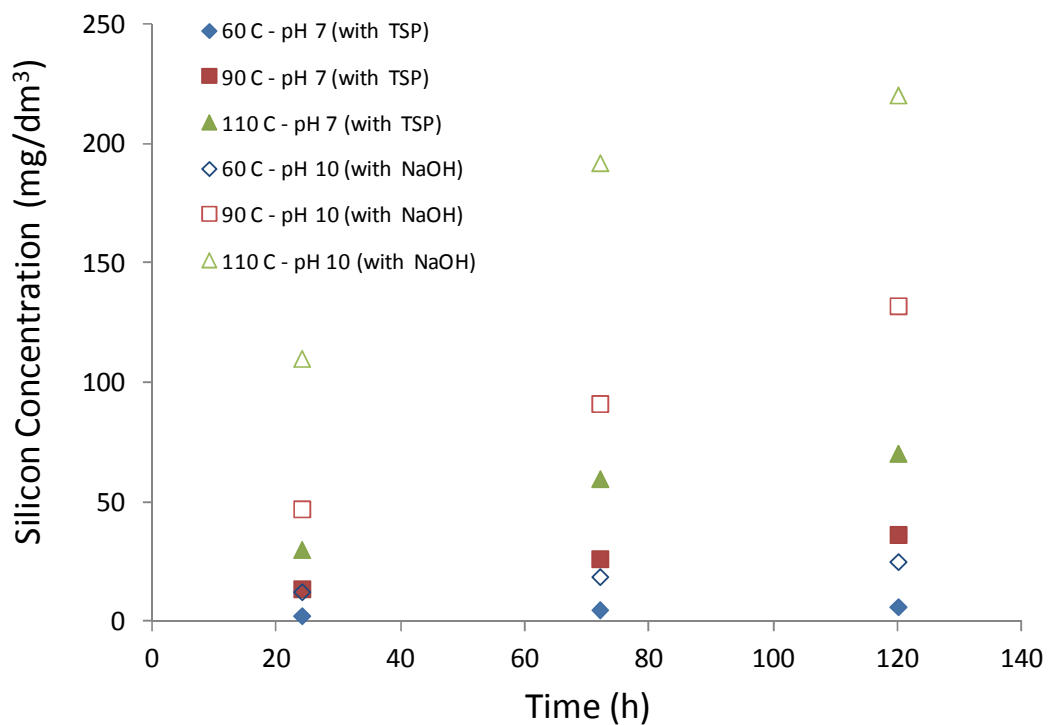
Figure 5-9: Silicon Release from Nukon Glass Fibers as a Function of Time for Different Temperatures and pH Values. The pH was adjusted to 10 using NaOH and adjusted to 7 using TSP. Adapted from Reference 5-30.
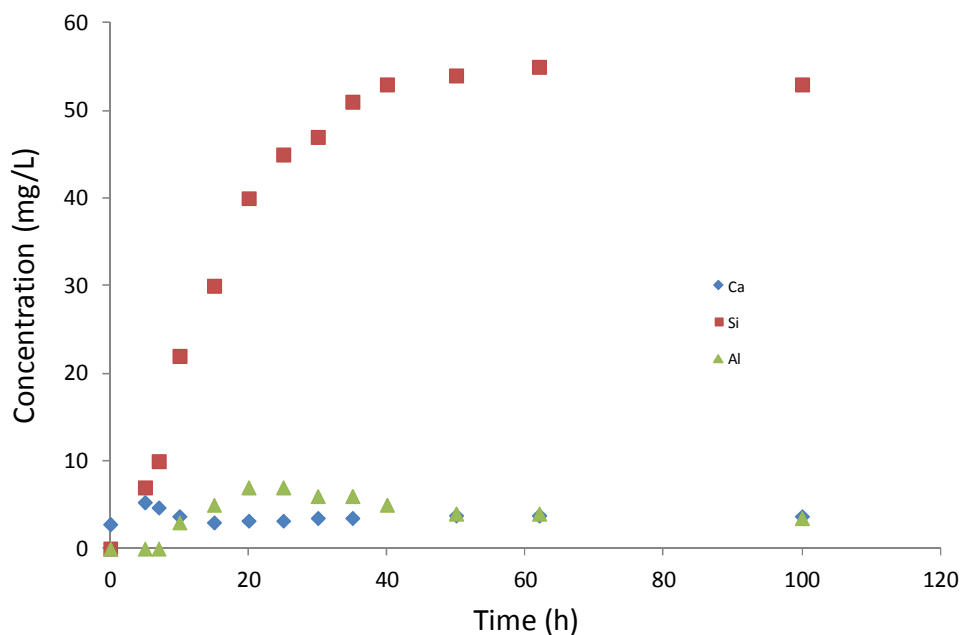
Figure 5-10: Measured Release of Ca, Si and Al from Glass Fibers at pH 8.1 (adjusted using TSP) at a Temperature of 85 °C [5-32].

Devreux et al. [5-33] summarized the experimental data and presented a simple model for glass dissolution in water that is helpful in understanding the relevant processes. They note that the dissolution behavior depends on both the glass composition and the composition of the leaching solution. In the pH range 6-9, the hydrolysis reactions of the Si-O-Si bonds is slow. For glasses with low boron content (such as Nukon fiberglass), selective extraction of boron and sodium occurs. This suggests that testing in borated and unborated water could lead to different silicon releases. Their model shows that the presence of less soluble oxides such as Al_2O_3 decreases the silicon release rate and the concentration in solution at saturation, as observed.

5.3.3   Calcium Release

Three sources of calcium have been identified; concrete, fibrous insulation and calcium silicate. Figure 5-11 summarizes the Ca release data from ICET test 1, 2, 4 and 5. ICET tests 1, 2, and 5 contained concrete and fiber, while calcium silicate was included in the debris mixture in test 4. The concentration of Ca in solution is significantly higher when calcium silicate is present than without calcium silicate.

The solubility of calcium silicates depends on parameters such as the compound structure, the Ca/Si ratio, pH, temperature and the concentration of electrolytes in solution. Generally, as the dissolved calcium concentration increases, the concentration of silicon species in the solution decreases. Figure 5-12 shows the dissolved silicon and calcium concentrations as a function of Ca/Si ratio in the solid phase [5-34]. The relative concentrations of dissolved calcium and silicon in the ICET tests are in reasonable agreement with literature data. Analysis of the calcium silicate used in the ICET tests showed that it was composed of calcite and tobermorite. More detailed interpretation of the ICET data on the relationship between the concentration of calcium and silicon is difficult, as the dissolved calcium concentration will also depend on the dissolution of calcite, which exhibits a strong dependence on pH, and on the presence of phosphate ions. In an open system, the uptake of CO_2 from the air plays a major role in calcite dissolution. Argonne National Laboratory (ANL) [5-35] reported the results of dissolution tests of commercial $CaSiO_3$ in NaOH at pH 7.14 at a temperature of 60 °C. The measured calcium concentration after 362 h was 254 ppm.
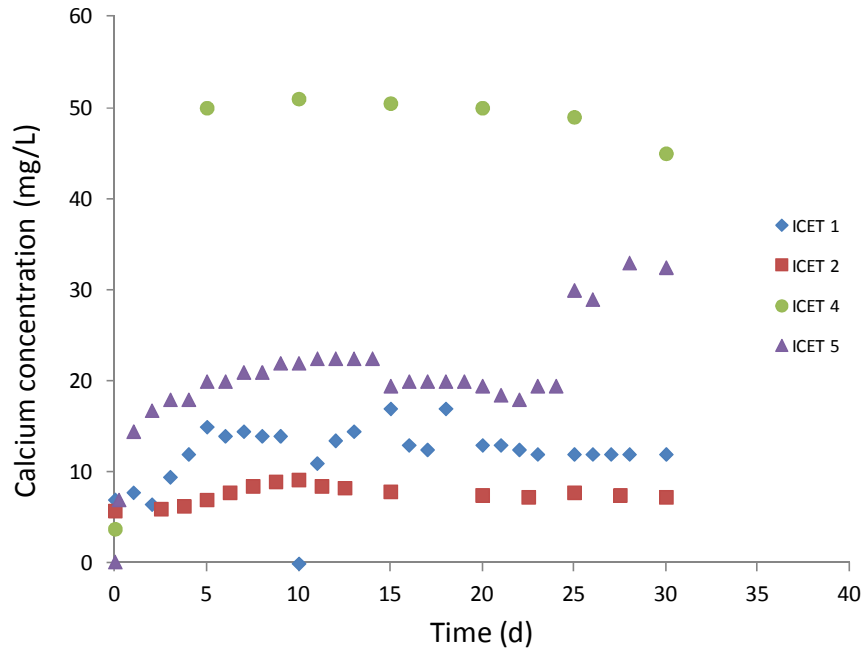
Figure 5-11: Ca Release Data from ICET Tests 1, 2, 4 and 5. ICET tests 1, 2, and 5 contained concrete and fiber, while in test 4, calcium silicate was included in the debris mixture [5-7]).
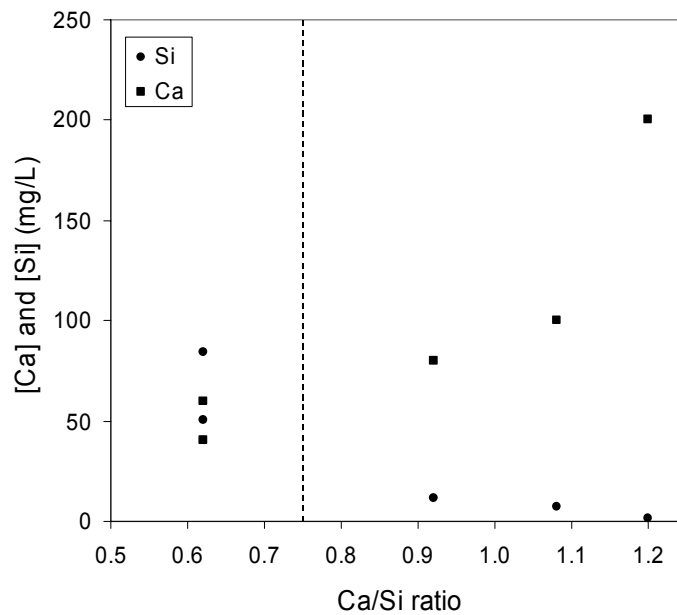
Figure 5-12. Solubility of Calcium Silicates in Water as a Function of the Ratio of Ca/Si in the Solid Phase at 22 °C. The dotted vertical line represents the Ca/Si ratio for tobermorite (Adapted from Reference 5-34).

The results from tests 1, 2 and 5, in which no calcium silicate was present, show that the release of Ca into solution is highest at pH 8.5 and lowest at pH 7. However, the test at pH 7 contained TSP, and it is possible that Ca release was inhibited in these tests by the formation of a Ca-phosphate surface film. In all of the tests (except test 5) the Ca concentration reached its maximum value after 5-10 days. In the single effects tests performed for the PWROG and reported by Lane et al. [5-9], the release of Ca decreased as the pH increased (Figure 5-13).
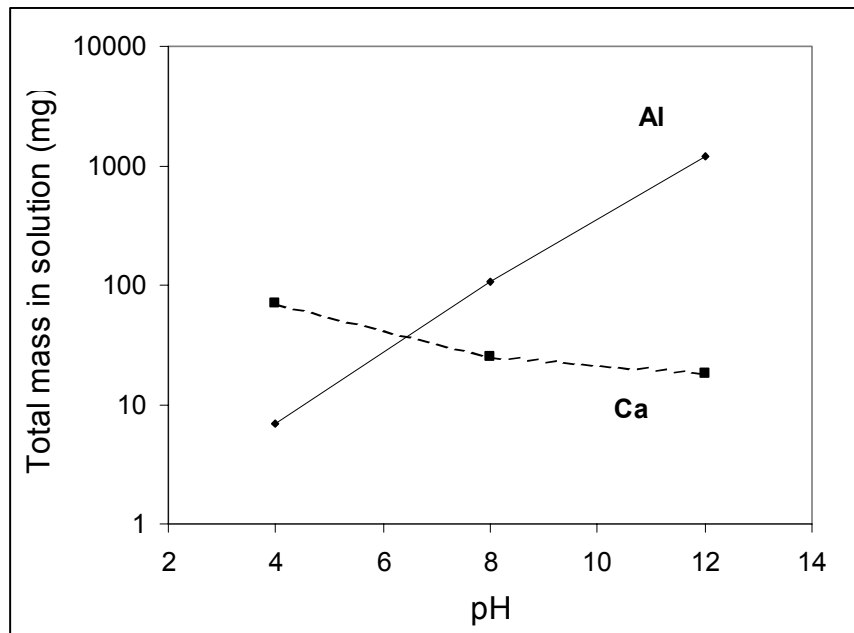
Figure 5-13: Dependence of Release of Aluminum and Calcium on pH Measured in the WOG Single Effects Tests.

Concrete is a mixture of calcium silicates and calcium aluminate. It is inherently basic and concrete dissolution rates in aqueous solutions are expected to increase as the solution becomes more acidic. In the tests reported by Lane et al. [5-9] (Figure 5-14), the amount of Ca released from powdered concrete was observed to decrease as the pH increased from 4.1 to 8, but the amount released at pH 12 was essentially the same as that released at pH 8 within the experimental uncertainty (roughly ±50% based on data from replicate runs). In bench-top tests that AECL conducted for Dominion, low-grade concrete was found to dissolve readily below pH 8 but in the presence of TSP, dissolution was almost completely inhibited [5-36]. This may have been the result of the formation of a protective calcium phosphate surface film on the concrete.
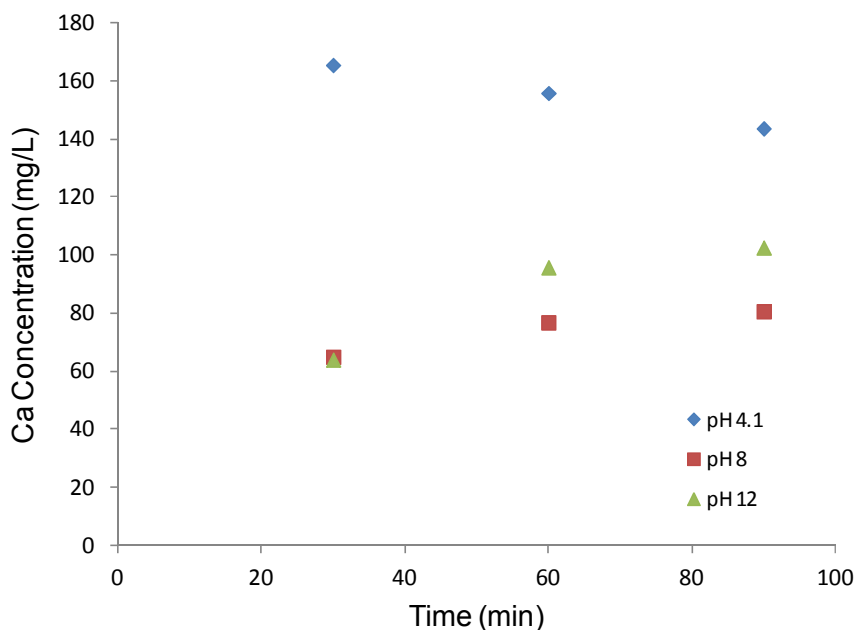
Figure 5-14: Ca Release from Powdered Concrete as a Function of Time at pH 4.1, 8 and 12 at a Test Temperature of 76 °C.

146

5.3.4   *Zinc Release*

Zinc corrosion can occur via the reaction:

$$Zn + 2H_2O \rightarrow Zn(OH)_2 + H_2 \qquad \text{Equation 5-5}$$

or by a reaction involving the reduction of O_2:

$$2Zn + O_2 + 2H_2O \rightarrow 2Zn(OH)_2. \qquad \text{Equation 5-6}$$
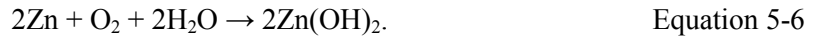
The ICET program included representative amounts of galvanized steels and Inorganic Zinc (IOZ) primer. The relative amounts of immersed versus non-immersed (sprayed for 4 h) areas for galvanized steel and IOZ primer were about 5% and 95%, respectively for each material. The ICET results illustrate some important features with respect to the post-LOCA behaviour of zinc at pH 7 and 10. In all tests, the galvanized steel and IOZ coupons showed little or no weight change, with the largest change being a 2.7% increase in the weight of the galvanized steel over the course of 30 days at pH 7. The pH 7 test also showed the highest concentration of total Zn in the surrogate recovery water, at 10 mg Zn/kg. Taken in conjunction with the weight gain/loss data, the concentration results indicate that the corrosion and mobilization rates of zinc are low. Analysis of the solids produced in the ICET tests showed that zinc was a very minor contributor to the formation of solids in those tests [5-7].

Ghosh et al. [5-37] reported data on zinc corrosion under post-LOCA chemistry conditions (3.3 x 10^{-2} M boric acid, 2.0 x 10^{-4} M LiOH, adjusted to pH 7 using HCl or NaOH). They studied the corrosion of zinc granules (20 mesh size), zinc coupons (1.3 cm x 15.3 cm x 0.263 cm), and IOZ primer (dried and crumbled). The corrosion was quantified by weight change and the zinc release quantified by measurement of the zinc concentration in the solution. The tests were carried out for up to 96 h and at 22 and 40 °C. Piippo et al. [5-29] also reported corrosion data for zinc under a range of conditions. The data from Ghosh et al. [5-37] and Piippo et al. [5-29] are listed in Table 5-9.

Table 5-9: Corrosion Data for Zinc in Borated Water

Temperature (°C)	Corrosion Rate (kg/m²/h)	Reference
22	0.055 x 10^{-3}	[5-37]
40	0.057 x 10^{-3}	[5-37]
50	0.05 x 10^{-3}	[5-29]
70	0.03 x 10^{-3}	[5-29]
90	0.04 x 10^{-3}	[5-29]

Laboratory-scale investigations performed by the HZDR showed that the corrosion mechanism of hot-dip galvanized ferritic steel in boric acid-containing media is complex. An intact Zn coating on the sample surfaces protected the base material and no significant amount of iron corrosion products were found on sample surfaces or in the test solution and fibers if demineralized water was used as the coolant. Consequently, no significant head loss increases across fiber-laden strainers were observed.

A significant increase in local corrosion resulted when there was sufficient hydrodynamic impact of borated coolant (PWR conditions), whereas in demineralized water (BWR conditions) such an effect was not observed. The Zn layer dissolved quickly in borated solution only within the impinging jet area (i.e., gratings directly exposed to a water shower) by flow-induced corrosion without formation of solid Zn corrosion products while corrosion of submerged surfaces did not lead to a significant increase of the head loss. The hydrodynamic impact of the jet on the surface, the water chemistry (e.g. pH), the ratio of the exposed surface to the coolant volume, as well as the relative surface areas of material exposed to the jet versus submerged were identified as the main parameters influencing strainer clogging by corrosion. The corrosion rates of zinc and iron were

reduced by zinc dissolution into the coolant and/ or by increasing the pH (e.g. addition of lithium hydroxide) [5-38]. The results of the laboratory-scale studies were confirmed by investigations using semi-industrial-scale test facilities at IPM Zittau/Goerlitz.

The experiments showed that the subsequent steel corrosion may lead to the clogging of mineral wool fiber beds (Rockwool MD2) within one day. Chemical analysis of deposits on clogged fiber beds point to corrosion products of iron as main component with lower amounts of zinc and confirm that steel corrosion was the main reason for clogging.

The cooling water chemistry (e.g. pH), the coolant jet impact and the coolant temperature were considered to be the main influencing parameters. In addition, the corrosion of zinc to form dissolved zinc (Zn^{2+}) causes a small pH increase whereas the pH is not influenced by rust particle formation resulting from Fe corrosion under these conditions; the buffer effect of boric acid starts to act in this pH region. Finally, the increasing concentration of dissolved Zn in the coolant reduces the potential of Zn/Zn^{2+} as the anodic corrosion process, therefore reducing Zn corrosion. As a result, strainer clogging due to corrosion depends to a great extent on the ratio of coolant volume to corrosion material surface area. The impact of the coolant provokes rapid localized Zn corrosion leading to the formation of bare steel. The coolant jet also transports the rust to the sump strainer and prevents rust deposition on steel that could limit further corrosion. The temperature is expected to influence such electrochemical processes, but experiments at 25 °C and 70 °C showed a delayed clogging compared to experiments at 45 °C.

A very long-term experiment on the influence of borated water at room temperature on step gratings was performed by a NPP. Within 2 years the submerged part of the zinc coating was visibly damaged (Fig. 5-15). The ferritic steel showed holes with an average depth of 2.5 mm due to corrosion.

Based on the laboratory tests, it was proposed to increase the pH at the beginning of the LOCA (borax was recommended) to suppresses steel corrosion, which was predicted to lead to a significant reduction of the potential for clogging. A similar effect cause large areas of submerged galvanized steel generating an accelerated pH increase by Zn corrosion. However, higher concentrations of dissolved zinc seem to induce disadvantageous consequences due to deposition of solid precipitates of sparingly soluble zinc borate and/or its derivatives. A joint research project was established by HZDR and IPM Zittau/Goerlitz to investigate this type of problem during the later phases of LOCA.

Additional problems are expected due to the formation of solid zinc borate compounds in boric acid solutions at elevated temperatures if the Zn concentration in solution exceeds the saturation concentration. Due to the negative solubility coefficient of zinc borate, the crystallization process can be initiated by a temperature increase of the coolant as well as by evaporation.

Figure 5-15: Hot-dip Galvanized Step Grating after having been Submerged in Borated Water for 2 Years.

5.3.5   Summary

1.   Precipitant release generally shows a time dependence, often of the form:

$$Release = (1-exp^{-kt})$$

or

$$Release = kt^{-1/2}$$

2.   Synergistic effects are important and can inhibit corrosion or dissolution reactions (e.g., corrosion inhibition by phosphates or silicates). Therefore the results obtained in single effects tests can be conservative;

3.   Aluminum alloys have a low corrosion rate in the pH range 4-7; at pH values less than 4 or greater than 7, the corrosion rate increases significantly;

4.   Aluminum corrosion is higher in borated solutions than in non-borated solutions;

5.   Aluminum release can be modeled by equations of the form $RR= f(pH, T, t)$;

6.   Silicon release increases with increasing temperature and pH;

7.   Silicon release can be inhibited by the presence of aluminum in solution and by the use of TSP;

8.   Silicon release may be different in borated versus non-borated solutions;

9.   Calcium release generally decreases as the pH increases;

10.   Concrete and fiberglass do not appear to be significant calcium sources;

11.   Zinc release from galvanized steels and IOZ primer is low.

12. Erosion-corrosion can be a serious concern given the right combination of water chemistries and flow conditions.

5.4   Precipitation

Thermodynamics predicts that a large number of compounds could potentially form in the post-LOCA sump given the mixture of chemical species expected to be present. Preliminary thermodynamic simulation modeling, carried out before the first ICET results were available, used input values from peer-reviewed literature (corrosion/dissolution rates) and the ICET test plan (surfaces areas, water composition) [5-30]. It was assumed that the system was in thermodynamic equilibrium and the model allowed the most oversaturated phase to precipitate; i.e., no kinetic information was included. The reactions were limited to those materials used in the ICET tests and excluded the uptake of CO_2 from air. At pH 10, various silicate species were predicted to form over time; however, silicate phases were not observed to form in the ICET tests. It was noted that, while these silicates are the thermodynamically stable phases, their formation is kinetically slow. Hence, the simulations were repeated with the formation of some species suppressed.

When the revised simulations were run for ICET Test 1 [5-39], reasonable predictions of the aluminum and calcium concentrations in solution were obtained for the first 720 h, after which the model overpredicted the concentrations of Al and Ca. This overprediction was attributed to the passivation of the surfaces. The model also overpredicted the concentration of Si in solution at all times, possibly because the model assumed that all the concrete dissolved instantly. The model also predicted the formation of $Fe(OH)_2$ after 148 h and $Zn(OH)_2$ after 32 h. Some conclusions regarding ability of the thermodynamic modeling to simulate the concentrations of the precipitating species identified in the five ICET tests are summarized in Table 5-10.

The study authors suggested [5-21] that there are likely only a few elements (e.g., aluminum, silicon) that contribute to the formation of chemical products in containment water. This is a key result, as it limits the number of compounds that need to be considered in assessing possible chemical effects.

Table 5-10: Assessment of the Ability of the Chemical Speciation Modeling to Predict the Concentrations of the Precipitating Species Identified in the Five ICET Tests.

Test	Assessment
1	Good correlation with major elements up to 360 h. Simulation predicts higher concentrations in solution at 720 h.
2	Good correlation with major elements, except Ca, up to 360 h. Simulation predicts Ca will precipitate as phosphate.
3	Good correlation with major elements, except Ca, up to 360 h. Simulation overpredicts [Ca] in solution after 96 h.
4	Prediction did not correlate with ICET results. Simulation inputs were based on separate corrosion measurements for cal-sil insulation and aluminum. ICET data indicate strong synergistic effects between cal-sil and aluminum corrosion.
5	Predictions did not correlate with ICET results because the simulations were based on corrosion data measured at pH 10 or at pH 7.

IRSN have used the thermodynamic modeling code PHREEQC[9] to predict the type and amount of precipitate that could be produced for a given set of test conditions [5-40].

5.4.1 Aluminum Precipitation

Accurately predicting the amount, form and properties of aluminum precipitates expected to be formed in a post-LOCA sump environment is difficult due to the complex nature of precipitation from neutral to basic solutions containing aluminum species. Many compounds are thermodynamically possible, but the kinetics of formation may be slow, and the observed precipitates and their properties will depend on the temperature, pH, solution chemistry and the presence of solid surfaces such as a debris bed. Possible aluminum-bearing precipitates include aluminum hydroxide or oxyhydroxide, aluminum phosphate and calcium aluminum phosphates. Aluminum silicates are thermodynamically stable, but were not observed in ICET tests [5-7].

Test data show that the measured dissolved aluminum concentrations are often much higher than the solubility of gibbsite (γ-Al(OH)$_3$) at similar temperatures [5-41]. These high aluminum concentrations result in precipitation of some of the aluminum as a non-crystalline material in which carbonate, aluminum, boron and sodium were the major components. The precipitate was described as "a white, nearly neutrally buoyant material which qualitatively looked like aluminum hydroxide with boron" [5-13]. Since the precipitating phase was not unambiguously identified, it is not known whether the presence of boron in the precipitates was due to inclusion or adsorption resulting in the co-precipitation of boron with aluminum hydroxide, or was due to the formation of an aluminum-boron compound.

The amount of precipitate formed in the ICET tests was temperature and time dependent. Filtered water held at 60 ^{o}C was never observed to form precipitates, but as the temperature was decreased to 23 ^{o}C, precipitates formed gradually with time, i.e., the solubility of the precipitate decreases with temperature. It was noted [5-21] that there was never any visible precipitate, but that when a raw sample was extracted, it would immediately flocculate. Total suspended solids measurements on end-of-test solutions as a function of temperature found a roughly linear increase in total suspended solids as the temperature decreased. Control tests in which a fibreglass sample was gently rinsed with water purified by reverse osmosis showed that the film deposits on the fiberglass

---

9   PHREEQ is a computer program for simulating chemical reactions and transport processes in natural or contaminated water, available at http://wwwbrr.cr.usgs.gov/projects/GWC_coupled/phreeqc/index.html

were water-soluble, suggesting that they were actually formed by chemical precipitation during the drying of the fiberglass for the SEM and ESEM analyses.

Aluminum hydroxide is amphoteric and dissolves readily in strong acids and bases. Figure 5-16 shows the dissolved species in equilibrium with gibbsite as a function of pH at 50 °C. Over the pH range 4 to 9 it has been found that a small change in pH towards the neutral point results in rapid and voluminous precipitation of colloidal aluminum hydroxide, which readily forms a gel containing considerable excess water and variable amounts of anions. The gel composition and properties depends largely on the method of preparation and can crystallize on aging. Above pH 9, the dominant aluminum species in solution is $Al(OH)_4^-$.
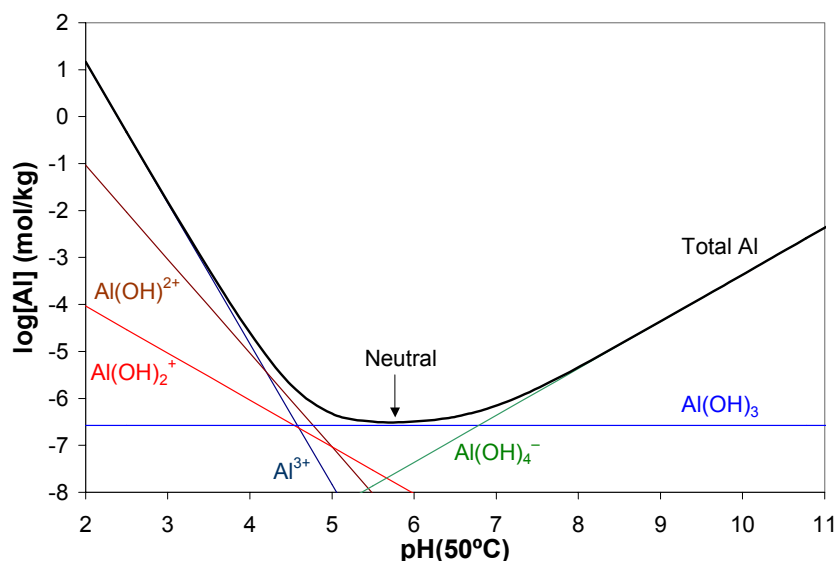
Figure 5-16: Logarithm of the Molality of Monomeric Aluminum Hydrolysis Species, $Al(OH)_y^{3-y}$ in Equilibrium with Gibbsite as a Function of pH at 50 °C and Infinite Dilution[10]

Aluminum hydroxide ($Al(OH)_3$) may exist in an amorphous form or as one of three crystalline forms: gibbsite, bayerite, or nordstrandite. Various forms of AlOOH (boehmite, diaspore, or pseudoboehmite) could also precipitate. The solubilities of the crystalline compounds in deionised water are very low; for example, at pH 8, the solubilities of gibbsite, bayerite, diaspore and boehmite are all less than 1 mg/L. However, in tests performed for the PWROG [5-22] in 2500 mg/L B solution, no aluminum oxyhydroxide precipitation was observed below 50 mg/L aluminum at pH 8 and 60 °C. As noted below, there appears to be an interaction between Al and B that results in higher apparent Al solubilities in borated solutions.

The precipitation of aluminum hydroxide phases from supersaturated aluminate solutions has been studied by a number of groups (e.g., [5-42]; [5-43]). Wesolowski [5-44] noted that approach to equilibrium from supersaturated aluminum solutions can be very slow (15–90 days); the formation of a metastable surface or bulk phase with a higher solubility than gibbsite was suggested. Van Straten and De Bruyn [5-42] reported that when a suspension of aluminum hydroxide in water is aged at a pH of 7 or higher, it undergoes a two-step aging process: amorphous aluminum hydroxide transforms into poorly ordered boehmite (pseuoboehmite), which in turn transforms into bayerite, the stable polymorph. It has also been shown that supersaturated aluminate solutions form the most-soluble phase first, become saturated with that phase, and subsequently form the next soluble phase[11].

---

[10] The thick solid curve is the total solubility of gibbsite.

[11] This trend follows the Ostwald rule of stages, which predicts that the thermodynamically least stable phase should form first, followed by the more thermodynamically stable phases.

Experiments in which solutions of aluminate ions were titrated with acids at various rates showed that the formation of a crystalline phase was favoured by very low titration rates, with amorphous phases being favoured at high titration rates. They also noted that an amorphous phase was formed immediately once a critical value of the supersaturation was reached and if the titration speed was quite rapid.[12] The degree of supersaturation in these tests was (pAl – pOH) ≤ –1.9. Based on this conclusion, the supersaturated aluminium concentration required for precipitation should be greater than 2.1 mg/kg at pH 7 and 25 ºC, 100 times higher than the solubility of crystalline aluminium hydroxides.

The temperature and pH dependencies of the solubilities of gibbsite, bayerite, diaspore and boehmite [5-45], [5-46] are similar; bayerite has the highest solubility relative to the other three aluminium phases at the same pH. The calculated solubility of gibbsite in non-borated water as a function of temperature at various pH values (Figure 5-17) is a weak function of temperature, decreasing by a factor of about 10 as the temperature is decreased from 100 ºC to 25 ºC at pH 10. The solubility of gibbsite is a very strong function of pH, dropping by a factor of ~300 when the pH is lowered from 10 to 6.5 at 50 ºC.

The solubility of amorphous aluminum hydroxide is much higher than that of the crystalline forms. Park et al. [5-35] reported a K_{sp} value[13] of 8.0×10^{-13} for the amorphous phase at 25 ºC, approximately 400 times larger than the solubility of gibbsite at the same temperature, consistent with the high measured aluminum concentrations in ICET Test 1.

Anions present during precipitation can be absorbed by the aluminum hydroxide gel and may stabilize or destabilize the colloid [5-48]. Literature data indicate a strong interaction between boron and aluminum that can lead to a significant increase in the solubilities of gibbsite and boehmite (up to factors of 6) [5-48], [5-49]. The presence of borate ion in solution may significantly change the flocculation behaviour of the aluminum hydroxide or oxyhydroxide, and therefore the surface chemistry of the precipitates must be considered. For precipitates formed near the point-of-zero-charge (in the range 8-9 [5-50]), the behaviour of the precipitate will be a strong function of pH, and borate ion adsorption could promote or prevent flocculation.

---

[12] These conditions are met by the method for precipitate preparation recommended by WCAP-16530-NP.

[13] This value was taken from Van Straten et al. [5-47]
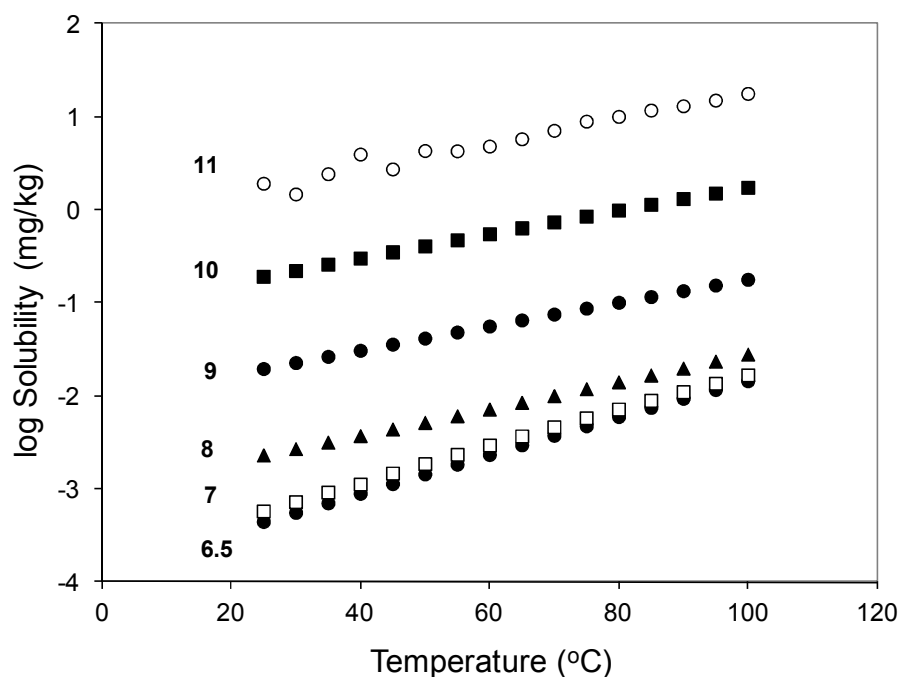
Figure 5-17: Solubility of Gibbsite as a Function of Temperature at Various pH Values (pH value listed to the left of each data set). Calculated from thermodynamic data reported by Wesolowski [5-44].

The initial ANL head loss testing of aluminum hydroxide precipitates used surrogates proposed by industry or prepared by in-situ precipitation of aluminum nitrate, $Al(NO_3)_3$. In a post-LOCA environment, however, the Al source will be dissolution of Al by corrosion of Al metal, and in alkaline solutions sodium aluminate is a much more representative aluminum source. In addition, nitrate ions would not likely be present in the post-LOCA sump water at concentrations comparable to those obtained when $Al(NO_3)_3$ is the source of dissolved Al.

Recently, ANL performed a series of head loss tests in which the source of Al was corrosion of Alloy 1100 and Alloy 6061 Al plates [5-10]. The objective of these tests was to compare the head loss resulting from precipitates formed from aluminum coupon corrosion with the head loss resulting from the use of precipitates prepared using the methodology presented in WCAP-16530-NP [5-9] or precipitates formed *in-situ* as a result of chemical injection.

Post-test examination of the glass fiber bed and bench top test results showed that Fe-Cu enriched intermetallic[14] particles were released by corrosion of the alloys and captured in the bed during the loop test. Differences in head loss behavior associated with the intermetallic particles were attributed to differences in the sizes of the intermetallic particles in Alloy 6061 and Alloy 1100. Variations in head loss suggested that the solubility of Al in these tests was lower than that measured in tests where the source of Al was chemical addition, possibly due to heterogeneous nucleation of Al hydroxide on intermetallic particles and/or on the surfaces of pre-existing Al hydroxide precipitates. It was suggested that the potential for corrosion of an Al alloy to result in increased head loss may be dependent on its microstructure as well as on the Al release rate.

Table 5-11 and Figure 5-18 summarize most of the available Al solubility data under PWR post-LOCA sump water conditions as a function of solution pH presented by Bahn et al. [5-10].

The graph has been divided into a "Precipitation" and a "No Precipitation" region; the data

---

[14] Primarily (FeSiAl) ternary compounds ranging in diameter from a few tenths of a micrometer to 10 μm.

strongly suggest that, at a given pH, precipitation does not occur at Al concentrations in the "No Precipitation" zone.

Table 5-11: Summary of Relevant Al Solubility Data under PWR post-LOCA Sump Water Conditions

[B] (mg/L)	Temperature (°C)	pH	Solubility (mg/L)	Source
2800	60	9.3	126	[5-49] pg 74
2800	60	8.7	80	[5-49] pg 74
3120	60	10	380	[5-7]
2860	60	8.5	54	[5-7]
2860	60	8.5	34	[5-7]
2800	60	10	260	[5-35] C5
2800	60	9.8	115	[5-35] C5
2800	60	9.5	60	[5-35] C5
2800	60	9.6	53	[5-35] pg 63
2800	60	9.6	35	[5-35] pg 63
2800	60	9.6	49	[5-35] pg 63
2800	25	7	20	AECL unpublished data

The observed decrease of pH + p[Al] as a function of temperature in Figure 5-18 is a consequence of the dominant equilibrium:

$$Al(OH)_4^- = Al(OH)_3(s) + OH^- \qquad \text{Equation 5-7}$$
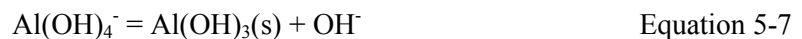
Since $Al(OH)_4^-$ is the dominant dissolved Al species in alkaline solution, the overall aluminum concentration is approximately equal to $[Al(OH)_4^-]$, and it can be shown that

$$pH + p[Al] = \log K_{14} + pK_w \qquad \text{Equation 5-8}$$

and pH + p[Al] represents the sum of $\log K_{14}$ and pK_w.

Recently, Bahn et al. [5-10] reported bounding estimates of aluminum solubility in alkaline environments containing boron. Their most conservative curve, which bounds all the available data, is reproduced in Figure 5-18. At pH 7.5, the predicted aluminum concentration lies just below the most conservative solubility estimate. As both the calculated aluminum concentration and the solubility limit are considered conservative, precipitation is unlikely.
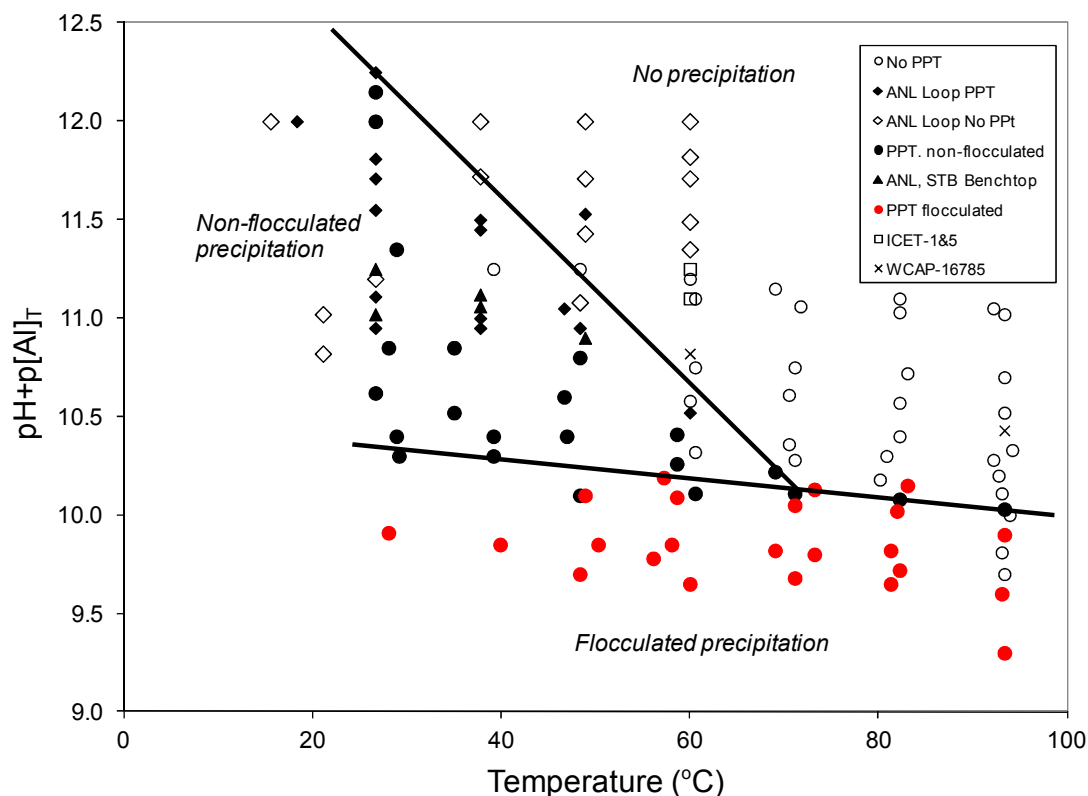
Figure 5-18: pH + p[Al] as a Function of Temperature for Amorphous Aluminum Hydroxide in Borated Alkaline Water. Data from Table 5. Open symbols indicate no precipitation, solid symbols indicate precipitation.

5.4.2   *Calcium Precipitation*

Calcium and phosphate ions can form a variety of low solubility salts (e.g., hydroxyapatite, $Ca_5(PO_4)_3OH$, whitlockite, β-$Ca_3(PO_4)_2$, octacalcium phosphate, $Ca_8H_2(PO_4)_6 \cdot 5H_2O$, monetite, $CaHPO_4$, and brushite, $CaHPO_4 \cdot 2H_2O$) in aqueous solution depending on the temperature, ions present, pH and the Ca/P ratio in solution. The solubilities of these phases have been typically measured around ambient temperature; the reported results can differ significantly from group to group [5-52]. Hydroxyapatite has been found to be the least soluble of these phases in water above pH 4 and is the thermodynamically most stable phase of calcium phosphate [5-53], [5-54]. It is expected that hydroxyapatite is the first phase to precipitate from a saturated solution, but $CaHPO_4 \cdot 2H_2O$ and $Ca_8H_2(PO_4)_6 \cdot 5H_2O$ can also precipitate, particularly at ambient temperatures and if the degree of supersaturation with respect to hydroxyapatite is high. These precipitates tend to transform to more stable phases such as hydroxyapatite but the process may be slow [5-55], again highlighting the importance of kinetics.

The concentrations of calcium and phosphate species in solution from the dissolution of calcium phosphates exhibit a range of behaviours as a function of pH. In acidic solutions, the dissolved calcium and phosphate species concentrations decrease with increasing pH. Chow [5-54] reported that at 25 ºC, sparingly soluble calcium phosphates showed a minimum in the dissolved calcium concentration at pH 8 to pH 10 depending on the phosphate species. Hydroxyapatite exhibited a minimum dissolved calcium concentration around pH 8.5. The dissolved phosphate concentration at 25 ºC decreased or increased with increasing pH in alkaline solution depending on the individual phosphate [5-54]. The concentration of phosphate species released from hydroxyapatite continuously decreases with pH up to 12. The different dissolution behaviours of calcium and phosphate species

may be due to the incongruent dissolution of calcium phosphates, i.e., the molar ratio of Ca/P in solution differs from that in solid state.

Sparingly soluble calcium phosphates show different dissolution behaviours at low and high temperatures. Below 40 ºC, calcium phosphate solubilities decrease with increasing temperatures (Figure 5-19) [5-56], [5-57]. At higher temperatures, the limited experimental data from conductivity measurements and solubility experiments show that dissolved calcium and phosphate concentrations increase with increasing temperatures (Figure 5-20) [5-58], [5-59], [5-60]. As solubility data for calcium phosphates between 40 and 100 ºC relevant to understanding precipitation in post-LOCA sump water are not available, the data from Figure 5-19 were extrapolated to pH 7 and included in Figure 5-20. These data suggest a solubility minimum near 50 ºC.

The literature data suggest that the solubility of calcium phosphate is lowest at pH values around 7 and temperatures below 100 ºC. The ICET test results are consistent with these observations.
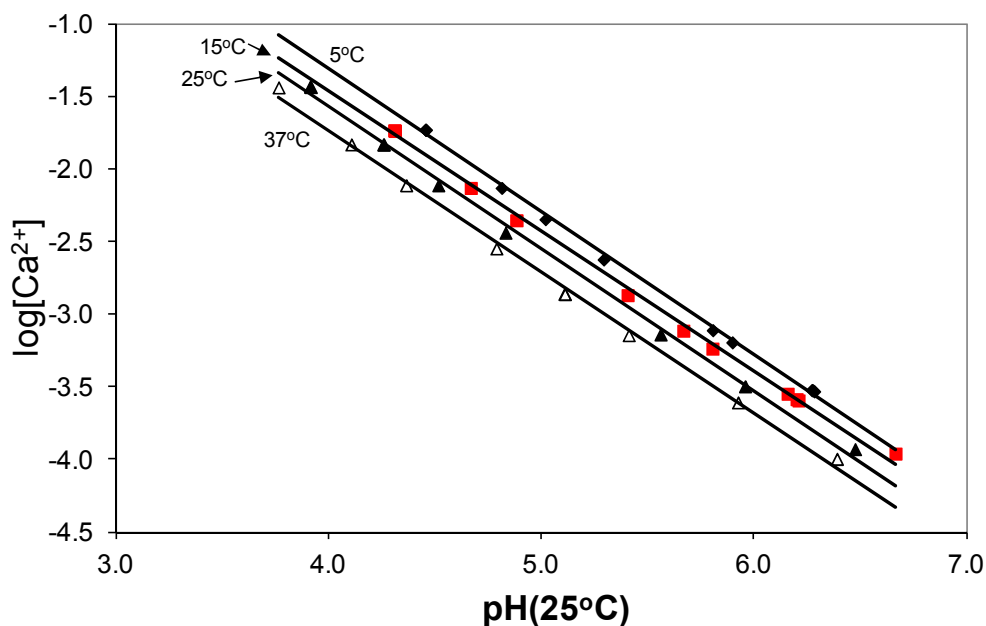
Figure 5-19. Dissolved Ca^{2+} Concentration (mol/kg) in Equilibrium with Hydroxyapatite as a Function of pH and Temperature [5-57].

In single effects tests sponsored by the PWROG [5-9], calcium phosphate was found to precipitate either as a single phase or as a mixture with an aluminum-bearing compound (e.g., aluminum hydroxide or calcium aluminum phosphate) when TSP was used as a buffer at pH 8 in tests containing calcium silicate and powdered concrete. SEM/EDS results showed that the precipitates had a Ca/P molar ratio of 1.2; however, the actual chemical phases present in the precipitate were not characterized, and it was not reported whether the precipitates were crystalline or amorphous.
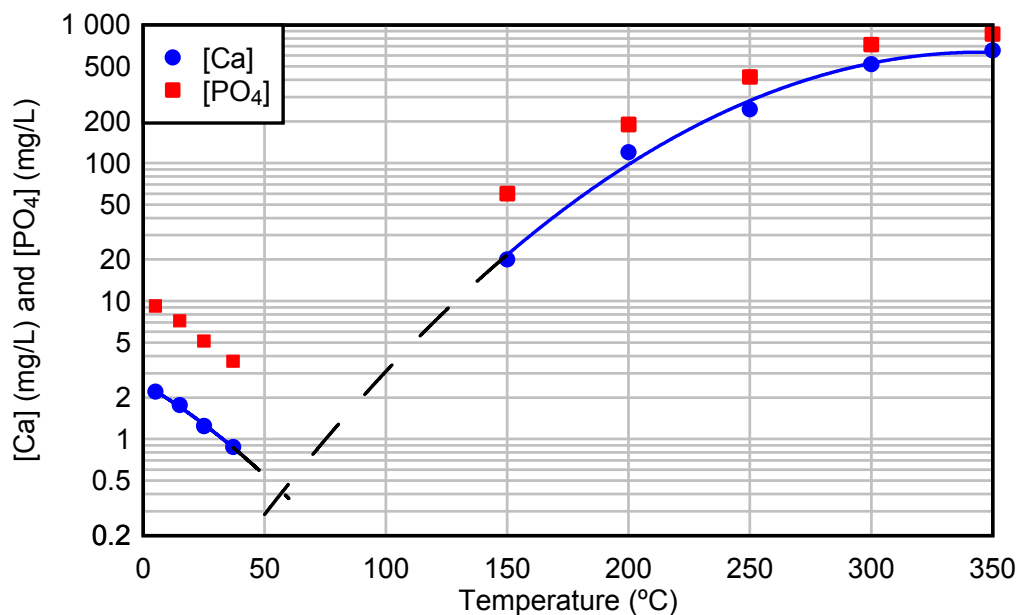
Figure 5-20: Dissolved Ca²⁺ and PO₄³⁻ Concentrations in Equilibrium with Hydroxyapatite as a Function of Temperature at pH 7 [5-60]. The data below 50 ⁰C were extrapolated from the data of McDowell et al. [5-56] (Figure 5-19).

In ICET Test 3, a white gel-like precipitate was observed [5-15] when TSP was added to simulated sump water containing 80% cal-sil and 20% fibreglass at pH 7. However, no precipitation was observed by visual examination in ICET Test 2, in which only fibreglass was added to the test vessel. Chemical composition analysis shows that 92% of the gel in ICET Test 3 was composed of Ca, O, and P. The formation of one of three calcium phosphate species was suggested, but it is more likely that it was an amorphous hydroxyapatite. The formation of amorphous materials rather than a pure calcium phosphate salt is often observed in other industries due to the incongruent dissolution behaviour of calcium phosphates.

The solubility data for crystalline calcium phosphates suggest that in all of the experiments discussed above, the calcium and phosphate concentrations were well above the solubility of the most stable calcium phosphate phases. However, both the Westinghouse short-term tests (24 h) and long-term ICET tests (30 days) show that, in the absence of added cal-sil, the amounts of calcium released from fibreglass are insufficient to result in the precipitation of calcium phosphate. As with aluminum hydroxide precipitation, kinetic factors appear to play a major role in the precipitation process, and high degrees of supersaturation are required to produce rapid precipitation. Calcium phosphate precipitation was found in the Westinghouse test PPT Run 38 using TSP and powdered concrete [5-9]. As noted by Lane et al. [5-9], the mass of powdered concrete used in these tests was several orders of magnitude too high compared to the desired surface area to coolant volume ratio. A conversion factor was used to convert concrete surface area to an equivalent mass of pulverized concrete, and it was concluded that concrete is an insignificant source of calcium.

5.4.3   *Silicon Precipitation*

As silicates or silica dissolve in water, various silicon-containing species form depending on the pH of the solution. These include monomeric silicon species, e.g.,

$$H_4SiO_4 = H_3SiO_4^- + H^+$$ `Equation 5-9

and polymeric silicon species, e.g.,

$$H_2O + 2SiO_4^{4-} = Si_2O_7^{6-} + 2\ OH^-$$ Equation 5-10
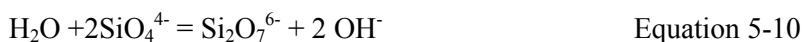
Over the pH range 6.8 to 9.3 at 25 ^{o}C, the dominant dissolved silicon species is H_4SiO_4 [5-61]. When aluminum and silicon species are present in aqueous solution, polymerization of aluminum and silicon can occur to form aluminosilicates. Depending on the Al/Si ratio and pH, various aluminosilicates such as feldspars, nepheline, and zeolites can be produced in which the molar ratio of Al/Si ranges from 0 to 1. The molar ratio of Al/Si in aluminosilicates usually follows Loewenstein's law [5-62], which states that an AlO_4^{5-} tetrahedron cannot be connected with another AlO_4^{5-} tetrahedron by a common oxygen atom, and the maximum Al/Si ratio in aluminosilicates is 1:1.

The solubilities of aluminosilicates depend on pH, temperature, Si/Al ratio and ionic strength. The crystalline materials generally have very low solubilities in water, lower than the corresponding amorphous materials. For example, the solubility of amorphous sodium aluminosilicate is about six times that of crystalline zeolite A in 3 M NaOH solutions at 25 ^{o}C [5-63] although both have the same chemical formula, $NaAlSiO_4$.

In alkaline solutions, high pH generally increases the solubility of aluminosilicates; in acidic solutions, increasing acid concentration destroys the framework of aluminosilicates and increases solubility. Figure 5-21 shows the solubility of nepheline ($NaAlSiO_4$) glass at 25 ^{o}C as a function of pH. Near neutral pH, nepheline has a solubility minimum, and this behavior is also observed in solubility data for jadeite and albite glasses [5-64].
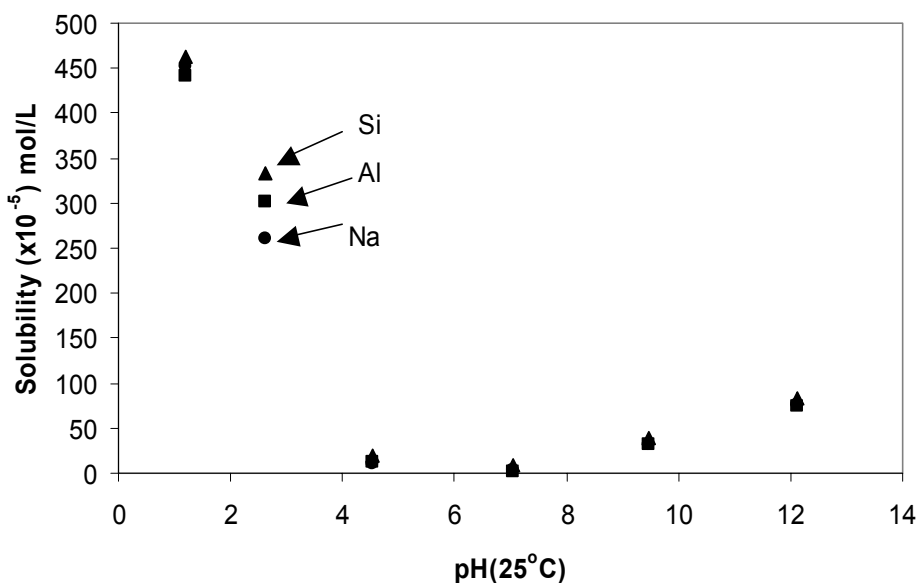
Figure 5-21. Solubility of Nepheline Glass as a Function of pH at 25 ^{o}C.

The effect of temperature on the solubility of aluminosilicates appears to not be well understood. Both positive and negative temperature coefficients of solubility are observed, even for same type of material. The common ion effect can decrease the solubility, but an increase in the ionic strength can increase the solubility of aluminosilicates in aqueous solution. Mensah et al. [5-63] measured the solubility of amorphous sodium aluminosilicate and crystalline zeolite at different aluminum concentrations and found that increasing the aluminum concentration decreased the solubility of aluminosilicates (Figure 5-22).
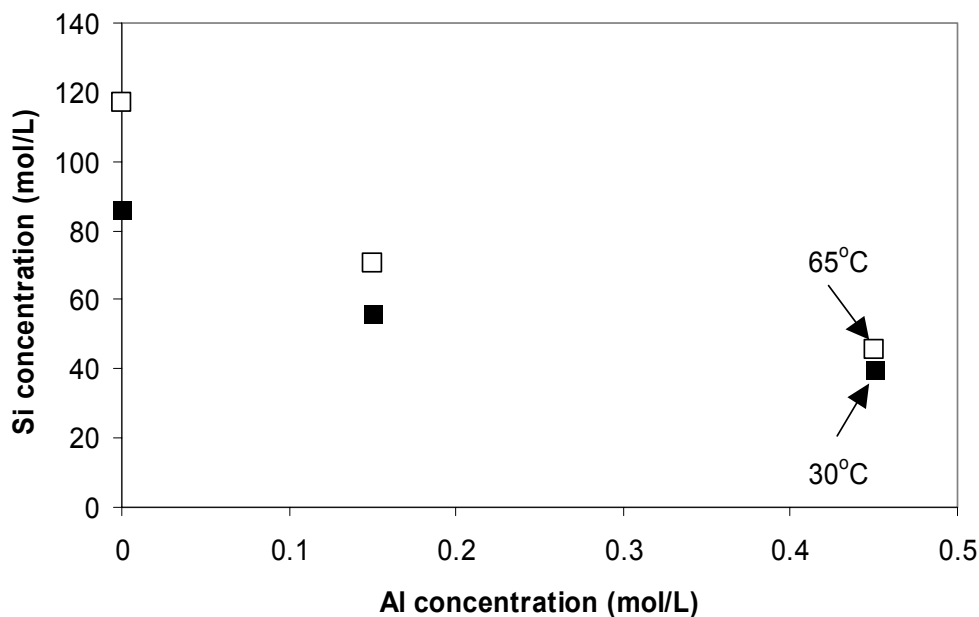
Figure 5-22. Solubility of Amorphous Sodium Aluminum Silicate (NaAlSiO$_4$) as a Function of Aluminum Concentration at 30 and 65 ^{o}C. The base solution contains 4.0 M of NaOH, 1.0 M NaNO$_3$ and 1.0 M NaNO$_2$ [5-63].

Park and Englezos [5-65] constructed a solubility map to predict the conditions under which sodium aluminosilicates could precipitate (Figure 5-23). It was found that the concentration of aluminum decreases with increasing concentration of silicon in solution and vice versa. Table 5-12 gives the maximum concentrations of selected elements in water samples taken from the ICET tests. Based on Figure 5-24, sodium aluminosilicates should not have precipitated in these tests, as observed. It should be noted that the pH in Figure 5-24 ([OH$^-$] = 0.89 M) is greater than that of ICET tests; as discussed above, high pH increases the solubility of aluminosilicates. However, the dependence of solubility of aluminosilicates on pH is weak at low hydroxide concentration ([OH$^-$] < 1 M) [5-66], [5-63], so the agreement between Figure 5-24 and the ICET observations is reasonable.

Table 5-12: Concentration of Selected Elements in Water Samples taken during the ICET Testing.

Test ID	pH	Maximum concentration in water samples (mg/L)									
		Al	Fe	Ni	Cu	Zn	Mg	Si	Ca	Na	P
Test 1	10 (no TSP)	380	Nr	nr	1.2	1.8	nr	8.5	15	5500	nr
Test 2	7 (TSP)	bd	bd	bd	bd	10	8	90	8	900	nr
Test 3	7 (TSP)	0.1	0.4	nr	0.2	0.1	3.5	100	100	2000	0.7
Test 4	10 (no TSP)	bd (5.5)	bd	nr	0.3	bd (0.3)	bd	180	50	11500	nr
Test 5	8.5 (borax)	54	bd	nr	0.9	0.8	1	12	34	1400	nr

bd – below detection
nr – not reported
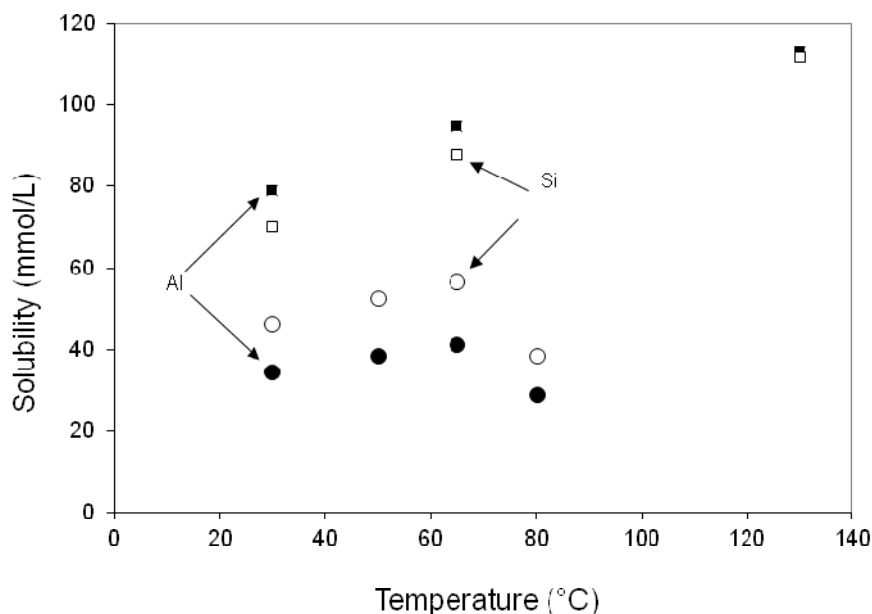
Figure 5-23: Precipitation Zones of Sodium Aluminosilicates at 25 $^{\circ}$C and 0.89 M Hydroxide. Adapted from Park and Englezos [5-65].

The mixing of alkaline aluminate and silicate solutions typically results in the formation of aluminosilicate gels which, upon heating in contact with the supernatant solution, are converted to aluminosilicate materials or zeolites. Gelation or precipitation may be delayed for long periods depending on the Al and Si concentrations, pH, temperature and the nature of the cation. Generally, the chosen synthesis conditions are far away from the equilibrium states, and supersaturated Al and Si solutions are commonly used to speed up the nucleation during the preparation of aluminosilicates. It has been found that increasing the temperature and supersaturation ratio decreases the induction time of aluminosilicates.

The pH appears to have two opposite effects on the precipitation of sodium aluminosilicate. Thermodynamically, lowering the pH decreases the solubility and increases the supersaturation ratio. On the other hand, kinetic experiments show that sodium aluminosilicate solutions with relatively low [Al] and [Si] (0.05 mol/kg) and low alkalinity (2 M) were slow to precipitate [5-66]. This is one reason why high alkaline concentrations are used to shorten the crystallization time of aluminosilicates [5-67]. In the ICET tests, the low pH (pH < 12) probably made sodium aluminosilicates difficult to precipitate.

5.4.4   *Zinc Precipitation*

The solubility of zinc in water is essentially determined by the solubility of zinc hydroxide ($Zn(OH)_2$), which has been measured by a number of investigators. Figure 5-24 shows the solubility of crystalline $Zn(OH)_2$ as function of pH and temperature, using the data of Reichle et al.[5-68]. The solubility of zinc increases as the pH decreases below about 9, and for pH values below about 8.5 the solubility of zinc hydroxide become retrograde, increasing as the temperature decreases. Thus, as the pH and temperature decrease with time in the post-LOCA sump water the solubility of zinc corrosion products will increase, a favourable situation from the perspective of solids formation.

At 40 °C and pH 8 the solubility of crystalline $Zn(OH)_2$ is about 1.5 mg/kg, reaching about 25 mg/kg at pH 7. The solubility of amorphous $Zn(OH)_2$ is known to be even higher; for a given pH, the solubility of amorphous zinc hydroxide is about 20-fold greater than the solubility of the crystalline form. As the initial corrosion film formed on metallic zinc surfaces is more likely to be amorphous $Zn(OH)_2$, the equilibrium solubility data indicate that zinc hydroxide (both crystalline and amorphous) is potentially quite soluble.
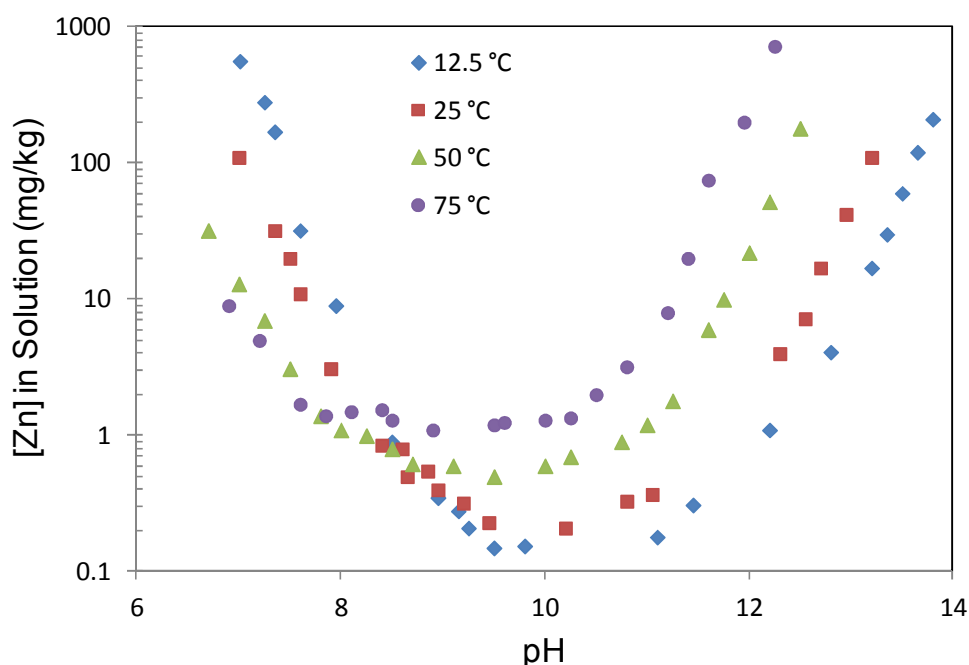
Figure 5-24: Solubility of Crystalline Zinc Hydroxide in Water as a Function of pH and Temperature (from data in Reichle et al., [5-68]).

5.4.5   *Summary*

1. The solubilities of aluminum hydroxides and oxyhydroxides in non-borated water are weak functions of temperature and very strong functions of pH;

2. The solubility of amorphous aluminum hydroxide is much higher than that of the crystalline forms;

3. The formation of crystalline aluminum hydroxide phases is favoured by very slow approaches to precipitation while amorphous phases are favoured by rapid condition changes;

4. The strong interaction between boron and aluminum can lead to a significant increase in the apparent solubilities of aluminum hydroxides and oxyhydroxides; the presence of borate ion in solution can change the flocculation behaviour of aluminum hydroxide or oxyhydroxide;

5. The solubilities of aluminosilicates depend on pH, temperature, Si/Al ratio and ionic strength;

6. The crystalline aluminosilicates generally have very low solubilities in water, lower than the corresponding amorphous materials;

7. Mixing of alkaline aluminate and silicate solutions typically results in the formation of aluminosilicate gels which can slowly convert to crystalline phases;

8. The effect of temperature on the solubility of aluminosilicates appears to not be well understood;

9. The limited solubility data for calcium phosphates between 40 and 100 ºC suggest a solubility minimum near 50 ºC;

10. Literature data suggest that the solubility of calcium phosphate is lowest at pH values around 7 and temperatures below 100 ºC;

11. Hydroxyapatite is the least soluble of calcium phosphate phases in water above pH 4 and is the thermodynamically most stable phase of calcium phosphate;

12. The solubility of zinc hydroxide increases as the pH decreases below about 9, and below about 8.5 increases as the temperature decreases.

5.5 Release and Precipitation - Implications for Chemical Effects Evaluation

In Sections 5.2 and 5.3, the release and precipitation behavior of the major species shown to give rise to chemical effects were described, and a number of conclusions made. The implications of these conclusions for chemical effects evaluations are as follows:

1. In general, Al, Si and Ca are the most problematic elements with respect to release under post-LOCA sump chemistry conditions and the subsequent formation of precipitates that can lead to high head loss. While Zn and Fe can also be released into the sump by corrosion, the solubilities of the Zn and Fe hydroxides and oxides increases as the pH decreases. In the absence of strong buffering of the sump pH, various radiolysis processes (air, paints, etc.) will cause the sump pH to decrease with time after a LOCA, so that precipitation of Zn and Fe hydroxides or oxides is not favoured.

2. The presence of boric acid in PWR and VVER sump water significantly increases both the corrosion rate of aluminum and the solubility of aluminum hydroxides and oxyhydroxides. While in principle these effects offset each other (more Al released but higher capacity of the solution for Al), in practice the higher Al loading is undesirable due to the strong sensitivity of Al precipitation on pH changes.

3. Short-term, single effects tests tend to overestimate both release and precipitation because factors such as passivation and inhibition are neglected. While inhibition effects can also be evaluated in single effects tests, it is difficult to model them in a conservative manner, and there has been reluctance for regulators to accept their occurrence in the absence of integrated testing.

4. The ICET tests and data from the literature show that the precipitation of aluminosilicates, while often thermodynamically favoured, is often kinetically unfavourable. In the absence of test data demonstrating their formation, it is recommended to assume aluminum precipitation only as aluminum hydroxide or oxyhydroxide.

5.5.1 Chemical Debris in BWRs

There have been fewer studies of chemical effects arising from interactions of solutes in the post-LOCA coolant with containment materials in BWRs. Unlike the PWR coolant, which contains a boric acid chemical shim, the BWR coolant is essentially pure water and does not contain solutes. However, some BWRs add sodium pentaborate (SPB) to the post-LOCA coolant and the SPB

additions may lead to chemical effects similar to those observed in PWRs. Although BWR coolant is chemically simpler than that of PWRs, chemical reactions in BWRs are still possible in the post-LOCA coolant sump because of the high temperatures and pH changes that will occur as the result of water radiolysis. Dissolution and/or corrosion processes can also lead to pH changes in unbuffered systems. Chemical effects in BWRs have to date not been a subject of study in the United States. The Japanese reported the results of integrated chemical effects tests under BWR water chemistry conditions as part of the ICAN integrated chemical effects test series (see Section 5.6). Tests under BWR conditions were also performed at the VENE test facilities in Hamburg, at the IPM Zittau/Goerlitz and the HZDR (see Section 5.6).

5.6   Testing

If the amount or nature of the chemical precipitates predicted to be formed in the post-LOCA sump water is outside the bounds of existing test data, plant-specific chemical effects testing can be performed to obtain the data required to ensure acceptable strainer performance. A number of conservative assumptions and calculations are typically used to develop bounding test conditions for chemical effects testing. The evolution of post-LOCA sump water chemistry will be very complex, and no simple model and short-term testing program can properly evaluate the synergistic effects that could be expected to occur. By necessity, models of release must be based on limited, often single effects laboratory scale tests in order to elucidate the influence of the major variables (e.g., pH, T). Exact simulation of all relevant parameters (e.g., debris surface area to solution volume ratio, mass transport, rate of chemical addition) is not feasible during bench-top or reduced-scale testing. As a result, the testing can become excessively conservative.

This type of testing is obviously very specific to each plant design and their operational characteristics. As a result, different countries and vendors have developed their own test protocols and facilities. The following section summarizes the actions undertaken in the US, Korea, Japan and Germany during the past decade as part of their programs to address this issue.

The US NRC developed guidance for the evaluation of chemical effects [5-69], and has outlined a generic chemical effects evaluation process. Figure 5-25 is a simplified flowchart adapted from the US NRC process.
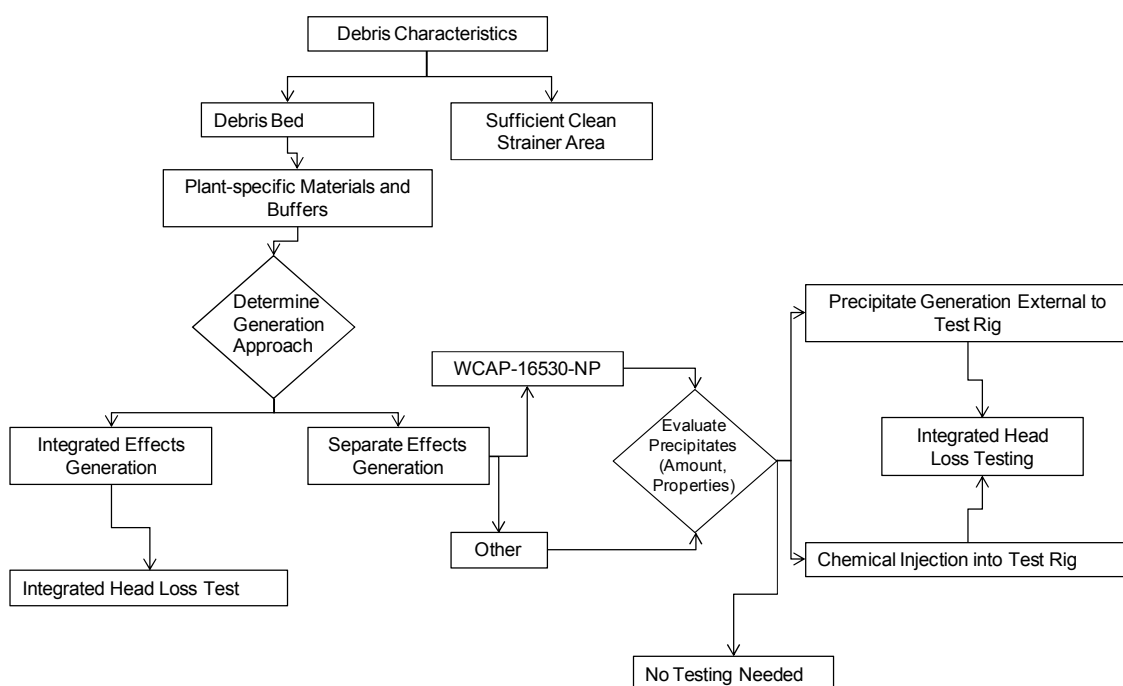
Figure 5-25: Simplified Flowchart for Chemical Effects Resolution (adapted from US NRC guidance document [5-70]).

It is necessary to identify the expected precipitates in the post-LOCA sump and also important to consider the impact of the kinetics of precipitate formation on the precipitates formed and their morphology. Table 5-13 lists the precipitates considered by various countries in their test programs.

Table 5-13: Precipitates Considered by Various Countries in their Test Programs.

Country	Precipitates	Reference
Canada	$Al(OH)_3$	-
France	Identified from integrated testing	[5-40]
Germany	none	[5-75], [5-76], [5-77]
Korea	$Al(OOH)$, $Ca_3(PO4)_2$, $NaAlSi_3O_8$	[5-70]
Japan	$AlOOH$, $NaAlSi_3O_8$, $FeOOH$, $Zn(OH)_2$	[5-72], [5-73], [5-74]
Spain[15]	$Al(OOH)$, $Ca_3(PO4)_2$, $NaAlSi_3O_8$	
United States	$Al(OOH)$, $Ca_3(PO4)_2$, $NaAlSi_3O_8$	[5-7], [5-9][a]

a - these are the precipitates used by those plants using WCAP 16530 as their basis for precipitate formation and preparation. Some plants used plant-specific tests with plant-specific materials to determine what precipitates form.

There is no agreement on what constitutes "prototypical" behaviour (e.g., settling rates, particle size), and this might be expected to differ from plant to plant. WCAP-16530-NP proposes that precipitates for testing should settle by less than 40% within the first hour of preparation. This value was selected to replicate the settling rate observed in Westinghouse tests where solutions from dissolution of aluminum sheet at pH 8 and pH 10 were rapidly cooled. In these tests, precipitates settled by about 30% within 4 hours. Settling rates were found to be a function of the concentration of aluminum oxyhydroxide in the mixing tank before dilution.

To be truly prototypical (least conservative), precipitates for chemical effects testing should be prepared in-situ in integrated tests in which the construction materials (aluminum, concrete, etc.) and debris are exposed to simulated sump water (with chemistry, pH and temperature correctly simulated), allowed to corrode (dissolve) and then to react to form precipitates slowly over time. In this way the various passivation and inhibition reactions that can limit release can occur, and the reactants reach their saturation concentrations slowly (as in Figure 5-2). In Figure 5-26, this is denoted 'Integrated Effects Generation'. The ICET tests are a good example of prototypical precipitate formation, and provide valuable insights into the expected behavior.

This consideration allows three levels of chemical effects testing sophistication to be defined:

1. Integrated tests in which the construction materials and debris are exposed to simulated sump water, allowing the various chemical reactions (corrosion, dissolution, precipitation, and aging) to occur over time;
2. Tests in which the corrosion and dissolution step are simulated by the addition of chemical reactants to the test rig based on a detailed model of the time-dependent post-LOCA sump chemistry;
3. Tests in which surrogate precipitates are added to the test rig.

Typically the degree of conservatism increases as one moves from 1 to 3 in the list while the complexity of the testing decreases. These three types of testing are discussed below.

---

[15] Note that the Trillo plant (a PWR of German design) did not consider precipitate formation but instead considered the effects of iron and zinc particulate corrosion products.

A typical 30-day integrated chemical effect test for PWRs was performed in Korea [5-71]. This test method was developed to simulate the chemical conditions of the post-LOCA containment recirculation sump to evaluate the head loss associated with the formation of chemical products. The test rig consisted of five individual loops, each of whose chamber was established to detect chemical product formation and to measure the head loss through a sample filter. The screen area in each chamber and the amounts of materials from the reactor building of interest were scaled according to the specific plant condition.

A series of tests were performed to evaluate the effects of calcium silicate, reactor building spray, TSP, and materials composition on head loss. The results showed that the head loss across the debris bed with even a small amount of calcium silicate debris instantaneously increased as soon as TSP was added to the test solution (Figure 5-26). The head loss across the screen was strongly affected by the spray duration and the increase of head loss was rapid during early stages of the test because of the high dissolution and precipitation of aluminum and zinc. After passivation of aluminum and zinc by corrosion, the rate of head loss increase slowed significantly, and mainly resulted from materials such as calcium, silicon, and magnesium leached from NUKON and concrete. It was found that the spray buffer agent, TSP, formed a protective coating on aluminum surfaces and reduced aluminum release, but was not effective for large amounts of aluminum and long spray duration.
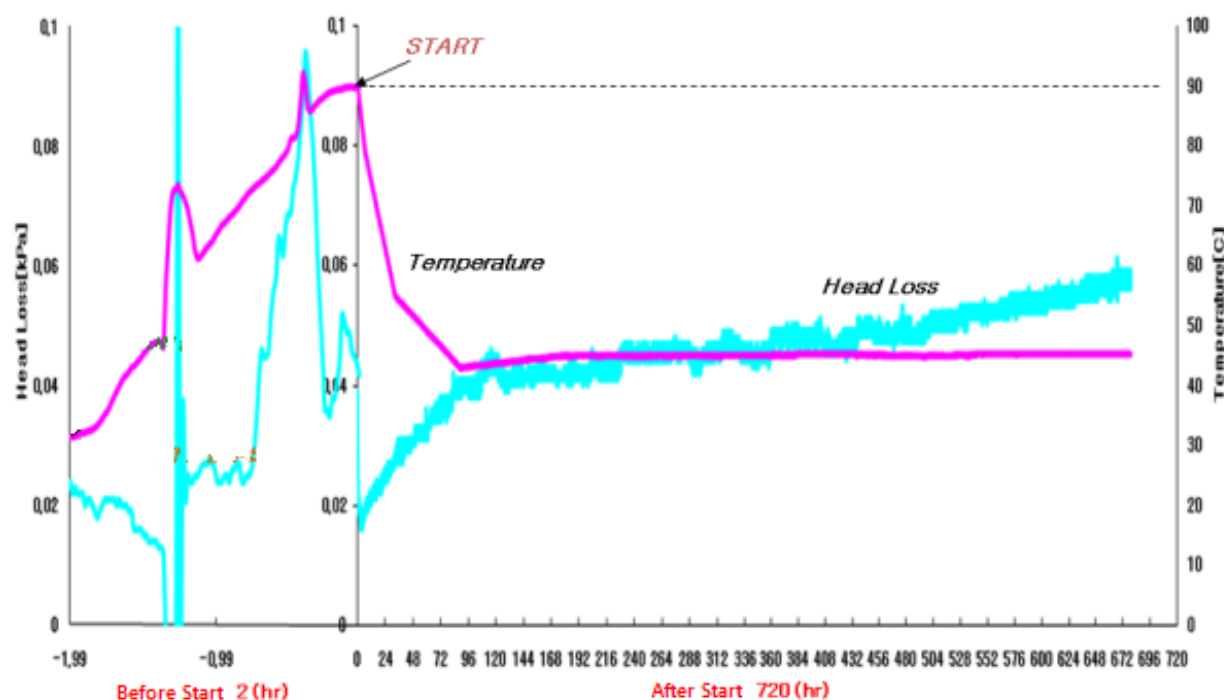
Figure 5-26: 30-Day Integrated Chemical Effects Test Data for a PWR [5-71].

Researchers at the Japanese Nuclear Energy Safety (JNES) reported the results of thirteen tests simulating the containment vessel of a PWR and simulating BWR conditions. These ~800 h (~33 day) integrated chemical assessment tests (denoted ICAN 1-13) were performed to examine head loss and dissolved element concentrations in recirculating 60 °C coolant accompanied by spray flow in gas spaces. Test parameters such as scale (1,000 L) and types, quantities, and placements of material surfaces were patterned on the ICET experiments. Two types of insulation material (calcium silicate and rock wool) were tested. The experiments are outlined in Table 5-14.

Details on the configurations of ICAN experiments can be found in [5-72], [5-73], [5-74], [5-75]. The dissolved concentrations of aluminum, silicon, iron, and copper were found to roughly match the solubilities of the corresponding oxides and hydroxides observed in the testing (gibbsite, $Al(OH)_3$, and amorphous $Al(OH)_3$, quartz, SiO_2, and amorphous silica, $SiO_2(am)$, hematite, Fe_2O_3, goethite, $FeOOH$, cupric oxide, CuO, and zinc oxide, ZnO). The changes in head loss with time were complex for these tests and the report provided observations but little overall interpretation.

JNES also conducted colloid tests, in which head loss terms in amount of each colloid were measured for aluminum, iron, copper, and zinc hydroxides and for $CaSiO_3$ particles. In the colloid tests, rock wool debris was deposited on the screen and then colloid solution was added stepwise into the test loop to measure the head loss increase.

Table 5-14: Summary of JNES Integrated Chemical Effects Tests. The insulation used was rock wool. ICAN tests 1-3 were preliminary tests and are not listed in the table, and ICAN 12 was not an integrated test and is also not listed.

Test	Boric Acid	Buffer	pH		Wt. Loss per Submerged Coupon (g)		Comments
			End of spray cycle	After 33 days of testing	Al (13 mm x 13mm)	Fe (315 mm x 315 mm)	
4	Yes (+ HCl)	Na_2B4O_7	8.3	8.4	-0.05	6.60	Ice condenser
5	Yes (+ HCl)	N_2H_4, NaOH	7.5	7.0	0.67	18.5	Hydrazine conditions
6	No (+ HCl)	None	3.2	5.9	0.67	59.0	Like BWR; galvanized steel also tested
7	Yes (+ HCl)	NaOH	9.9	9.9	0.44	0.63	Dry condenser
8	Yes (+ HCl)	N_2H_4, NaOH	7.5	7.3	0.02	9.5	Like ICAN 5 but galvanized steel added in place of some of the carbon steel
9	Yes (no HCl)	NaOH	10.1	~10.1	0.03	0.5	Like ICAN 7, but galvanized steel added
10	Yes (no HCl)	N_2H_4, NaOH	7.5	~7.5	0.0	4.0	Like ICAN 5, but galvanized steel added
11	No (no HCl)	No	~6.3	8.3	-	36.0	Like ICAN 6
13	Yes (no HCl)	N_2H_4, NaOH	~7.7	~7.5	8.9 (315 mm x 315 mm)	5.2	Like ICAN 10 but Al coupon area increased.

Major findings from the experiments for representative Japanese plant conditions were as follows:

- Hydrochloric acid severely corrodes rock wool debris and suppresses head loss increase;

- Corrosion of carbon steel can increase the head loss significantly;

- The head loss increase in NaOH-buffered solution is greater than in N_2H_4-buffered solution;

- Enlarging the sump screen to decrease the approach velocity is very effective in preventing unacceptable head loss increase;

- Head loss is larger when the particles deposit on the fibre debris than when the debris deposits after the particles or the debris and particles are premixed;

- The head loss increases sharply after a certain amount of colloid is deposited on the debris.

JNES also proposed a method to include the chemical effects of iron and zinc into the WCAP method. In this method, the dissolution rate of carbon steel is analyzed with StreamAnalyzer[16], additional precipitates of iron and zinc hydroxide are assumed and conversion factors to estimate the amount of the surrogate precipitate are estimated based on the colloid tests. Head loss under ICAN test conditions, estimated by summing up each chemical effect of the specified precipitates measured in the colloid test including AlOOH, FeOOH, NaAlSi$_3$O8, and Zn(OH)$_2$ are holistically conservative for typical Japanese plant conditions. The conservativeness of the evaluation method is mainly caused by the assumption that all of the Si dissolved from the rock wool insulation precipitates.

For PWR long-term conditions an increasing head-loss at the strainer that was completely covered by a bed of insulation fiber was demonstrated by experiments performed by AREVA at the "Erlanger Wanne". In those experiments, zinc-coated step gratings were inserted into a waterfall of borated water. The head-loss due to the fibrous material at the strainer was around 50 mbar. After 10 h, a rising head-loss across the strainer was measured (Figure 5-27) [5-77]. Due to zinc erosion and subsequent iron corrosion, the head loss across the strainers exceeded the design limit of the strainers.
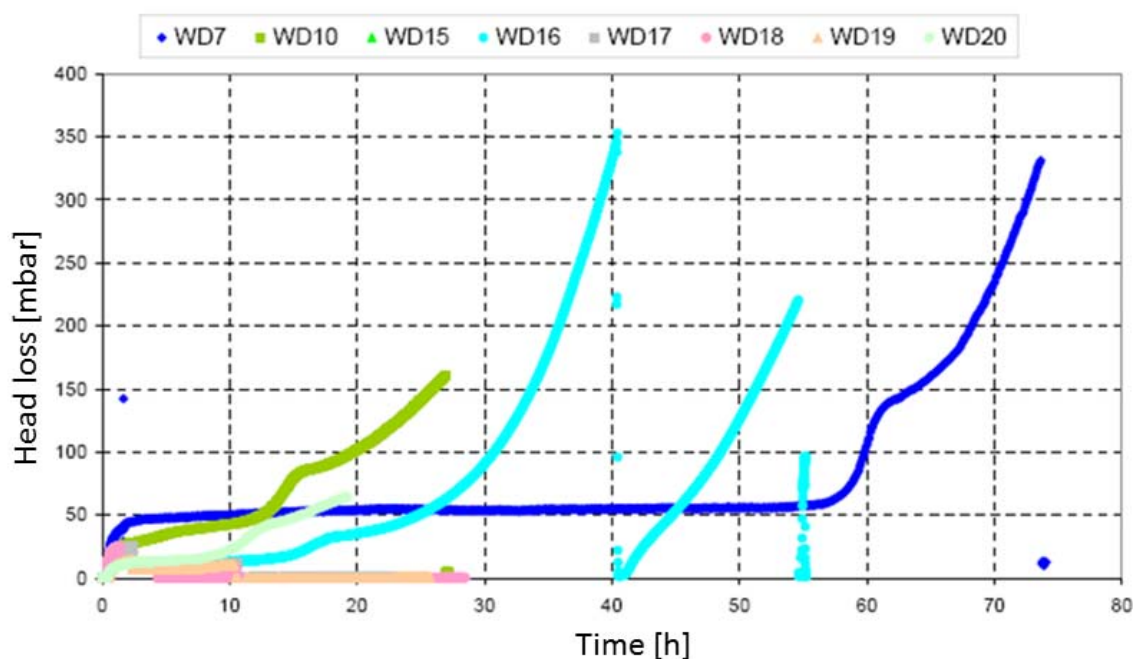
Figure 5-27:   Head Loss across Strainers Including the Influence of Erosion and Corrosion of Step Gratings in a Jet of Borated Water [5-77].

As a result of the increase of the head-loss across the strainers up to the design limit, the RSK requested monitoring and the limitation/reduction of the head-loss across the strainers [5-77] with a

---

[16] OLI Systems, Inc.

qualification according to safeguard systems. Within the test facility a reduction of the head-loss across the strainers was sometimes possible by shut-down of the pumps. However, a reliable limitation/reduction of the head-loss across the strainer was only achieved by backflushing by reversing the flow of water.

Tests under BWR conditions were performed at the VENE test facilities in Hamburg, at the IPM Zittau/Goerlitz and the HZDR. At the VENE test facilities, no increase of the head loss across fuel elements with deposited fibrous insulation material was measured for zinc-coated step gratings submerged in pure water [5-77]. For step gratings within a waterfall the head-loss across fuel elements increased after 5 to 10 days by a factor of 2 to 5 (Figure 5-28).
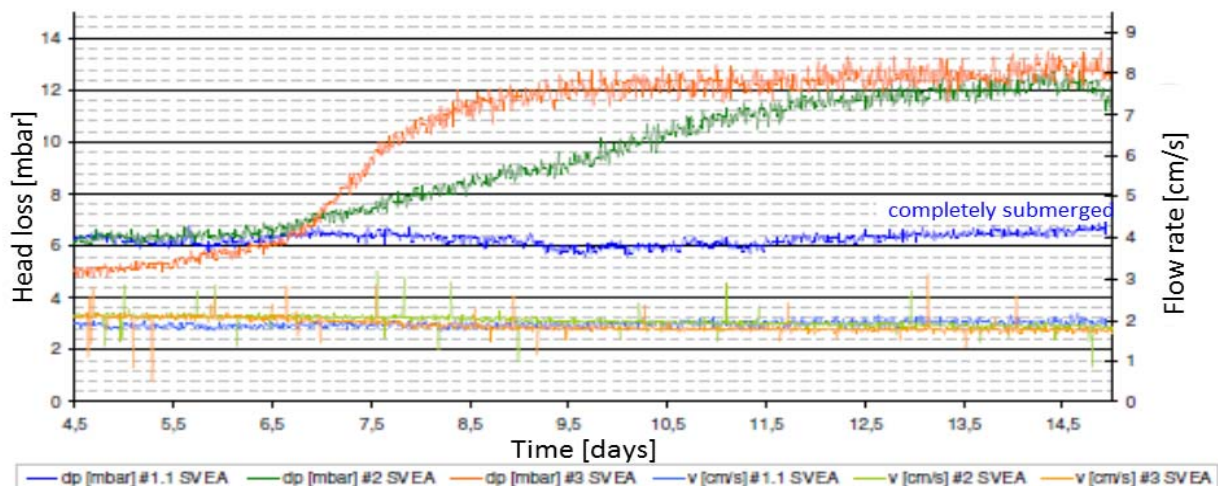
Figure 5-28:   Head Loss across a Fuel Element with Zinc-coated Step Gratings in a Jet of Pure Water (red, green) and Submerged in Pure Water (blue) [5-78].

Another investigation was performed by GES at the VENE test facility to study the influence of erosion and corrosion products on the head loss across the strainer debris bed. No increase in head-loss was observed due to zinc and iron embedded in the debris bed. The debris bed was created by manual deposition of the fibrous material onto the strainer; it is possible that manual deposition of the fibers led to an unrepresentative debris bed structure and therefore effect of zinc and iron. Strong zinc corrosion was shown for a water temperature of 70 °C. Additionally, the zinc corrosion was faster for new step gratings compared to older ones due to the lack of passivation of the zinc surface. The results are described in [5-78].

Moving down one level of test complexity, the corrosion and dissolution step can be simulated by the addition of chemical reactants to the test rig based on a detailed model of the time-dependent post-LOCA sump chemistry ('Separate Effects Generation' in Figure 5-25). Such a model can be developed using the type of information on release summarized in Section 5.2. The generation models developed in WCAP-16530-NP [5-9] are perhaps the most widely used of such models. Various thermodynamic database programs (e.g., PHREEQC, OLI Systems StreamAnalyzer) can also be used if care is taken to benchmark the results against the ICET tests or other all-effects tests to ensure prototypical precipitate behavior [5-40]. Once an appropriate release model has been developed, postulated post-LOCA temperature and pH profiles can be used to determine release rates of the major precipitants as a function of time. Release rates can be converted to accumulated releases, and accumulated releases to sump concentrations.

Chemical addition is then performed by adding precipitants such as sodium aluminate or calcium chloride to the test rig, usually with the debris bed preformed, at times determined by the release model ('Precipitate Generation External to Test Rig' in Figure 5-25). This approach reduces two key conservatisms by:

- Allowing the added reactants to form precipitates both in solution and on rig surfaces; and
- Explicitly accounting for solubility effects.

As an example of this type of testing, Figure 5-29 shows a representative head loss curve from a test conducted for the US utility Dominion Generation in borated deionised water at pH 7 and 40 ºC [5-36]. Additions of sodium aluminate ($NaAlO_2$) solutions were observed by AECL to result in increases in pressure drop (head loss) in all cases tested. Frequently, head loss peaked after additions, only to stabilize to a lower value. Aluminum concentrations in the all tests seldom exceeded 0.4 mg/L Al (the method detection limit of aluminum), suggesting nearly complete precipitation of the aluminum added. The peak head losses are plotted against the amount of aluminum precipitated per unit area of strainer (the strainer aluminum load) in Figure 5-30. Using the available pump suction head margin, the maximum allowable strainer aluminum load can be calculated and used to justify the existing aluminum components in containment or their replacement.
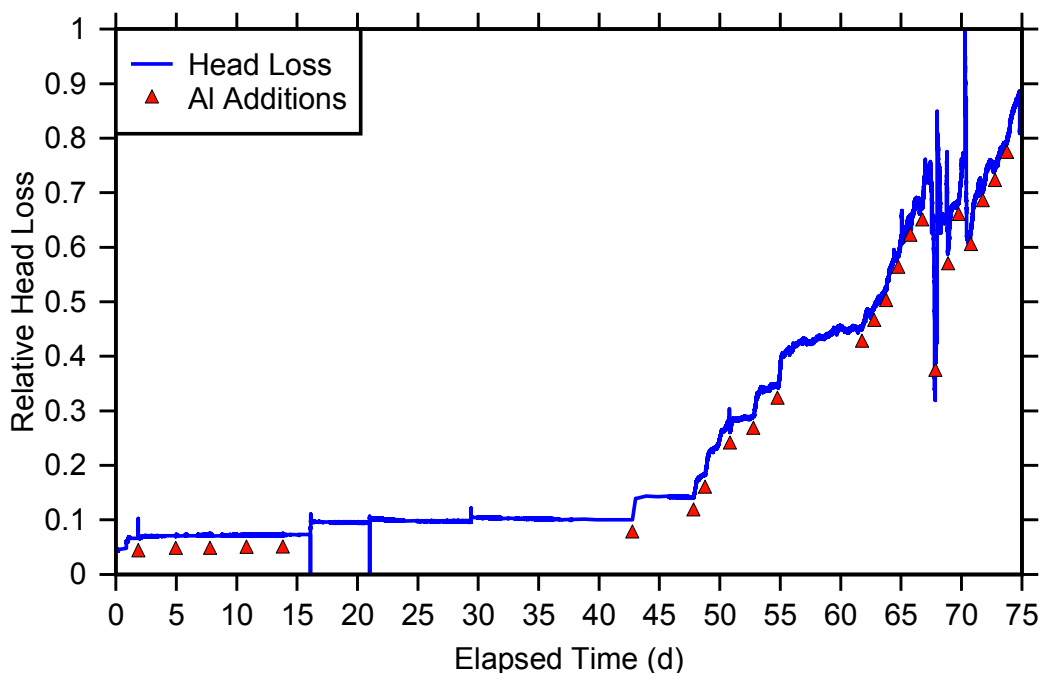
Figure 5-29: Head Loss Observed during a Typical Chemical Effects Test [5-36]. Dominion Generation reduced-scale chemical effects test data.
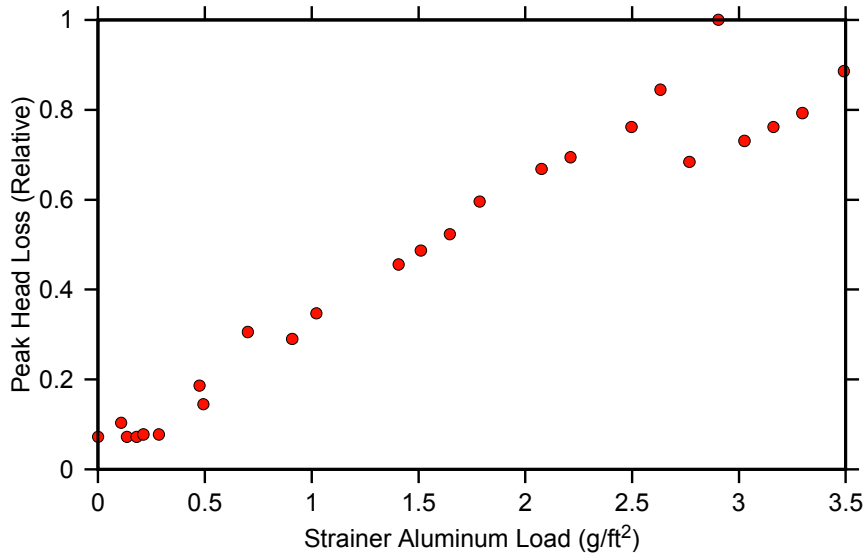
Figure 5-30: Peak Head Loss as a Function of Precipitated Aluminum per Unit Area of Strainer (Strainer Aluminum Load) [5-36]. Dominion reduced-scale chemical effects test data.

This test method also allows synergistic effects to be observed. As an example, in reduced-scale chemical-effects tests for Dominion Generation [5-36], additions of calcium chloride had a negligible effect on strainer head loss. SEM analysis of debris bed fibres in tests where calcium was added showed indications of a Ca-Al-P precipitate, and the calcium concentration decreased in a one-to-one molar ratio with aluminum additions (Figure 5-31). Thermodynamic analysis indicated that $CaAlH(PO_4)_2$ may form under certain conditions, but has been reported to be unstable with respect to hydrolysis.
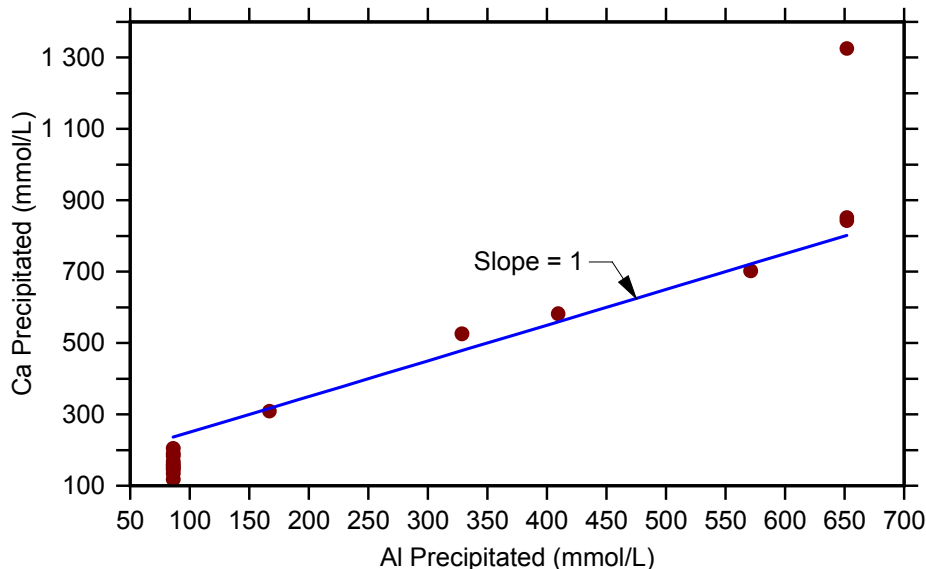
Figure 5-31: Calcium and Aluminum Co-precipitation in the Presence of Phosphate [5-36]. Dominion Generation reduced-scale chemical effects test data.

The least prototypical (most conservative) test method is to produce precipitates outside the test rig ('Chemical Injection into Test Rig' in Figure 5-25); the amount added is based on the calculated full chemical loading at the end of the mission time. The surrogate precipitates are added to the test

rig after formation of the debris bed. This approach ignores the effects of time, concentration, competing anions and debris bed surfaces on the particle size and distribution of the resulting precipitates. To produce the relatively large masses of precipitates required for testing using reasonable volumes of reagents, unrealistically high reagent concentrations may be required during precipitate generation. For example, the procedure for preparation of aluminum oxyhydroxide given in WCAP-16530-NP recommends that the concentration of aluminum oxyhydroxide in a mixing tank not exceed 11 g/L, corresponding to an aluminum concentration of 5000 mg/L. This is an unrealistically high concentration of aluminum, far above the amount of aluminum that could be produced in solution by corrosion of aluminum. The physical properties of precipitates formed by rapid precipitation at very high concentrations will be very different from the properties of precipitates formed slowly at much lower concentrations.

5.7   Gaps

The US NRC convened an external peer review panel to review the NRC-sponsored research conducted through the end of 2005 and to identify technical gaps that the original NRC-sponsored research either did not resolved or did not consider; NUREG-1861, "Peer Review of GSI-191 Chemical Effects Research Program" [5-80] summarizes this review. They also conducted a PIRT exercise between March 2006 and June 2006 to identify **additional** chemical effects that may affect the performance of the ECCS. The PIRT panelists independently ranked the significance and current knowledge associated with chemical phenomena most likely to (1) contribute to strainer screen clogging, (2) affect downstream component performance, (3) impact core heat transfer, or (4) degrade structural integrity. The PIRT process identified three types of issues:

- Issues that had been evaluated during previous research activities;

- Remaining follow-on issues or questions stemming from the prior research; and

- New issues not addressed by previous research.

NUREG-1918, "Phenomena Identification and Ranking Table Evaluation of Chemical Effects Associated with Generic Safety Issue 191" [5-81], details the results of the PIRT exercise.

The PIRT panelists identified and evaluated over 100 chemical effects phenomena pertaining to the underlying containment pool chemistry: radiological considerations; physical, chemical, and biological debris sources; solid species precipitation; solid species growth and transport; organics and coatings; and downstream effects. These phenomena fell into one of four different categories:

1. Category I - phenomena or issues that are generally known or have been demonstrated to be significant by prior research;

2. Category II - phenomena or issues that either are expected to be significant by the PIRT panelists or have been demonstrated to be significant by prior research, but whose implications with respect to ECCS performance are not well known;

3. Category III - phenomena that are potentially significant but are not well understood, and whose ECCS performance implications are highly uncertain;

4. Category IV - phenomena that have no engineering significance as determined by both the aggregate PIRT rankings and individual rankings and justifications.

After the PIRT process was completed, NRC staff evaluated the phenomena and reduced the list to those considered to be potential contributors to ECCS performance degradation, including issues that needed additional study to determine their significance. The 41 items in the final list fell mostly in Categories II and III such that further evaluation was deemed necessary to assess ECCS performance implications. US NRC staff used available information to determine the significance of, and implications associated with, each issue; the evaluation and the technical justification supporting

their disposition are documented in "Evaluation of Chemical Effects Phenomena Identification and Ranking Table Results" [5-82]. It was concluded that the implications of these issues are either not generically significant or are appropriately addressed within the guidance associated with assessing chemical effects on ECCS performance in response to GL 2004-02. Although several issues associated with downstream in-vessel effects remain, the staff did not anticipate the need for additional research in these areas since ongoing testing will establish the limiting amount of debris within the core that will ensure adequate flow to provide acceptable peak clad temperatures. The remaining issues to be resolved by testing and/or analysis are:

- The deposition of precipitates on reactor fuel and its effects on core cooling;

- The effect of physical and chemical debris contained within the core on the ability of the coolant to remove heat from the core;

- The effect of debris settling on the grid straps to block flow and prevent heat transfer from the fuel cladding;

- The potential for particulate settling on the grid straps to block flow and prevent heat transfer from the fuel cladding.

It was noted that the US NRC would review licensee's in-vessel effects evaluations to ensure these issues were adequately addressed.

REFERENCES

5-1   United States Nuclear Regulatory Commission (2004) "Potential Impact of Debris Blockage on Emergency Recirculation during Design Basis Accidents at Pressurized-Water Reactors", NRC Generic Letter 2004-02.

5-2   NEA (2004) "Debris Impact on Emergency Coolant Recirculation", Nuclear Safety Workshop proceedings; 2004 February 25-27; Albuquerque, NM.

5-3   Rao, D.V.; Letellier, C.; Shaffer, C.; Ashbaugh, S.; Bartlein, L.S. (2002) "GSI-191 Technical Assessment: Parametric Evaluations for Pressurized Water Reactor Recirculation Sump Performance", USNRC Report NUREG/CR-6762 (LA-UR-01-4083), Vol.1, Washington (DC).

5-4   ACRS (2003) Official Transcript of Proceedings of the Advisory Committee on Reactor Safeguards Thermal Hydraulics Subcommittee, February, 2003.

5-5   Hart, G.H. (2004) "A Short History of the Sump Clogging Issue and Analysis of the Problem", Nuclear News, 24.

5-6   Johns, R.C.; Letellier, B.C.; Howe, K.J.; Ghosh, A.K. (2005) "Small-scale Experiments: Effects of Chemical Reactions on Debris-bed Head Loss; A Subtask of GSI-191", USNRC Report NUREG/CR-6868 (LA-UR-03-6415), 2005, Washington (DC).

5-7   Dallman J, Letellier B, Garcia J, Madrid J, Roesch W, Chen D, Howe K, Archuleta L, Sciacca F, Jain BP. (2006) "Integrated Chemical Effects Test Project: Consolidated Data Report", USNRC Report NUREG/CR–6914.

5-8   NEA (2000) "Insights into the Control of the Release of Iodine, Cesium, Strontium and Other Fission Products in the Containment by Severe Accident Management", NEA/CSNI/R(2000)9.

5-9   Lane A.E.; Andreychek T.S.; Byers W.A.; Jacko R.J.; Lahoda E.J.; Reid R.D. (2008) "Evaluation of Post-accident Chemical Effects in Containment Sump Fluids to Support GSI-191", Westinghouse Report WCAP-16530-NP-A. ADAMS Accession Number: ML081150379.

5-10   Bahn C.B.; Kasza K.E.; Shack W.J.; Natesan K. (2008) "Aluminum Solubility in Boron Containing Solutions as a Function of pH and Temperature", Argonne National Laboratory

Report. ADAMS Accession Number: ML091610696.

5-11   Torres, P.; Oras, J; Park, J. H.; Kasza, K.; Natesan, K.; Shack, W. J. (2006) "Chemical Effects/Head Loss Testing", slides for presentation during ACRS Thermal-Hydraulics Subcommittee Meeting, 2006 February 14-16.

5-12   Andreychek, T.S. (2005) "Test Plan: Characterization of Chemical and Corrosion Effects Potentially Occurring Inside a PWR Containment Following a LOCA", Revision 12.c. Westinghouse Electric Company, LLC.

5-13   Dallman, J.; Garcia, J.; Klasky, M.; Letellier, B.; Howe, K. (2005a) "Integrated Chemical Effects Test Project: Test #1 Data Report", Los Alamos National Laboratory, LA-UR-05-0124.

5-14   Dallman, J.; Letellier, B.; Garcia, J.; Klasky, M.; Roesch, W.; Madrid, J. (2005b) "Integrated Chemical Effects Test Project: Test #2 Data Report", Los Alamos National Laboratory, LA-UR-05-6146.

5-15   Dallman, J.; Letellier, B.; Garcia, J.; Madrid, J.; Roesch, W. (2005c) "Integrated Chemical Effects Test Project: Test #3 Data Report", Los Alamos National Laboratory, LA-UR-05-6996.

5-16   Dallman, J.; Letellier, B.; Garcia, J.; Madrid, J.; Roesch, W.; Chen, D.; Howe, K.; Archuleta, L.; Sciacca, F.; Jain, B.P. (2005d) "Integrated Chemical Effects Test Project: Test #4 Data Report", Los Alamos National Laboratory, LA-UR-05-8735.

5-17   Dallman, J.; Letellier, B.; Garcia, J.; Madrid, J.; Roesch, W.; Chen, D.; Howe, K.; Archuleta, L.; Sciacca, F.; Jain, B.P. (2005e) "Integrated Chemical Effects Test Project: Test #5 Data Report", Los Alamos National Laboratory, LA-UR-05-9177.

5-18   Chen, D.; Howe, K.J.; Dallman, J., Letellier, B.C.; Klasky, M.; Leavitt, J.; Jain, B. (2007) "Experimental Analysis of the Aqueous Chemical Environment Following a Loss-of-Coolant Accident", Nuclear Engineering and Design, **237**, 2126.

5-19   Chen, D.; Howe, K.J.; Dallman, J., Letellier (2008) "Corrosion of Aluminum in the Aqueous Chemical Environment of a Loss-of-Coolant Accident at a Nuclear Power Plant", Corrosion Science, **50**, 1046.

5-20   United States Nuclear Regulatory Commission (2006) "NRC Information Notice 2005-26, Supplement 1: Additional Results of the Chemical Effects Test in a Simulated PWR Sump Pool Environment", January 20, 2006.

5-21   ACRS (2006) Official Transcript of Proceedings of the Advisory Committee on Reactor Safeguards Thermal Hydraulics Subcommittee, Tuesday, February 14, 2006.

5-22   Westinghouse (2007) "Incorporation of Additional Plant Inputs in the Chemical Effects Spreadsheet PA-SEE-0354", presented at the USNRC GSI-191 meeting, 2007 April18, Washington DC.

5-23   Etteyeb, N.; Douibi, L.; Sanchez, M.; Alonso, C.; Andrade, C.; Triko, E. (2007) "Electrochemical Study of Corrosion Inhibition of Steel Reinforcement in Alkaline Solutions Containing Phosphate Based Components", J. Materials Science, **42**, 4721.

5-24   McMurry J.; Jain V.; He X.; Pickett V.D.; Pabalan R.; Pan Y.M. (2006) "GSI PWR Sump Screen Blockage Chemical Effects Tests: Thermodynamic Simulations", U.S. Nuclear Regulatory Commission Report No.: NUREG/CR-6912. ADAMS Accession Number: ML071900449.

5-25   Pourbaix, M. (1974) Aluminum. In Atlas of Electrochemical Equilibrium in Aqueous Solutions, NACE International (Houston, TX) Section 5.2.

5-26   ASM (1999) Corrosion of Aluminum and its Alloys, J.R. Davis, ed., ASM International, Materials Park, OH.

5-27   Griess, J.C.; Bacarella, A.L. (1969) "Design Considerations of Reactor Containment Spray Systems – Part III: The Corrosion of Materials in Spray Solutions", ORNL-TM-2412, Part III.

Oak Ridge, Tennessee, Oak Ridge National Laboratory.

5-28   Niyogi, K.K.; Lunt, R.R.; Mackenzie, J.S. (1982) "Corrosion of Aluminum and Zinc in Containment Following a LOCA and Potential for Precipitation of Corrosion Products in the Sump",   Proceedings of the Second Int. Conf. on the Impact of Hydrogen on Water Reactor Safety, Albuquerque, NM, 1982 October 3-7. NUREG/CP-0038, pp 410-423.

5-29   Piippo, J.; Laitinen, T.; Sirkai, P. (1997) "Corrosion Behavior of Zinc and Aluminum in Simulated Nuclear Accident Environments", STUK-YTO-TR 123. Helsinki, Finland: Finnish Centre for Radiation and Nuclear Safety.

5-30   Jain, V.; He, X.; Pan, Y.-M. (2005) "Corrosion Rate Measurements and Chemical Speciation of Corrosion Products Using Thermodynamic Modeling of Debris Components to Support GSI-191", NUREG/CR-6873.

5-31   Bell, M.J.; Bulkowski, J.E.; Picone, L.F. (1975) "Investigation of Chemical Additives for Reactor Containment Sprays", WCAP-7153A.

5-32   Soltész, V.; Vicena, I.; Chromčikova, M.; Liška, M.; Mattei, J.-M. (2008) "Chemical Durability of Glass Thermal Insulation Fibers in Borate and Phosphate Water Solutions", Advanced Materials Research, **39-40**, 363.

5-33   Devreux, F.; Barboux, Ph.; Filoche, M.; Sapoval, B. (2001) "A Simplified Model for Glass Dissolution in Water", J. Materials Science, **36**, 1331.

5-34   Chen, J.J.; Thomas, J.J.; Taylor, H.F.W.; Jennings, H.M. (2004) "Solubility and Structure of Calcium Silicate Hydrate", Cement and Concrete Research, **34**, 1499.

5-35   Park, J.H.; Kasza, K.; Fisher, B.; Oras, J.; Natesan, K.; Shack, W.J. (2006) "Chemical Effects Head-Loss Research in Support of Generic Safety Issue 191", NUREG/CR-6913.

5-36   Edwards, M.K.; Qiu, L.; Guzonas, D.A. (2010) "Emergency Core Cooling System Sump Chemical Effects on Strainer Head Loss", Nuclear Plant Chemistry Conference 2010 (NPC 2010), 2010 October 3-8, Quebec City, Canada, ISBN# 978-1-926773-00-1.

5-37   Ghosh, A.K.; Howe, K.J.; Maji, A. K.; Letellier, B.C.; Jones, R.C. (2007) "Head Loss Characteristics of a Fibrous Bed in a PWR Chemical Environment", Nucl. Technology, **157**, 196.

5-38   H. Kryk et al. "Influence of corrosion processes on the head loss across ECCS sump strainers", Kerntechnik 76/1, March 2011.

5-39   Jain, B.P.; Jain, V.; McMurry, J.; He, X.; Pan, Y.-M.; Pabalan, R; Pickkett, D.; Yang. L; Chiang, K. (2006) "Chemical Speciation Prediction: Technical Program and Results", slides for presentation during ACRS Thermal-Hydraulics Subcommittee Meeting, 2006 February 14-16.

5-40   Mattei, J.-M.; Vicena, I.; Soltesz, B.; Batalik, J.; Liska, M.; Galuskova, D. ; Klementova, A. "Experimental Program on Chemical Effects and Head Loss Modelling", IRSN Report DAI No. 2012/006.

5-41   Wesolowski, D. J.; Palmer, D.A. (1994) "Aluminum Speciation and Equilibria in Aqueous Solution: V. Gibbsite Solubility at 50 °C and pH 3-9 in 0.1 Molal NaCl Solutions (a General Model for Aluminum Speciation; Analytical Methods)", Geochimica et Cosmochimica Acta, **58**, 2947.

5-42   Van Straten, H.A.; De Bruyn, P.L. (1984) "Precipitation from Supersaturated Aluminate Solutions II Role of Temperature", J. Colloid Interface Sci., **102**, 260.

5-43   Vermeulen, A.C. (1975) "Hydrolysis-Precipitation Studies of Aluminum (III) Solutions 1. Titration of Acidified Aluminum Nitrate Solutions", J. Colloid and Interface Sci. **51**, 449.

5-44   Wesolowski, D.J. (1992) "Aluminum Speciation and Equilibria in Aqueous Solutions: I The Solubility of Gibbsite in the System Na-K-Cl-OH-Al(OH)$_4$ from 0 to 100C", Geochimica and Cosmochimica Acta **56**, 1065.

5-45   Benezeth, P.; Palmer, D.A.; Wesolowski, D.J. (2001) "Aqueous High Temperature Solubility Studies. II. The Solubility of Boehmite at 0.03 m Ionic Strength as a Function of Temperature and pH as Determined by In-situ Measurements", Geochimica et Cosmochimica Acta, **65**, 2097.

5-46   Apps, J.A.; Neil, J.M.; Jun, C.H. (1988) "Thermodynamic Properties of Gibbsite, Bayerite, Boehmite, Diaspore and the Aluminate Ion between 0 and 350 $^{\circ}$C", Lawrence Berkeley Laboratory Report, LBL-21482.

5-47   Van Straten, H.A.; Schoonen, M.A.A.; De Bruyn, P.L. (1985) "Precipitation from Supersaturated Aluminate Solutions II. Influence of Alkali Ions with Special Reference to Li^{+}", J. Colloid Interface Sci., **103**, 493.

5-48   Klasky, M.; Zhang, J.; Ding, M; Letellier, B. (2006) "Aluminum Chemistry in a Prototypical Post-Loss-of-Coolant-Accident, Pressurized-Water-Reactor Containment Environment", U.S. Nuclear Regulatory Commission Report No NUREG/CR-6915, LA-UR-05-4881. ADAMS Accession Number: ML070160448

5-49   Zhang, J.; Klasky, M.; Letellier, B.C. (2009) "The Aluminum Chemistry and Corrosion in Alkaline Solutions", J. Nucl. Mat., **384**, 175.

5-50   Szekeres, M.; Tombacz, E.; Ferencz, K.; Dekany, I. (1998) "Adsorption of Salicylate on Alumina Surfaces", Colloids and Surfaces A, **141,** 319.

5-51   Bahn C.B.; Kasza K.E.; Shack W.J.; Natesan K.; Klein, P. (2011) "Evaluation of Precipitates used in Strainer Head Loss Testing: Part III. Long-term Aluminum Hydroxide Precipitation Tests in Borated Water", Nuclear Engineering and Design, Vol. 241 p. 1914-1925.

5-52   Jaynes, W.F.; Morre, P.A. Jr.; Miller, D.M. (1999) "Solubility and Ion Activity Productivity of Calcium Phosphate Minerals", Journal of Environmental Quality, **28**, 530.

5-53   Dabrowska, D.S. (1989) "Change of Solubility of Calcium Phosphates in Aqueous Solutions in the Presence of Amberlite IRA-400. PART III $Ca_3(PO_4)_2$", Polish J. Chemistry, **63**, 51.

5-54   Chow, L.C. (2001) "Solubility of Calcium Phosphates", Monogr. Oral Sci. Basel, Karger, 2001, Vol. 18, pp 94-111.

5-55   Brown, W.E. (1973) "Solubilities of Phosphates and Other Sparing Soluble Compounds", in Environmental Phosphorous Handbook, Wiley.

5-56   McDowell, H.; Gregory, T.M. Brown, W.E. (1977) "Solubility of $Ca_5(PO_4)_3$ in the System $Ca(OH)_2$-H_3PO_4-H_2O at 5, 15, 25, and 37 $^{\circ}$C", J. Research of the National Bureau of Standards-A. Physical and Chemistry, **81A**, 273.

5-57   Gregory, T.M.; Moreno, E.C.; Patel, J.M.; Brown, W.E. (1974) "Solubility of β-$Ca_3(PO_4)_2$ in the System $Ca(OH)_2$-H_3PO_4-H_2O at 5, 15, 25, and 37°C", J. Research of the National Bureau of Standards-A. Physical and Chemistry, **78A**, 667.

5-58   Prakash, K.H.; Kumar, R.; Ooi, C.P.; Cheang, P.; Khor, K.A. (2006) "Apparent Solubility of Hydroxyapatite in Aqueous Medium and Its Influence on the Morphology of Nanocrystallites with Precipitation Temperature", Langmuir, **22**, 11002.

5-59   Kaufman, H.W.; Kleinberg, I. (1979) "Studies on the Incongruent Solubility of Hydroxyapatite", Calcified Tissue International, **27**, 143.

5-60   Zhang, H.; Li, S.; Yan, Y. (2001) "Dissolution Behavior of Hydroxyapatite Power in Hydrothermal Solution. Ceramics International", **27**, 451.

5-61   Wilkin, R.T.; Barnes, H.L. (1998) "Solubility and Stability of Zeolites in Aqueous Solution: I. Analcime, Na, and K-clinoptilolite", Amer. Mineral., **83**, 746.

5-62   Löwenstein, W. (1954) "The Distribution of Aluminum in the Tetrahedra of Silicates and Aluminates", Amer. Mineral. **39**, 92.

5-63 Mensah, J. A.; Li, J.; Rosencrance, S.; Wilmarth, W. (2004) "Solubility of Amorphous Sodium Aluminosilicate and Zeolite A Crystals in Caustic and Nitrate/Nitrite –Rich Caustic Aluminate Liquors", J. Chem. Eng. Data, 49, 1682.

5-64 Hamilton, J. P.; Brantley, S. L.; Pantano, C. G.; Criscenti, L. J.; Kubicki, J. D. (2001) "Dissolution of Nepheline, Jadeite, and Albite Glasses: Toward Better Models for Aluminosilicate Dissolution", Geochimica et Cosmochimica Acta, **65**, 3683.

5-65 Park, H.; Englezos, P. (2001) "Precipitation Conditions of Aluminosilicate Scales in the Recovery Cycle of Kraft Pulp Mills", Pulp & Paper Canada, **102**, 20.

5-66 Gasteiger, H. A.; Frederick, W. J.; Streisel, R. C. (1992) "Solubility of Aluminosilicates in Alkaline Solutions and a Thermodynamic Equilibrium Model", Ind. Eng. Chem. Res., **31**, 1183.

5-67 North, M.R.; Fleischer, A.; Swaddle, T.W. (2001) "Precipitation from Alkaline Aqueous Aluminosilicate Solution", Can. J. Chem. **79**, 75.

5-68 Ejaz, T.; Jones, A. G. (1999) "Solubility of Zeolite A and Its Amorphous Precursor under Synthesis Conditions", J. Chem. Eng. Data, **44**, 574.

5-69 Reichle, R.A.; McCurdy, K.G.; Hepler, L.G. (1975) "Zinc Hydroxide Solubility Product and Hydroxy-complex Stability Constants from 12.5-75 °C", Can. J. Chemistry, **53**, 3841.

5-70 United States Nuclear Regulatory Commission (2007) "Evaluation Guidance for the Review of GSI-191 - Plant-Specific Chemical Effect Evaluations", ADAMS Accession Number ML072600372.

5-71 Chung, Y.W.; Cho, J.S.; Kwon, B.I.; Ku, H.K.; Choi, Y.J.; Kim, H.T. (2011) "Development of Methodology for Evaluation of Chemical Effects on Sump Screen Performance Testing", 2011 Korea Nuclear Society Spring Meeting, May 26~27, 2011.

5-72 Park, J. W.; Park, B. G.; Kim, C. H. (2009) "Experimental Investigation of Material Chemical Effects on Emergency Core Cooling Pump Suction Filter Performance after Loss of Coolant Accident", Nuclear Engineering and Design, **239**, 3161.

5-73 JNES-SS-0703 JNES-SS "Report on the Assessment of the Impact and Chemical Deposition Morphology PWR Sump Screen Blockage", in Japanese.

5-74 JNES-SS-0804 "PWR Sump Screen Chemical Effect Test", English version available from US NRC website, Accession Number: ML082350151.

5-75 "Survey and Test Events PWR Sump Screen Blockage" (10原熱報-0006), in Japanese.

5-76 Arbeitsbericht NGPS4/2005/de/0113, Auswertung Experimenteller Untersuchungen zur Entwicklung des Differenzdruckes über die Sumpfsiebe im Nach-Störfallbetrieb unter Berücksichtigung von Korrosionseffekten, AREVA, 15.05.2006

5-77 RSK statement, "Loss-of-coolant Accidents Involving the Release of Insulation Material and Other Substances in Pressurized Water Reactors – Removal of Deposits on Sump Strainers", 406th RSK meeting, 13.03.2008

5-78 VENE-Bericht, Experimentelle Ermittlung von Differenzdrücken in SWR-Brennelementen unter Einfluss von Isolationsmaterial MD2 und Korrosion, VENE, 17.09.2010

5-79 GES-Bericht 08/11, "Experimentelle Untersuchungen zum Einfluss der Zinkkorrosion auf das Differenzdruckverhalten von Isolationsmaterial an Siebflächen und in einem SWR-BE-Dummy", GES, 08.10.2009

5-80 Torres, P.A. (2006) "Peer Review of GSI-191 Chemical Effects Research Program", NUREG-1861, 2006 December.

5-81   Tregoning R.T.; Apps, J.A.; Chen, W.; Delegard, C.H.; Litman, R.; MacDonald, D.D. (2009) "Phenomena Identification and Ranking Table Evaluation of Chemical Effects Associated with Generic Safety Issue 191", NUREG-1918, 2009 February.

5-82   US NRC, "Evaluation of Chemical Effects Phenomena Identification and Ranking Table Results", March 2011, http://pbadupws.nrc.gov/docs/ML1022/ML102280594.pdf.

6.   STRAINER PRESSURE DROP

This chapter discusses information related to estimating the head loss (pressure drop) across ECCS suction strainers caused by debris from a LOCA transported to and accumulated on such strainers. Although the knowledge base that can be used for such evaluations has grown since the release of NEA/CSNI/R(95)11, calculations are still limited by the scope of experiments and the large variabilities introduced by materials present in NPPs. For example, estimating head losses in mixed fibrous debris beds coupled with the filtration of particulates such as suppression pool "sludge," paint chips, precipitated corrosion products, and other LOCA-generated debris is highly plant- and materials-specific. As a result of these variables, plant specific head loss testing is the preferred method of qualifying ECCS suction strainers.

This chapter summarizes the present understanding of the underlying phenomena and their effect on the head loss, and focuses on identification of various factors that affect head loss across the strainer, and experimental databases and analytical methodologies available for strainer design and performance evaluation. Table 6-2 at the end of this chapter summarizes individual head loss test reports that establish strainer blockage models or correlation equations to estimate the head loss/pressure drop across a strainer due to debris build-up.

6.1   Factors Affecting Debris Bed Buildup and Head Loss

Debris comprising fibrous and non-fibrous insulation fragments and particulates (e.g., sludge, chemical corrosion products, failed coatings and dust particles) would be transported to the strainer by the ECCS and containment spray (where applicable) flows. The relative concentrations of various types of debris approaching the strainer are expected to vary with time and will be strongly influenced by the assumptions about the types and quantities of debris generated and the transport of these materials in the containment pool. Materials already present in the containment pool (such as "sludge" or latent debris) will also be transported. The subject of debris generation and transport was discussed in detail in Chapters 2 to 5.

The size and shape of the insulation debris reaching the strainer will depend on a variety of factors, including the type and make of the material (e.g., NUKON vs. mineral wool vs. Thermal-Wrap, calcium silicate, RMI); plant-aging effects such as the duration of exposure to high temperatures; the mode of transport (blowdown vs. washdown); and the containment pool hydrodynamics at the time of the materials' transport (e.g., pool chugging, break flow impingement). Qualitatively, the fibrous debris would vary in size from individual fibers, typically a few millimeters in length, to shreds or small pieces that retain some of the original structure of the insulation blankets, (See Figure 4-1). Because individual fibers and the finer shreds have generally lost their original blanket structure, the finer debris is more compressible than large pieces of debris. Based on this observation, it can be concluded that considerable attention should be paid to ensure that the size of debris used in determining the head loss is representative of the debris expected to reach the strainer following a LOCA. Ultimately, engineering judgment must be relied upon to arrive at the debris sizes to be used in the experiments, and should be based partially on the following considerations:

(a)   The debris-size is influenced strongly by the type of insulation, the mode of encapsulation, and the duration of its exposure to harsh environments (i.e., its age); and,

(b)   Debris disintegration would occur not only during its generation but also during its transport (e.g. thrashing due to pool turbulence and erosion).

Debris transport analysis requires the conservative specification of a size distribution for each type of debris. Finer debris is transported much more readily than coarser debris. The first step in specifying the debris size distribution is characterizing debris categories with respect to the transport properties of the various debris sizes.

Debris generation analysis assumes some damage to all insulation within the break-region ZOI such that all of the insulation within the ZOI is assumed to be debris. The damage could range from slight (e.g., insulation erosion occurring through a rip in the blanket cover), which leaves the blanket attached to its piping, to the total destruction of a blanket with its insulation reduced to small or very fine debris. Fibrous debris can also be categorized into one of four categories based on transport properties so that the transport of each type of debris can be analyzed independently. Table 6-1 shows these categories and their properties. The two smaller and two larger categories differ primarily with regard to whether the debris was likely to pass through a grating typical of those found in NPPs. Thus, fines and small pieces pass through gratings but large and intact pieces do not. The fines and small pieces are much more transportable than the large debris. The fines were then distinguished from the small pieces because the fines would tend to remain in suspension in a sump or suppression pool, even under relatively quiescent conditions, whereas the small pieces would tend to sink. Furthermore, the fines tended to transport more like an aerosol in the containment-air/steam flows and were slower to settle than the small pieces when airflow turbulence decreased.

Table 6-1: Debris-Size Categories and Their Capture and Retention Properties

Size	Description	Airborne Behavior	Waterborne Behavior	Debris-Capture Mechanisms	Requirements for Crediting Retention
Fines	Individual fibers or small groups of fibers.	Readily moves with airflows and slow to settle out of air, even after completion of blowdown.	Easily remains suspended in water, even relatively quiescent water.	Inertial impaction Diffusiophoresis Diffusion Gravitational settling Spray washout	Should be deposited onto surface that is not subsequently subjected to CSs or to spray drainage. Natural-circulation airflow likely will transport residual airborne debris into a sprayed region. Retention in quiescent pools without significant flow through the pool may be possible.
Small Pieces	Pieces of debris that easily pass through gratings.	Readily moves with depressurization airflows and tends to settle out when airflows slow.	Readily sinks in hot water, then transports along the floor when flow velocities and pool turbulence are sufficient. Subject to subsequent erosion by flow water and by turbulent pool agitation.	Inertial impaction Gravitational settling Spray washout	Should be deposited onto surface that is not subsequently subjected to high rates of CSs or to substantial drainage of spray water. Retention in quiescent pools (e.g., reactor cavity). Subject to subsequent erosion.
Large Pieces	Pieces of debris that do not easily pass through gratings.	Transports with dynamic depressurization flows but generally is stopped by gratings.	Readily sinks in hot water and can transport along the floor at faster flow velocities. Subject to subsequent erosion by flow water and by turbulent pool agitation.	Trapped by structures (e.g., gratings) Gravitational settling	Should be either firmly captured by structure or on a floor where spray drainage and/or pool flow velocities are not sufficient to move the object. Subject to subsequent erosion.
Intact	Damaged but relatively intact pillows.	Transports with dynamic depressurization flows, stopped by a grating, or may even remain attached to its piping.	Readily sinks in hot water and can transport along the floor at faster flow velocities. Assumed to remain encased in its cover, thus, it is not subject to significant subsequent erosion by water and by turbulent pool agitation.	Trapped by structures (e.g., gratings) Gravitational settling Not detached from piping	Should be either firmly captured by structure or on a floor where spray drainage and/or pool flow velocities are not sufficient to move the object. Intact debris subsequently would not erode because of its encasement.

Experiments have been performed on fibrous and RMI insulation to categorize debris generation. Continuum Dynamics, Inc (CDI) Test report 96-06 is an attachment to the BWROG URG [6-2]. This test report evaluated fibrous and RMI insulation air jet impact tests conducted at CEESI using typical BWR pressures and temperatures. In other tests of RMI such as the MIJIT by Swedish utilities and the US NRC, summarized in [6-3], RMI debris generated tended to be crumpled pieces rather than small pieces that would readily transport. The current regulatory position[17] in the US is that for plants with large surface area modern strainers and resultant low flow velocities, RMI debris will not transport to the strainer in sufficient quantities to impact head loss unless there are hydrodynamic forces such as chugging in BWRs to keep the metallic foils in suspension.

Particulate debris may also be generated by the LOCA jet stream as insulation, concrete and coatings are eroded, or may already be present in containment as latent debris. The particulates will vary in size from sub-micron (microporous insulation) to a few microns (e.g., rust particles) to 10 microns and larger (e.g., paint chips and calcium silicate), depending on the type of debris and its mode of generation. The material composition and size class of the debris should be carefully considered while designing experiments to estimate the head loss. The primary characteristic of concern for particulate debris is that it tends to stays in suspension and readily transports to the strainers.

Head loss across the strainer is dependent on the quantity and arrival sequence of the fibrous and particulate debris trapped on the strainer surface. A convenient measure for the quantity of fibrous debris trapped on the strainer is the debris bed thickness

Typically, head loss varies linearly with fiber bed thickness for beds that are uniform or nearly uniform in composition and surface area. Large deviations from this linear behavior have been seen when debris accumulates in a non-uniform manner on the strainer surface or when the particulate debris arrives at the strainer in sufficient quantity to effective plug the gaps between individual fibers. A thin fiber bed can be a very effective filter of particulate debris, creating larger than anticipated head losses.

The non-uniformity of the debris bed may also lead to lower filtration efficiencies for entrapment of debris passing through the strainer. As a result, the pressure drop for non-uniform beds could be lower than that predicted by extrapolating data obtained for uniform beds. This is an important issue that should be taken into account when evaluating specialized strainers designed to collect debris in a non-uniform manner (e.g., a pocket or star strainer).

Filtration efficiencies close to 100% are possible for particulates such as paint chips and concrete dust, but efficiencies on the order of 25 to 50 percent have been reported for filtration of sludge particles ranging in size from 1-10 microns [6-1]. In view of this finding, the quantity of particulate debris filtered by the fiber bed and the resulting head loss across the strainer (which is an increasing function of the amount of debris trapped on the strainer) are strong functions of the size distribution of the particulate debris reaching the strainer. Consequently, it is not appropriate to extrapolate head loss obtained for one mixture of particulate debris to another without carefully considering their relative size distributions and effects of the shape of the particulate; walnut shell, calcium silicate and iron oxide tend to result in higher head losses than similar sized particles of silicon carbide. This also brings into focus the important role played by filtration efficiency in determining the head loss.

The aforementioned filtration of the particulate debris by fibrous beds leads to the formation of mixed beds in which the fibers are intermixed with particulates. SEM images of a clean and a mixed bed are presented as Figure 6-1. As evident from these images, the mixed beds tend to be more compact, and, as a result, they have been known to induce higher head losses across the strainer. This differential pressure serves to further compact the bed, resulting in actual bed thickness being lower

---

[17] See Section 2.1 of Ref 6.32

than the theoretical thickness. In some cases, compaction ratios[18] as high as four times that of the original bed have been reported for purely fibrous beds at high approach velocities.
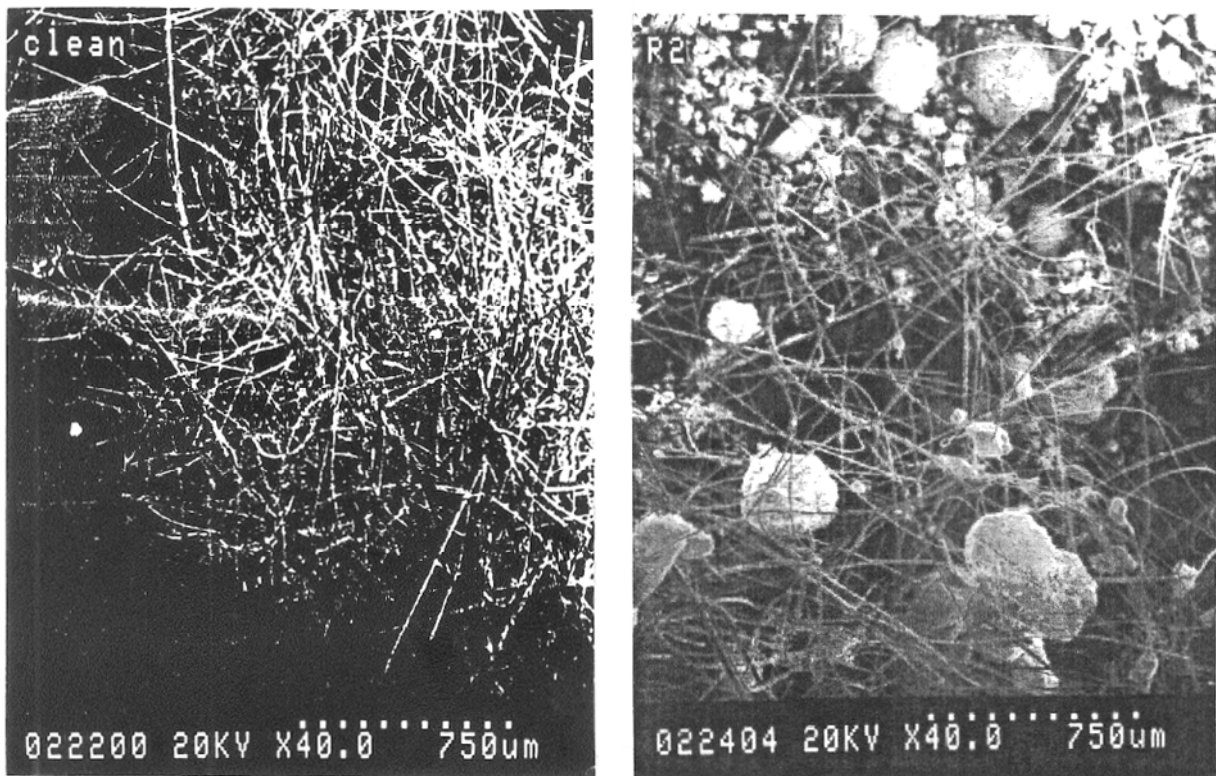
Figure 6-1: Scanning Electron Micrographs of Pure and Mixed Fiber Beds.

Insights from numerous head loss tests show that bed compaction is influenced by such factors as the size class of the debris and the makeup of the debris bed. For example, beds formed of individual fibers and finer shreds are more compressible than those formed of larger pieces. Similarly, beds loaded with particulate debris are much more compact and less porous than pure fiber beds. The compressed beds are typically associated with lower porosity, which in turn leads to higher pressure drops and also to higher filtration efficiencies.

The experiments also established that for a fixed amount of particulate debris, pressure differentials across the bed are significantly higher for smaller, rather than larger, quantities of fibrous material. This effect, which is often referred to as the thin-bed effect, has been studied extensively. Closer examination of the bed morphology reveals that thin beds closely resemble granular beds (rather than fibrous beds) and that higher head loss is a direct result of bed morphology.

Note that head losses for thick beds only exceed those of thin beds when there are large volumes of fiber. Even if a plant has large quantities of fiber that could lead to potentially thick mixed beds of debris, the initial bed formation would often begin with a thin layer of fibers that could cause a thin bed head loss relatively early into the accident (depending on the break location and break specific debris generation and transport).

The debris accumulation and debris bed compression continue until a steady state condition is created, the containment pool water is cleared of debris by filtration or settlement, or the ECCS pumps have failed because of the loss of NPSH margin.

---

[18] Defined as the ratio of the theoretical thickness to the actual thickness.

The head loss incurred during the debris bed buildup and the time at which such head loss exceeds the available NPSH margin are important factors in design considerations and in planning for mitigative actions. The rate of head loss increase and the magnitude thereof will be influenced by the following factors:

- The amounts of various types of debris reaching the strainer and their rates of transport at any given time;

- Size distribution of the debris reaching the strainer;

- The filtration efficiency of the fibrous bed for particulates;

- ECCS flow rate (i.e., approach velocity) and containment pool temperature;

- Plant-specific considerations such as geometrical design and strainer arrangement;

- Plant-specific chemical corrosion/dissolution products and their subsequent transport to strainers; and

- Strainer design (conical, star, top hat, or stacked disc).

The detail to which such phenomena can be physically modeled or simulated can significantly affect the quality of the head loss testing.

6.2   Design Approaches

Current ECCS strainer design approaches generally rely on large-area passive strainers (i.e., strainers having a large filtration area without the need for additional mechanical features); passive strainers supplemented with a backflush capability; and passive strainers that include mechanical design features (i.e., debris scraper blades) designed to clear off the debris layer as it is formed— these are called "active" strainers in the United States. The uses of strainer types vary widely by country. Totally passive systems are designed to provide large surface areas for debris deposition, which in turn would result in thinner debris beds. The Swedish Radiation Safety Authority (SSM) "robust" design concept is based on a very large strainer surface area, which in turn reduces approach velocities, and is further augmented with backflush and/or self cleaning capability. Several other OECD member countries promote strainer designs with backflush capabilities.

Where backflush capability is provided, it should be able to prevent the accumulation and entry into the ECCS of debris that may block restrictions found in systems served by the ECCS pumps. The operation of the active component or backflush system should not adversely affect the operation of other ECCS components or systems. Under some operational modes, an active system may allow more debris to pass through the strainer. If this is the case, then the downstream effects analysis should be performed accordingly. Performance characteristics of an active system should be supported by appropriate test data that address head loss performance. Active systems should meet the requirements for defense-in-depth and redundancy for active components. Appropriate instrumentation must be provided to be able to accurately initiate the backflushing procedures.

In the U.S., strainer design concepts using complex, non-linear surfaces (e.g., pockets, top hats, or stacked disk designs) to maximize available surface area within a selected spatial envelope to enhance strainer capacity are being used to replace the original strainers installed when the plants were constructed 30 to 40 years ago. Some of these designs intentionally introduce non-uniform flow distribution across the strainer flow area with the intent of directing the debris to selected locations on the strainer surface.

The lack of directly applicable experimental data (prior to 2005) and verified analysis methods (or models) for large passive strainers has led U.S. strainer vendors, NPP licensees, the PWROG and the BWROG to conduct independent design qualification programs. Independent plant-specific evaluation of these strainers requires scaled physical model testing to determine the maximum head loss for a given combination of fibrous and non-fibrous debris added to the containment pool. Such

tests are highly dependent on the testing approach employed and the strainer scale or size. Any independent evaluation of these tests should carefully consider the following factors:

- Maximum head loss may not necessarily correspond to the break that transports the largest volume of fibrous debris to the containment pool. Instead, the most severe case may correspond to a thin-bed effect of a layer of fibers trapping a large quantity of particulate debris;

- The head loss is a strong function of debris size classes and transportability. As a result, considerable attention must be paid to ensure that size classes of debris used in vendor testing are an acceptable representation of the debris expected to reach the strainer following a LOCA;

- In some cases, it may not be appropriate to extrapolate strainer performance to operating parameters beyond the original range of testing;

- Sufficient time should be available for operator response, if needed, in cases where the designs incorporate active systems. Also, operability of active systems under harsh containment pool conditions should be evaluated, including the associated instrumentation.

6.3 Head Loss Test Considerations

Table 6.2[19] provides a compilation of the testing and data, results, and pressure drop relationships, where developed, by those organizations submitting them for review to include in this report. Summaries of those investigations are presented in Appendix D. The insulating materials used or simulated in the experiments consisted of:

- Mineral wool (rockwool)
- ISaVER type mineral wool (Germany)
- Low-density fiberglass (NUKON,Transco-Thermal-wrap)
- High-density fiberglass
- Caposil (Unibestos) (calcium silicate containing asbestos[2] fibers)
- Calcium silicate (diatomaceous earth, "Newtherm")
- Insulation particulates (e.g., calcium silicate and alumina)
- Reflective metallic insulation with stainless steel foils.
- Reflective metallic insulation with aluminum foils

Other debris materials included in some tests were:

- Paint chips and particulates
- Rust (iron oxide corrosion products)
- Metallic particulates (e.g., zinc dust from galvanized steel)
- Chemical reaction products (e.g., aluminum-based precipitates)
- Latent debris-dirt/dust
- Suppression pool sludge

6.3.1 Debris Preparation

Various techniques have been used to generate insulation debris of representative size classes. For fibrous insulation, these include manual (hand) shredding, mechanical shredding (meat mincer,

---

[19] For ease of reading, Table 6.2 has been placed at the end of this chapter.

leaf shredder, food processors) and jet fragmentation (steam jets, water jets, and air jets). In the US, the NEI has developed a procedure for preparation of fibrous debris [6-36]. The actual size class of the fibrous debris varied from as-fabricated blankets (without covers or scrims) to finely destroyed debris consisting of a significant quantity of individual fibers. Production techniques such as manual shearing and jet fragmentation were used for generation of non-fibrous RMI insulation fragments used in the experiments. Debris should be shredded finely enough to be prototypical of what would be expected in the post-LOCA containment pool. In general, the finer the fibrous debris is prepared, the higher the pressure drop will be. The use of excessively coarse fibrous debris in testing will likely result in non-conservative results. Head loss testing should be conducted with the most problematic mixture of debris that could realistically occur at the plant. The use of particulate debris that is too large or that may not transport prototypically is another factor that influences the test protocol and must be considered.

For several reasons, it may be impractical to obtain test debris that exactly replicates the debris expected to be formed in the plant following a LOCA. The material may no longer be commercially available, or it may be too hazardous to handle from a practical standpoint. Therefore, surrogate materials are often used to simulate the postulated plant debris. Assurance is needed that debris created using surrogate materials is prototypical of the postulated plant debris. The similitude considerations for the surrogate debris include selection of surrogate materials, preparation of the surrogate debris, and prevention of non-prototypical agglomeration of the prepared debris before and during the debris introduction process. For chemical effects precipitates, in addition to preparation of the precipitates, the potential for chemical interactions with other surrogate debris, such as coatings, should be considered. Chemical stability of the surrogate solution is also a consideration. Some chemical surrogates used in testing may produce unexpected results if the surrogate material is not used in a reasonable time frame after it is prepared. Head loss testing should be conducted such that the surrogate precipitate is introduced in a way to ensure transportation of all the material in a realistic way (see Chapter 5). This requirement means that integral experiments may often give the best results.

For test strainer head losses to be considered representative the plant strainer and the debris used in the test should conservatively represent the postulated plant debris. Debris generation and transport analyses are used to estimate both the quantities and the characteristics of debris expected to arrive at the strainers. For each type of debris, a number of characteristics govern the behavior of that debris with regard to transport, accumulation, and head loss, and significant uncertainty is typically associated with estimating these characteristics (e.g. size distributions). Debris substitutions in testing add to the uncertainty in the head loss results. The important characteristics include debris settling tendencies, filtration, and head loss parameters.

To determine the similitude of surrogate debris, the first step is to characterize the postulated debris as LOCA-generated, post-LOCA-generated, and latent debris. Second, the proposed surrogate debris should be characterized and compared to the expected plant debris. This comparison should be performed for each characteristic parameter that significantly affects strainer head loss to ensure either realism or conservatism. The characteristics include those parameters that govern debris transport, accumulation, and head loss. For example, fibers introduced into the test to represent latent fibers should not only be of characteristic diameters but should effectively be transported as individual fibers.

Surrogates are frequently used to represent coatings debris. In chip form, the transport of coating debris depends on chip size, thickness, density, and shape. A conservative approach is to generate the debris in the form of particulates if chips are proved not transportable. If chips are transportable and may be generated during the event, separate or repeat testing may be needed to ensure that conservative head loss is measured. RMI debris should be manufactured from insulation samples if the manufacturing of replicated debris is not feasible.

Surrogate debris preparation should first render the material into debris sizes that reasonably

represent the size distribution determined by the debris generation and transport analyses. Once the debris has been generated, debris is typically pre-wetted to remove trapped air. The debris is usually added to a relatively large volume of water and mixed well to reduce subsequent agglomeration before introducing the debris into the test tank. For some head loss testing, fibrous debris is preheated to effectively age new insulation material so that it resembles insulation that has been installed at a plant for an extended period of time. This step is necessary only if the aging process significantly alters the head loss characteristics of the insulation material. Boiling or mixing the prepared fibrous debris in hot water can shorten the time required for entrained air to escape. The specification for surrogate fibrous debris should consider filtration characteristics such as bed porosity and compressibility. The debris should be prototypical in the transport characteristics such as floor tumbling velocities and settling velocities. The specification of surrogate particulate and fibrous debris should consider head loss characteristics such as specific surface areas, porosity, compressibility, and fiber diameter. The debris surrogate should also consider the settling characteristics of the various sizes of debris. Specific surface area has typically been related to particle size distribution. The specific surface area for a perfect sphere is 6 divided by the diameter and many particulates can be approximated as spheres of varied diameters; however some particulates can be distinctly non-spherical. Settlement behavior of potential surrogate precipitates for chemical effects tests should be considered during material selection and preparation process.

In summary, the debris materials used in head loss testing should be either the actual plant materials or suitable surrogate substitutions. Substitutions should be justified by comparing the important characteristics of the plant debris sources and the surrogate to ensure that the debris preparation creates prototypical or conservative debris characteristics.

6.3.2   Suppression Pool Sludge

Corrosion products, along with dirt, dust, and other residues commonly found in BWR suppression pools are referred to as BWR sludge. Significant quantities of sludge can be present in the suppression pools, depending on materials of construction (carbon steel vs. stainless steel), and primary circuit water chemistry.

The head loss effects of sludge were found to depend on the size distribution of the sludge. The U.S. NRC and BWROG established a consensus position on the sludge size distribution for use in experiments, based on surveys of 14 U.S. BWR suppression pools conducted between 1994 and 1996 ([6-2] Vol 4) (Table 4.23). The surveys also concluded that the sludge was nearly 100% iron oxide and is generated at an average of 68 kg (150 lbm) per year. However, the amount of sludge present in a pool is also controlled by frequency and thoroughness of pool cleaning and the rate at which new corrosion products are generated. BWRs in other OECD member countries could have more or less suppression pool sludge, depending on materials of construction, and water chemistry control practices.

6.3.3   Latent Debris

Latent debris (general area dirt and dust) can be a significant contributor to strainer head loss for some plants. NEI topical reports NEI 02-01 Revision 1 [6-4] and NEI 04-07 [6-5] describe one method to determine the quantity and size distribution of latent debris that has been accepted by the US NRC.

In some plant designs that are very compartmentalized, or do not use containment spray systems after a DBA, latent debris may not transport readily to the suction strainers. For those plants, latent debris would be less of a debris concern than those plants designs where debris transports without many geometrical restrictions.

Similar methods have been used in other countries. As noted previously in Section 1.4, in Canadian CANDU plants, the quantity of floor debris to be used for the strainer performance evaluation was estimated based on plant walk-downs and a review of FME programs. Floor swipes were used to estimate the quantity of rust, dust or dirt particulate per unit area; this was then multiplied over the entire area of interest to give an overall estimate. Some conservatism was applied to account for uncertainties. First, the amount of rust, dust and dirt in the entire area of interest was calculated based on the upper range of measured debris per unit area (as determined by the floor swipes), rather than on the mean value. Second, all this debris was assumed to be transported to the strainer; no credit was allowed for any debris that might fall out of suspension along the way or get caught in stagnant areas.

6.3.4   Coating Debris

Protective coatings have been evaluated in two widely varying methods for their impact on suction strainer pressure drop. For US BWRs, paint chip debris varied from 3 mm (0.125 in) to 6.3 mm (0.25 in.) in size and from 0.02 g to 0.16 g in weight. The size of the paint chips used in the experiments was based on engineering analyses provided by the BWROG for BWR containment coatings. Using generic material properties, film thickness, and size of jet, 38.6 kg (85 lbm) of chips was determined to be a generic value for coating debris that was used to qualify the strainers.

PWR strainer evaluations used much smaller paint debris sizes, as was specified by the US NRC [6-5]. Both coatings qualified to withstand DBA environments and those coatings that were not qualified are including the debris mixture, depending on the location relative to the jet ZOI.

For coatings qualified to ANSI N101.2, ASTM D3911 or equivalent, the only coating debris generated is from the jet impingement from the broken pipe. The coatings within this jet zone of influence are postulated to be destroyed down to their base constituent size of 10 μm. All other qualified coatings remain intact. Those coatings in containment not tested or qualified to be resistant to DBA environmental conditions are considered unqualified. All unqualified coatings are postulated to fail as 10 μm particulate debris and readily transport to the strainer. The quantity of paint debris for PWRs is plant specific and depends on the size of the jet zone of influence, plant specific coating materials and plant specific coating thicknesses.

6.4   Strainer Qualification Tests

The strainer qualification tests conducted can be broadly categorized as (1) separate effects experiments, (2) small-scale strainer qualification tests, and 3) plant-specific scaled tests. The focus of the separate effects tests was to develop relationships that correlate strainer head loss to flow velocity and the amount of debris on the strainer. The intent of the investigators was to use these relationships, together with engineering judgment and assumptions regarding debris generation and transport, to provide the basis for design and sizing of the strainers. Typically, these tests employed a flat plate strainer and a closed test loop to conduct experiments. Note that the results from tests

performed in a once-through column and in closed-loop and open-loop recirculating facilities can produce significantly different results if these experiments are not carefully designed to separate such effects. Tests conducted with flat plate strainers may not produce results that can be applied to strainers with complex flow surfaces.

Typical data reported by the closed-loop experiments included head loss as a function of strainer-approach velocity and the quantity and type of debris added to the test loop. Some of the European experimental data were reported in the form of coverage (kg/m^2) of insulation material required to produce a head loss of 2 m of water across the strainer as a function of velocity. Table 6-1 presents the range of parameters studied in each experiment. Some of the head loss data were reported for theoretical bed thicknesses in the range of 3 mm to about 25 cm; approach velocities in the range of 1 cm/s to 0.5 m/s; at temperatures of 20-25 °C and 50-55 °C; and for nominal sludge-to-fiber mass ratios in the range of 0 to 60. For cases involving sludge, most experimenters did not attempt to estimate the quantity of sludge trapped on the filter at the time steady-state head loss was achieved. Instead, head loss was provided as a function of the quantity of sludge added to the loop. Only one investigation provided concentration estimates that can be used to estimate filtration efficiency and subsequently the quantity of debris trapped on the strainer when the head loss was measured.

The actual data reported by various investigators are provided in a standardized plot format in Appendix A of. NEA/CSNI/R(95)11 "Knowledge Base for Emergency Core Cooling System Recirculation Reliability" As evident from these figures, considerable scatter exists in head loss data from different sources. Careful examination of the experimental data available prior to 1996 suggests that the scatter can be attributed to the following factors:

- Variation in size classes of debris used in the experiments to simulate LOCA-generated debris. Typically, debris produced by manual methods is larger in size, that is, classes 6 and 7, and resulted in lower pressure drops. On the other hand, debris produced by mechanical methods and jet fragmentation was much smaller in size and resulted in higher pressure drops. Further discussions related to the effect of size class on the head loss across the strainer were presented in previous sections;

- Variation in the age of the fibrous insulation debris;

- Differences in experimental test loops;

- Differences in the range of experimental parameters. For example, European experiments were conducted at very low velocities, 1-10 cm/s, while the U.S. experiments were conducted at much higher velocities, 5-50 cm/s;

- The chosen method of correlating the data. In most cases, purely empirical relationships were sought to correlate the head loss data that were obtained for a limited range of experimental parameters. This seriously limited extendibility of these individual correlations beyond their original range of study.

For pure fiber beds, many of these early studies developed empirical relationships to relate velocity and bed theoretical thickness to strainer pressure drop. The relationships were usually of the following form:

$$\Delta H = a V^b e^c \hspace{3cm} \text{Equation 6.1}$$

where,

ΔH is the strainer head loss (ft)

V is the strainer approach velocity (ft/s)

e is debris bed theoretical thickness[20] (ft)

a, b, and c are empirical constants determined in experiments

Similar relationships were used to correlate experimental data obtained for mixed beds. These relationships[21], together with engineering judgment and assumptions regarding the debris generation and transport, provide the basis for design and sizing of the strainers. The various correlations developed for debris beds formed of pure mineral wool beds, pure low-density fiberglass beds (NUKON and Transco-Thermal-Wrap), and mixed beds formed of NUKON and sludge mixtures are listed in Table 6-3. The predictions of the correlations for low-density fiberglass are illustrated in Figure 6-2 and clearly illustrate the variabilities and uncertainties associated with this simplified correlation that is applicable only to the low-density fiberglass tested. Other insulation materials will exhibit different head loss characteristics.

6.4.1 U.S. NRC (NUREG/CR-6224 Correlation) Characterization of Insulation Debris Head Loss Data

In the 1994/1995 time frame the U.S. NRC sought a semi-theoretical approach for BWR suction strainer design and developed what has become known as the NUREG 6224 correlation. Appendix B of NUREG/CR-6224 [6-6] provides the theoretical basis and limitations for the correlation given below as Equation 6.2.

$$\frac{\Delta P}{t} = 3.5 S_v^2 (1-\varepsilon)^{1.3} [1 + 37(1-\varepsilon)^3] \mu V + \frac{0.66 S_v (1-\varepsilon)}{\varepsilon} \rho V^2 \qquad \text{Equation 6.2}$$

where,

ΔP is the pressure drop that is due to flow across the bed (dynes/cm^2)

t is the height or thickness of the fibrous bed (cm)

μ is the fluid dynamic viscosity (poise)

ρ is the fluid density (g/cc)

V is the fluid velocity (cm/s)

ε is bed porosity

S_v is the specific surface area (cm/cm^3)

6.4.2 Specific Limitations on the NUREG/CR-6224 Correlation

There are basic limitations with the use of any analytical correlation. Specifically, the head loss predictions are only as good as the correlation input parameters and at least two of the input parameters can only be determined by using an applicable head loss correlation to deduce the parameter from applicable head loss data. These two parameters are the debris bed porosity and the debris bed specific surface area. Since these parameters must be deduced using an appropriate head loss correlation, the deduced parameters should then be used in conjunction with that correlation. To make matters more complicated, a typical strainer blockage calculation will have multiple types of debris such as fibrous insulation, latent fibers, coatings particulates, calcium silicate, chemical effects, dirt, etc., and the experimental head losses will include synergistic effects among the debris types that are difficult to simulate analytically. Therefore, analytical correlations are most useful for scoping purposes such as the initial sizing of a new strainer design or the extrapolation of head loss test data from the test conditions to alternate conditions, such as a slightly smaller or larger strainer area. The

---

[20] Some investigators used mass spread (kg/m^1) instead of theoretical thickness in their correlations' development

[21] In most cases, these relationships are based on testing conducted by insulation manufacturers and laboratories representing the utility industry. Vendor tests are usually considered as applicable only to the vendor's product, since the tests were performed only on the vendor's product.

further the extrapolation beyond the original dataset used to develop the correlation, the greater the uncertainty in the result.

It should also be pointed out that any correlation has inherent assumptions built into its development. For example, the 6224 correlation assume that particulates cannot be deformed under the pressures encountered in a strainer debris bed. Particulates such as dirt or iron oxide corrosion products look like little rocks under a microscope and when compressed in a solid layer, particulate will not compress further once the particles make complete contact, such as a thin layer of dirt particles. Some materials, such as calcium silicate, derived from limestone and diatomaceous earth (fossilized plankton), have a fine crystalline structure that can undergo shape changes under pressure affecting head loss correlation predictions involving significant quantities of calcium silicate, i.e., the bed porosity and specific surface area could have a pressure dependency.

The correlation may not be applicable for non-uniform debris beds since the correlation was developed based on the assumption that the debris forms a uniform bed. This may limit equation applicability to very thin beds or thin beds formed on specialized strainers.

The correlation assumes that the debris bed is homogeneous. Its use for mixed beds can lead to significant underprediction of debris bed head loss.

The sequence of debris accumulation (fiber versus particulates) on the strainer will affect the correlation.

The correlation's model for debris bed compression under differential pressure loading is inaccurate and can contribute to the underprediction of debris bed head loss.

The development and validation of the correlation considered limited types of fibrous debris and iron oxide particulate only.

Chemical effects precipitates were not included as debris types.

Debris preparation methods used in the head loss testing have been found to greatly affect results. In general, debris used for the NUREG/CR-6224 studies was courser than debris used in PWR tests in the 2007 and later time frame.

The correlation cannot accurately predict head losses for debris beds that include calcium silicate pipe insulation debris and other microporous debris

The correlation may not be applicable to thin fiber beds coupled with high particulate-to-fiber mass ratios since non-uniform debris bed thicknesses, including open spaces, were observed in the ARL experiments. The thin-bed effect was not considered to the same rigor in developing the correlation as was done later for GSI-191. Because the development and validation database for the NUREG/CR-6224 correlation did not adequately treat this condition, the correlation can lead to the underprediction of thin bed head losses.

The NUREG/CR-6224 correlation may be useful for scoping calculations and preliminary design work in conjunction with engineering judgment to account for its limitations. However, the US NRC staff expects physical prototypical head loss testing to verify acceptable performance for suction strainers for both PWRs and BWRs.

Although this correlation may provide a reasonable approximation for the head loss, these limitations and other factors presented in NUREG/CR-6224 should be reviewed before using this correlation without confirming results with head loss testing.

As a result of these limitations on the use of the correlation, details on its use are not included in

this Chapter. The reader is referred to the initial publication of this document [1-1] and reference 6-2, 6-6, and 6-11 if more information on the use of the correlation is needed.

6.4.3   *General Observations and Insights from Tests*

In examining the data from the tests and experiments (Table 6-2), the following observations can be made:

- The most striking observation is that the pressure drop across a bed consisting of fibrous and particulate debris is significantly greater than that produced by fibrous material alone. This trend is illustrated in Figure 6.3 below using experimental data obtained from the U.S. NRC experiments summarized in NUREG/CR-6367 [6-1].
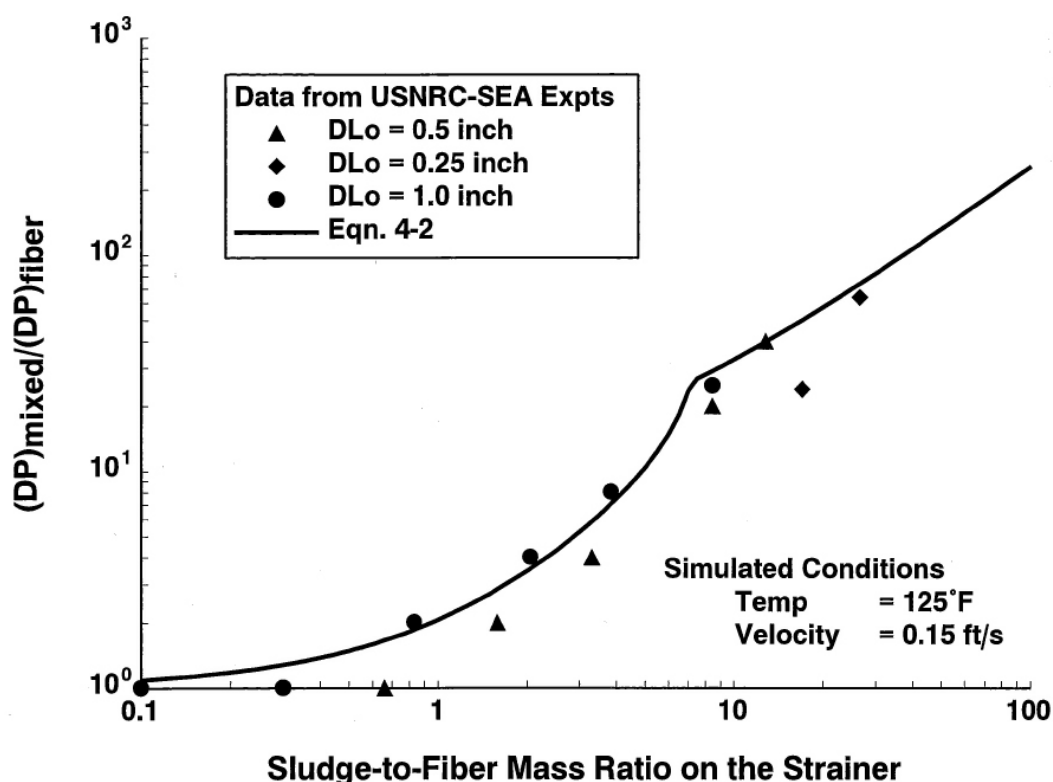
Figure 6-3: Effect of Filtration of Sludge Particles by Fiber Beds on the Head Loss

As evident from this figure, the ratio of pressure drops (i.e., ratio of pressure drop for fiber + nonfiber beds-to-pressure drop for fiber beds formed of the same volume of fibers) increases rapidly as the particulate-to-fiber mass ratio on the fiber bed increases. In some cases this increase is two orders of magnitude while the mass of nonfibrous debris added is only ten times that of the fibrous debris. This illustrates the important role played by particulate debris in determining the head loss.

The particulate debris size distribution significantly influences the head loss across the strainers. Experiments have revealed that larger particles are more likely to be filtered by the fibrous beds whereas smaller particles (such as sludge) are more likely to penetrate the bed. As a result, it is not appropriate to extrapolate the head loss measurements obtained for one size distribution to the other without accounting for these differences in filtration efficiency.

Some data (Vattenfall and BWROG) have shown that for a given amount of particulate material, larger pressure drops may occur for smaller, rather than larger, quantities of fibrous material[22]. This

---

[22] This trend should not be generalized for all types of particulates. For finer particulate debris, much more

trend is illustrated in Figure 6.4, which plots head loss vs. debris-bed thickness for three different quantities of particulate debris added to the suppression pool. As shown in this figure, for a given quantity of nonfibrous debris added to the suppression pool, the maximum head loss occurs for thinner beds where particulate-to-fiber mass ratios are largest. This maximum head loss increases as greater quantities of sludge are added, but always occurs for thinner beds. This somewhat counterintuitive trend displayed in Figure 6.4 can be explained as follows. Very thin beds tend to be highly non-uniform and will filter out only a small fraction of the particulate debris. For such beds, no noticeable increase in pressure drop would be expected. As the beds become thicker, the filtration efficiency increases and, consequently, a larger fraction of the particulate debris is filtered. A critical point is reached when the bed is still relatively thin but consists of a large mass fraction of nonfibrous debris. These beds are very compact and resemble granular beds rather than fibrous beds. As more fibers are added, the bed starts to behave more and more as a fiber-only bed. Finally, a state is reached where the bed behaves essentially as a fiber bed as the mass fraction of particulates becomes negligibly small compared to that of the fibrous debris.

Filtration is an important phenomenon that plays a key role in determining the head loss. Predictions of analytical tools developed without considering filtration may be associated with large uncertainties.

Fibrous and RMI debris have the capability themselves to increase pressure drop across a strainer. Granular insulation materials such as calcium silicate can act as particulates on or within a bed, further increasing the pressure drop across a bed.
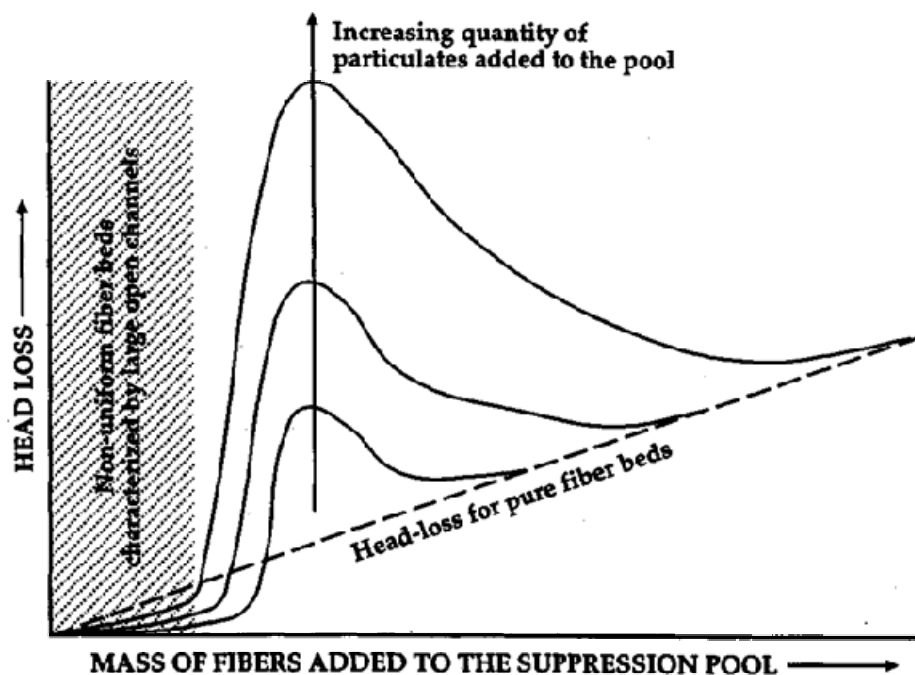
Figure 6-4: Schematic Representation of Head Loss Observed for Mixed Debris Added to a Once-Through Loop.

The flow regimes encountered at the BWR strainers range from laminar to transitional[23]. Darcy's law holds for some of the data where the approach velocity is low (<0.1m/s). On the other hand, Stokes' law *($\Delta P \propto V^2$)* holds for turbulent flows. A combination of these two extremes can be used

---

moderate head loss increase was observed.

[23] Typically, almost all European BWRs operate in the laminar region (1-10 cm/s), whereas most U.S. BWRs operate in the transitional region (20-50 cm/s). (Before strainers were enlarged in the 1996 time frame)

for describing head loss corresponding to transitional flows.

No significant variation was observed for similar materials (e.g., fiberglass) fabricated by different vendors. A single test debris preparation procedure such as shredding in a meat mincer or leaf shredder produces shorter fibers that result in a more dense bed with higher pressure drop characteristics than a bed with "as-fabricated" material.

The effect of baking the material to remove organic binder materials, simulating service on hot piping (thermal aging), has mixed reports from researchers. However, most data support the need to remove the binder to provide insulation with realistic characteristics.

When a debris-laden strainer is in service for an extended period (days), there is a noticeable increase in head loss. The magnitude of the increase is dependent on the initial size of the bed. Results reported by the different vendors vary.

A decrease in head loss as temperature increases is due to viscosity and density effects.

An increase in sump water pH is expected to result in an increase in head loss owing to devitrification and subsequent compaction of fiberglass in an alkaline environment for extended time periods [6-35]. This was reported in a vendor test [6-19], with an increase in head loss up to 45 percent attributable to pH effects. In testing performed by another vendor [6-23], the effect of pH was not considered to be significant in light of other effects involving longer term operation.

Fragments of metallic insulation generate turbulent head losses down to an approach velocity of 0.01 m/s (0.033 ft/s). The magnitude of the head loss is a strong function of foil piece size and shape. Generally, the larger the pieces the higher the head loss, and the more crumpled the pieces the smaller the head loss. In the US BWRs, flow velocities with the replacement strainers installed range between about 0.03 m/s (0.1 ft/s) and 0.0003 m/s (0.001 ft/s), with a typical value being less than 0.003 m/s (0.01 ft/s) [6-37]. At these lower velocities, RMI debris does not transport once chugging ceases.

Reference [6-26] provides data for one particular metallic insulation internal foil type that can be used for bounding purposes. However the variability of different vendor products (e.g., dimpled foils, waffle patterns, or smooth patterns) suggests caution and review of product lines before extrapolating results. In addition, [6-26] results show that mixtures of foil pieces and fibrous debris can result in significantly higher head losses than would be derived from summing the individual contributions.

6.4.4   PWR Strainer Testing

Typical large passive PWR replacement strainer approach velocities are so low (< 0.003 m/s) that the approaching debris consists primarily of suspended fibers and particles that are not significantly affected by gravity. Further, the velocities are typically so low that the debris can accumulate relatively uniformly even when the first accumulations preferentially occur nearer the pump connection to the strainer. As a result, thin-bed formation is not only possible on these complex strainers but could be the most likely and problematic type of bed formation in PWRs, with the potential to cause severe head losses.

The key requirement when simulating debris accumulation is to ensure that the suspended matter is prototypically or conservatively represented. Further, the non-suspended matter must not be artificially forced to accumulate on the strainer by non-prototypical agitation or debris addition that could be used with the objective of enhancing the quantities of debris on the strainer. Testing has demonstrated that the most severe head losses are associated with a relatively slow accumulation process that allows the flow to systematically seek the locations of higher flow through a debris bed and slowly plug these locations. Rapid bulk accumulations can leave channels within a bulky debris bed that would not exist for slow accumulations. Moreover, the fiber bed accumulates more uniformly in the presence of particulates than without particulates because particulate filtration

increases localized head losses and forces the flow toward uncovered surfaces. In conclusion, the most severe head losses are simulated with only suspended matter approaching the strainer, with the particulate added first, and with the fibrous debris introduced very slowly.

6.4.4.1   *Integrated Head Loss Strainer Testing*

Integrated strainer head loss test facilities have been built in several countries (see Appendix D). Tests were carried out by IRSN and VUEZ in the ELISA loop [6-38] and VIKTORIA loop to characterize the temperature dependence of chemical effects on the strainer head loss. Depending on the decrease of temperature of the solution versus the residual heat, at the beginning of the test, the head loss curve usually exhibited a constant increase due mainly to change of the solution viscosity. After that, additional increase in head loss was observed due to chemical effects in the fiber bed, and a sudden peak often occurred during the decrease of the temperature close to 40-50 °C (Figure 6-5), after which the head loss slowly decreased and returned to exhibiting a constant increase.
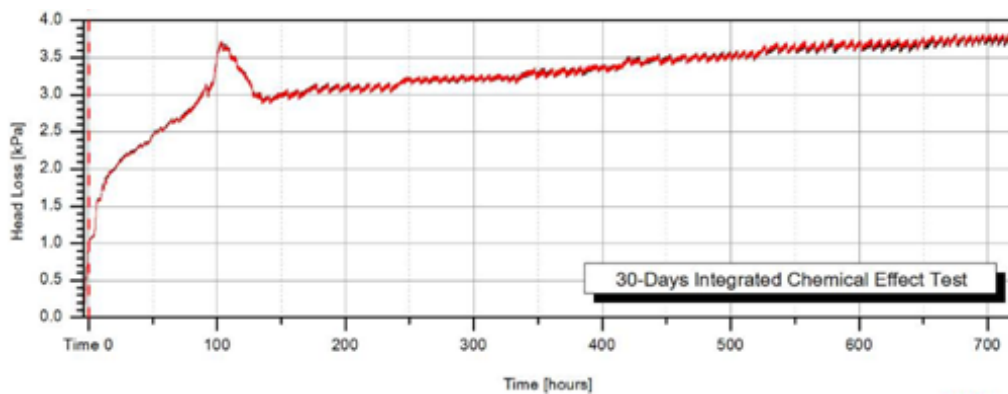
Example 1
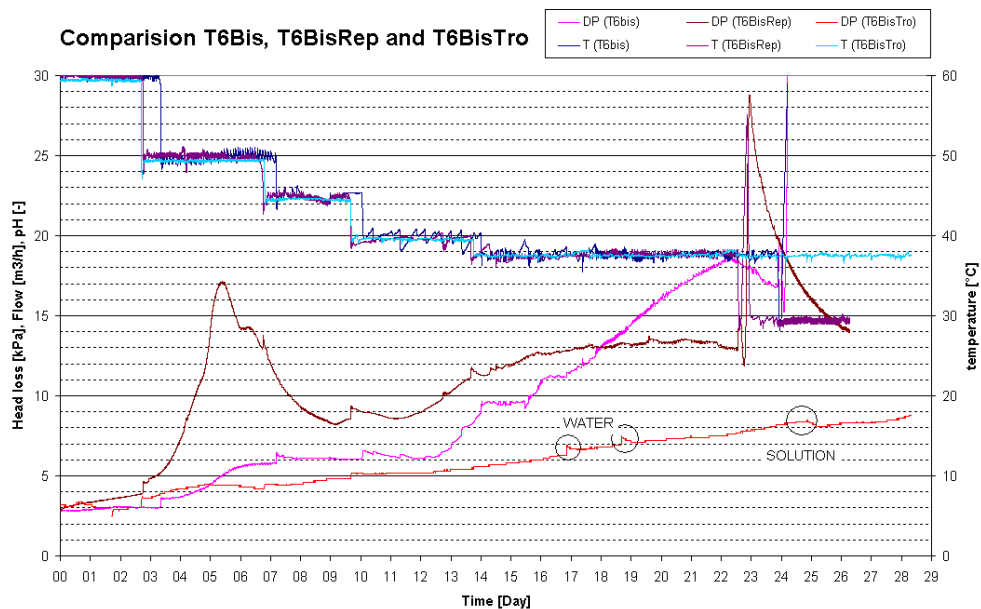
Example 2

Figure 6-5: Examples of Head Loss Changes in Integrated Tests Performed by IRSN and VUEZ.

To better understand the origin of this peak, IRSN and VUEZ investigated different possibilities:

I.   Spurious release of gas dissolved in the solution or produced by chemical reactions

For this purpose, the variation of the solution level inside the filter was used. The corresponding curve did not show any spurious decrease. Consequently, it was concluded that the peak was not related to spurious release of gas inside the filter.

II.   Chemical changes

During the change of temperature, some precipitates captured or created in the fiber bed changed their form by:

- o   Dissolution of the initial precipitates which were present under crystalline forms;
- o   Creation of new ones (possibly gels);
- o   Dissolution of the newly created precipitates.

To test this hypothesis, the concentrations of chemical species present in the solution when the head loss peak occurred were assessed and fluctuations were observed for some of them. Additional investigations, still underway, were carried out using the PHREEQC computer code to identify if any of the possible precipitates have the capability to change over the range of temperature to be considered. For example, Figure 6-6 shows the results of a simulation using PHREEQC for a temperature of 60 °C.
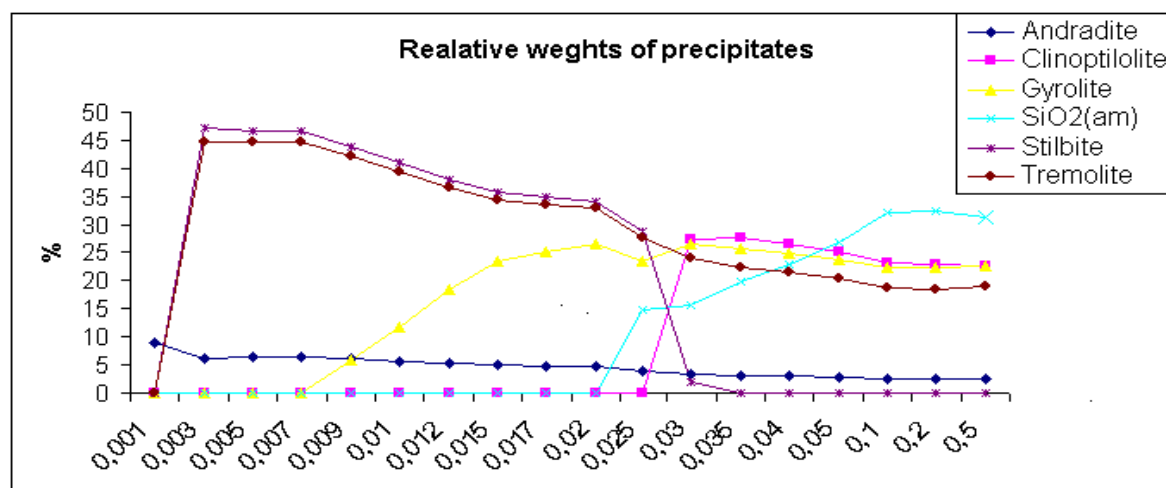
Figure 6-6:   Composition of Precipitates for Various Amounts of Dissolved Glass.

6.4.5   *Clean Strainer Head Loss*

Clean Strainer Head Loss (CSHL) loss is the head loss associated with friction losses in the strainer internal structure, any manifold or plenum losses, and any exit losses associated with flow out of the strainer and from the manifold, without a contribution from debris accumulation. Not all aspects of the CSHL can be determined by testing because of size limitations. In general, the calculation of CSHL should be performed in accordance with industry-accepted methods for hydraulic calculations. If the clean strainer head loss cannot be calculated using theoretical methods, testing should be performed to clearly demonstrate the head loss of the clean strainer.

In addition to the friction head losses, the evaluations should include justification for any temperature scaling that was conducted during the clean strainer head loss evaluation. If scaling other than temperature scaling was performed, the methods and bases for the additional scaling should also be justified.

6.4.6   *Head Loss Test Termination Criteria*

The goal of head loss testing is to determine the plant specific peak head loss that could occur across a sump strainer during a postulated LOCA scenario over the strainer mission time for a design basis event. The mission time is the time from accident initiation to when the flow is permanently reduced by the licensee's Emergency Operating Procedures (EOPs) (typically 30 days or longer, 90 days for CANDU plants). Ideally, the head loss testing would continue until the mission time is reached, but practical considerations may limit the period of testing. Also, conservatism in the testing procedure tends to mitigate the need to run a test through the full length of the mission time. Under certain conditions, the peak head loss can be estimated by the extrapolation of the test head loss results. Extrapolation is possible when the test head loss can be demonstrated to have approached the peak head loss value reasonably closely. Head loss tests for severe accidents cases, or beyond design basis events conditions, have not been conducted. Extrapolating test data for longer term operating periods should be done with caution.

During testing, head loss may approach a steady state relatively soon after the majority of the debris has transported to the strainer. Once all debris has settled out or has been deposited on the debris bed, the water may appear clear indicating that the majority of fine particulate debris has been captured by the debris bed. In other situations, the filtration efficiency may be poor enough that the water remains cloudy. A final steady state head loss can sometimes require many pool turnovers as the filtration process gradually clears the water of finer and finer particles until the remaining particulate is too fine to be filtered or all of the particulate is removed. In addition, there are time-dependent phenomena that may result in longer-term head loss increases. Test termination and data extrapolation methods should consider this possibility as well. Some phenomena that can result in long-term head loss increases are bed compression due to differential pressure and physical or chemical degradation of debris bed components resulting in reduced bed porosity.

Some tests have simulated reduced flow rates and delayed chemical precipitate arrival when it has been demonstrated that these assumptions are conservative for the specific plant condition.

Although it is not practical to conduct all head loss tests over a long term, the head loss results can be more reliable if selected key design basis tests are run for extended periods. Test termination criteria should be based on experimental observations rather than on engineering judgment. The achievement of steady-state head loss can be affected by test conditions and the time required to reach steady state can vary significantly.

6.5   Knowledge Base for Strainer Head Loss

There have been many advances in the understanding of suction strainer performance. However, there are also many uncertainties associated with suction strainer design and qualification. The following items are considered to be sources of remaining uncertainties:

- Different testing methodologies, variations in debris preparation, and variations in adding debris to the test fixture all contribute to test data variability. For example, in one series of tests, material was added to the test section before the test commenced, and pressure drop was measured at varying velocities. This type of testing is prone to nonuniform bed formation, especially for small bed thicknesses. In another series of tests, a concentration of debris was maintained in the test tank water in which the strainer was located, and the test was conducted at constant velocities until a certain pressure drop was achieved. In both cases, some smaller material passed through the strainer. However, in the latter case, more fine material can pass through the strainer at low coverage and be returned and deposited later during recirculation. Significant differences (factors of 2 or 3) have been reported between tests performed using variations of these methods of debris introduction;

- The differing methods of preparing sample material (blast generation, hand shredding, and mechanical shredding) can affect the fiber size and effective bed density and head loss.

In light of these uncertainties, it is recommended that plant specific head loss testing be conducted to qualify strainer designs, in lieu of using an analytical approach, such as the use of the NUREG 6224 correlation.

6.6   On-going Research Needs

The effect of debris by-pass, i.e. debris that passes through the strainers and downstream into the ECCS, on the potential for blockage of flow channels in fuel assemblies needs additional research to determine the allowable debris limits. In the US, this research has been conducted by the PWROG and is documented in Westinghouse report WCAP-16793-NP Revision 2. The acceptance criteria may be fuel fabrication vendor specific. Chapter 7 contains more information on this issue.

Integrated head loss testing that includes a debris tank, suction strainer assembly, and downstream components such as a fuel assembly has had only limited use in qualifying strainers. More extensive use of such facilities could reduce some of the uncertainties in strainer testing.

Table 6.2: Summary of Experiments and Tests

Sponsor: Swiss Federal Nuclear Safety Inspectorate; **Authors**: R. Wanner, H. Eitschberger, and D. Burris; **Date:** April 1993 [6-13]

Variables Studied	Ranges	Results/Relationships	Comments
Materials tested	Mineral wool	$AH=141V^{113}t^{1.14}$ V is velocity in m/s, t is thickness in inches, and head loss is in bars.	Experiments started at the largest approach velocity, so compaction existed at smaller velocities.
Insulation preparation - baking, cutting, shredding, blast, etc.	The wool was stirred in water to simulate the effect of steam jet.		
Material introduction method			
Particulates	None		
Coverage or thickness	16.1,19.32,7.8,9.36,4.1, 4.92 cm		
Approach velocity	0-16 cm/s		
Pressure drop	0.6 bar		
Temperature	15 °C		
pH	Not investigated		
Duration	Not reported		

Table 6.2: Summary of Experiments and Tests-Continued
Sponsor: Vattenfall Utveckling AB; **Author:** M. Henriksson; **Date:** December 1992 [6-14]

Variables Studied	Ranges	Results/Relationships	Comments
Materials tested	Rockwool, Transco K	Mineral wool u AP/AL [m/s] [m-water/m] 0.01 9.09 0.02 22.2 0.03 40 0.04 100	Mineral wool is compressed at high loads, so the pressure drop increases.
Insulation preparation - baking, cutting, shredding, blast, etc.	Shredded with high-pressure water. Shredded with hydraulic pumps.		
Material introduction method	Insulation added in small portions and mixed well.		
Particulates	None		
Coverage or thickness	To achieve 2 MVP		
Approach velocity	0-0.1 m/s		
Pressure drop	2MVP		
Temperature	15 °C		
pH	Not investigated		
Duration	To achieve 2 MVP		

Table 6.2: Summary of Experiments and Tests-Continued

Sponsor: ABB-Atom; **Author:** P.O. Andersson; **Date:** December 1992 [6-15]

Variables Studied	Ranges	Results/Relationships	Comments
Materials tested	Mineral wool (old and new), Filomat	Old rockwool (small shreds) v AP/AL [m/s] [m-water/m] 0.06 17.5 0.07 23.7 0.1 47.3 0.2 102.7	New mineral wool produces higher head losses. Small shreds produce higher head losses.
Insulation preparation -baking, cutting, shredding, blast, etc.	Hand-shredded, trimmer		
Material introduction method			
Particulates	None		
Coverage or thickness	27.8,13.9,6.3,6.4,4.3,11.8, 2.8, 5.6, 7.5, 27.8,2.6, 3.8 kg/m^2		
Approach velocity	0.06-0.22 m/s		
Pressure drop	-0.9 bar		
Temperature	40 °C		
pH	Not investigated		
Duration			

Table 6.2: Summary of Experiments and Tests-Continued
Sponsor: NRC; **Test Facility:** Alden Research Laboratory, Inc.; **Author:** D. N. Brocard; **Date:** July 1983 [6-16]

Variables Studied	Ranges	Results/Relationships	Comments
Materials tested	Mineral wool, fiberglass	Mineral wool $\Delta H = 123 V^{1.51} e^{1.36}$ Fiberglass $\Delta H = 1653 V^{1.84} e^{1.54}$ V in ft/s, e = bed thickness (inches)	Fiberglass shreds produce higher head loss than mineral wool.
Insulation preparation - baking, cutting, shredding, blast, etc.	Manual shredding, Smallest 1" X 1/2" X 1/8"		
Material introduction method	Manually introduced		
Particulates	None		
Coverage or thickness (inch)	0.25', 0.50", 0.1", 2", 5", and 10"		
Approach velocity	0.1-0.5 ft/s		
Pressure drop	<70ft		
Temperature	56-131 °F		
pH	Not investigated		
Duration			

Table 6.2: Summary of Experiments and Tests - Continued

Sponsor: NRC; Test Facility: Alden Research Laboratory, Inc.; **Author:** D. V. Rao and F. Souto; Date: February 1996 [6-1]

Variables Studied	Ranges	Results/Relationships	Comments
Materials tested	NUKON™	NUREG/CR-6224 head loss correlation fits the experimental results per undamaged mixed bed. Overestimates the results for damaged beds.	The approach velocity at which the debris bed is formed does not affect head loss. Particulate debris significantly increases the head loss. Head loss very sensitive to the method by which fibrous debris and particles are introduced.
Insulation preparation - baking, cutting, shredding, blast, etc.	Aged according to ASTM standards; shredded in a leaf shredder.		
Material introduction method	Manually at each approach velocity after particles were circulating in the test loop.		
Particulates	Iron oxide (Fe_3O_4) particles, paint chips		
Coverage or thickness	0.25-2"		
Approach velocity	0.15,0.25,0.50,0.75,1.0, 1.25, 1.50 ft/s		
Pressure drop	<50 ft		
Temperature	125 °F		
pH	Not investigated		
Duration	Until stable head loss at 1.5 ft/s or 50 ft water.		

Table 6.2: Summary of Experiments and Tests - Continued
Sponsor: Owens/Coming Fiberglass Corp; **Test Facility:** Alden Research Laboratory, Inc.; **Date:** September 1983 [6-17]

Variables Studied	Ranges	Results/Relationships	Comments
Materials tested	NUKON™ Base Wool	$\Delta H = 68.3 V^{1.79} e^{107}$ $\Delta H = ft$ $V = ft/s$ $e = ft$ (as manufactured)	Lower coverage (<1") required repeat testing. Distribution on screen may be non-uniform.
Insulation preparation - baking, cutting, shredding, blast, etc.	Cutting into: l" x l" x l/8"; manually tearing to l/4" x l/4" x l/8"		
Material introduction method	Placed into test section with no flow		
Particulates	None		
Coverage or thickness	1/8", 1/4", 1/2", 1", 2", 5", 10"		
Approach velocity	0.1, 0.2, 0.3, 0.4, 0.5 f/s		
Pressure drop	0-18.1 ft		
Temperature	Ambient		
pH	Neutral		
Duration	Short		

Table 6.2: Summary of Experiments and Tests - Continued

Sponsor: Performance Contracting, Inc.; **Test Facility:** Alden Research Laboratory; **Date:** October 1989 [6-18]

Variables Studied	Ranges	Results/Relationships	Comments
Materials tested	NUKON™ Base Wool	$\Delta H = 410V^{1.62}e^{1.45}$	
Insulation preparation - baking, cutting, shredding, blast, etc.	Bake at 650 °F for 96 hours, manually shredded	ΔH in ft	
Material introduction method	Placed into test section at low velocity	V in ft/s	
Particulates	None	e in ft (as manufactured)	
Coverage or thickness	1/4" to 1-1/8"		
Approach velocity	0.2ft/s		
Pressure drop			
Temperature	Ambient, 38 °C, 80 °C		
pH	Neutral, 9.1	~8-ft increase in ΔP due to pH effect	
Duration	0-5 days	No long-term effect neutral, ambient. Slight (1~ft) increase at elevated (80 °C) temperature	

Table 6.2: Summary of Experiments and Tests - Continued
Sponsor: Performance Contracting, Inc.; **Test Facility:** Alden Research Laboratory, Inc.; **Date:** April 1991 [6-19]

Variables Studied	Ranges	Results/Relationships	Comments
Materials tested	NUKON™ Base Wool	pH has a time-dependent effect on head loss. See Fig. 12 in Ref. 4.16.	
Insulation preparation - baking, cutting, shredding, blast, etc.	Bake at 650 °F for 96 hours, manually shredded		
Material introduction method	Placed into test section slowly at low velocity		
Particulates	None		
Coverage or thickness	2"		
Approach velocity	0.05 to 0.35 ft/s		
Pressure drop	<8ft		
Temperature	80 °C		
pH	7-9.5		
Duration	1-24 hr		

Table 6.2: Summary of Experiments and Tests - Continued
Sponsor: Performance Contracting, Inc.; **Test Facility:** Alden Research Laboratory, Inc.; **Date:** October 1993 [6-20]

Variables Studied	Ranges	Results/Relationships	Comments
Materials tested	NUKON™ Base Wool	$\Delta H = 173V^{1.96}e^{1.46}$ ΔH in ft V in ft/s e in ft	Reasonable correlation with 1983 measurements.
Insulation preparation - baking, cutting, shredding, blast, etc.	Bake at >550 °F, air blast to simulate LOCA		
Material introduction method	Slowly placed into test section at low velocity		
Particulates	None		
Coverage or thickness	1/4", 1/2", 1.5", 2.5", 4"		
Approach velocity	0.2,0.4,0.8,1.5,1.65 ft/s		
Pressure drop	14 ft		
Temperature	Ambient		
pH	Neutral		
Duration	15 min to constant dp		

Table 6.2: Summary of Experiments and Tests - Continued

Sponsor: Performance Contracting, Inc.; **Test Facility:** Alden Research Laboratory, Inc.; **Date:** April 1994 [6-21]

Variables Studied	Ranges	Results/Relationships	Comments
Materials tested	NUKON™ Base Wool and particulate iron oxide debris	Small amounts of particulate caused large increases in head loss (up to 1000%), particularly for smaller insulation thickness (see Fig. 6 in Ref. [6-21]). Loss is insensitive to sequence of debris addition.	Wide variance in results between tests for same conditions. Concentration based on measured contaminant levels of Perry pool.
Insulation preparation - baking, cutting, shredding, blast, etc	Bake, air blast		
Material introduction method	Note l		
Particulates	≤ 0.5 lb/ft^2		
Coverage or thickness	1/2" 1", 2"		
Approach velocity	≤ 0.6ft/s		
Pressure drop	<13ft		
Temperature	Ambient		
pH	Neutral		
Duration	2 hours (typical)		

1. Procedure A—Insulation introduced at low velocity and allowed to settle on screen. Particulates added. Velocity increased to 0/37 ft/s.
Procedure B—Particulates added. Insulation added at low velocity and allowed to settle on screen. Velocity increased.

Table 6.2: Summary of Experiments and Tests - Continued
Sponsor: Pennsylvania Power & Light, Co.; **Test Facility:** Alden Research Laboratory, Inc.; Date: May 1994 [6-22]

Variables Studied	Ranges	Results/Relationships	Comments
Materials tested	NUKON™ fiber, iron oxide, zinc paint particulates, and "dirt" sludge	Head loss with combination dirt, sludge, and insulation was significantly greater than for insulation only. Moreover, this condition can manifest itself in a short period of time, depending on the contaminant concentration in the water. Paint chips and rust have less effect. The following equation relates head loss to sludge thickness as well as insulation: $\Delta H = 1059\ V^{1.3}\ e_s^{\ 0.197}\ e_i^{\ 0.72}$ ΔH = head loss, ft V - approach V, ft/s e_i = insulation thickness, ft e_s = sludge thickness, ft Refer to Figs. 18, 20, 24, and 29 in [6-22] for representative test behavior.	This combined equation is judged to poorly fit the data and is presented for information only.
Insulation preparation -baking, cutting, shredding, blast, etc.	Some baked, some fresh NUKON™ either cut into clumps or shredded to simulate debris. Refer to Ref. 6-22 for details on debris preparation.		
Material introduction method	Concentration maintained in tank with 1:4 scale ECCS strainer.		
Particulates	Note 2		
Coverage or thickness	1/4" to 3" Note l		
Approach velocity	0.67 & 0.96 ft/s		
Pressure drop	<30ft		
Temperature	Ambient		
pH	Neutral		
Duration	Variable, minutes to 7 h		

Insulation concentration in water approaching strainer varied from 0.00005 to 0.003%.

Paint chip concentration: 0.0005%; rust concentration 0.0008%; sludge concentration varied from 0.0133% to 0.133% (% units in weight %).

Table 6.2: Summary of Experiments and Tests - Continued
Sponsor: Transco Products, Inc.; **Test Facility:** Fluid Mechanics Laboratory, Illinois Institute of Technology; **Date:** May, 1992 [6-23]

Variables Studied	Ranges	Results/Relationships	Comments
Materials tested	Thermal-Wrap blanket insulation	$\Delta H = aV^b e^c$ H, ft; V,,ft/s; e; ft; as manufactured values at 52 °C	Shreds/fragments probably represent LOCA-destroyed material; as-fabricated does not.
Insulation preparation - baking, cutting, shredding, blast, etc.	Cutting into 1"x l" or l/4" x l/4" pieces. Precondition by soaking in water. One test performed after baking.	Material **a** **b** **c** Series A shreds 103 1.45 1.32 Fragments 182 1.60 1.61 "As fabricated" 161 0 .56 1.28 B shreds 72 1.48 0.938 Fragments 67.7 1.91 1.13 "As fabricated" 123 1.53 1.03	
Material introduction method	Manually introduced at no flow	Unconditioned shreds $\Delta H = 1285 T^{0.54} V^{2.08} e^{1.32}$	Method of introduction may not represent actual strainer buildup for small thicknesses.
Particulates	None		
Coverage or thickness	1/8", 1/4", 1/2", 1", 2", 3", 6"		
Approach velocity	0.1-0.5		
Pressure drop	<22 ft	No significant effect due to baking	
Temperature	52 °C	dP decreases with increasing temperature	
pH	1 test at 9.5	No significant effect	
Duration	Some testing to 16 days	Up to 10 ft. change noted over 7 day period for 6" bed at 0.5 ft/s	

Table 6.2: Summary of Experiments and Tests - Continued
Sponsor: Vattenfall Development Co.; **Test Facility:** Wilhelmsson and Tinoco; **Date:** March 1994 [6-24]

Variables Studied	Ranges	Results/Relationships	Comments
Materials tested	Various fibrous insulation - Transco, Transco B, Glava, Rockwool	Pressure drop equation for fresh Rockwool: $$\Delta P = 5.26 \left(\frac{M}{A}\right)^{0.71} V^{0.92}$$ ΔP = MVP (meters of water), M = Strainer mass, kg dry material, A = Strainer area (m^2) V = Approach velocity, m/s	Uncertainty due to holes or channelling in beds, especially at higher velocities.
Insulation preparation - baking, cutting, shredding, blast, etc.	Baked to remove binder, shredded	See Figures in Ref. 6.24 [BIL4.INC (April 2, 1992) and BIL9x.INC (April 23, 1993) for additional results.	
Material introduction method			
Particulates			Some materials were removed more effectively by strainer. Fresh Rockwool and Glava removed by strainer. Laxa tends to pass through strainer.
Coverage or thickness			
Approach velocity			
Pressure drop			
Temperature			
pH			
Duration			

Table 6.2: Summary of Experiments and Tests - Continued
Sponsor: Vattenfall Development Co.; **Test Facility:** Wilde; **Date:** June 1993 [6-25]

Variables Studied	Ranges	Results/Relationships	Comments
Materials tested	Mineral wool and fiberglass in combination with particulates from asbestos-reinforced Caposil or Newtherm Aged, baked, steam blasted, shredded, minced Mixture introduced into agitated recirculating tank with strainer.	Mixed debris (fibrous and particulates). Significantly increases strainer pressure drop.	Holes or channels developed in beds with high dp or flow and nonuniform beds.
Insulation preparation - baking, cutting, shredding, blast, etc			Clumps from steam-blasted low-density fiberglass caused difficulties in establishing concentration and bed uniformity.
Material introduction method			
Particulates	Caposil, Newtherm	See App. 3/1/20, 3/8/27, and 3/39/58 in Ref. 6.25.	
Coverage or thickness			
Approach velocity	1,2,4 cm/sec		
Pressure drop	<~2MVP		
Temperature	Ambient		Difficulties experienced in maintaining constant temperature.
pH	Neutral		
Duration			

Table 6.2: Summary of Experiments and Tests - Continued
Sponsor: Finnish Centre for Radiation and Nuclear Safety (STUK); **Test Facility:** IVO Power Plant Laboratory; **Date:** July 1994 [6-26]

Variables Studied	Ranges	Results/Relationships	Comments
Materials tested	DARMET metallic insulation	Pressure drop is roughly proportional to approach velocity squared: $dp = dp_0 (v/v_0)^2$	This relation is highly approximate. See figures in [6-26] for more accurate data. (Appendix D in [6-26])
Insulation preparation - baking, cutting, shredding, blast, etc.	DARMET inner foils cut to regular pieces, ranging from 0.01 to 1.3 m.		
Material introduction method	Foils placed onto strainer or added into circulating flow. Three experiments run: (1) one large foil, (2) many intermediate (0.3-m) foil pieces, (3) large batch of small (2-cm) pieces.	The following apply: 1) large piece (1.2 m^2/m^2): $dp_0 = 18$ kPa, $v_0 = 2.5$ cm/s 2) intermediates (1.2 m^2/m^2): $dp_0 = 18$ kPa, $v_0 = 8.6$ cm/s 3) small pieces (11 m^2/m^2): $dp_0 = 3.0$ kPa, $v_0 = l\,1$ cm/s	
Coverage or thickness	1/2 m^2/m^2 for large and intermediate pieces, up to 12 m^2/m^2 for small pieces.		Adding a few small pieces on top of larger ones can raise dp by 3 to 5 kPa. Linear load dependency holds for uniform size distribution only.
Approach velocity	From 0.5 to 11.4 cm/s	At over 100% coverage, for uniform pieces, dp depends linearly on debris load (see Comments).	
Pressure drop	See Results and Figures		
Temperature	20 °C		
pH	Neutral		

Table 6.2: Summary of Experiments and Tests - Continued

Sponsor: Finnish Centre for Radiation and Nuclear Safety (STUK); Test Facility: IVO Power Plant Laboratory; **Date:** July 1994

Variables Studied	Ranges	Results/Relationships	Comments
Materials tested	DARMET metallic insulation mixed with mineral wool debris.	Pressure drop is roughly proportional to a power of approach velocity: $dp = dp_0(v/v_0)^n$ The following apply: (1) thick fibers, some foil: $n=1$, $dp_0= 11$ kPa, $v_0=0.8$ cm/s at foil coverage 75%.	These relations are approximate. See figures in Ref. 6-26 for more accurate data.
Insulation preparation - baking, cutting, shredding, blast, etc.	DARMET as above; wool heated in an oven to remove binder completely and fragmented under a high-pressure jet.		
Material introduction method	Foils placed onto strainer or added into circulating flow. Fibrous slurry poured on circulating flow. Two experiments run: (1) thick fibrous bed + some larger foils (2) large batch small (2-cm) pieces + some fibers.	(2) thick foil bed, some fibers: $n=1.4$, $dp_0=10$ kPa, $v_0=5.0$ cm/s at $v>3$ cm/s $n=2$, $dp_0=2$ kPa, $v_0=2.2$ cm/s.	In case 2, rapid compression was observed. Particulates were not present in either experiment.
Coverage or thickness	(1) 5 to 7.5 kg/m^2 fibers + 50% & 75% larger pieces, (2) 11 m^2/m^2 small pieces and 1 kg/m^2 fibers	For thick fibrous beds (foil coverage below 100%), dp linear with fiber load (no particulate).	Pressure drops are primarily determined by the fibers and are consequently sensitive to temperature and possible chemistry.
Approach velocity	From 0.5 to 11.4 cm/s		
Pressure drop	See Results and Figures		
Temperature	20 °C		
pH	neutral		

Table 6.2: Summary of Experiments and Tests - Continued

Sponsor: Boiling Water Reactor Owner's Group; **Test Facility:** Continuum Dynamics, Inc.; **Date:** December 1994 [6-27]

Variables Studied	Ranges	Results/Relationships	Comments
Materials tested: Combined debris • Fibrous insulation (NUKON™ & others) • Iron oxide particulate material	45 to 231 micron: Size %Pass 100μ 90 75 μ 70 45μ 48.1	$\Delta H = aU + bU^2$ $a = 17.71\left(M_L^{.95}\right)\left(1 + .23\left(\frac{M_C}{M_L}\right)^{1.37}\right)$ $b = 17.0\left(M_L^{.95}\right)\left(1 + .27\left(\frac{M_C}{M_L}\right)^{1.37}\right)$ Where: U the strainer approach velocity in ft/s M_L pounds mass of fiber on the strainer per ft^2 of strainer area M_c pounds mass of corrosion products per ft^2 of strainer area which has passed onto or through the fiber bed ΔH head loss across the strainer in feet of water	Particulate iron oxide used is larger than what exists in U.S. suppression pools, yielding conservative results Once-through, non-recirculating test facility may not attain equilibrium head loss.
Insulation preparation	Baked, manually shredded fibrous insulation. Particulate material obtained in size range from laboratory.		
Material introduction method	Mixtures of fibers only or fibers and iron oxide in water introduced into vertical column, flow was subsequently established		
Coverage	0.11 to 0.44 lb/ft^2		
Approach velocity	0.1 to 2.0 ft/s		
Maximum Head Loss	15 ft H$_2$0		
Temperature	Ambient		
pH	Neutral		

Table 6.2: Summary of Experiments and Tests - Continued

Sponsor: Performance Contracting, Inc (PCI); **Authors**: R. Biasca; **Date:** September 19, 1997 [6-28]

Variables Studied	Ranges	Results/Relationships	Comments
Materials tested	Fibrous, particulate and reflective metallic insulation	$HL_c = A + K_1 v V_{es} + K_2 (V_{es}^2 / 2g)$	12 separate tests at EPRI's facility, by CDI, were reported. Varying the amount of fiber, RMI and particulates. Stainless steel foils from RMI increased head loss < 1 ft H_2O
Insulation preparation – Shredded NUKON and shredded stainless steel foil RMI	Up to 300 lbs of NUKON, size of shreds not reported		
Material introduction method			
Particulates	Up to 100 lbs of iron oxide		
Coverage or thickness	Up to 14 inch thick		
Approach velocity	Not reported Flow rate up to 10,000 gpm		
Pressure drop	Curves developed for various conditions		
Temperature	Ambient, 57-73 °F, adjusted to 60 °F		
pH	Not investigated		
Duration	Not reported		

Table 6.2: Summary of Experiments and Tests – Continued,
Sponsor: U. S. NRC; **Authors**; C. J. Shaffer et al., **Test Facility**: University of New Mexico; **Date:** May 2005 [6-29]

Variables Studied	Ranges	Results/Relationships	Comments
Materials tested Crushed calcium silicate and shredded NUKON insulation with RMI	Specific sizes not recorded.	NUREG/CR-6224 correlation parameters developed for calcium silicate and NUKON for various ratios of NUKON and calcium silicate	The confirmatory tests were intended to provide reasonable assurance that NUREG/CR-6224 can be used as a scoping tool to calculate the pressure drop across calcium silicate debris beds. However, the NRC staff position is the NUREG/CR-6224 correlation cannot be used as a design tool to calculate the head loss across a calcium silicate debris bed on sump screens.
Insulation preparation - baking, cutting, shredding, blast, etc.	NUKON put through a Leaf shredder, then a blender. Calcium silicate was pulverized		
Material introduction method	Not recorded		
Coverage or thickness	Various		
Approach velocity	various		
Pressure drop	Various, up to 20 ft		
Temperature	72 °F and 125 °F		
pH	Not recorded		

Table 6.2. Summary of Experiments and Tests - Continued

Sponsor: U. S. NRC; **Authors**; B. Letellier et al. **Test Facility**: Los Alamos National Lab & Univ. of New Mexico; **Date:** July 2005 [6-30]

Variables Studied	Ranges	Results/Relationships	Comments
Materials tested Latent debris samples from 5 PWR plants	84% to 95% was particulate, remainder was fiber		Latent debris fiber / particulate ratio of 15/85 recommended for future use Specific surface area for using NUREG/CR-6224 correlation was evaluated.
Insulation preparation	Surrogate debris of fiberglass fibers and soil particles used for head loss tests.		
Material introduction method	Blended debris mixture added slowly to produce very thin, uniform bed		
Coverage or thickness	Not reported		
Approach velocity	Up to 0.45 ft/sec		
Pressure drop	various		
Temperature	Not recorded		
pH	Not recorded		

Table 6.2: Summary of Experiments and Tests - Continued
Sponsor: U. S. NRC; **Authors:** C.W. Enderlin, et al.; **Test Facility**: Pacific Northwest National Lab; **Date:** January, 2007 [6-31]

Variables Studied	Ranges	Results/Relationships	Comments
Materials tested NUKON Fiberglass and calcium silicate			A total 156 tests were conducted with the following test conditions: 5 screen-only tests, 11 calcium silicate-only tests, 90 NUKON-only tests, 45 NUKON/calcium silicate tests, and 5 coatings tests. Of the 156 tests, 43 were performed in the large-scale test loop, and 16 of those tests were conducted at elevated temperatures of 129 and 180 °F (54 and 82 °C).
Insulation preparation	NUKON shredded by wood chipper then commercial blender. Calcium silicate crushed with mortar and pestle.		
Material introduction method	As a slurry		
Coverage or thickness	Varied by test		
Approach velocity	various		
Pressure drop	various		
Temperature	various		
pH	Not recorded		

Table 6.2: Summary of Experiments and Tests – Continued,
Sponsor: BWROG; **Author(s):** A. Bilanin; **Test Facility**: EPRI NDE Center and CDI lab; **Date:** November 1996 ([6-2] Vol. 2)

Variables Studied	Ranges	Results/Relationships	Comments
Materials tested	Reflective metallic insulation, iron oxide mixed with NUKON wool debris.	Pressure drop is proportional approach velocity and velocity squared: CDI 95-09 Rev 4 gives results by strainer type	See CDI Report 95-09 Rev 4, which is included in Vol. 2 of the URG 7 strainer designs tested
Insulation preparation - baking, cutting, shredding, blast, etc.	RMI manually cut up; NUKON fragmented with a garden shredder.		
Material introduction method	RMI Foils added into circulating flow. Fibrous debris added uniformly. Iron oxide added in dry form.		
Coverage or thickness	varies		
Approach velocity	Flow rate recorded		
Pressure drop	See Results in report		
Temperature	Not given		
pH	Not given		

Table 6.2: Summary of Experiments and Tests – Continued,
Sponsor: Northeast Nuclear Energy Company; **Test Facility**: Continuum Dynamics, Inc. **Date:** February 1999 ([6-5] Table E-2)

Variable Studied	Range	Results/Relationships	Comments
Materials tested Coatings, Nukon, RMI			Debris on floor does not readily transport Boric acid does not increase transportability
Insulation preparation - baking, cutting, shredding, blast, etc	Coating, RMI and Nukon shredded manually. Coatings ranges 1/8 inch to ¾ inch Nukon less than ½ inch RMI crumpled		
Material introduction method	Debris wetted then added to tank		
Coverage or thickness	500 sq ft paint, 0.115 sq ft fiber, 2.5 sq ft RMI		
Approach velocity	0-0.25 ft/sec		
Pressure drop	1.3 inch H_2O		
Temperature	Ambient		
pH	Greater than 6.0 with boric acid		

References

6-1   U.S. Nuclear Regulatory Commission NUREG/CR-6367, "Experimental Study of Head Loss and Filtration for LOCA Debris", Science and Engineering Associates, Inc., February1996.

6-2   Utility Resolution Guide for ECCS Suction Strainer Blockage by GE Nuclear Energy, NEDO-32686-A October 1998, 4 Volumes.

6-3   "Experimental Investigation of Head Loss and Sedimentation Characteristics of Reflective Metallic Insulation Debris", SEA No.95-970-01-A: 2, May 1996 by G. Zigler, et al, for the US Nuclear Regulatory Commission.

6-4   Nuclear Energy Institute Topical Report NEI-02-01 Revision 1 "Condition Assessment Guidelines Debris Sources Inside PWR Containments ", September 2002.

6-5   Topical Report NEI 04-07 "Pressurized Water Reactor Sump Performance Evaluation Methodology" Revision 0, December 2004 Volume 1 and 2, by the Nuclear Energy Institute.

6-6   U.S. Nuclear Regulatory Commission, "Parametric Study of the Potential for BWR ECCS Strainer Blockage Due to LOCA-Generated Debris", NUREG/CR-6224, October 1995.

6-7   U.S. Nuclear Regulatory Commission, "Blockage 2.5 User's Manual", NUREG/CR-6370, December 1996.

6-8   U.S. Nuclear Regulatory Commission, "Blockage 2.5 Reference Manual", NUREG/CR-6371, December 1996.

6-9   Boiling Water Reactor Owners Group ECCS Suction Strainer Committee, "Interim Report", December 1994.

6-10   Vattenfall Utveckling AB, "Research and Experiment in Support of Back Fitting Measures at the Swedish BWRs", January, 1994.

6-11   NUREG-1862 "Development of a Pressure Drop Calculation Method for Debris-Covered Sump Screens in Support of Generic Safety Issue", W. Krotiac, February 2007.

6-12   Information Systems Laboratories, 2005, "Development and Implementation of an Algorithm for Void Fraction Calculation in the '6224 Correlation' Software Package", ISL-NSAD-TR-05-01.

6-13   ABB-Atom, "Guaranteed Emergency Core and Containment Cooling", RVD-92-193, December 1992.6.13.

6-14   Kernkraftwerk, Leibstadt, AG, Swiss Federal Nuclear Safety Inspectorate, "KKL-Specific ECCS Strainer Plugging Analysis According to Regulatory Guide 1.82, Rev. 1, for a Loss of Coolant Accident", BET/93/031, April 1993.

6-15   Vattenfall Utveckling AB, "Ringhals 1: Strainer Systems 322/323", VU-592.56, December 18, 1992

6-16   ABB-Atom, "Guaranteed Emergency Core and Containment Cooling," RVD-92-193, December 1992.

6-17   U.S. Nuclear Regulatory Commission, "Buoyancy, Transport, and Head Loss of Fibrous Reactor Insulation", NUREG/CR-2982, Rev. 1, July 1983

6-18   Alden Research Laboratory, Inc., "Transport and Head Loss Tests of Owens-Corning NUKON™ Fiberglass Insulation", September 1983.

6-19   Performance Contracting, Inc., "NUKON™ Insulation Head Loss Tests", October 1989.

6-20   Performance Contracting, Inc., "Investigation of the Effect of pH on Head Loss of NUKON™ Insulation Base", April 1991.

6-21   Performance Contracting, Inc., "Head Loss Tests with Blast Generated NUKON™ Insulation Debris", ARL: 140-93/M670F, October 1993.

6-22   Performance Contracting, Inc., "Head Loss with Blast Generated NUKON™ Insulation Debris Mixed With Iron Oxide Particulates", April 1994.

6-23   Alden Research Laboratory, Inc., "Results of Hydraulic Tests on ECCS Strainer Blockage and Material Transport in a BWR Suppression Pool", May 1994. (Pennsylvania Power & Light Company report No EC-059-1006 Revision 0).

6-24   Transco Products, Inc., "Experimental Measurements on the Characteristics of Flow Transport, Pressure Drop, and Jet Impact on Thermal Insulation", Test Report No. ITR-92-03N, May 18, 1992.

6-25   Vattenfall Development Co., "Forsmark 1 & 2 Strainer Systems 322/323, Wilhelmsson and Tinoco Test Facility", Sweden, March 1994.

6-26   Vattenfall Development Co., "Strainer Test with Fiber Insulation and Reactor Tank Insulation, Results From Small Model", Sweden, June 1993.

6-27   Finnish Centre for Radiation and Nuclear Safety (STUK) Imatran Voima Oy, "Metallic Insulation Transport and Strainer Clogging Tests", STUK-YTO-TR 73/DLVI-G 380-383, July 1994.

6-28   Boiling Water Reactor Owners Group ECCS Suction Strainer Committee, "Interim Report", December 1994.

6-29   Summary Report on Performance of Performance Contracting, Inc.'s Sure-Flow™ Suction Strainer with Various Mixes of Simulated Post-LOCA Debris Revision 1 and Revision 2, R. Biasca, September 1997.

6-30   NUREG/CR-6874, "GSI-191: Experimental Studies of Loss-of-Coolant-Accident-Generated Debris Accumulation and Head Loss with Emphasis on the Effects of Calcium Silicate Insulation", U.S. Nuclear Regulatory Commission, May 2005.

6-31   NUREG/CR- 6877 "Characterization and Head-Loss Testing of Latent Debris from Pressurized-Water-Reactor Containment Buildings", U.S. Nuclear Regulatory Commission, July 2005.

6-32   NUREG/CR-6917, "Experimental Measurements of Pressure Drop across Sump Screen Debris Beds in Support of Generic Safety Issue 191", U.S. Nuclear Regulatory Commission, February 2007.

6-33   Revised Guidance for Review of Final Licensee Responses to Generic Letter 2004-02, "Potential Impact of Debris Blockage on Emergency Recirculation during Design Basis Accidents at Pressurized-Water-Reactors", March 2008, US NRC (ADAMS Accession No. ML080230234).

6-34   NUREG/CR-6913, "Chemical Effects Head-Loss Research in Support of Generic Safety Issue 191", U.S. Nuclear Regulatory Commission, December 2006.

6-35   NUREG/CR-6808, "Knowledge Base for the Effect of Debris on Pressurized Water Reactor Emergency Core Cooling Sump Performance", U.S. Nuclear Regulatory Commission, February 2003.

6-36   US NRC Information Notice 90-07, "New Information Regarding Insulation Material Performance and Debris Blockage of PWR Containment Sumps", U.S. Nuclear Regulatory

Commission, January 1990.

6-37 "ZOI Fibrous Debris Preparation: Processing, Storage and Handling", Revision 1, January 2012, Nuclear Energy Institute, ADAMS No. ML120481057.

6-38 LA-UR-01-1595 "BWR ECCS Strainer Blockage Issue: Summary of Research and Resolution Actions", Los Alamos National Laboratory, March 21, 2001.

6-39 Mattei, J.-M.; Vicena, I.; Soltesz, B.; Batalik, J.; Liska, M.; Galuskova, D. ; Klementova, A. "Experimental Program on Chemical Effects and Head Loss Modelling", IRSN Report DAI No. 2012/006.

7.   DOWNSTREAM EFFECTS

7.1   Introduction

The downstream effect issue is highly linked to the topics of "debris source term", "debris retention system performance" and "chemical effects". The phrase "downstream effect" identifies all phenomena that apply to components after the water/debris mixture has passed the sump strainer. This chapter gives an overview on research programs performed by industry groups and regulatory bodies and highlights questions with respect to debris accumulation at specific components.

The U.S. NRC Generic Letter 2004-2 identified component- and system-related concerns within the framework of GSI-191. In Germany, VGB ordered testing with respect to strainer pressure loss, downstream effects (Fuel Assembly (FA) clogging) and chemical effects starting in the 1990s following the "Weiterleitungsnachricht 14-92" triggered by the Barsebäck event. Many other countries also started investigations regarding the downstream effects issue.

The downstream effect issue separates in general into two subject areas: ex-vessel and in-vessel. The ex-vessel subject deals with components like pumps, valves, heat exchangers and nozzles while the in-vessel subject is focused mainly on the clogging of fuel assemblies.

It is important to note that the evaluation of downstream effects is very plant-specific, as it depends on the specific components (valves, pumps) present in the plant, the core and fuel assembly design, and the specific sequence of ECCS events following a LOCA.

7.2   Debris Penetration through the Strainer

Actual strainer designs use either perforated plates or wire mesh as the filtering agent. The size of the opening and the free flow area differ over a wide range depending on the strainer design. The total installed strainer area differs over the range of some tens of m² to several hundred m² per unit. In combination with the different types and amounts of debris material that can be produced during a LOCA it is very difficult to describe the debris penetration behavior through the strainer. G. Zigler (Alion Science) presented a linear correlation between strainer approach velocity and fiber bypass fraction for NUKON fibers based on test results obtained by Alion Science. The US NRC has not accepted this linear correlation because it was based on a limited number of tests.

NUREG/CR-6885 [7-1] addresses the propensity of different types of insulation debris (fibrous, particulate, and RMI) to penetrate PWR sump screens. The variables under consideration include: the size of screen openings; the size, shape, and type of debris; the flow velocity upstream of the screen; and the manner in which the debris reaches the screen (on the floor or in the flow). The test matrix consisted of 44 tests using combinations of representative screen-opening sizes (1/4 in., 1/8 in., and 1/16 in.) and debris sizes and shapes. Insulation debris consisting of NUKON fiberglass, calcium silicate, and stainless-steel RMI was tested individually within a linear hydraulic flume. Approach velocities ranged from 0.2 to 1.0 ft/s. These velocities are representative of containment pool approach velocities at the sump screen for current designs, but modifications in many plants may result in lower approach velocities.

Debris screen penetration depends to some extent on all of the test variables examined: screen size; debris size, shape, and type; flow velocity; and method of introduction (on the floor versus in the

flow). The debris type determines the relative importance of the remaining test variables. Under certain conditions, results indicate the potential for significant debris screen penetration. It was observed that a significant amount of particulate calcium silicate insulation (up to 70% in some cases) can pass through a screen opening of any size. Higher flow velocities cause large calcium silicate clumps to break up, allowing more calcium silicate to be transported to, and pass through, the sump screen. A significant amount of fibrous NUKON debris (up to 90% in some cases) arriving at the screen in finely separated fibers can pass through the screens. However, if the NUKON debris arrives at the screen in larger, agglomerated pieces, only a small amount (<5%) may pass through the screens. Finally, when RMI debris was introduced on the floor, the RMI tended to remain stationary on the floor and not transport to the screen. The result was that <22% of the RMI introduced on the floor passed through the screen for all tests. However, a significant percentage (up to 75%) of the RMI passed through the screen when the RMI was introduced directly into the flow immediately before the test screen.

WCAP-16406-P Rev 1 [7-2] describes the development and application of a "Debris Ingestion Model" that licensees can apply to plant-specific conditions. The shape and size distributions of the debris are the main constraints on the amount of debris that can get through the strainers. The model ignores the effect of filtering due to the debris bed and assumes instead that any particulate material in the coolant that is small enough to pass through the strainer will do so.

The Debris Ingestion Model assumes that there is no settling of debris within the floor pool of the sump. Large heavy particles are expected to settle out in the lower plenum of the reactor vessel, but small light particles are assumed to carry through back to the sump and into the recirculation loop repeatedly without settling out.

The topical report also contains a methodology for calculating the reduction in fibrous debris in the recirculating fluid due to capture on the strainers, using a model from NUREG/CR-6885. This model is recommended for plant-specific analysis where a "more realistic but still conservative" approach is required to appropriately characterize debris transport through the suction strainers.

As the strainer penetration behavior depends on (but is not limited to):

- screen opening size;
- debris size;
- debris shape;
- debris type;
- screen approach velocity;
- transport and sedimentation effects;
- debris mixture ratio (fibers to particles);
- change of debris mixture ratio during long term sump operation;
- filtering of debris on the strainer during recirculation period;
- influence of recirculation pumps on debris size and shape;
- short and long term chemical effects;
- debris erosion,

it is challenging to develop correlations to describe the debris source term downstream of the strainer. The application of correlations has to be done carefully taken into account design or plant specifics, possibly complemented by specific tests with plant specific debris mixtures.

In NUREG/CR-7011 [7-3], the subsection "Debris Carried Through Sump or Suppression Pool Suction Strainers" discusses guidance provided for determining the amount and type of debris that

could be expected to pass through a suction strainer during a LOCA event and post-LOCA recirculation cooling (excerpt on the following pages). This subsection also discusses guidance provided for determining the amount and type of damage that such debris could cause in downstream components of the ECC, CS, and RHR systems.

Suction strainers are designed to severely limit the debris that can enter the ECCS, CSS, and RHR loops, but it is not possible to completely exclude all debris without incurring unacceptable head losses across the strainers. Regulatory Position 1.3.8 from Regulatory Guidance 1.82, Revision 4 specify that the possibility of debris clogging at flow restrictions downstream of the suction strainers should be assessed to ensure adequate long term cooling following a LOCA event.

For BWR systems, the original design criterion for determining the size of the openings in the suction strainers depended on the plant design. For BWR/2, /3, /4, and /5 designs, the strainer hole size was determined by the throat diameter for the containment spray nozzles or the core spray nozzles. For the BWR/6 design, the hole size was determined by the size of the cyclone separator orifices in the flushing subsystem for the ECCS pump seals. Suction strainer hole sizes prior to installation of new designs in response to strainer clogging issues are reported in the BWROG guidance document as ranging from 0.06 inch to 0.6 inch, based on sampling from 16 plants (47% of all operating US BWRs). Of the sampled plants, 50% reported hole sizes of 0.125 inch (1/8 inch) and approximately 38% reported hole sizes of 0.094 inch (3/32 inch). For PWR systems, the original design criterion for strainer openings was defined by the containment spray nozzle throat size. Typically, this dictated an upper limit of 1/8 inch (0.125 inch) for the size of the openings. New replacement strainers installed in response to GSI-191 issues resolution typically have openings 0.094 inch (3/32 inch), and in some designs are only 0.0625 inch (1/16 inch) or smaller.

However, even the smallest strainer openings are large compared to the expected size ranges of fibrous and particulate debris, which have mean values on the order of 0.01 to 0.001 inch. Paint chips and some types of particulate debris have typical sizes in the micron and sub-micron range. It is therefore inevitable that some amount of debris would be carried through the strainers and subsequently reach the downstream components, including the reactor pressure vessel and core, and it is necessary to determine the quantity and characteristics of debris material that could get through.

The two main concerns with the presence of debris in the coolant being pumped through the ECCS and CSS systems and the reactor vessel are the possibility of plugging at flow restrictions, and excessive wear that could lead to failure of components within these systems. Both of these concerns could result in loss of recirculation cooling. The plant piping for these systems and the primary system are unlikely to be at risk since the pipes are relatively large in diameter and are thick-walled stainless steel with a high resistance to abrasive wear. The components of interest in evaluating the effect of debris in the coolant are pumps, valves, orifices, heat exchangers, areas within the reactor and core, and instrumentation tubing. Table 7-1 summarizes the types of these components that are found in PWR and BWR plants, and potential problems due to debris that could compromise ECCS, CSS, or RHR system performance.

The common causes of potential damage due to debris for all of the components listed in Table 7.1 are flow blockage or excessive wear due to abrasion. Flow blockage could shut down the recirculation loop for emergency cooling, and abrasion could lead to a secondary failure in the loop, which would also shut down emergency cooling. It is therefore advisable to determine where and how such problems could occur, and assess the severity of the consequences.

Section 7.1 describes the approach recommended by the BWROG for BWR systems.

Section 7.2 describes the industry guidance for PWR systems. Regulatory guidance on this issue is summarized in Section 7.3, and the treatment of BWR and PWR systems is compared in Section 7.4. Recommendations for appropriate development of consistent guidance for the two systems are provided in Section 7.5.

Table 7.1: Typical Downstream Components for ECCS and CSS in Light Water Reactors.

(not all reactor designs use all of these types of components)

Component	Potential Problems due to Debris
Pumps	
Centrifugal (single- and multi-stage)	Wear on bearing surfaces, seals, impeller, causing: • Increased pressure drop • Decreased flow rate at given speed • Increased vibration • Leaking at shaft seals • Loss of pressure boundary integrity
Valves	
Needle valves Manual globe valves (with and without diaphragm seals) Check valves • Lift type • Piston type • Swing type • Tilting disc type	General hazards of debris in flow: Wear on seals Sticking open (when valve should be shut) Sticking shut (when valve should be open) Plugging hazard for small valves: Needle valves wit labyrinthine flow paths Globe valves with small-diameter holes in cage Sealed globe valves (limited clearance between seal and base)
Orifices	
Spray nozzles (typically 3/8 in)	Erosion due to abrasion Plugging due to accumulation of debris
Heat Exchangers	
Primary side tubing	Debris accumulation in U-bend Scale buildup on tube inner wall Erosion of tube wall; potential for leakage of primary coolant
Instrumentation lines and tubing	
In-vessel, recirculation loop, sump or suppression pool	Plugging due to debris entering the tubing, settled debris covering taps

7.2.1 *Guidance from the BWROG for Debris Transport through Suction Strainers and Effects on Downstream Components*

The BWROG guidance document does not provide recommendations for methods of determining the amount of debris that could be carried through the strainers. It is assumed that passive strainers will allow essentially no particulate to pass through because of the fibrous debris bed that very quickly develops on the strainer. Significant amounts of debris are assumed to pass through the strainers only if a fiber bed fails to develop, or if the plant has installed self-cleaning strainers. With the lessons learned from more recent testing conducted for PWRs in response to Generic Letter 2004-02, US NRC staff has requested the BWROG to reconsider that position and perform a more detailed evaluation of the effects of debris on downstream components. The BWROG has agreed to conduct downstream effects testing over the next few years.

This guidance is based on a General Electric study of the effects of debris on components downstream of the strainers, GE-NE-T23-00700-15-21 (Rev. 1) [7-4] Evaluation of the Effects of Debris on ECCS Performance (Reference 11 of NEDO-32686-A). Based on the General Electric evaluation, the guidance document concludes that there is no safety concern for the potential failure of the ECCS pumps, inadequate cooling capacity from the RHR heat exchangers, plugging of the core spray header nozzles, plugging of containment spray nozzles, corrosion or chemical reaction with other reactor materials, or fuel bundle flow blockage due to debris in the recirculating coolant. The guidance document considers the issue essentially closed, based on the work reported in GE-NE-T23-

00700-15-21 Revision 1, and does not include any suggestions, recommendations, or methodology for determining effects of debris on components downstream of the suction strainers. It also neglects any effects of suppression pool sludge, which may reach the suction strainers well before incoming material from the drywell can establish a debris bed.

7.2.2   *Industry Guidance for PWRs on Debris Transport through Suction Strainers and Effects on Downstream Components*

The industry guidance document containing recommendations related to this issue is WCAP-16406-P, Revision 1, Evaluation of Downstream Sump Debris Effects in Support of GSI-191. This document was developed to supplement NEI 04-07 [7-5] in response to the US NRC staff's finding that the guidance in NEI 04-07 did not fully address the potential safety impact of LOCA generated debris on downstream components. The guidance provided in WCAP-16406-P is comprehensive and detailed, and includes sample calculations illustrating applications to hypothetical plant conditions.

To address the specific question of how much debris can get through the strainers, WCAP-16406-P describes the development and application of a Debris Ingestion Model that licensees can apply to plant-specific conditions. The shape and size distributions of the debris are the main constraints on the amount of debris that can get through the strainers. The model ignores the effect of filtering due to the debris bed and assumes instead that any particulate material in the coolant that is small enough to pass through the strainer will do so. The guidance document also suggests that in plant-specific analysis, additional conservatism can be introduced by assuming that debris particulate considerably larger than the strainer hole size can still pass through and contribute to the debris load.

The Debris Ingestion Model assumes that there is no settling of debris within the floor pool of the sump. In addition, the guidance document suggests that in plant-specific analysis, the licensee could apply the extremely conservative assumption that the debris concentration remains constant in the ECCS throughout the post-LOCA recirculation period. Alternatively, the guidance document develops a methodology for calculating the reduction in debris concentration due to settling within the reactor vessel and elsewhere in the system. In general, this approach is based on simple one-dimensional modeling of the system, assuming velocity dependence for settling rates. Large heavy particles are expected to settle out in the lower plenum of the reactor vessel, but small light particles are assumed to carry through back to the sump and into the recirculation loop repeatedly without settling out.

The guidance document also contains a methodology for calculating the reduction in fibrous debris in the recirculating fluid due to capture on the strainers, using a model from LANL report LA-UR-04-5416.34 This model is recommended for plant-specific analysis where a more realistic but still conservative approach is required to appropriately characterize debris transport through the suction strainers.

In general, the perspective of the industry guidance document for PWRs is that debris effects on downstream components will not be a problem for long-term operation under post-LOCA conditions. However, this is not treated as a blanket assumption for all PWRs, and the document provides recommendations for specific analyses that should be done to evaluate this issue for plant-specific conditions.

The industry guidance document for PWRs describes the development of two empirical models to represent wear due to debris in the coolant; one based on abrasive wear, the other on erosive wear. Abrasive wear is defined as the removal of material due to the presence of hard or sharp particles between two moving surfaces in close proximity. Examples of affected surfaces in pumps are wear rings, impeller hubs, bushings, and diffuser rings. Erosive wear is defined as the removal of material due to particles in the flowing fluid impinging on a component surface or edge. Examples of surfaces that might be affected by erosive wear are valve internal flow paths, spray nozzle orifices, and heat exchanger tubing, particularly in the vicinity of sharp bends.

The industry guidance document presents detailed examples of evaluation methods applying the abrasive wear model to pumps used in the ECCS, CSS, and RHRS. Using plant-specific data, the licensee can obtain estimates of wear rates and evaluate the consequences of such wear for the specific components of the plant. Similarly, the guidance document presents examples for the erosive wear model, which applies to pumps, valves, orifices, and heat exchangers. The document specifically recommends evaluating both hot-leg and cold-leg break scenarios to determine the worst-case conditions of debris loading for potential wear damage to the system components. However, the document fails to note that these may not be the same conditions that lead to the worst case for head loss across the strainers due to the formation of the debris bed.

The worst-case break location for debris load on the strainer may not be the same worst-case break location for debris downstream of the strainer. For suction strainer performance, the worst case probably would include a high percentage of fiber debris. For effects on downstream components, debris loading that is high in particulate, especially small sharp-edged particles that have high hardness values, is likely to be the most adverse.

To evaluate potential effects of debris on instruments that have sensing lines connected to the recirculation flow path and must function to support Emergency Operations Procedures (EOPs), the guidance document recommends specific methods to evaluate the potential for abrasive wear or erosion, or the possibility of plugging of such lines. The guidance document concludes that such analyses can show that instrumentation lines will not be subjected to abrasive wear or erosion and that debris blocking of instrument lines is not a viable failure mechanism.

The guidance document considers flow blockage due to plugging of pumps, orifices, nozzles, valves, or heat exchanger tubing an unlikely mode of failure for the recirculation loop. This is based on analyses using conservatively-bounding assumptions on the size of particles that can pass through the suction strainer openings. The design-basis for the size of these openings is the smallest flow path that the recirculating fluid is expected to encounter.

Based on these assumptions, the industry guidance document expects that licensees will be able to show in plant-specific analyses that debris particulate (both particles and fiber) will be too small to plug even the narrowest flow paths in the loop. The flow velocity in the narrow regions is expected to be high enough to preclude settling, and particulate debris will simply be swept through the system. However, the guidance document strongly reminds licensees that the recommendations provided were developed assuming passive strainers. For active strainers, the licensee must determine the size of particulate material that can pass through the holes, the debris concentration, and the resulting wear and plugging potential of this debris, which may be quite different from that of debris passed through passive strainers.

7.2.3 Regulatory Guidance on Debris Transport through Suction Strainers and Effects on Downstream Components

In the US NRC SE for the BWROG guidance document, there is no discussion of the BWROG position that there is no safety concern due to potential effects of debris on downstream components. This issue is also not discussed in the memorandum on completion of NRC staff reviews of NRC Bulletin 96-03 and NRC Bulletin 95-02 in October, 2001 (ML0129702290).

In the SE for the industry guidance document for PWRs (NEI 04-07), issued in 2004, NRC staff found the guidance in NEI 04-07 was insufficient in that it did not fully address the potential safety impact of LOCA-generated debris on components downstream of the containment sump. The SE offered specific guidance on what should be considered to address this issue. The major positions are summarized as follows:

1. Evaluations for resolution of GSI-191 should include the effects of debris on pumps and rotating equipment, piping and valves, and heat exchangers downstream of the containment

sump related to ECCS and CSS. In particular, any throttling valves installed in the ECCS for flow balancing should be evaluated for blockage potential;

2. Evaluations should consider, on a plant-specific basis, equipment used for both long-term and short-term system operation lineups, conditions of operation, and mission times, at the maximum flow rates expected during operation;

   a) for pumps and rotating equipment, consideration should be given to wear and abrasion of surfaces (e.g., running surfaces, bushings, wear rings); tight clearance components, or components where process water is used to either lubricate or cool should be identified and evaluated;

   b) component rotor dynamics changes and long term effects of vibrations caused by potential wear should be evaluated in the context of pump and rotating equipment operability and reliability, including potential impact on pump internal loads, to address such concerns as rotor and shaft cracking;

   c) for system piping, containment spray nozzles, and instrumentation tubing, consideration should be given to how settling of debris and fines in low fluid velocity areas could impact system operating characteristics; evaluations should include tubing connections such as those provided for differential pressure from flow orifices, elbow taps, venturi nozzles, and reactor vessel/RCS leg connections for reactor vessel level;

   d) for valves and heat exchangers, wetted materials should be evaluated for susceptibility to wear, surface abrasion, and plugging.

3. Evaluations should consider the effect of possible decreased heat exchanger performance resulting from plugging, blocking, plating out of slurry materials, or tube degradation with respect to overall system required hydraulic and heat removal capability;

4. An overall ECC or CS system evaluation integrating limiting or worst-case pump, valve, piping, and heat exchanger conditions should be performed and include the potential for reduced pump/system capacity resulting from internal bypass leakage or external leakage;

5. The potential for leakage past seals and rings to areas outside containment caused by wear from debris fines should be evaluated with respect to fluid inventory, overall accident scenario design, and licensing bases environmental and dose consequences In the SE for WCAP-16406-P, Revision 1, which was developed by the PWROG in response to the guidance from the SE of NEI 04-07, NRC staff found the approach for performing assessments of the impact of debris on various equipment required by the ECCS, CSS and NSSS acceptable, subject to certain conditions and limitations. These conditions and limitations are specified in detail in Section 4 of the SE, but can be summarized as three main concepts:

   a) licensees must use plant-specific information in performing the analyses;

   b) licensees must verify that models and/or data are applicable to plant-specific conditions;

   c) licensees must show that they have considered all equipment that could see debris-laden coolant, and analyzed the worst case conditions in all particulars.

7.2.4   Comparison of Regulatory Guidance for BWRs and PWRs

In the 1998 timeframe, the US NRC staff accepted the BWROG position that there was no safety concern related to effects of debris on downstream components, and it was not necessary to perform plant-specific analyses to address this issue. However, with the lessons learned from more recent testing conducted for PWRs in response to Generic Letter 2004-02, US NRC staff has requested the BWROG to reconsider that position and perform a more detailed evaluation of the effects of debris on downstream components.

US NRC staff treats this issue as a significant concern in the SE for the industry guidance document for PWRs, and have developed detailed and specific guidance on how the issue should be

addressed.

The difference in the regulatory positions for BWRs and PWRs is due to the evolving nature of debris clogging concerns in nuclear power plants, and the earlier development of guidance for the BWRs, compared to PWRs. The actual nature of the technical issues involved is essentially the same for the two reactor types. There is nothing unique to PWRs that make them more susceptible to problems due to debris in downstream ECCS and CSS components, compared to BWRs, except possibly the greater likelihood of chemical interaction problems in PWRs.

Rather, the reverse might be considered more likely, at least in terms of potential damage due to material debris, as BWR systems have the suppression pool and its latent debris to deal with immediately upon activation of the ECCS, while PWRs would draw clean emergency cooling water from storage tanks for approximately the first 30 minutes of an event.

7.2.5   *Recommendations for Guidance on Debris Transport through Suction Strainers and Effects on Downstream Components*

The BWROG guidance is over-generalized from limited data and liberal assumptions regarding the amount of debris that can be transported through the strainers. The industry guidance for PWRs, as expanded in WCAP-16406-P, Revision 1 and the additional regulatory guidance from US NRC staff included in the SE for that document, defines a sound engineering approach to this issue. However, it requires appropriate experimental validation to verify overall conservatism in the methodology. Guidance on this issue should also be cognizant of the fact that for debris ingestion models, a conservative estimate of debris passing through the strainer is not the same as a conservative estimate of the amount of debris trapped on the strainer. In some plants, the bounding case for each analysis may not be the same postulated LOCA event.

These observations suggest the following recommendations:

- Require validation of debris ingestion models with experimental data obtained for conditions where the maximum amount of debris is able to pass through the suction strainers. This should include the evaluation of conditions where an incomplete debris bed might form, and generally corresponds to conditions where the effect of debris on strainer head loss may be relatively low;
- Require validation of abrasion and erosion wear models for specific particulate materials and ranges of particle sizes postulated for debris generated in BWR and PWR LOCA scenarios;
- Apply the same standards and guidance to evaluations of submittals from BWR licensees regarding effect of debris in the recirculation coolant on downstream components as are applied to submittals from PWR licensees.

7.3   Ex-Vessel Components

7.3.1   *Piping*

The plant piping for ECCS, CSS, and RHRS systems and the primary system are unlikely to be at risk since the pipes are relatively large in diameter and are thick-walled with a high resistance to abrasive wear. This argumentation is also used in the non-proprietary version of MHI US-APWR Sump Strainer Downstream Effects MUAP-08013-NP (R1) January 2011 [7-6].

7.3.2   *Pumps*

WCAP-16406-P Rev 1 presents detailed examples of evaluation methods applying the abrasive wear model to pumps used in the ECCS, CSS, and. Using plant-specific data, the licensee can obtain estimates of wear rates and evaluate the consequences of such wear for the specific components of the plant. Similarly, the guidance document presents examples for the erosive wear model, which applies to pumps, valves, orifices, and heat exchangers. The document specifically recommends evaluating both hot-leg and cold-leg break scenarios to determine the worst-case conditions of debris loading for

potential wear damage to the system components.

Pumps that are used are single or multi-stage centrifugal pumps with internal or external seal water supply. Tests performed by AREVA [7-7] show that multi-stage pumps withstand fiber-particle debris mixtures during long term operation. The tests showed in addition that frequent switch on - switch off operations are possible during operation with debris laden water.

7.3.3   Heat Exchangers

BWROG guidance is based on a General Electric study of the effects of debris on components downstream of the strainers, GE-NE-T23-00700-15-21 (Rev. 1), Evaluation of the Effects of Debris on ECCS Performance (Reference 11 of NEDO-32686-A). Based on the General Electric evaluation, the guidance document concludes that there is no safety concern for the potential failure of the ECCS pumps, inadequate cooling capacity from the RHR heat exchangers, plugging of the core spray header nozzles, plugging of containment spray nozzles, corrosion or chemical reaction with other reactor materials, or fuel bundle flow blockage due to debris in the recirculating coolant.

The PWR guidance document considers flow blockage due to plugging of pumps, orifices, nozzles, valves, or heat exchanger tubing an unlikely mode of failure for the recirculation loop. This is based on analyses using conservatively bounding assumptions on the size of particles that can pass through the suction strainer openings.

The NRC SE for PWRs provides the following summary:

1. Evaluations for resolution of GSI-191should include the effects of debris on pumps and rotating equipment, piping and valves, and heat exchangers downstream of the containment sump related to ECCS and CSS. In particular, any throttling valves installed in the ECCS for flow balancing should be evaluated for blockage potential;
2. Evaluations should consider, on a plant-specific basis, equipment used for both long-term and short-term system operation lineups, conditions of operation, and mission times, at the maximum flow rates expected during operation for valves and heat exchangers, wetted materials should be evaluated for susceptibility to wear, surface abrasion, and plugging;
3. Evaluations should consider the effect of possible decreased heat exchanger performance resulting from plugging, blocking, plating out of slurry materials, or tube degradation with respect to overall system required hydraulic and heat removal capability an overall ECC or CS system evaluation integrating limiting or worst-case pump, valve, piping, and heat exchanger conditions should be performed and include the potential for reduced pump/system capacity resulting from internal bypass leakage or external leakage.

Recent tests (AREVA) show that free flow heat exchangers with a plate distance of about 10 mm can be plugged by a fiber-particle debris mixture which is able to pass sump strainers with a hole size of 2 mm.

7.3.4   Valves

NUREG/CR 6902 [7-8] describes a series of tests conducted to assess the potential for LOCA-generated debris to be trapped in the HPSI throttle valve downstream of the sump screen.

Trapping of debris in the valve has important consequences for ECCS operation because it may result in unacceptably high pressure losses in the system and consequent degradation of ECCS performance. Tests have been performed using a range of loadings and compositions of insulation introduced either as a single batch or as a set of successive batches. The tests used a surrogate throttle valve designed to simulate a range of representative valve configurations in use within US PWRs. This test program was the second in a series of NRC-sponsored tests that were conducted to address the effects downstream of the ECCS sump screens.

The first test program in this series addressed the potential for LOCA-generated debris materials to penetrate the sump screen. The current tests addressed the downstream effects of the debris that was able to penetrate the sump screen in these earlier tests. The test data provided information on the potential blockage of the HPSI throttle valves caused by single slugs of unmixed debris, as well as the potential for enhanced blockage caused by single or multiple batches of combinations of debris types. The insulation debris that was tested included calcium silicate insulation, NUKON fiberglass insulation, and RMI; however, many other types of insulation exist in plants. The range of debris sizes was based on the results of the screen penetration tests.

Debris blockage in the valve was gauged using the valve-loss-coefficient K, which was calculated using measured data for the pressure drop across the valve, the flow rate through the valve, and the temperature of the water. As the effective flow area of the valve decreased because of blockage, the loss coefficient increased. The overall approach was first to establish baseline loss coefficients for each valve configuration of interest and then to compare loss coefficients for various debris flow conditions with the data to get an indication of the extent of blockage caused by the debris. In addition, baseline loss coefficients were determined for selected known blockages (blockage-area fractions simulated using shims) to determine the relationship between K and the blocked-area fraction, as well as the blockage detection threshold of the system (~5%–8%). Loss coefficients for debris flow conditions then were compared with those for shim blockage data to obtain estimates of the blockage-area fractions.

Data from tests with single batches of unmixed debris showed that, in general, higher debris loadings and larger debris sizes (relative to the throttle-valve opening) resulted in higher observed increases in K. The K increases were higher for RMI than for NUKON for equivalent mass loadings. However, NUKON is judged to be more likely than RMI or calcium silicate to cause throttle valve blockage because of the propensity for NUKON to transport and penetrate the sump screen.

Tests using calcium silicate-RMI mixtures were the only two-component combinations that exhibited clear increases in K when compared with results from analogous single-debris calcium silicate and RMI tests. The results of tests performed using NUKON-RMI or calcium silicate-NUKON mixtures did not differ significantly from results for analogous separate tests, with one possible exception: one mixture test performed using unsieved calcium silicate with NUKON showed an appreciable increase in valve blockage compared with single-debris NUKON tests. However, it is unclear if this result should be attributed to clumping within the unsieved calcium silicate or to retention by NUKON fibers within the valve.

The three-component mixture tests were divided into two types of tests: (1) homogeneous mixtures of RMI, calcium silicate, and NUKON; and (2) sequential additions of each debris type using different ordering. Tests using homogeneous mixtures of RMI, calcium silicate, and NUKON showed an increase in valve blockage when compared with analogous single-debris RMI tests. However, no particular debris introduction sequence resulted in increases in valve blockage compared with results for homogeneous mixtures. Further, in the tests where NUKON was introduced first in the debris sequence, the blockage was much less than for homogeneous mixtures.

Three accumulation tests were performed to investigate the potential for a cumulative increase in valve clogging as the result of a stream of debris batches reaching the valve. In these tests, multiple batches of debris were introduced at ~15-min intervals over a period of 3 h. Three debris types and loadings were tested. The tests with 25 g each of successive additions of NUKON-calcium silicate showed a sustained increase in K over time as more and more debris reached the valve. However, consistent with the variability observed in other tests, the increase in K was not observed following all additions of debris. Some debris additions did not result in any increase in K, suggesting that no net increase in valve blockage occurred at that step. Accumulation tests with periodic additions of calcium silicate alone (after early introduction of NUKON) also showed that some calcium silicate additions triggered increases in K, whereas others did not. Relative to single-debris calcium silicate tests, larger K increases were observed after some calcium silicate additions, which suggests that the

potential exists for calcium silicate to be trapped by NUKON or RMI that may be present in the valve.

The results for replicated single-debris, multiple-debris, and accumulation tests exhibited significant test-to-test variability. This variability is consistent with the inherent randomness involved in the process; the propensity for trapping of debris in the valve gap is a function of the random orientation of the individual pieces as they enter the valve gap. Further, the bending or thrashing of the debris pieces inside the valve also is a random process. This variability makes it difficult to quantify trends in these results because only a limited number of replicate tests were performed for any single condition.

Spain has applied WCAP-16406-P Rev 1 to their W-design plants with the result to change some of the valves because of restrictions for clearances, sedimentation and wear.

In France tests on throttle valves used in ECCS systems have been performed that led to the replacement of throttle valves by cage valves, as it was found that downstream debris questioned the operability of the type of throttle valves used.

7.3.5 *Spray Nozzles*

No test results regarding plugging of spray nozzles or wear at the nozzles are available. Because of the large dimension of the openings inside the nozzles (> 10mm) it seems unlikely that nozzles can get plugged, but experimental evidence is missing.

7.3.6 *Instrumentation Nozzles and Lines*

Instrumentation nozzles and lines of safety related measurement equipment are a subject of interest. Sedimentation of fibrous or particulate debris or crystallization of e.g., boric acid could plug nozzles even if there is no flow in the lines and therefore influence the reliability of measured values. This effect could be important, especially in a long term post-LOCA period together with chemical effects.

7.4 In-Vessel Components

A sub-section of NUREG/CR-7011 discusses guidance provided for evaluating the effect on flow in the vessel and core as a result of debris that passes through the sump screen or suction strainer during a LOCA event and post-LOCA recirculation cooling (excerpt on the following pages). As noted in Section 7.2, the issue of debris in the emergency cooling water is addressed by Regulatory Position 1.3.8 from Regulatory Guidance 1.82, Revision 4. This Regulatory Position specifically requires consideration of the buildup of debris in the core fuel assemblies and fuel assembly inlet debris screens when assessing long-term cooling following a LOCA event.

The main concern with the presence of debris in the coolant being pumped into the reactor vessel is the possibility of flow blockage, resulting in loss of adequate cooling of the fuel rods, leading to high fuel cladding temperatures that could cause fuel damage. The time frame of greatest interest is long-term post-LOCA cooling. This is mainly because it will take time for sufficient debris to build up to cause problems, but also because during the initial stages of the LOCA event, coolant is leaving the core and vessel, generally at an extremely rapid rate, and debris blockage is essentially impossible. However, the main function of the ECCS is to get coolant to the core as quickly as possible following a LOCA. In a relatively short time, debris-laden water will enter the core.

For PWRs, there will be a delay of approximately 20-30 minutes duration while the storage tank empties and before ECCS pumps start drawing from the sump. For BWRs, ECCS pumps drawing from the suppression pool are activated very early in the LOCA scenario. For both systems, a significant amount of debris will be present as soon as the ECCS pumps begin to draw cooling water

from the sump or suppression pool. The amount of debris will tend to increase for some time interval, as debris is washed into the sump or suppression pool from containment.

The BWR ECCS components that can draw water from the suppression pool vary with plant design, as summarized in Table 7.2. All BWR designs have two or three ECCS components that can inject suppression pool water into the vessel (with the exception of the BWR/2 design, which has only the core spray system.) These components create two main paths for debris to reach the core. The core spray systems (both high- and low-pressure) spray water containing debris directly over the top of the core, or directly into the top of the core bypass region (BWR/5 and BWR/6). The coolant injection systems, when drawing from the suppression pool rather than the condensate storage tank, inject water containing debris into one of the vessel feedwater lines or recirculation lines. From the injection point, water containing debris can flow into the downcomer, through the jet pumps, into the lower plenum, and upward into the core.

The PWR ECCS components that draw water from the sump are essentially the same for all plants, although with significant variation in design details. The basic systems are summarized in Table 7.3. The location at which the ECCS water is injected can be the hot leg or the cold leg, depending on the LOCA scenario. In some Westinghouse plants, ECCS water can be injected directly into the vessel upper plenum or upper head. As with the BWR systems, this creates two main paths for debris to reach the core. Cold-leg injection sends sump water into the vessel downcomer where it can flow into the lower plenum and from the lower plenum up through the core. Hot-leg injection (and upper plenum or upper head injection) sends sump water into the vessel above the core, and debris-laden coolant enters the core from the top.

For both PWR and BWR primary systems, the design basis for long-term core cooling in post-LOCA conditions postulates a stable two-phase flow configuration in the core for some break locations. The inlet flow rate is just sufficient to match a boil-off rate in the partially submerged core, and this has been shown analytically to maintain fuel rod temperatures within acceptable limits. Because the coolant leaves the core as steam, any debris in the recirculating flow will be left behind in the core. This is another source of potential blockage in the fuel assemblies, in addition to the potential plugging of inlet orifices and other flow paths for cooling water entering at the bottom or top of the core.

The approach for evaluating the effect of debris in the vessel and core recommended by the BWROG for BWR systems is described in Section 7.4.1. Section 7.4.2 describes the industry recommended approach for PWR systems. Regulatory guidance for BWRs and PWRs on this issue is summarized and compared in Section 7.4.3. Recommendations for appropriate development of consistent guidance for the two systems are provided in Section 7.4.4.

Table 7.2: Summary of BWR ECCS Components that Draw from the Suppression Pool.

ECCS Component	Action	Plant Type(s)
Core Spray System	• Sprays water on top of core through nozzles on 2 independent sparger rings within core shroud above the fuel assemblies • 2 low-pressure loops (activated at 285 psig) • Draws water from suppression pool	BWR/2 BWR/3 BWR/4
High Pressure Core Spray System	• Provides high pressure core cooling for small, intermediate, and large line breaks • Single loop system, with motor-driven pump • Draws water from the condensate storage tank • Alternatively, draws water from suppression pool • Pumps water to sparger on upper core shroud	BWR/5 BWR/6
Low Pressure Core Spray System	• Single loop system with motor-driven pump • Draws water from suppression pool • Discharges water through core spray sparger directly into core bypass region inside the core shroud	BWR/5 BWR/6
Low Pressure Coolant Injection System	• Can be part of Residual Heat Removal system, or a separate system • 2 recirculation loops • Injects water into recirculation system discharge lines • Draws water from suppression pool	BWR/3 BWR/4 BWR/5 BWR/6
High Pressure Coolant Injection System	• Turbine-driven; needs no external power • Pumps water into vessel feedwater piping • Draws water from condensate storage tank • Alternatively, draws water from suppression pool • For core cooling during small and intermediate break LOCAs	BWR/3 BWR/4

Table 7.3: Summary of PWR ECCS Components that Draw from the Water Storage Tank or Sump.

ECCS Component	Action	Plant Type(s)
Cold Leg Accumulators (Core Flood Tank System, Safety Injection Tanks)	• Passive system consisting of a pressurized tank filled with borated water on each cold leg of the reactor vessel • Activated by drop in reactor coolant system pressure below 600 psig • Injects coolant directly into reactor vessel to rapidly reflood core following a LOCA	Westinghouse Combustion Engineering Babcock and Wilcox
High Head (Pressure) Injection System	• Provides high-pressure core cooling for small to intermediate-size LOCAs • Two-loop system, with centrifugal charging pumps • Draws water from borated water storage tank during injection phase • Draws water from boron injection tank to maintain shutdown margin following steamline break accident • (optionally) can be used during recirculation phase following a LOCA	Westinghouse Combustion Engineering Babcock and Wilcox
Intermediate Head (Pressure) Injection System	• Provides intermediate-pressure core cooling for small- or intermediate-size break LOCAs • 2-loop system with 2 multi-stage centrifugal pumps • Draws water from the borated water storage tank during injection phase • Draws water from the containment sump during recirculation phase • Normal alignment injects directly into cold leg; can be manually aligned to inject into hot leg	Westinghouse
Low Head (Pressure) Injection System	• Injection portion of Residual Heat Removal System; provides low-pressure core cooling for large break LOCAs • Two-loop system with single stage centrifugal pumps • Draws water from the borate water storage tank during injection phase • Draws water from the containment recirculation sump during recirculation phase • Normal alignment inject directly into cold leg; can be manually aligned to inject into hot leg • (optionally) can supply coolant top the intermediate and high pressure injection systems.	Westinghouse Combustion Engineering Babcock and Wilcox

7.4.1 Guidance from BWROG for Debris Effects in Reactor Vessel and Core

The BWROG guidance on evaluating debris effects in the reactor vessel and core is based on the same General Electric study in which the effects of debris on ECCS components are evaluated (see Section 4.2.1). It is assumed that debris will be transported to the reactor vessel only if the plant is equipped with self-cleaning strainers. The guidance document asserts that the General Electric study demonstrates that debris in the coolant will not adversely affect core cooling. This is based on the assumption that because flow velocities in the lower plenum will be quite low, much of the debris suspended in the coolant from the suppression pool will settle out in the lower plenum and will never reach the core inlet. Because most of the debris will not remain suspended in the flowing fluid, very little will be available to be caught on the lower tie plate, inlet debris screen, or other narrow flow paths at the core inlet. If some local blockage occurs, the guidance document assumes it will be innocuous since very little material will remain in suspension after the coolant passes through the lower plenum. The possibility of creating a flow blockage due to the build-up of debris in the lower plenum is dismissed as not credible in the General Electric study. In addition, the guidance document asserts that because the core flow rate is relatively low in the latter stages of the transient, even if some local blockage might occur due to debris, it is unlikely to cause problems, as the flow rate has only to remain high enough to balance the core boil-off rate. The guidance document does not present any recommendations for considering the potential effect of debris left behind in the fuel assemblies as a result of the boil-off, due to local blockages or degraded heat transfer from the fuel rods.

The guidance document dismisses the potential for fuel bundle flow blockage and fuel damage on the strength of General Electric's judgment that, on a best-estimate basis, it would not adversely affect core cooling, even in the highly unlikely situation of a blocked bundle inlet.

This argument is based on a SE of the GE11 and GE13 fuel (General Electric Report). This report shows that adequate core cooling would be maintained, even with complete flow blockage of the lower tie plate debris filter for a single bundle. Core spray cooling would deposit enough water from the top to keep the core below the 2200 ºF (~1200 ºC) peak cladding temperature limit.

The guidance document does not consider the potential effect of debris in the coolant sprayed into the core from the top, which would be left behind in the fuel assemblies as a result of the boil-off.

The guidance provided consists only of the suggestion that licensees should review their plant specific conditions to assure they are bounded by the GE evaluation and address any unresolved issues. However, it is noted that the BWROG has begun a task to reevaluate fuel blockage in a manner similar that used by the PWROG and described in the following sub-sections.

7.4.2 Industry Guidance for PWRs on Debris Effects in Reactor Vessel and Core

The industry guidance document for PWRs (WCAP-16406-P) was evaluated by the US NRC staff as incomplete in the treatment of debris effects in the reactor vessel and core (SE WCAP-16406-P). A second document was submitted for review (WCAP-16793-NP, Revision 0) [7-9] as a supplement to WCAP-16406-P, providing more specific and detailed guidance on assessing the impact on long-term core cooling of debris in the ECCS the effects of debris that could form blockages in the fuel bundles or adhere to the cladding surface the effects of chemical precipitates that could plate out on fuel cladding surfaces.

Revision 2 of WCAP-16793-NP was accepted for review by the US NRC and the SE on this document has been completed [7-11]. Because of this extended time frame, the industry guidance described in this section is based only on WCAP-16406-P, Revision 1 and its corresponding SE.

The guidance document provides recommendations for specific analyses that should be done to evaluate this issue for plant-specific conditions.

As in the case of the BWROG guidance, the industry guidance for PWRs asserts that collection of a large volume of fibrous debris in the lower plenum (or upper plenum) sufficient to completely block flow to the core is not considered credible. However, the effect of debris carried to the core should be evaluated based on plant-specific debris loading (as determined in responses to GL 2004-02 provided in NEI 04-07).

Because fibrous debris has the capability to collect on any structure in the reactor vessel, the guidance document recommends that plant-specific analyses should be performed to determine the effect of fibrous, mixed fibrous-particulate, and particulate debris on flow through the fuel assemblies. In cold-leg recirculation mode (which can be used for both hot-leg and cold-leg postulated breaks), ECCS water is injected into the cold leg and follows the normal flow path through the reactor; i.e., through the downcomer, the lower plenum, and on up through the core.

For a cold-leg break, long-term core cooling is achieved by relatively low velocity flow (typically about 0.2 ft/sec) from the lower plenum driven by a matching boil-off of liquid inventory in the core. For a hot-leg break, core flow is driven directly by the recirculation loop and can be up to an order of magnitude higher (i.e., up to about 2 ft/sec). Boiling may occur in the core, depending on the specific break scenario. The guidance document offers recommendations for determining the rate of accumulation of debris in the lower plenum, due mainly to settling of particulate, but generally assumes that fiber will not settle out even at low flow velocities because of its low density. The tight clearances in the lower core plate support structure and between the rods and spacer grids are expected to be very effective at trapping debris, and the guidance document outlines general steps for determining the flow reduction due to local blockages, based on geometry and hydraulics modeling.

In hot-leg recirculation mode, the flow path through the vessel is the reverse of normal. ECCS water is injected into the hot leg, flows into the upper plenum and then down through the core.

In some break scenarios, the ECCS flow rate is balanced with the core boil-off rate to achieve adequate core cooling. In such cases, the flow regime in the two-phase region of the core will be counter-current, with steam flowing upward (carrying some entrained liquid droplets) and saturated liquid water flowing downward. As a result, the velocities are even lower in the lower plenum compared to cold-leg injection. The guidance document offers general recommendations for determining the rate of accumulation of debris in the lower plenum, due mainly to settling of particulate, and models for determining fibrous debris build up on fuel rods and spacer grids.

The guidance document suggests options for remedial actions that might be taken if the plant specific analysis shows problems with reduced core flow and elevated core temperatures due to the capture of debris within the fuel assemblies or core inlet structures. These suggestions include removing all fibrous insulation from containment, installing pre-conditioned suction strainers or intermediate debris interceptors to trap a larger amount of debris before it enters the ECCS loop(s), switching to hot-leg recirculation to back-flush the core (as per current EOPs for hot-leg switchover, but with additional justification), if a problem occurs in cold-leg recirculation.

The guidance document notes that this list is not exhaustive. Plant-specific features should be evaluated to determine additional strategies to mitigate debris collection in the core during ECCS recirculation.

7.4.3   *Regulatory Guidance for Debris Effects in Reactor Vessel and Core*

As noted in the introduction to this section, Regulatory Position 1.3.8 from Regulatory Guidance 1.82, Revision 4 specifically require consideration of the build-up of debris in the core fuel assemblies and fuel assembly inlet debris screens when assessing long-term cooling following a LOCA event. In the SE for the BWROG guidance document (NEDO-32686-A), issued in 1998, US NRC staff did not reject the BWROG position that there is no safety concern related to effects of debris on downstream

components, including the reactor vessel and core, nor did the SE offer any guidance on plant-specific analyses to address this issue. In direct contrast, US NRC staff treated this issue as a significant concern in the SE for the industry guidance documents for PWRs, and developed detailed and specific guidance on how the issue should be addressed. In the SE for WCAP-16406-P, Revision 1, NRC staff found the treatment of debris effects in the reactor vessel and core incomplete. The SE states that US NRC staff has reached no conclusions regarding the information presented in WCAP-16406-P, Section 9, which addresses reactor internal and fuel blockage evaluations. The SE further states that Licensees should refer to TR WCAP-16793-NP and the NRC staff's SE of the TR WCAP-16793-NP in performing their reactor internal and fuel blockage evaluations.

In the SE of WCAP-16406-P, US NRC staff identified seven specific issues regarding the evaluation of reactor internal components and fuel. These are summarized below:

1. The evaluation methodology should account for differences in PWR RCS and ECCS designs that could affect core conditions such as boiling time;

2. The evaluation methodology should consider that hot spots could be produced from debris trapped by swelled and/or ruptured cladding;

3. Long-term core boiling effects on debris and chemical concentrations in the core should be accounted for;

4. The evaluation methodology should consider debris and chemicals that might be trapped behind spacer grids and could potentially affect heat transfer from the fuel rods;

5. Consideration should be included for plating out of debris and/or chemicals on the fuel rods during long-term boiling;

6. Evaluations should address the effect of high concentrations of debris and chemicals in the core (due to long-term boiling) on the natural circulation elevation head that brings coolant into the core;

7. If hot spots are found to occur, evaluations should address cladding embrittlement and demonstrate that a coolable geometry is maintained.

The methodology presented in WCAP-16793-NP addresses these seven issues.

The US NRC Safety Evaluation on WCAP-16793, Rev. 2 accepted a fibrous debris limit of 15 g per fuel assembly for operating US PWRs. Testing demonstrated that in the absence of fibrous debris, other types of debris small enough to pass through the ECCS sump strainer did not cause a significant head loss. Testing also demonstrated that at some fiber loads above 15 grams, head loss can increase significantly when chemical precipitates are present. For example, some tests with 20 g of fiber resulted in relatively high head losses. The US NRC concluded that at some fiber loads above 15 g, head loss can increase significantly

Testing was accomplished using a single, partial height fuel assembly with the core support plate modeled in the test rig. The test fuel assemblies consisted of a prototypical inlet nozzle, fuel protective filter, and spacer grids (usually 4 or 5 grids), and prototypically sized fuel rods and instrument tubes. The assemblies were about one-third full height. Testing was generally conducted with room temperature tap water, but some tests were run at about 130 $^{\circ}$F. Tests were run at various flow rates. It was determined that the maximum flow rate resulted in the limiting head loss.

Tests to simulate the fuel response to hot-leg and cold-leg breaks were conducted because each condition has different flow conditions and available driving head. The cold-leg break condition has a much lower flow rate, but also has less driving head to force coolant into the core. It was determined that if a plant meets the hot-leg break fiber limit of 15 g then the cold-leg break will also be acceptable.

Tests showed that small fibers can become trapped in the spacer grids or fuel filters. These fibers are effective at filtering particulate debris and chemical precipitates. If enough fiber becomes trapped within a limited volume in the fuel assembly it can capture other debris and cause significant head loss. It was observed that the greatest head losses occurred when all or most of the debris was trapped at a single elevation within the assembly.

Fuel assembly testing included NUKON fiberglass as the fibrous debris and silicon carbide as the particulate. The particulate had a nominal diameter of 10 microns. The fiber size distribution was based on samples of fibers collected downstream of prototypical strainers during testing. Some tests also included microporous-type insulation. In these fuel assembly tests, microporous insulation behaved similarly to silicon carbide. Aluminum oxyhydroxide chemical precipitates (prepared in accordance with WCAP-16530) were added after all particulate and fiber debris was added. Tests showed that a relatively small amount of chemical surrogate could result in a significant head loss with further additions having little effect. It was discovered that the head loss depended on the amount of particulate that was included in the test. The particulate to fiber ratio (p/f) was varied. For high flow rate (hot-leg break) cases it was determined that a low p/f ratio resulted in the limiting head loss when chemicals were added. For lower flow rates (cold-leg break response) a higher p/f ratio resulted in the limiting head loss after chemicals were added. Without chemical surrogates added, the p/f ratio that results in the highest head loss is different.

The 15 g fiber limit, which is applicable to all US PWR plants, was determined using the most conservative inputs in all areas that were varied during the testing. It is unlikely that the most limiting conditions would occur following a LOCA. However, because review of the test program identified many uncertainties regarding fuel blockage behavior and a theoretical model for blockage behavior has not been developed, the US NRC concluded that the limit is appropriate. The US NRC will review additional information as it becomes available to determine if the limit can be increased under plant specific conditions or if the limit should be changed based on updated analyses. The US NRC safety evaluation on WCAP-16793, Rev. 2 [7-11] contains a number of limitations and conditions in Section 4.0 of the document.

7.4.4   *Recommendations on Determining Debris Effects in Reactor Vessel and Core*

The BWROG guidance is inadequate in that it over-generalizes from limited data and does not consider the wide variation of plant-specific conditions. The industry guidance for PWRs uses a sound approach, but any approach must be validated with appropriate experimental data and its applicability verified for specific plant conditions. Given the current state of knowledge about debris blockage in fuel assemblies and core inlet structures, it is very difficult to define conservative assumptions with confidence. Testing in prototypic geometries is needed to explore effects of such factors as the amount and type of debris and the debris mixture. The effects of debris left behind by core boil-off should also be investigated. The limited studies that have been performed have dealt only with debris deposited by forced flow through such structures as the bundle inlet plate, debris screen, and spacer grids.

- Require prototypic testing of debris mixtures in core flow at pressures and temperatures corresponding to post-LOCA conditions to determine the effect of local blockages on local fuel rod cladding temperatures for postulated for BWR and PWR LOCA scenarios. Include testing to show the effects of debris left behind by core boil-off;

- For PWRs, require testing to determine the effects on local fuel rod cladding temperatures of chemical plate-out (with and without trapped debris) for forced flow and core boil-off conditions in postulated for LOCA scenarios;

- Apply similar standards and guidance to evaluations of submittals from BWR licensees regarding effects of debris in the reactor vessel and core as are applied to submittals from PWR licensees.

7.4.5   *Integral Tests and Analyses on Determining Debris Effects in Reactor Vessel and Core*

A number of test facilities (see Appendix D) are available to address the core (fuel assembly) clogging question. Tests can be performed either in an "integrated mode" where, for example, a time dependent reduction of downstream debris concentration caused by sedimentation or by a debris retention system is taken into account, or in an "separate effects" mode where a specified amount of debris is added to a FA only. As an example, with this option the pressure loss caused by a specific debris mass and mixture can be evaluated for a specific FA design.

Integrated tests are able to reduce conservatism in test performance as they represent more realistically the feedback that exists between the strainer and the FA with respect to debris deposition. Some of the projects that have been performed on that subject are described below.

Between 2000 and 2010 in Germany, VGB and single utilities commissioned a large test series (several hundred integrated tests performed at the AREVA Technical Center) to investigate the effect of the combination of different debris mixtures with different sump screen designs on FA clogging of German-design PWRs. A large number of these tests included the influence of chemical effects. One main result was that sump screens with a 2 mm mesh width in combination with a fast build up of a closed debris filter cake (based on relatively small filter area) lead to very low debris bypass amounts, and therefore very low debris depositions on FAs (less than 5 g per FA) for the debris mixtures used for the tests.

This concept is valid in combination with the ability to back-flush the sump screens if the pressure loss on the screen exceeds the defined limits.

For BWR sump screen designs, similar tests have been performed at the University of Zittau. Some ATHLET calculations related to the ensured core cooling were also carried out in Germany. Calculations were performed with ATHLET for the BWR KKP-1 with a 0.1A leak of a main steam line. The intake of fibers was calculated using the data in Table 7-4.

For the calculations the inner bypass was assumed to be closed.

Table 7-4: Input data for ATHLET calculations for the German BWR KKP-1.

Release	**80 kg**
Transport to Condensation chamber	17.50 %
Insulation material within condensation chamber	14.00 kg
Water in condensation chamber	2500000 kg
Water transport (TK+4*TH)	1600 kg/s
Emergency core cooling phase I without sedimentation	
Time	500 s
Water transport from condensation chamber	800000 kg
Outtake from condensation chamber phase I	4.48 kg
Emergency core cooling phase II with sedimentation	
Remaining insulation material within condensation chamber	9.52 kg
Sedimentation within condensation chamber	50 %
Outtake from condensation chamber phase II	4.76 kg
Transport to fuel rod room	20.00 %
From fuel rod room to condensation chamber	3.20 kg
Maximal core intake in case of no retention at strainers	**12.44 kg**
Number of fuel elements	592

Free area per fuel element	0.01 m²
Material per fuel element	**21.013514 g**
Coverage per m²	2.10 kg/m²

Different pump operation modes, different loads and an increase by a factor of 9 due to the embedding of corrosion products into the fiber bed at the spacers were modeled. It was found that, for the case of large quantities of fibers at the spacers and conservative conditions, residual heat removal was possible. Under those conditions, the coolant consists of water and steam in the upper part of the fuel elements. Cooling is ensured by an alternating production and release of steam and subsequent ingress of water from the upper part into the fuel elements. For the case of a load of 20 kg/cm² at the spacers and for the case of embedded corrosion products, residual heat removal was also ensured. Table 7-5 gives the most important parameters of the calculations. All results are documented in the GRS report 3643 [7-12].

Table 7-5: Calculated Residual Heat Removal from ATHLET calculations for KKP-1.

	Residual heat [MW]	Residual heat removal due to flow through the fuel element [MW]	Residual heat removal via fuel element bypass [MW]	Condition of cooling in the upper part of the fuel elements
TK + 4 TH, closed outer bypass, embedding of corrosion products	11	10.5	0.34	two-phase
3 TH, closed outer bypass, embedding of corrosion products	11	10.5	0.42	one-phase
TK + 4 TH, closed outer bypass, load of 25 kg/m²	42	38 water inrush and evaporation	0.36	two-phase
3 TH, closed outer bypass, load of fibers increased by a factor of 10	36.6	32 water inrush and evaporation	0.65	two-phase
TK + 4TH, open outer bypass, embedding of corrosion products	11	4	7	one-phase
3 TH, open outer bypass, embedding of corrosion products	11	3.5	7.5	one-phase
TK + 4 TH, open outer bypass	42.7	26 water inrush and evaporation	5.2	two-phase
3 TH, open outer bypass, load of fibers increased by a factor of 10	39	15 water inrush and evaporation	19	two-phase

Calculations were performed to show ensured core cooling for a PWR of the KONVOI type. The calculations were performed for a reactor power of 106 %, loss of offsite power and non-availability of 2 emergency diesels. A feeding was possible into leg 1 and 3. The 8%-leak (353 cm²) was positioned at a cold leg. The insulation material was deposited on the upper spacers of the fuel elements. The fiber load was 0.3 kg/m² and for the area with feed at the hot leg the fiber load was 0.4 kg/m² (11 g at the spacer). The resulting head loss at the spacers was 40 mbar for a mass flow of 1.9 kg/s. Within 22 h, the flow within the core is reverted and the deposits from the upper spacers will be removed. If the deposits create a head loss of more than 20 mbar, steam will be generated at the fuel element and will escape. As a result, the deposits will be removed from the upper spacers and water can flow into the fuel element. This process will be repeated. The core was not heated up in between. The results showed a temperature in the hot channel of 40 K below the boiling temperature immediately after the LOCA and, in the long term, 90 K below the boiling temperature. Detailed information is described in [7-13].

In Finland, the University of Lappeenranta performed downstream effect tests for the VVER plant at Loviisa [7-10]. One main result was that the change of the sump filter design from a 2 mm perforated plate opening to a 0.7 mm wire mesh reduced the fiber debris bypass mass by about 80%. The additional pressure loss in the FA caused by fibers sticking at the spacer grids stayed within acceptable limits.

In Korea, the CRI (Central Research Institute) of KHNP (Korea Hydro and Nuclear Power Co. Ltd) and FNC (Future and Challenge Technology Co. Ltd) performed some in-vessel downstream effect tests for the APR1400 plants and for CANDU plants [7-14, 7-15]. The pressure drop across the fuel region of the APR1400 with a PLUS7 fuel assembly was measured. The test results showed that the pressure drop in the mockup PLUS7 due to debris under LOCA condition was less than the head loss allowed for core cooling. In the experiment for CANDU plants, the pressure drop through a horizontal fuel channel composed of 38 fuel rods was measured under conditions such that debris such as silica, fiber, and chemical product (AlOOH) were intruded to the channel in conservatively estimated manner. The results showed that the measured pressure drop was acceptable for ensuring fuel channel cooling under the simulated LOCA condition.

In Japan, JNES performed several test series to investigate material deposition (caused by downstream or chemical effects) on heated fuel cladding surface [7-16]. It was found that the build-up of precipitate depends on pH and affects the cladding surface temperature only by a few tens of a degree centigrade under the boundary conditions applied.

Other parties performed or are planning to perform experiments of a similar type.

To confirm long term core coolability in the case of core inlet clogging due to debris that has passed through the sump screen, JNES has conducted an analysis with the thermal-hydraulic code TRACE [7-17]. It was assumed that the core inlet was 99% clogged with an additional pressure loss coefficient and chemical precipitates were deposited on the cladding of all fuel rods just after the ECCS recirculation operation started during the cold-leg or hot-leg break LOCA in a PWR plant. The additional pressure loss coefficient was treated as a parameter. The three loop PWR plant TRACE analytical model was used and the pressure vessel was divided into 18 levels and 4 rings using cylindrical coordinates. It was found that:

- The cold-leg break is critical for long term core cooling because the core inlet flow is less than the hot-leg break due to the lower downcomer water head.

- Long term core coolability was confirmed even if the core inlet was 99% clogged with an additional pressure loss coefficient up to 20 during the cold-leg break LOCA in a PWR.

- The core inlet flow clogging condition has been obtained with a relation of flow velocity and pressure loss required for long term core cooling during the cold-leg break LOCA in a PWR.

Other parties have performed analytical or CFD calculations for similar scenarios.

See Section 4.5, page 10 of General Electric Report, 10 CFR 50.59 Safety Evaluation of the GE11 and GE13 Fuel Bundle Debris Filter, prepared by J.L. Embley, dated September 7, 1995 (GE Class III Proprietary Information). This document is Reference 12 of Reference 11 of NEDO-32686-A.

7.5 Summary and Conclusion

In the past years a lot of research and development work was performed in order to understand and optimize the performance of sump strainers. The work mainly focused on a combination of high general debris retention capacity combined with low pressure loss at the debris-covered strainer. As the debris layer itself is the effective filtering agent the performance of the strainer regarding debris retention is better the faster a closed debris bed is built up. This reduces the time and possibility for debris bypass and therefore downstream effects.

The downstream effects issue separates in general into two subjects: ex-vessel effects (e.g., pumps, valves, heat exchangers and nozzles) and in-vessel effects (focused mainly on the clogging of FAs). Aspects of the downstream effects issue are closely linked to the chemical effects issue.

The downstream effects issue was identified in recent years as an important subject as relatively small amounts of debris captured by the FAs can have a drastic impact on thermal hydraulics in the core under post-LOCA conditions. In addition, the performance of components of the ECCS systems can be influenced by debris.

Investigations regarding downstream effects have been performed and will continue be performed in the upcoming years for existing and new plant designs. A lot of information obtained is proprietary to the industry and is therefore not publically available.

To minimize the downstream effect issue one should carefully consider the selection of materials to be used inside the containment (e.g., thermal insulation and coating materials). This can reduce and simplify the debris source term in case of a LOCA and facilitate all other necessary steps.

References

7-1   Los Alamos National Laboratory, NUREG/CR-6885, "Screen Penetration Test Report", October 2005.

7-2   WCAP-16406-P, "Evaluation of Downstream Sump Debris Effects in Support of GSI 191", Revision 1 (proprietary).

7-3   Pacific Northwest National Laboratory, NUREG/CR-7011, "Evaluation of Treatment of Effects of Debris in Coolant on ECCS and CSS Performance in Pressurized Water Reactors and Boiling Water Reactors", May 2010.

7-4   GE-NE-T23-00700-15-21 (Rev. 1).

7-5   Nuclear Energy Institute, NEI 04-07, "Pressurized Water Reactor Sump Performance Evaluation Methodology", May 2004, ML041550279, ML041550332, ML041550359, ML041550380.

7-6   MHI "US-APWR Sump Strainer Downstream Effects", MUAP-08013-NP (R1) January 2011.

7-7   I. Ganzmann, C. Schulte; "Test einer LHSI (Low Head Safety Injection) Notkühlpumpe für den EPR™ bei Betrieb mit Feststoffbeladenem Wasser", Jahrestagung Kerntechnik, 2010.

7-8   Los Alamos National Laboratory, NUREG/CR 6902, "Effects of Insulation Debris on Throttle Valve Flow Performance", March 2006

7-9   T.S. Andreycheck et al.; "Evaluation of Long-Term Cooling Considering Particulate and Chemical Debris in the Recirculating Fluid", Westinghouse Electric Company, WCAP-16793-NP, Revision 2, October 2011, ML11292A021.

7-10   J. Laine, A. Räsänen and H. Purhonen, "Sump Strainer Performance Experiments for VVER 440", NURETH 14-473, Toronto, Canada, September 2011.

7-11   US NRC Safety Evaluation for WCAP-16793-NP Revision 2, "Evaluation of Long-Term Cooling Considering Particulate and Chemical Debris in the Recirculating Fluid", ADAMS Accession Number ML13084A154.

7-12   Report GRS-A-3643, Technical Notice 3, "ATHLET Calculations on Residual Heat Removal in Case of Fibrous Debris at the Spacers of BWR Fuel Elements", GRS, December 2011 [in German]. For further information contact Mr. Pointner (mailto:winfried.pointner@grs.de).

7-13   Report GRS-A-3526, Technical Report, "Extension and Testing of the Model on Deposition of Insulation Material within the Core", GRS, May 2010 [in German]. For further information contact Mr. Pointner (mailto:winfried.pointner@grs.de).

7-14   Jeongkwan Suh et al., "In-vessel Downstream Effect Tests for the APR1400", Paper KF125, 2013 International Congress of Advanced Power Plants (ICAPP), Jeju, Korea, April 2013.

7-15   In-Hwan Kim, Hwang-Yong Jun and Je-Joong Sung, "In-Core Downstream Effect for CANDU", Transactions of the Korean Nuclear Society Autumn Meeting, Gyeongju, Korea, October 25-26, 2012.

7-16   JNES Report, "Survey and Test Events PWR Sump Screen Blockage," 10原熱報-0006, http://www.jnes.go.jp/gijyutsu/seika/2009_genshi.html [in Japanese].

7-17   JNES Annual Safety Research Report, JFY 2011, "Investigation, Experiment and Analysis on PWR Sump Screen Clogging Issue", JNES-RE-2012-0001, pp.25-32, August, 2012, http://www.jnes.go.jp/gijyutsu/seika/re_report_2012.html [in Japanese].

8.   RISK ASSESSMENT AND SEVERE ACCIDENT RELATED ISSUES

8.1   Introduction

The technical safety and operational reliability of NPPs is a highly relevant issue that permanently and on a long-term basis faces the increased attention not only of the technical community but also of the broad public. Although NPPs are a highly reliable and safe source of production of electrical energy and heat, the principle of a conservative approach to safety is relevant. In the 1980s, after the real emergency accident in an operating NPP, the new phenomenon of the possibility of a functional failure of the emergency safety systems for cooling of the nuclear reactor occurred. This functional failure with hypothetically potential over-designed implications could arise if technological elements become clogged by thermal insulation, preventing coolant access to reactor core. Thermal insulation based on glass or mineral fibers, broadly used in the industry and specifically in nuclear power engineering, can thus become a serious technical and safety problem, if, as in the case of an accident with coolant leakage (LOCA), mechanically dislodged and disintegrated thermal insulation (e.g. by the exit flow of the steam-air mixture from the split pipeline) is mixed with working fluids such that it can impair the functionality and reliability of various systems (operation of pumps, strainer structures, gratings, etc.).

The assessment of the operational characteristics of the filtration function used during the recirculation phase of the safety injection and containment spray system in the event of a primary system break in containment, is one of the main issues to be addressed for nuclear reactors belonging to the 2nd and 3rd generations.

After the accident in the Barsebäck Kraft AB NPP in 1992 (described in Appendix B), individual NPP operators as well as regulatory bodies began to consider this phenomenon. The question concerning the adequacy of the emergency systems and protective strainer structures for suction of emergency pumps to handle the various scenarios of LOCAs was being investigated.

8.2   State of the Art

The operational characteristics of the filtration function used in a reactor during the recirculation phase of the safety injection system (SIS) and CSS in the event of a primary system break in the containment (LOCA) is one of the main concerns of nuclear safety worldwide. The assessment of this issue has to be addressed for existing NPPs as well as future ones. To estimate the associated risk, the following points have already been studied (Figure 8-1):

1. Inventory of debris generated by the jet effect of the postulated break (insulation fibers, paint and particulates, concrete, oxides, dust, etc. present in the containment, in suspension or on the walls);
2. Vertical transport of debris;
3. Structural modification of debris in the containment (mechanical and/or chemical degradation);
4. Horizontal transport of debris at the bottom of the containment;
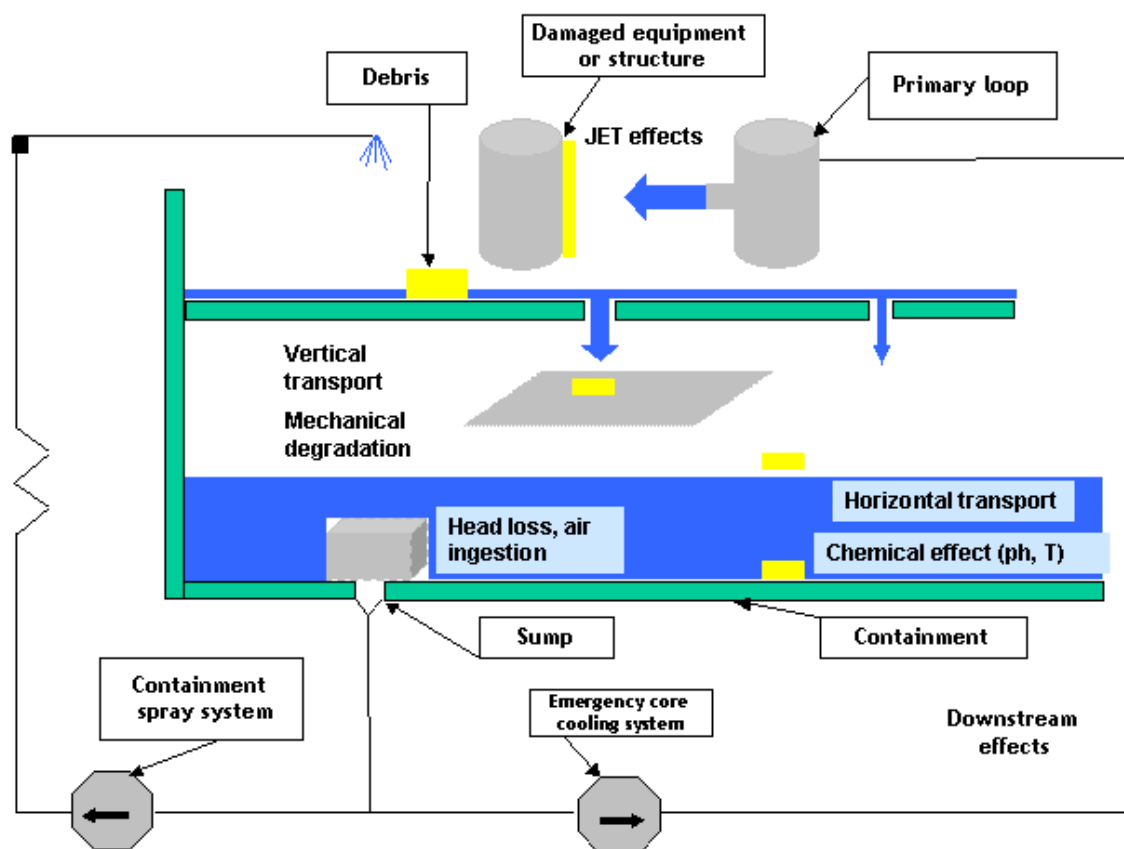5. Filtration efficiency and operation of safety systems.

Figure 8-1: Functional Scheme of the Spray and Emergency Core Cooling Systems during Post-accident Conditions, including Elements of the Protective Strainer Structure and Sump

A large amount of activity and research has been performed since 2000, mainly in the USA with the support of the US NRC. The results obtained, mainly from laboratory tests (i.e., small-scale experiments) were reported in NUREG documents (e.g. NUREGs 6224, 6773, 6868 and 6874). This work mainly relates to operating US BWRs and PWRs and their specific operating conditions. Despite these extensive activities, it is not possible to unambiguously declare that all necessary work has been finished and the problem fully resolved.

Most technological systems are designed so that installing various protective barriers (e.g., strainer structures designed to collect debris) should eliminate such failure conditions. These protective systems are sized so as to be able to collect the dispersed volume of insulation without endangering the functionality or reducing the capacity of the technological systems.

Worldwide, important developments can be underlined, and solutions have been implemented for units under operation and for new-build reactors of the last generation. However, the problem remains that in the existing designs and technical solutions of enhancement of the NPP operational safety, only physical/mechanical effects of insulation on protective barriers have been considered so far.

8.3   Risk Assessment

Concerning breaks leading to recirculation process, we can define the following:

On the main coolant system:

- Large LOCA
- Medium LOCA

- Small LOCA,

- Primary feed and bleed.

On the secondary coolant system:

- Secondary line (steam and feed-water) break inside containment.

The assessment of the effectiveness of emergency core cooling during a LOCA with release of insulation material and other material has to be done in a deterministic way, mainly in agreement with RG 1.82. This guide describes methods acceptable for implementing these requirements with respect to the sumps and suppression pools performing the functions of water sources for emergency core cooling, containment heat removal, or containment atmosphere clean up. The RG also provides guidelines for evaluating the adequacy of the availability of the sump and suppression pool for long-term recirculation cooling following a LOCA.

Initially, this guide was applied to BWRs, but has been revised to enhance the debris blockage evaluation guidance for PWRs. This regulatory guide has also been revised to include guidance previously provided in Regulatory Guide 1.1, "Net Positive Suction Head for Emergency Core Cooling and Containment Heat Removal Pumps."

The predicted frequencies of the corresponding breaks are different depending on the countries. Hereafter are given some examples.

USA

For the USA, in NUREG 1829 the NRC has established a risk-informed revision of the design-basis pipe break size requirements in 10 CFR 50.46, Appendix K to Part 50, and GDC 35 which requires estimates of LOCA frequencies as a function of break size. Separate BWR and PWR piping and non-piping passive system LOCA frequency estimates were developed as a function of effective break size and operating time through the end of the plant license-renewal period. The estimates were based on an expert elicitation process which consolidated operating experience and insights from probabilistic fracture mechanics studies with knowledge of plant design, operation, and material performance. The quantitative responses were combined to develop BWR and PWR total LOCA frequency estimates for each contributing panelist. The distributions for the six LOCA size categories and three time periods evaluated are represented by four parameters (mean, median, 5th and 95th percentiles). Finally, the individual estimates were aggregated to obtain group estimates, along with measures of panel diversity.

The risk significance study that supported a parametric evaluation of operating US PWR plants to assess whether or not ECCS recirculation sump failure was considered as a plausible concern was part of the NRC GSI-191 study tasked to determine if the transport and accumulation of debris in a containment following a LOCA will impede the operation of the ECCS in operating PWRs. The parametric evaluation identified a range of conditions under which a PWR ECCS could fail in the recirculation mode of operation. These conditions stem from the destruction and transport of piping insulation materials, containment surface coatings (paint), and particulate matter (e.g., dirt) by the steam/water jet emerging from a postulated break in reactor coolant piping. The likelihood that sufficient quantities could transport and accumulate on the recirculation sump screen to severely impede recirculation flow is plant specific and a review of PWR plant design features indicated adverse conditions exist in several plants.

The specific goal of the risk significance study was to estimate the amount by which the CDF would increase if failure of PWR ECCS recirculation cooling due to debris accumulation on the sump screen were accounted for in a manner that reflects the results of recent experimental and analytical work. Further, the estimate was made in a manner that reflected the total population of US PWR plants. Results suggest the conditional probability of recirculation sump failure (given a demand for

recirculation cooling) is sufficiently high at many U. S. plants to cause an increase in the total CDF of an order of magnitude or more.

France

In France, leak before break or break preclusion are not applied to the design of Generation II reactors. The design of the sumps filters is based on agreement to RG 1.82.

Concerning Generation III reactors, the break preclusion concept is applied in particular for the EPR, in agreement with the Technical Guidelines recommended by the French Standing Group.

In 2003, using the results of a research program carried out by IRSN, the French Permanent Group recommended a global reassessment of the sump plugging issue. At the end of 2004, the French Permanent Group performed a review of the Utility guidelines for reassessment of the sumps and requested the inclusion of investigations on chemical effects in all the situations which require the recirculation mode. In April 2005, the French ASN (Nuclear Safety Authority) endorsed the advisory committee conclusions. The utility reply to the ASN request was mainly to increase filtering areas and to carry out additional investigations on chemical effects. This topic is still under discussion.

Germany

In Germany, the assessment of the effectiveness of emergency core cooling during a LOCA with a release of insulation material and other substances has to be done in a deterministic way. For this purpose: *"It has to be demonstrated for each plant that:*

- *the amount of the insulation material deposited inside the core remains below the amount at which core cooling is no longer guaranteed,*

- *load transfer resulting from the pressure differences due to the deposition of insulation material on the sump suction strainers and their supporting structural elements is ensured,*

- *no cavitation takes place in the residual-heat removal pumps that will lead to an inadmissible reduction in flow rate."* [8-1].

For PWRs, requirements for the provision of evidence and for associated measures were developed [8-1] for:

- Leak location;

- Release of insulation material and other substances;

- Transport within the containment;

- Transport in the sump water;

- Head loss across the strainers;

- Penetration of insulation material through the strainer;

- Pump suction head;

- Head loss inside the core due to the deposition of insulation material;

- Residual-heat removal system components;

- Long-term behavior;

- Cleanliness of the plant;

- Accident management measures.

"Leak location: Those leaks have to be considered for the provision of evidence for which the insulation material released will lead to the most adverse conditions as regards pressure loss at the strainers or entrainment into the core. This has to be explained in the analysis comprehensively and specifically for each plant." [8-1]

It has to be pointed out that the "most adverse conditions" are not always a maximal release. In particular, mixtures of debris can induce a high head loss across the strainers and/or in the core. Due to partially covered strainers for smaller amounts of release, intake into the core can be higher than for completely covered strainers.

Risk assessments have been carried out to evaluate probabilities of different leaks. For a KONVOI-type PWR, the probability of a leak in the MCL > 200 cm² is less than E-7 per year. The probability of a leak in the MCL with 80 – 200 cm² is 9.0 E-5 per year. However, these results were not used for the sump clogging issue in Germany.

Break preclusion is based on the basic safety concept for construction, material and inspection. It is applied to the MCLs of German PWRs and main steam lines and feed-water lines of German BWRs. As regards break preclusion, the release of insulation material has to be considered up to a leak size of 0.1A. Effectiveness of emergency core cooling has to be demonstrated up to a 2A break, independent on the release of insulation material.

Taking advantage of some favorable technical circumstances in the design of plants in operation and a common strategy to implement technical modifications to reduce complexity in the sump issue and to improve system performances, a status was reached in 2010/2011 for PWRs where the nuclear authorities in Germany decided that successful and sufficient sump recirculation had been demonstrated for all known phenomena and LOCA-scenarios to be considered. For the BWR type 72 the evaluation is ongoing.

8.4   Open Topics

Important developments can be underlined, and solutions implemented for units under operation and for new-built reactors of the last generation. Nevertheless, certain topics are investigated, in particular:

- Topic 1: LOCA-induced long-term debris effects (chemical effects on the strainer bed or downstream effects), as a combined action of temperature and the chemical composition of the solution;
- Topic 2: Downstream effects due to bypass areas of the strainers, taking into account the large increase of their area and/or chemical effects downstream of the strainers;
- Topic 3: The specificities of the sump plugging issue in the case of a severe accident due to the characteristics of the primary circuit and conditions inside containment.

8.4.1   Chemical Effects

The assessment of chemical effects (Topic 1) is in progress for a large number of reactors. Chemical interactions between materials in the containment sump and cooling water additives may affect performance of the sump strainers (Chapter 5). The key effect is generation of precipitates that may increase head-loss across the fiber beds.

This topic could affect:

- the operation of the safety pumps by increasing the head loss at their suction;
- the operation of equipment located in the safety system or in the primary circuit.

Some key input parameters can have large variations based on ranges for normal operating conditions and differences in accident scenarios and plant responses. Such parameters include:

- Sump temperature;

- pH of the solution;

- Debris types and quantities;

- Leached structures.

The issue of chemical effects deals with the transformations of materials inside containment due to the combined effects of temperature and water chemistry. The alkaline solution contained in the sumps can cause significant corrosion-dissolution of materials accompanied by precipitation of the dissolved materials, which can in some cases be accompanied by the generation of thermodynamically unstable intermediates in colloidal form. The chemical species leading to precipitate formation can also be trapped in the thin layer of the filtration bed adhering to the screens, or carried through the primary circuit and give rise to downstream effects. Consequently, the head loss across the containment sump screen in the post-LOCA environment could increase due to the collection of corrosion products on fibrous insulation or equipment can be plugged (e.g., core structures).

Chemical effects started to be investigated in 2004. This is confirmed by newest initiatives of US NRC and NPP operators that have the obligation to qualify or modernize their equipment according to the new conditions including chemical effects (NRC GL-2004-02, Potential Impact of Debris Blockage on Emergency Recirculation during Design Basis Accidents at Pressurized Water Reactors).

In March 2007, the PWROG submitted for US NRC review and approval the Westinghouse non-proprietary topical report WCAP-16530-NP, "Evaluation of Post-Accident Chemical Effects in Containment Sump Fluids to Support GSI- 191," dated February 2006. WCAP-16530-NP provides one approach for plants to evaluate chemical effects that may occur in a post-accident containment sump pool.

For the purpose of this SE, the issue of chemical effects involved interactions between the post-accident PWR containment environment and containment materials that may produce corrosion products, gelatinous material, or other chemical reaction products capable of affecting head loss across the sump strainer or components downstream of the sump strainers. This topical report is applicable to PWRs only. Topical Report WCAP-16793-NP, "Evaluation of Long-Term Cooling Considering Particulate, Fibrous, and Chemical Debris in the Recirculating Fluid," evaluates potential chemical effects in the reactor vessel, so these effects are not addressed in WCAP-16530-NP.

Testing was conducted to identify key interactions, and to develop generically applicable tools to evaluate post-accident chemical effects at plants. The purpose of the ICET Program conducted by the US NRC, EPRI and the PWR Owners Group was to assess if chemical products would form. The program included integrated testing using typical plant materials at bounding material loadings and sump chemistries. The program demonstrated that chemical products would form over time and identified the dominant chemical products (aluminum, sodium and calcium). The objective was to support replacement sump screen testing by developing testing and development of a generic chemical model. Results were used by licensees to perform sump screen testing.

In Europe, since 2004 a program aimed at increasing knowledge of chemical effects on the fiber bed created on filtering systems during recirculation was performed by IRSN in collaboration with VUEZ and the TRENCIN academy (Slovakia).

In 2011, 41 potentially significant issues that required further evaluation based on an original list of over 100 chemical effects phenomena identified in NUREG-1918, "Phenomena Identification and Ranking Table Evaluation of Chemical Effects Associated with Generic Safety Issue 191", were selected. The NRC provided an evaluation of the remaining 41 issues in the March 2011 report, and

assessed each item as either having a negligible impact on the results or having been adequately addressed in the current plant-specific analyses.

In 2011, the WCAP-16530-NP conservatism was underlined in terms of chemical effects, illustrating how aluminum corrosion rates were determined in studies of relatively short duration which results in conservative estimates of soluble metal concentration.

New assessments are in progress based on a risk-informed approach. In an effort to understand the true impact that chemical effects could have on long-term core cooling in a plant-specific post-LOCA environment, several plants are considering the option of performing chemical effects testing under conditions that are more realistic than previous tests. Since the testing will attempt to reduce or eliminate overly-conservative methods that were used previously, it is also necessary to consider potentially significant issues that were not directly addressed previously.

Today, a corresponding assessment is in progress to reach agreement on the conditions that must be explicitly modeled in realistic chemical effects tests (NEI summit, January 2012).

The assessment of the chemical process is important not only in terms of its impact on the head loss of the filters but also its impact on downstream effects.

8.4.2 *Downstream Effects*

The solutions implemented by NPPs to cope with the sump plugging issue lead to the possible formation of bypass areas. Increased filtering surface area could increase the downstream effects risk due to the creation of clean strainer area, allowing the transported fibers, particles and chemical species to pass through the strainers. Therefore, in addition to possible chemical effects impacting the head loss of the strainers, downstream effects (due to particles, fibers or chemical effects) can occur on critical equipment (fuel assemblies, heat exchangers, orifices, pumps, valves, see Chapter 7). This issue could impact the operation of equipment located in the safety systems or in the primary circuit.

The assessment of downstream effects (Topic 2) is still open (refer to US NRC letter dated 23rd of December 2010 "Staff Requirements – SEC 10-0113 – Closure Options for Generic Safety Issue – 191, Assessment of Debris Accumulation on Pressurized Water Sump Performance").

Research on downstream effects is being conducted to characterize the importance of the problem. For this purpose, downstream effects are assessed in particular on heat exchanger tubes, fuel assemblies, orifices, diaphragms and most critical parts of pumps or valves. Changes of temperatures able to modify chemical processes and consequent downstream effects have to be taken into account.

WCAP-16793-NP provides methods and information that can be used to perform an assessment of the following:

- Impact of debris ingested into the ECCS to affect long-term core cooling when recirculating coolant from the containment sump;

- Debris that has been postulated to either form blockages or adhere to the fuel cladding, thereby reducing the ability of the coolant to remove decay heat from the core;

- Chemical precipitants that have been postulated to precipitate on the fuel cladding, again resulting in a reduction of the ability of the coolant to remove decay heat from the core.

Assessments are in progress to reach agreement on the conditions that must be explicitly modeled in realistic tests (NEI summit, January 2012). The South Texas Project (STP) has recently proposed the use of a risk-informed approach to assess chemical and downstream effects [8-2], [8-3]. The overall philosophy is to use stochastic analysis and uncertainty quantification to enable an

'educated' reduction of previously demonstrated conservatisms. Initial conclusions are that WCAP-16530-NP provides a conservative estimate of precipitate formation, and that chemical effects for an SBLOCA are negligible at STP. 'Realistic' testing is expected to show that chemical effects for an LBLOCA are relatively minor at STP. The goal of the project is to show that STP has margin to accommodate chemical effects on strainer for medium and small breaks, and margin to accommodate chemical effects within the core for all breaks. It is important to note that not all regulatory authorities have approved the use of a risk-informed solution; the STP approach has not yet been submitted for official US NRC approval.

In Europe, IRSN (France) and VUEZ (Slovakia), who have performed a large research program on the chemical effects issue, have decided to build a test loop with representative conditions, designed to perform 30 days integral chemical effects experiment to determine the impact of chemical effects on debris head loss and downstream effects on critical equipment.

8.4.3   Severe Accidents

The topic related to the recirculation process in case of a severe accident (Topic 3) is still open.

For Generation III reactors, this raises several different issues that need to be assessed:

1. Radionuclide effects: Radionuclides trapped in the debris bed may change the local chemistry (water radiolysis) and cause precipitation;

2. Debris generation: During severe accident progression, the temperature of the gas inside the primary circuit can increase significantly. These very high temperatures can affect materials; for example, insulation glass wool cannot withstand temperatures higher than 500 °C.

   In this case, the insulation could be damaged and could fall down at the bottom of its metallic covering. Under effect of the Containment Heat Removal System for the future reactors, this covering could be damaged. Consequently, a large amount of additional debris could be transported to the sumps. Knowledge of the quantity dislodged and transported to the sumps will allow verification of the relevance of the filtering areas. It is the same case for the coatings washed by radioactive solutions.

3. Containment bypass possibility: depending on the design of the plants, specific aspects as sump suction line installation can contribute significantly to the probability for late unfiltered releases.

Investigations are needed, using assumptions, model and experimental research to quantify the importance of the specific issues to be considered in case of severe accident and the efficiency of the system used to cool the core meltdown.

8.5   References

[8-1]   RSK Statement, "Requirements for the Demonstration of Effective Emergency Core Cooling during Loss-of-coolant accidents involving the Release of Insulation Material and other Substances", RSK 374th meeting, July 22, 2004

[8-2]   "Chemical Effects Implications of WCAP-16530-NP for South Texas Project", slides from G. Zigler, December 1, 2011.

[8-3]   "Risk Informing STP GSI-191 Chemical Effects", slides from Onsite Meeting at STP with NRC, NEI, STP, and STP Contractors, November 14 & 15, 2011

9.   CONCLUSIONS

9.1   Introduction

The art and science of 'sumpology' is complex and multidisciplinary. It was recognized at the start of the Task Group mandate that differences in issue resolution status and methods undertaken to achieve resolution (regulatory aspects, R and D actions, plant modifications) would make consensus difficult. Subtle differences in plant design and configuration (e.g., choice of insulation) make it almost impossible to specify a single solution to the problem of ensuring ECCS and containment spray reliability and long-term core cooling. While Figure 1-1 outlines the general approach to developing a solution, the specific approach taken to address each of the sub-tasks, for example, debris transport, must be tailored to the specific plant and the specific regulatory environment.

A key aspect of the mandate was to not only update the 1995 document, but also to address the new issues of chemical effects and downstream effects. With this in mind, three sub-groups were formed:

- Sub-group one to address chemical effects;

- Sub-group two on downstream effects;

- Sub-group three to address the update of the original 1995 SOAR.

Whereas the 1995 SOAR focused on BWRs, in fulfilling their mandate the Task Group members reviewed and summarized the massive amount of new information related to PWRs. This is reflected in the very much expanded Appendix on "Experimental Investigations and Test Facilities", which, at nearly 200 pages, highlights the large experimental and modelling efforts undertaken to address the sump clogging issue. At the same time, it must be recognized that while a significant amount of non-proprietary information is available on the topic of chemical effects, only limited public information is available on the topic of downstream effects.

9.2   General Conclusions

Many of the conclusions presented in NEA/CSNI/R(95)11 remain valid, and the discussion that follows highlights advances, gaps and new phenomena.

Any assessment of ECCS and core cooling reliability must start with quantification of the amounts of debris generated since this is the source term for transport through the containment to the strainers. Assessments must consider all materials known to be problematic, such as insulation, concrete, paint chips, latent debris, corrosion products that may come loose under a LOCA, as well as materials that can contribute to chemical effects. It is equally important that the key characteristics of the destroyed material be known, e.g., the size distribution of released fibers and particles. While new information on paint chips, latent debris and chemical effects are available, little new information on size distributions of released material is available.

The major mechanisms for dislodging material have been identified as the pressure wave associated with pipe rupture, jet impingement on insulated targets, and erosion due to interaction with the high-velocity fluid. While conceptual models have been established in order to quantify the

amount of debris, in general, the assessment of the models is rather limited.

Most debris transport/strainer head loss correlations rely on a few types of debris and the formation of homogeneous filter bed on the strainer surface. More recent head loss testing experiments have concluded the use of correlations are difficult to justify, as debris beds rarely form homogeneously and these correlations did not include contributions from chemical effects. Plant specific head loss testing with representative quantities and combinations of debris of types is recommended. However, the scaling effects associated with debris transport add uncertainties.

The reference plant study in NRC-SER-2004 developed a methodology that considers both transport phenomenology and plant features and divides the overall complex transport problem into many smaller problems amenable to solution by a combination of experiment and analysis or engineering judgment. The use of CFD for debris transport analyses is promising but complex, as analyses require a large number of nodes, the inclusion of turbulence in the model requires refined techniques, there is a lack of benchmarking of multi-phase flow models, and there is a need for more validation and verification. In general, conservatisms in debris transport evaluations are related to the unavailability of relevant data; in the absence of such data, the analysis should conservatively hedge toward assuming transport to the strainers.

The collection of phenomena referred to as chemical effects take place in a complex recirculating water system in contact with a large number of different materials. Chemical effects involves the release of chemical species into the sump water by corrosion or dissolution of materials in containment, followed by chemical reactions between these dissolved species leading to the formation of a precipitate. Most materials present within containment can undergo corrosion or dissolution under the right physical (e.g, temperature) and chemical (e.g., pH) conditions; these conditions are determined by the sump water chemistry. The post-LOCA pH evolution is complex and depends in part on whether chemical buffers are added to minimize iodine release. Under some post-LOCA water chemistry conditions, erosion-corrosion can be a concern. A significant knowledge base now exists with respect to the behaviour of chemical effects source terms under post-LOCA sump conditions, and this knowledge base has been summarized in this update.

While the fundamental principles underlying chemical effects are reasonably well understood, the post-LOCA sump is a non-equilibrium chemical system and precipitate formation is determined not only by thermodynamic considerations but by numerous kinetic factors. This can make prediction of precipitate formation from first principles extremely difficult and testing based on results obtained in single-effects tests can be excessively conservative. The use of integrated test facilities can reduce this conservatism.

The effect of debris by-pass, i.e. debris that passes through the strainers and downstream into the ECCS, on the potential for blockage of flow channels in FAs is an active area of research. In recent years this 'downstream effects' issue has become an important subject as relatively small amounts of debris captured by the FAs can have a drastic impact on thermal-hydraulics in the core under post-LOCA conditions. The performance of ECCS components can also be influenced by debris. In addition, aspects of the downstream effects issue are closely linked to the chemical effects issue. A significant knowledge base on downstream effects has also been developed, but unfortunately for the Task Group mandate, much of these data are proprietary. Downstream effects investigations are on-going and will continue to be performed in the upcoming years for both existing and new plant designs. Unfortunately for the mandate of this SOAR, much of information on this topic is proprietary to the industry and not publically available.

Much research and development work has been performed to understand and optimize the performance of sump strainers, focusing on both high debris retention capacity and a low pressure loss at the debris-covered strainer. As the debris layer itself is the effective filtering agent the performance of the strainer with respect to debris retention is better the faster a closed debris bed is built up. This reduces the time and possibility for debris bypass and potential downstream effects.

However, the Task Group highlights the seemingly conflicting requirements between a high degree of debris removal to minimize downstream effects and minimizing strainer head loss.

While differences in plant design and configuration (e.g., choice of insulation) make it impossible to specify a single solution to the problem of ensuring ECCS and containment spray reliability and long-term core cooling, the large knowledge base now available, supported by the extensive suite of test facilities described in the Appendix on "Experimental Investigations and Test Facilities", has made it possible for some member states to consider this issue closed.

9.3 Information Exchange

It is clear that work will continue on the topic of the Task Group mandate for some time into the future, and the Task Group highlighted the need to ensure that this new information is shared when possible. While most of the Task Group effort was focused on updating the SOAR, much less time was spent on investigating the feasibility of web-based information exchange on sump clogging. However, the Task Group was very positive concerning the usefulness and feasibility of such a tool, based on the feedback provided by Task Group members on the web page set-up by the NEA. In order to minimize the burden put on the NEA Secretariat to continuously update the NEA web page on sump clogging, the Task Group members agreed to provide links to their national web pages dealing with sump clogging issues to be included on the NEA sump clogging web page. In this way, modifications to the various national web pages will be directly reflected in the latter without an extra effort of maintenance. However, issues such as the language of the national web pages and the availability of test data have to be underscored as challenging. The NEA sump clogging web page will be cleaned up, restructured for easier use and made public as soon as the present report is published.

9.4 Recommendations

Given the differences in issue resolution status and approaches taken achieve resolution, specific recommendations that might become proscriptive. However, several generic recommendations can be made:

- To reduce the risk of sump clogging, one should reduce and simplify the debris source term in case of a LOCA by carefully considering the materials used inside the containment (e.g., thermal insulation, coating materials, potential chemical effects source terms). Good housekeeping to minimize latent debris is also an important aspect of minimizing the risk of strainer clogging.

- A large number of test facilities now exist that can be used both to provide insights into the fundamental phenomena underlying the topics discussed in this SOAR and to perform more targeted, plant-specific testing. Collaborative projects that take advantage of these facilities could be beneficial.

- It is clear that work will continue in this field for some time into the future. One concern raised by the Task Group was the need to ensure that this new information is shared when possible. The Task Group web page set-up by the NEA Secretariat was an effective method for information exchange on the sump clogging issue between the Task Group members and should be maintained and expanded as a means of facilitating information exchange in the future.